Universidad de Valladolid

Escuela de Doctorado Universidad de Valladolid

PROGRAMA DE DOCTORADO EN QUÍMICA: QUÍMICA DE SÍNTESIS, CATÁLISIS Y MATERIALES AVANZADOS

TESIS DOCTORAL:

New methods for organocatalyzed asymmetric synthesis of spirocyclic pyrazolones from pyrazole-4,5-diones and *N*-Boc protected pyrazolinone ketimines

Presentada por Marta Gil Ordóñez para optar al grado de
Doctora por la Universidad de Valladolid

Dirigida por:
Prof. Dr. José María Andrés García
Prof. Dr. Alicia Maestro Fernández

Esta Tesis Doctoral titulada "*New methods for organocatalyzed asymmetric synthesis of spirocyclic pyrazolones from pyrazole-4,5-diones and N-Boc protected pyrazolinone ketimines*" ha sido realizada en el Instituto CINQUIMA, en el Departamento de Química Orgánica de la Facultad de Ciencias de la Universidad de Valladolid (UVa) bajo la dirección del Prof. Dr. José María Andrés García y la Prof. Dra. Alicia Maestro Fernández.

Agradezco a la Junta de Castilla y León por la concesión de un contrato predoctoral (EDU/556/2019) y por las subvenciones concedidas a los proyectos de investigación FEDER-VA115P17 y VA149G18, y también al Laboratorio de Técnicas Instrumentales (LTI) de la UVa por la utilización de sus equipos.

Quiero agradecer especialmente su contribución al desarrollo de los trabajos descritos en esta memoria a Pablo Ortega y al Prof. Dr. Pablo G. Jambrina, así como al resto de coautores de las publicaciones: Cristopher Niño, Camille Aubry y Laura Martín.

Contents

Resumen

Los derivados de pirazol son una clase única de heterociclos conocidos por la amplia gama de propiedades que presentan. Entre todos ellos, las pirazolonas espirocíclicas y los derivados de 4-amino-5-pirazolona destacan por formar parte de la estructura de compuestos con actividades biológicas muy variadas (antitumoral, analgésica…) que se usan como fármacos. Debido a esto, muchos químicos están dedicando numerosos esfuerzos a la síntesis asimétrica de este tipo de derivados. Mientras que las pirazolin-5-onas y sus alquiliden derivados han sido ampliamente utilizados en la preparación de este tipo de compuestos, el uso de pirazolin-4,5-dionas y de sus correspondientes *N*-Boc cetiminas derivadas como sustratos de partida apenas ha sido desarrollado. Por otro lado, la organocatálisis asimétrica destaca como una de las herramientas de preparación de compuestos enantiopuros más atractivas, eficientes y respetuosas con el medio ambiente, y, debido a esto, es un campo en continuo desarrollo.

Por estos motivos, en esta Tesis Doctoral se aborda la síntesis asimétrica organocatalizada de pirazolonas espirocíclicas y de derivados de 4-amino-5-pirazolona a partir de pirazolin-4,5-dionas y de sus correspondientes *N*-Boc cetiminas derivadas. Se estudian dos estrategias diferentes: catálisis covalente, utilizando carbenos *N*-heterocíclicos quirales, y catálisis por enlace de hidrógeno, utilizando escuaramidas bifuncionales quirales.

Capítulo II: Carbenos *N*-heterocíclicos quirales como organocatalizadores para la anelación [3+2] de pirazolin-4,5-dionas y enales: síntesis de γ-butirolactonas espirocíclicas derivadas de pirazolona.

En el capítulo II se describe el primer ejemplo de síntesis enantioselectiva organocatalizada de γ-butirolactonas espirocíclicas derivadas de pirazolona mediante la reacción NHC-catalizada de pirazolin-4,5-dionas con enales. Se ha estudiado la actividad de diferentes carbenos *N*-heterocíclicos quirales como catalizadores, siendo el catalizador de Bode el que proporcionó las espiro pirazolonas deseadas con rendimientos moderados, diastereoselectividad excelente y elevados excesos enantioméricos. La reacción es compatible con un amplio rango de sustituyentes en ambos sustratos de partida.

Para establecer y comprender el mecanismo de la reacción y el origen de la estereoselectividad, se han llevado a cabo cálculos computacionales. Después de considerar varios mecanismos, se concluyó que la etapa limitante y la que determina la estereoselectividad del proceso es la etapa

de lactonización que ocurre después del ataque del homoenolato, formado a partir del enal y el carbeno quiral, al grupo carbonilo electrofílico de la pirazolin-4,5-diona.

Capítulo III: Síntesis de butenolidas espirocíclicas derivadas de pirazolona a partir de pirazolin-4,5-dionas y 3-bromoenales catalizada por carbenos *N*-heterocíclicos.

En el capítulo III, se estudia la reacción de anelación [3+2] de pirazolin-4,5-dionas y 3-bromoenales catalizada por carbenos *N*-heterocíclicos quirales que conduce a pirazolonas espirocíclicas con una unidad de butenolida. Un derivado del catalizador de Bode fue el más eficiente de todos los ensayados proporcionando las correspondientes butenolidas finales con buenos rendimientos y, generalmente, elevada enantioselectividad.

La reacción transcurre en condiciones suaves sobre una amplia gama de sustratos y es compatible con grupos arilo, heteroarilo y alquilo en el 3-bromoenal de partida, así como en las pirazolonas 1,3-disustituidas. La reacción del carbeno con el β-bromoenal genera un 3-bromo homoenolato, especie catalíticamente activa, que tras un proceso de adición/deshalogenización/lactonización dará lugar a las butenolidas espirocíclicas.

Capítulo IV: Síntesis asimétrica organocatalizada de espiropirazolona-oxazolidinas entre *N*-Boc cetiminas derivadas de pirazolonas y γ-hidroxienonas catalizada por escuaramidas bifuncionales quirales.

En este capítulo se describe la primera síntesis asimétrica de oxazolidinas espirocíclicas derivadas de pirazolona mediante la reacción, promovida por una escuaramida bifuncional derivada de la hidroquinina, de *N*-Boc cetiminas derivadas de pirazolin-5-onas con γ-hidroxienonas. La reacción transcurre en condiciones suaves, con elevados rendimientos y permite la creación de dos estereocentros en los productos finales con moderada diastereoselectividad y elevada enantioselectividad en ambos diastereoisómeros. El mecanismo de esta reacción dominó implica la formación inicial de un hemiaminal, seguida de una adición aza-Michael. Experimentos de control realizados permiten concluir que la etapa determinante de la diastereoselectividad del proceso es la *N*,*O*-acetilación.

Capítulo V: Síntesis de 4-pirazolil- y 4-isoxazolil-4-amino-pirazolonas a través de reacción de Mannich asimétrica entre *N*-Boc cetiminas derivadas de pirazolona y compuestos 1,3-dicarbonílicos catalizada por escuaramidas bifuncionales quirales.

En el capítulo V, se estudia la reacción de Mannich enantioselectiva organocatalizada de *N*-Boc cetiminas derivadas de pirazolona con compuestos 1,3-dicarbonílicos. Esta reacción constituye una vía directa de acceso a derivados de 4-amino-5-pirazolona con un estereocentro

tetrasustituido, que contienen dos motivos estructurales privilegiados, las subestructuras de β-dicetona y de pirazolinona. Los aductos se obtienen con excelentes rendimientos químicos y enantioselectividades empleando tan sólo un 2% de una escuaramida bifuncional derivada de la quinina como organocatalizador con una amplia variedad de sustratos. Además, se ha demostrado la utilidad de los productos obtenidos mediante su transformación en derivados de 4-pirazolil-pirazolona y 4-isoxazolil-pirazolona enantioenriquecidos de interés biológico.

Capítulo VI: Acoplamiento cruzado de nucleófilos a través de química oxidativa.

En el capítulo VI se recogen parte de los resultados obtenidos durante la estancia predoctoral llevaba a cabo bajo la supervisión del profesor Karl Anker Jørgensen en la Universidad de Aarhus (Dinamarca). La combinación de aldehídos y alcoholes en presencia de aminocatalizador y un oxidante permite el acoplamiento cruzado de ambos nucleófilos con rendimientos elevados y enantioselectividades excelentes. En este contexto, se ha estudiado del alcance de la reacción con diferentes alcoholes y realizado transformaciones del producto final obtenido dirigidas a la síntesis de compuestos biológicamente activos.

Abstract

Pyrazole derivatives are an interesting class of heterocycles known for the wide range of applications they enable. Among all of them, spirocyclic pyrazolones and 4-amino-5-pyrazolone derivatives belong to a wide family of compounds with well-known pharmacological properties (antitumoral, analgesic). Due to this, chemists have devoted efforts to the asymmetric synthesis of these compounds. Whereas pyrazolin-5-ones and unsaturated pyrazolones have been extensively used as starting materials in asymmetric reactions, pyrazolin-4,5-diones and their corresponding *N*-Boc ketimines derivatives have hardly been used. On the other hand, asymmetric organocatalysis constitutes one of the most useful, effective and eco-friendly strategies for the asymmetric synthesis of organic compounds, and, because of this, it is a growing field.

Consequently, the main objective in this Doctoral Thesis is the development of new methods for the asymmetric synthesis of spirocyclic pyrazolones and 4-amino-5-pirazolone derivatives from pyrazolin-4,5-diones and their *N*-Boc ketimines derivatives. Two different strategies will be used: covalent catalysis, by using chiral *N*-heterocyclic carbenes, and hydrogen bonding catalysis through the use of chiral bifunctional squaramides.

Chapter II: Chiral NHCs as organocatalysts for the synthesis of spirocyclic pyrazolone γ-butyrolactones from pyrazolin-4,5-diones.

The synthesis of spiropyrazolone γ-butyrolactones from 1*H*-pyrazol-4,5-diones and enals through *N*-heterocyclic carbene catalysis is described in Chapter II. After reaction conditions optimization, it was concluded that Bode catalyst is the best choice to perform the [3+2] annulation reaction between the starting materials affording the desired spirocyclic pyrazolones in moderate to good yield, total diastereoselectivity and high enantiomeric excess. The reaction tolerates a wide range of different substituents in both starting compounds.

To understand the catalytic mechanism, electronic structure calculations were carried out. After considering several pathways, it was concluded that the stereoselective-determining step is the lactonization step, which proceeds after the attack of the homoenolate to the electrophilic carbonyl group of the pyrazolin-4,5-dione.

Chapter III: Synthesis of spirocyclic pyrazolone-butenolides through *N*-heterocyclic carbene catalysis.

In Chapter III, the preparation of spiropyrazolones with a butenolide motif *via* NHC-catalyzed [3+2] annulation reaction between pyrazolin-4,5-diones and 3-bromoenals is studied. A modified Bode catalyst is able to promote the reaction in good yield and, generally, high enantioselectivity.

The reaction occurs in extremely mild conditions and tolerates a wide variety of different substituents on both the pyrazolin-4,5-diones and the 3-bromoenals. The reaction of the starting enal with the corresponding carbene generates a 3-bromo homoenolate, which through an addition/dehalogenization/lactonization process provides the spirocyclic butenolides.

Chapter IV: Squaramide-catalyzed asymmetric synthesis of spiropyrazolone-oxazolidines from *N*-Boc pyrazolinone ketimines and γ-hydroxyenones.

The synthesis of spirocyclic oxazolidino pyrazolones is shown in Chapter IV. A hydroquinine-derived squaramide is used to promote the reaction between *N*-Boc pyrazolinone ketimines and γ-hydroxyenones through a *N*,*O*-acetalization/aza-Michael sequence. This new protocol allows the construction of two contiguous stereocenters in the final products in good yield, moderate to good diastereoselectivity and high enantioselectivity. Control experiments were carried out to conclude that the *N*,*O*-acetalization is the diastereoselective-determining step.

Chapter V: Synthesis of 4-pyrazolyl and 4-isoxazolyl-4-amino-pyrazolones derivatives *via* squaramide-catalyzed asymmetric Mannich reaction between 1,3-dicarbonyl compounds and pyrazolinone ketimines.

In Chapter V, the enantioselective organocatalyzed Mannich reaction between *N*-Boc pyrazolinone ketimines and 1,3-dicarbonyl compounds is reported. This reaction provides a direct access to 4-amino-5-pyrazolone derivatives bearing a tetrasubstituted stereocenter with two privileged scaffolds: the β-diketone and pyrazolinone substructures. Mannich adducts are obtained in excellent yield and enantioselectivity with a low loading of a quinine-derived squaramide as catalyst on a wide range of substrates. Moreover, the utility of these products is demonstrated by their transformation into enantioenriched 4-pyrazolyl and 4-isoxazolyl-pyrazolone derivatives with biological interest.

Chapter VI: Cross-nucleophile couplings *via* oxidative chemistry.

In Chapter VI, the results obtained during the three-month stay in Aarhus University under the supervision of Prof. Karl Anker Jørgensen are shown. Combination of α-methyl substituted

aldehydes and propargylic alcohols through oxidative aminocatalysis allows the cross-coupling between the two nucleophiles. In this context, the scope of the reaction with different alcohols is studied. Products undergo further metal-catalyzed cyclization to methylene isochromanes with a quaternary stereocenter after deprotection and reduction.

Chapter I: Introduction.

1.1 Spirocyclic pyrazolones

Pyrazole is a five-membered heterocycle with two adjacent nitrogen atoms. Its possible structural diversity confers it a broad range of applications.[1] Among all the pyrazole derivatives, pyrazolin-5-one scaffolds, specifically, chiral spiropyrazolones with a spiro-ring fused at 4-position of the pyrazolone core, are widely found in medically relevant compounds exhibiting biological activities such as antitumor, antimicrobial, analgesic or anti-inflammatory activities, as well as an inhibitory effect for acetyl-CoA carboxylase and type 4-phosphodiesterase,[2] Figure 1.1. The synthesis of spirocyclic pyrazolones is in the spotlight of drug discovery due to the fact that spirocycles are more flexible than flat aromatic rings, which confers them the possibility to adapt to different targets and as consequence the chances of finding bioactive hits increase.

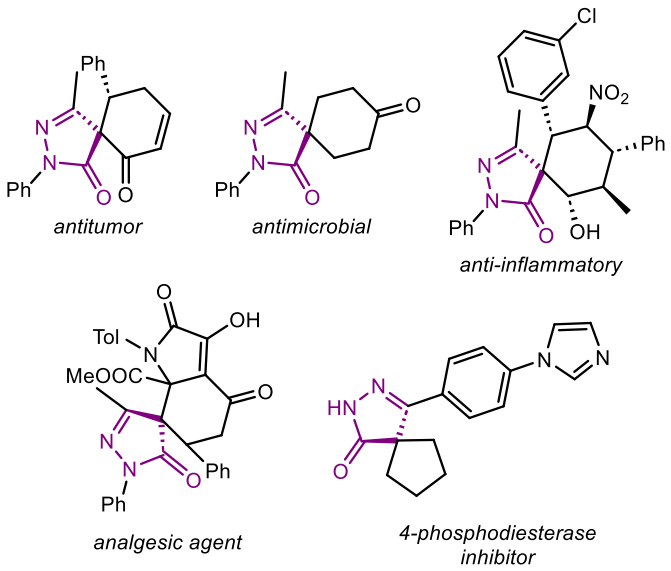

Figure 1.1: Selected bioactive compounds containing spiropyrazolone motif.

Accordingly, different strategies have been developed for the preparation of these interesting compounds. One of them uses metal-catalyzed asymmetric reactions for the synthesis of

[1] (a) P. K. Mykhailiuk *Chem. Rev.* **2021**, *121*, 1670–1715, (b) T. -F. Wang, S. R. Kosuru, S. -C. Yu, Y. -C. Chang, H. -Y. Lai, Y. -L. Chang, K. -H. Wu, S. Dingad, H. -Y. Chen *RSC Adv.* **2020**, *10*, 40690–40696, (c) M. J. Naim, O. Alam, F. Nawaz, M. J. Alam, P. Alam *J. Pharm. Bioallied Sci.* **2016**, *8*, 2–17, (d) S. Fustero, M. Sánchez-Roselló, P. Barrio, A. Simón-Fuentes *Chem. Rev.* **2011**, *111*, 6984–7034.

[2] *Some examples:* (a) O. Barreiro-Costa, G. Morales-Noboa, P. Rojas-Silva, E. Lara-Barba, J. Santamaría-Aguirre, N. Bailón-Moscoso, J. C. Romero-Benavides, A. Herrera, C. Cueva, L. Ron-Garrido, A. Poveda, J. Heredia-Moya *Molecules* **2021**, *26*, 4960, (b) J. Zaiter, A. Hibot, A. Hafid, M. Khouili, C. M. B. Neves, M. M. Q. Simoes, M. G. P. M. S. Neves, M. A. F. Faustino, T. Dagci, L. Saso, G. Armagan *Eur. J. Med. Chem.* **2021**, *213*, 113140, (c) Y. Zhang, C. Wang, W. Huang, P. Haruehanroengra, C. Peng, J. Sheng, B. Han, G. He *Org. Chem. Front.* **2018**, *5*, 2229–2233, (d) S. Wu, Y. Li, G. Xu, S. Chen, Y. Zhang, N. Liu, G. Dong, C. Miao, H. Su, W. Zhang, C. Sheng *Eur. J. Med. Chem.* **2016**, *115*, 141–147, (e) Y. Zhang, S. Wu, S. Wang, K. Fang, G. Dong, N. Liu, Z. Miao, J. Yao, J. Li, W. Zhang, C. Sheng, W. Wang *Eur. J. Org. Chem.* **2015**, *9*, 2030–2037.

spirocyclic pyrazolones.[3] However, asymmetric organocatalysis stands out as one of the most effective and environment-friendly strategies, and because of this, it has received a lot of attention from chemists and industry worldwide.[4]

Pyrazolin-5-one derivatives can undergo a wide range of transformations because of the different reactivity that can be achieved depending on their structure, Figure 1.2. For example, pyrazolin-5-one, **a**, acts as nucleophile at 4-position, due to the possibility of the existence of an enolate, and it is usually regarded as C1 synthon for transformations into spiropyrazolones. Moreover, α-arylidene pyrazolones, **b**, dispose of both nucleophilic and electrophilic positions, and have been recognized as excellent C2 synthons. Some alkylidene derivatives, **c**, can be used as nucleophiles in asymmetric vinylogous Michael additions, thus acting as dinucleophilic C3 synthons in asymmetric catalysis. 4-Isothiocyanato pyrazolones,[5] **d**, with the nucleophilic C-α of carbonyl and the electrophilic NCS group, can be used as another powerful C2 synthon for the construction of spirocyclic compounds. Finally, when pyrazolin-5-one is converted into pyrazole-4,5-dione or its corresponding *N*-protected ketimine, **e**, C-4 position turns to be electrophilic and can be used as C1 synthon. This variety of raw materials allows the possibility of the synthesis of different spirocyclic pyrazolones fused with different carbo- or heterocycles.[6]

[3] *Selected recent examples:* (a) B. Mao, J. Xu, W. Shi, W. Wang, Y. Wu, Y. Xiao, H. Guo *Org. Biomol. Chem.* **2022**, *20*, 4086–4090, (b) J. -M. Guo, X. -Z. Fan, H. -H. Wu, Z. Tang, X. -F. Bi, H. Zhang, L. -Y. Cai, H. -W. Zhao, Q. -D. Zhong *J. Org. Chem.* **2021**, *86*, 1712−1720, (c). K. Shukla, S. Shah, N. K. Rana, V. K. Sin *Tetrahedron Letters* **2019**, *60*, 92–97.

[4] Prof. B. List and Prof. D. W. C. MacMillan were awarded the Nobel Prize in Chemistry 2021 for their contributions to asymmetric organocatalysis.

[5] *Review:* Y. Yang, X. Wang, X. Ye, B. Wang, X. Bao, H. Wang *Org. Biomol. Chem*. **2021**, *19*, 4610–4621.

[6] *For reviews see:* (a) X. Bao, X. Wang, J. -M. Tian, X. Ye, B. Wang, H. Wang *Org. Biomol. Chem.* **2022**, *20*, 2370−2386, (b) L. Carceller-Ferrer, G. Blay, J. R. Pedro, C. Vila *Synthesis* **2021**, *53*, 215−237, (c). X. Xie, L. Xiang, C. Peng, B. Han *Chem. Rec.* **2019**, *19*, 2209–2235.

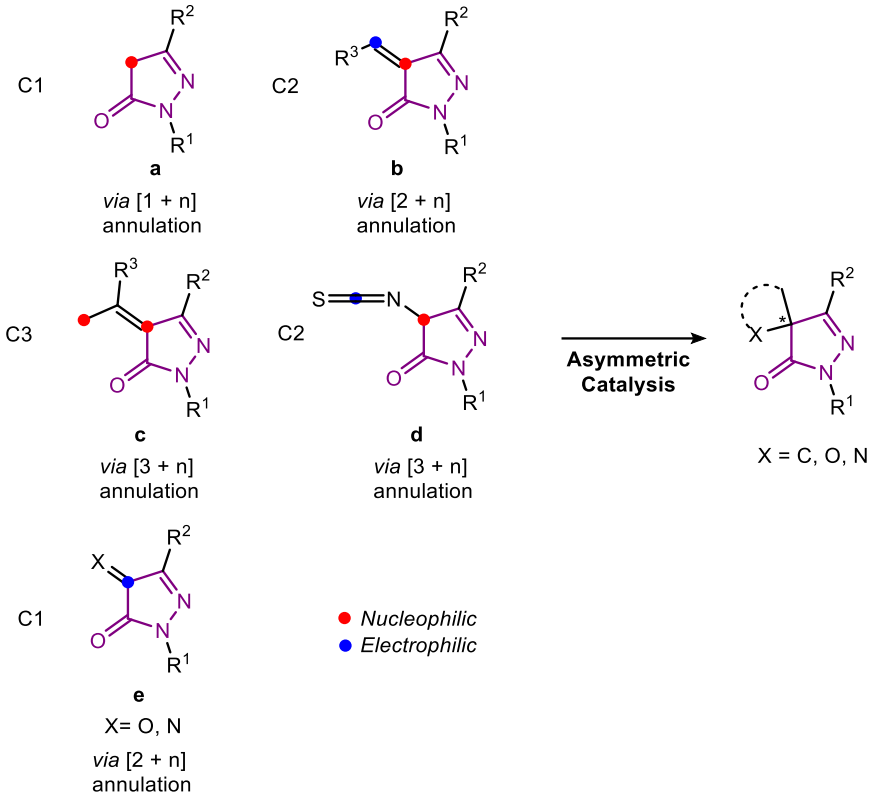

Figure 1.2: Different structures for pyrazolin-5-one derivatives as precursors for spiropyrazolones.

Several methods have been reported for the enantioselective synthesis of spiropyrazolones fused with three-, five-, and six-membered carbocycle *via* aminocatalysis,[7] bifunctional thiourea/squaramide catalysis,[8] or *N*-heterocyclic carbene (NHC) catalysis.[9] While the formation of enantioenriched 4-spiropyrazolones featuring an all carbon spirocenter has been widely studied, synthesis of spiropyrazolones bearing a heteroatom attached to the spirocenter is still a growing field.

[7] *Some examples:* (a) B. Wu, J. Chen, M. -Q. Li, J. -X. Zhang, X. -P. Xu, S. -J. Ji, X. -W. Wang *Eur. J. Org. Chem.* **2012**, 1318–1327, (b) A. -N. R. Alba, A. Zea, G. Valero, T. Calbet, M. Font-Bardía, A. Mazzanti, A. Moyano, R. Rios *Eur. J. Org. Chem.* **2011**, 1318–1325, (c) A. Zea, A. -N. R. Alba, A. Mazzanti, A. Moyano, R. Rios *Org. Biomol. Chem.* **2011**, *9*, 6519–6523.

[8] *Some examples:* (a) S. Meninno, A. Mazzanti, A. Lattanzi *Adv. Synth. Catal.* **2019**, *361*, 79–84, (b) Y. Lin, B. -L. Zhao, D. -M. Du *J. Org. Chem.* **2019**, *84*, 10209−10220, (c) J. -Y. Liu, J. Zhao, J. -L. Zhang, P. -F. Xu *Org. Lett.* **2017**, *19*, 1846–1849, (d) J. -H. Li, T. -F. Feng, D. -M. Du *J. Org. Chem.* **2015**, *80*, 11369–11377.

[9] *Some examples:* (a) C. Zhao, K. Shi, G. He, Q. Gu, Z. Ru, L. Yang, G. Zhong *Org. Lett*. **2019**, *21*, 7943−7947, (b) S. R. Yetra, S. Mondal, S. Mukherjee, R. G. Gonnade, A. T. Biju *Angew. Chem. Int. Ed*. **2016**, *55*, 268−272, (c) L. Wang, S. Li, P. Chauhan, D. Hack, A. R. Philipps, R. Puttreddy, K. Rissanen, G. Raabe, D. Enders *Chem. Eur. J.* **2016**, *22*, 5123−5127.

1.1.1 Synthesis of 4-Oxygen attached chiral spiropyrazolones

Different synthesis of 4-oxygen attached chiral spiropyrazolones using pyrazolones as nucleophiles have been reported. Xia, Xu and coworkers showed how spirodihydrobenzofuran pyrazolones can be prepared through a Michael/iodization/S_N2 nucleophilic substitution sequential catalytic reaction of pyrazolones and 2-hydroxy-β-nitrostyrene using a bifunctional squaramide as organocatalyst,[10] Scheme 1.1a. In a similar way, Wei and Xu described a one-pot asymmetric synthesis of spiropyrazolone-linked benzofurans from the same substrates and quinone methides through a 1,6-addition/chlorination/nucleophilic substitution sequence,[11] Scheme 1.1b.

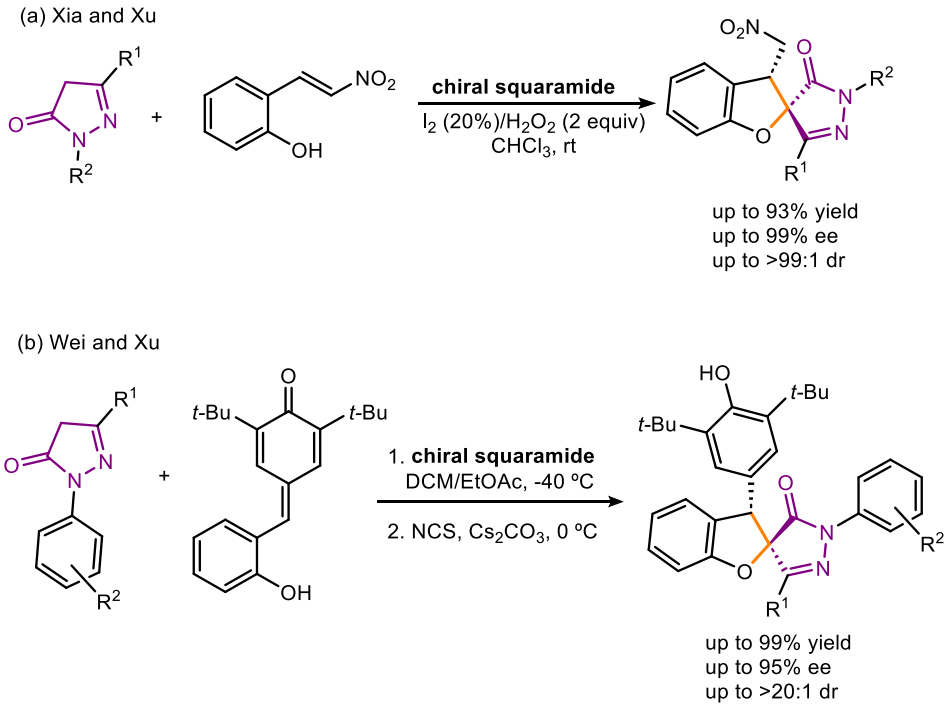

Scheme 1.1: O-attached spiropyrazolones synthesized from pyrazolin-5-ones.

Another example of the use of quinone methides is reported by Jiang group who developed a bifunctional squaramide-catalyzed reaction of pyrazolin-5-ones with *ortho*-quinone methides, *in situ* generated from 2-(1-tosylalkyl)phenols, followed by a cascade chlorination/cyclization reaction,[12] Scheme 1.2a. Later, Wang and Xu described a straightforward access to spiro-

[10] C. -K. Tang, Z. -Y. Zhou, A. -B. Xia, L. Bai, J. Liu, D. -Q. Xu, Z. -Y. Xu *Org. Lett.* **2018**, *20*, 5840–5844.
[11] H. Lu, H. -X. Zhang, C. -Y. Tan, J. -Y. Liu, H. Wei, P. -F. Xu *J. Org. Chem.* **2019**, *84*, 10292–10305.
[12] J. Zhou, W. J. Huang, G. F. Jiang *Org. Lett*. **2018**, *20*, 1158–1161.

benzofuran pyrazolones *via* organocatalytic asymmetric [4+1] annulation of *in situ* generated *o*-quinomethanes with 4-halo pyrazolones,[13] Scheme 1.2b.

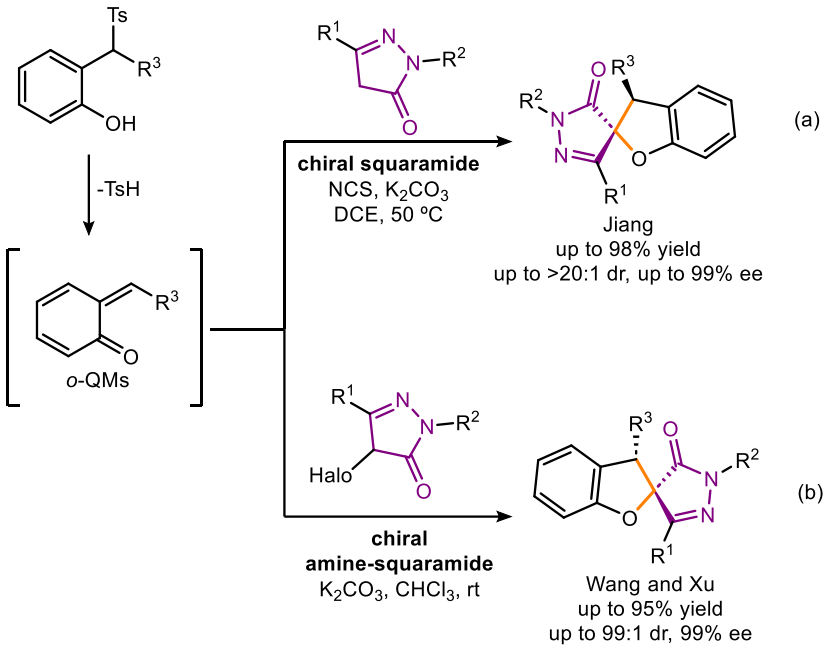

Scheme 1.2: *In situ* generated *ortho*-quinomethanes as starting reactants for the synthesis of spiropyrazolones.

Unsaturated pyrazolones have also proved to be versatile synthons to construct spiropyrazolone motifs. Lattanzi group found that the easily available amine-thiourea/*tert*-butyl hydroperoxide (TBHP) system can catalyze the asymmetric epoxidation of unsaturated pyrazolones, giving access to corresponding *trans*- or *cis*-spiro-epoxypyrazolones with good yields and moderate to high diastereoselectivities,[14] Scheme 1.3a. In 2017, Xu group reported a highly efficient enantioselective synthesis of spiro[dihydrofurocoumarin/pyrazolone] derivatives from readily available 4-hydroxycoumarins and unsaturated pyrazolones *via* an asymmetric one-pot Michael addition/I_2-mediated cyclization sequence.[15] Almost simultaneously, the same group applied this strategy to unsaturated pyrazolones and 1,3-diketones, providing access to chiral spiro-dihydrofuran pyrazolones,[16] Scheme 1.3b.

[13] M. -M. Chu, S. -S. Qi, Y. -F. Wang, B. Wang, Z. -H. Jiang, D. -Q. Xu, Z. -Y. Xu *Org. Chem. Front.* **2019**, *6*, 1977–1982.
[14] S. Meninno, A. Roselli, A. Capobianco, J. Overgaard, A. Lattanzi *Org. Lett.* **2017**, *19*, 5030–5033.
[15] A. B. Xia, X. L. Zhang, C. K. Tang, K. X. Feng, X. H. Du, D. Q. Xu *Org. Biomol. Chem*. **2017**, *15*, 5709–5718.
[16] X. L. Zhang, C. K. Tang, A. B. Xia, K. X. Feng, X. H. Du, D. Q. Xu *Eur. J. Org. Chem.* **2017**, *2017*, 3152–3160.

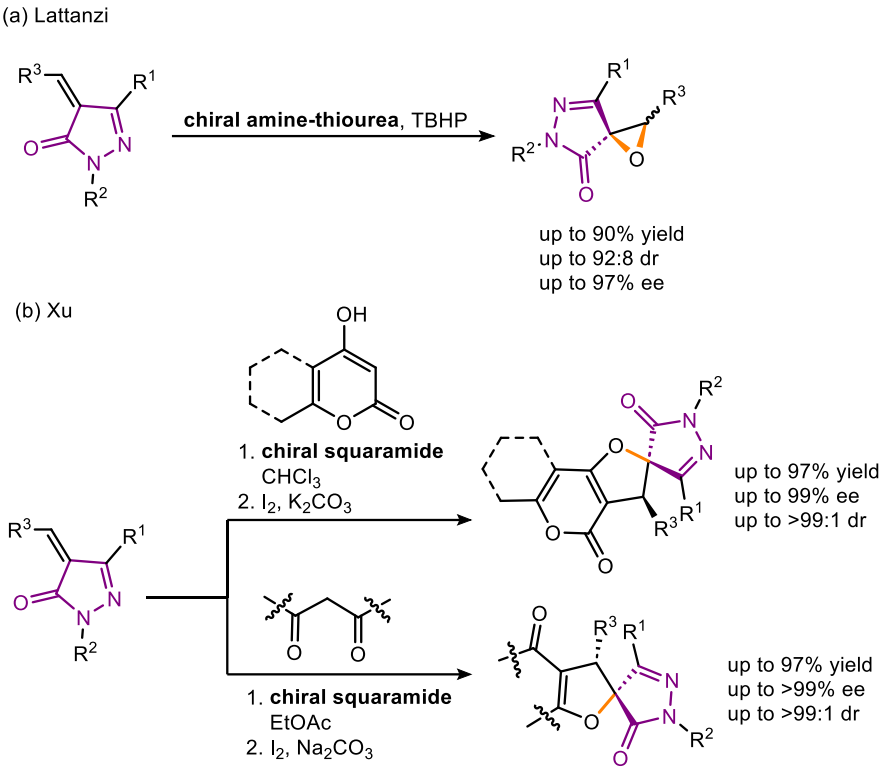

Scheme 1.3: Synthesis of O-attached spiropyrazolones from unsaturated pyrazolones.

Finally, the [3+2] annulation and cycloaddition of pyrazole-4,5-diones constitute another route for the preparation of oxaspirocyclic pyrazolones. Bhat and co-workers reported a tertiary amine-catalyzed highly diastereo- and enantioselective [3+2] annulation involving Morita–Baylis–Hillman (MBH) carbonates derived from isatin and pyrazolin-4,5-diones,[17] Scheme 1.4a. At the same time, Lu group developed an asymmetric oxa-1,3-dipolar cycloaddition of pyrazole-4,5-diones with trifluoroethylamine-derived azomethines,[18] Scheme 1.4b. This protocol provides a facile access to chiral CF_3-containing oxazolidines with excellent diastereo- and enantioselectivities. Recently, Zhao and Huang[19] showed how δ-lactone-fused spiropyrazolones can be prepared through a Lewis base-catalyzed asymmetric [4+2] annulation of cyclobutenones and pyrazole-4,5-diones with generally high yields and good enantioselectivities, Scheme 1.4c.

[17] P. K. Warghude, A. S. Sabale, R. G. Bhat *Org. Biomol. Chem*. **2020**, *18*, 1794–1799.
[18] W. -R. Zhu, Q. Su, N. Lin, Q. Chen, Z. -W. Zhang, J. Weng, G. Lu *Org. Chem. Front*. **2020**, *7*, 3452–3458.
[19] R. Qin, T. -T. Yu, S. -J. Liu, Y. -C. Wang, M. -Lan Luo, B. -H. Chen, Q. Zhao, W. Huang *J. Org. Chem.* **2022**, *87*, 5358−5370.

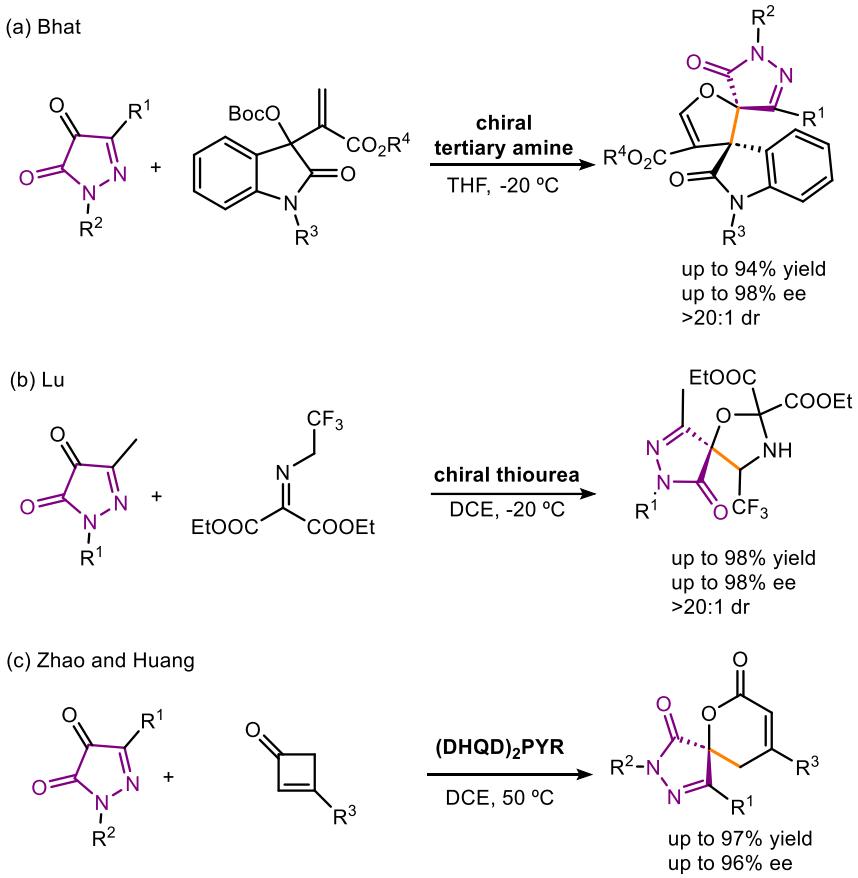

Scheme 1.4: Enantioselective [3+2] annulation of pyrazole-4,5-diones.

1.1.2 Synthesis of 4-Nitrogen attached chiral spiropyrazolones.

Otherwise, some examples of 4-nitrogen attached chiral spiropyrazolones derivatives have been displayed. In 2018, Wang and Zou developed a catalytic asymmetric [3+2] cyclization of 4-isothiocyanato pyrazolones and isatin-derived ketimines to construct a dispiro[pyrazolone/ethylenethiourea/oxindole] scaffold containing three pharmacophores with excellent diastereo- and enantioselectivity, Scheme 1.5a.[20] Wang also combined 4-isothiocyanato pyrazolones with alkynyl,[21] allenyl[22] or α,β-unsaturated ketones[23] giving rise to spiro[pyrrolidine–pyrazolones] and spiro[pyrrole–pyrazolone] cores *via* asymmetric [3+2] annulation reaction, Scheme 1.5b and c.

[20] X. Bao, S. Wei, X. Qian, J. Qu, B. Wang, L. Zou, G. Ge *Org. Lett.* **2018**, *20*, 3394–3398.
[21] W. Wang, S. Wei, X. Bao, S. Nawaz, J. Qu, B. Wang *Org. Biomol. Chem*. **2021**, *19*, 1145−1154.
[22] W. Wang, X. Bao, S. Wei, S. Nawaz, J. Qu, B. Wang *Chem. Commun*. **2021**, *57*, 363−366.
[23] W. Gong, X. Du, W. Wang, W. Zhang, B. Wang *Tetrahedron Letters* **2021**, *78*, 153259.

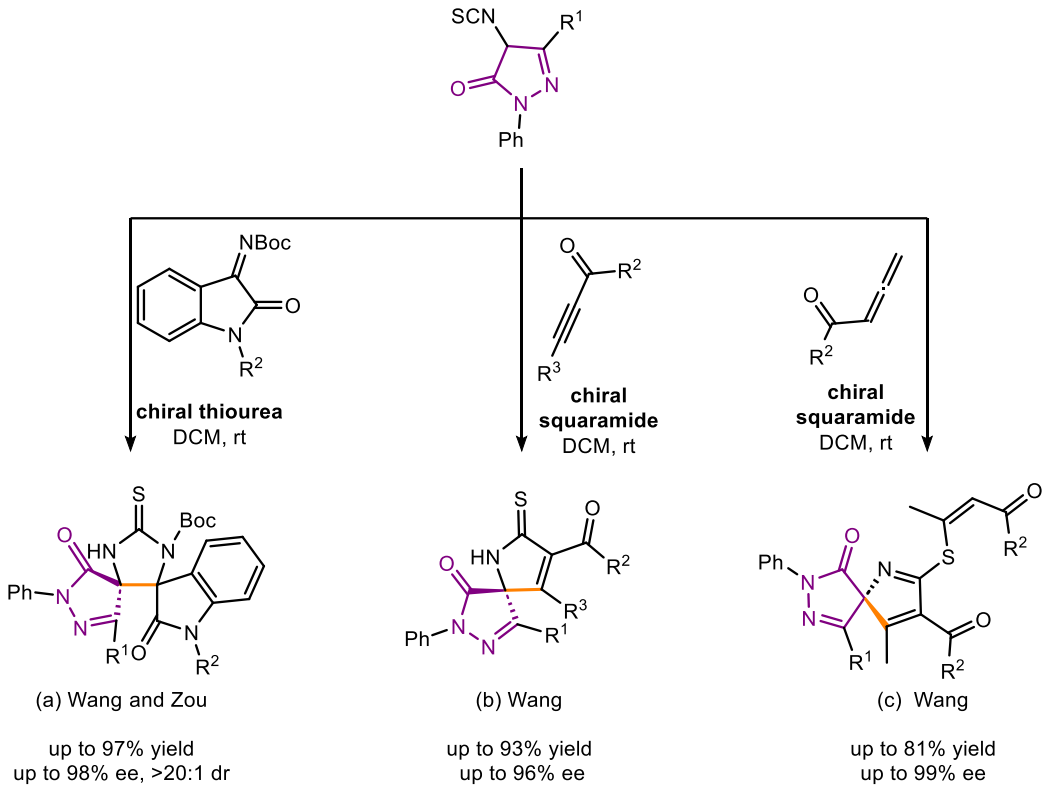

Scheme 1.5: Spiropyrazolones synthesized from 4-isothiocyanato pyrazolones.

In contrast to what has been shown so far, the preparation of a rigid but beneficial four-membered spirocyclic pyrazolone skeleton has been scarcely studied. Huang[24] reported the synthesis of the first spiropyrazolone-β-lactam through a visible-light-mediated sequential Wolff rearrangement/Staudinger cycloaddition by using *in situ* generated ketenes and pyrazolone-derived ketimines, Scheme 1.6.

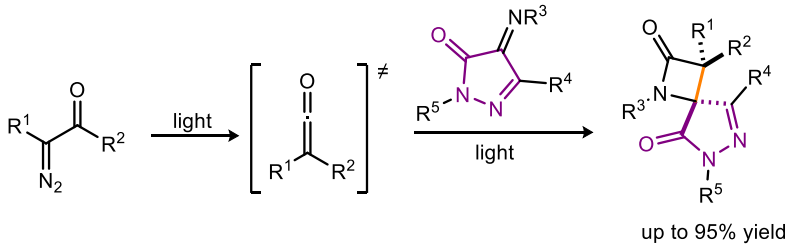

Scheme 1.6: Synthesis of spiro-pyrazolone-β-lactams reported by Huang.

[24] J. Tang, Z. -H. Yan, G. Zhan, Q. -Q. Yang, Y. -Y. Cheng, X. Li, W. Huang *Org. Chem. Front.* **2022**, *9*, 4341–4346.

1.2 4-Substituted-4-Aminopyrazolones.

Pyrazoles and pyrazolones constitute a privileged class of five-membered aza-heterocycles that, although not common components of biologically active natural products, exhibit significant pharmacological activities.[25] In addition, scaffolds with chiral α-tertiary amines are structural elements of a wide variety of natural products, bioactive molecules, pharmaceuticals and agrochemicals.[26] Considering the prominence of pyrazolones and chiral α-tertiary amines and aiming to seek new biologically active lead compounds, hybrid molecules incorporated with these two biologically relevant motifs provide new opportunities in diversity-oriented synthesis and modern drug discovery. However, only few examples are documented despite the potential these products could have,[20,27] Figure 1.3.

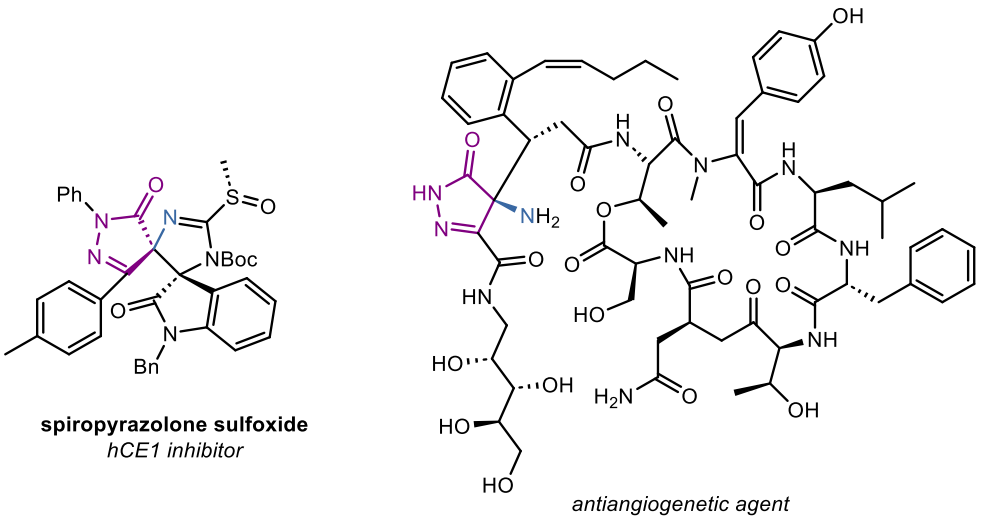

Figure 1.3: Pyrazolin-5-one derivatives with a nitrogen atom attached at C-4.

As a result, in recent years, great research efforts have been focused on the development of new strategies for the synthesis of various chiral amino-pyrazolone derivatives. Most of these methods employ the known reactivity of pyrazolin-5-one derivatives, especially the C-4 nucleophilicity. In this context, the groups of Feng[28] and Rios[29] reported the electrophilic α-amination reaction of 4-substituted pyrazolones with diazodicarboxylates using an *N,N'*-dioxide gadolinium(III) complex or quinine as catalysts, Scheme 1.7.

[25] Z. Zhao, X. Dai, C. Li, X. Wang, J. Tian, Y. Feng, J. Xie, C. Ma, Z. Nie, P. Fan, M. Qian, X. He, S. Wu, Y. Zhang, X. Zheng *Eur. J. Med. Chem.* **2020**, *186*, 11189.
[26] (a) A. Hager, N. Vrielink, D. Hager, J. Lefranc, D. Trauner *Nat. Prod. Rep*. **2016**, *33*, 491–522, (b) P. Chauhan, S. Mahajan, D. Enders *Chem. Commun.* **2015**, *51*, 12890–12907.
[27] M. Bae, J. Oh, E. S. Bae, J. Oh, J. Hur, Y. -G. Suh, S. K. Lee, J. Shin, D. -C. Oh *Org. Lett.* **2018**, *20*, 1999–2002.
[28] Z. Yang, Z. Wang, S. Bai, X. Liu, L. Lin, X. Feng *Org. Lett.* **2011**, *13*, 596–599.
[29] (a) B. Formánek, V. Šeferna, M. Meazza, R. Rios, M. Patil, J. Veselý *Eur. J. Org. Chem.* **2021**, *2021*, 2362–2366, (b) M. Šimek, M. Remeš, J. Veselý, R. Rios *Asian J. Org. Chem.* **2013**, *2*, 64–68.

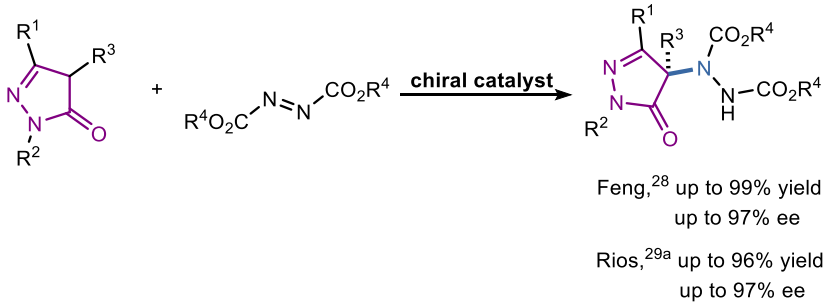

Scheme 1.7: α-Amination reaction of 4-substituted pyrazolones with diazodicarboxylates.

In 2017, Enders reported the synthesis of a new series of pyrazolin-5-one derivatives, *N*-Boc ketimines, where the C-4 position can act as an acceptor,[30] Figure 1.4. These ketimines can be used in nucleophilic 1,2-addition reactions to afford 4-aminopyrazolones bearing a tetra-substituted stereocenter.

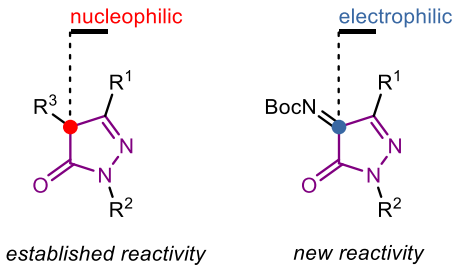

Figure 1.4: New reactivity of pyrazolone-derived ketimines reported by Enders.

In recent years, effort has been devoted to expanding the utility of these ketimines as synthons. For example, Enders group first described the squaramide-catalyzed enantioselective Strecker reaction of ketimines derived from pyrazolin-5-one with trimethylsilyl cyanide to produce pyrazolone α-aminonitrile derivatives,[31] Scheme 1.8a. Subsequently, 2-naphtols[32] and hydroxyindoles[33] were used as nucleophiles for enantioselective aza-Friedel-Crafts reactions with pyrazolinone ketimines, Scheme 1.8b and c, respectively. Some metal-catalyzed versions of

[30] P. Chauhan, S. Mahajan, U. Kaya, A. Peuronen, K. Rissanen, D. Enders *J. Org. Chem.* **2017**, *82*, 7050−7058.
[31] S. Mahajan, P. Chauhan, U. Kaya, K. Deckers, K. Rissanen, D. Enders *Chem. Commun.* **2017**, *53*, 6633−6636.
[32] U. Kaya, P. Chauhan, S. Mahajan, K. Deckers, A. Valkonen, K. Rissanen, D. Enders *Angew. Chem. Int. Ed.* **2017**, *56*, 15358–15362.
[33] Z. -T. Yang, W. -L. Yang, L. Chen, H. Sun, W. -P. Deng *Adv. Synth. Catal.* **2018**, *360*, 2049–2054.

pyrazolin-5-one-derived ketimines with various nucleophiles, such as silyl enol ethers,[34] benzyl but-3-ynoates[35] and arylboronic acids,[36] were also reported.

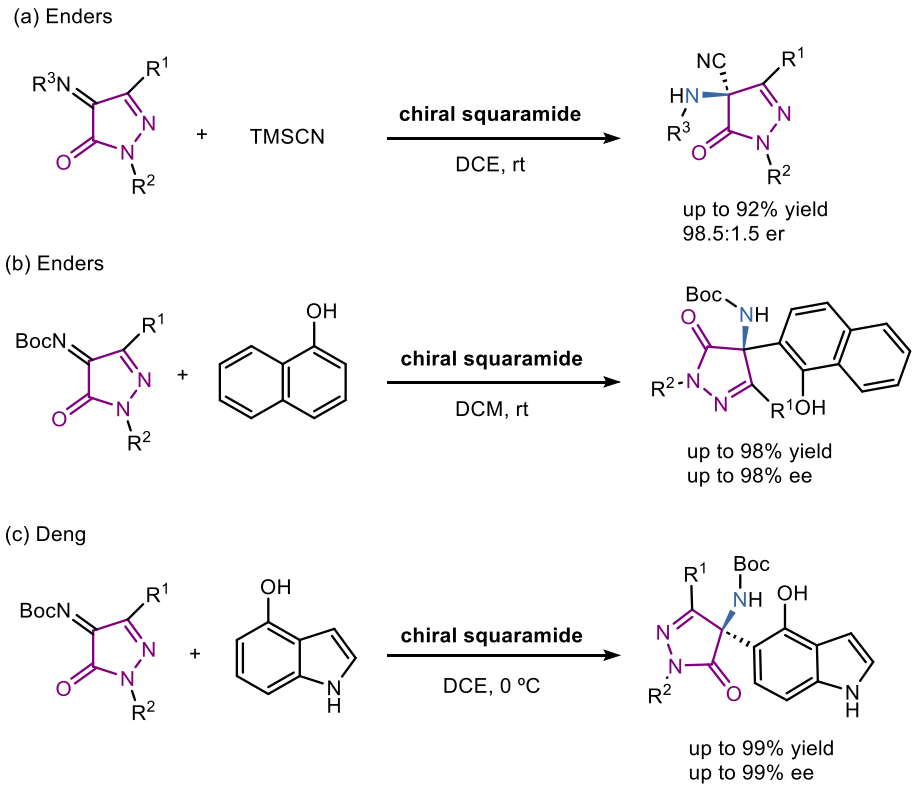

Scheme 1.8: Some 4-aminopyrazolone derivatives synthesized from *N*-protected ketimines.

However, despite the rapid growth in the number of new 4-aminopyrazolone derivatives, the study of their applications has been less investigated, especially their biological activities.

1.3 *N*-Heterocyclic Carbenes

A particular case within the formation of new C-C bonds are those reactions in which the classical reactivity is reversed (*umpolung*[37]). It was Sheehan and Hunneman[38] who described the first Benzoin reaction catalyzed by an *N*-Heterocyclic Carbene (NHC). Since then, asymmetric

[34] T. Kang, W. Cao, L. Hou, Q. Tang, S. Zou, X. Liu, X. Feng *Angew. Chem.* **2019**, *131*, 2486–2490.
[35] G. -Y. Ran, C. Chen, X. -X. Yang, Z. Zhao, W. Du, Y. -C. Chen *Org. Lett*. **2020**, *22*, 4732–4736.
[36] A. -Q. Miao, M. Zhou, J. -L, Chen, S. -C. Wang, W. -J. Hao, S. -J. Tu, B. Jiang *Adv. Synth. Catal*. **2021**, *363*, 5162–5166.
[37] Seebach's terminology to describe *umpolung* reactivity, D. Seebach *Angew. Chem. Int. Ed. Engl.* **1979**, *18*, 239–258.
[38] J. Sheehan, D. H. Hunneman *J. Am. Chem. Soc.* **1966**, *88*, 3666−3667.

organocatalysis enabled by *N*-heterocyclic carbenes (NHCs) has continued to evolve, especially during the last two decades.[39]

The role of NHCs depends on the reversible formation of the *Breslow intermediate*.[40] This intermediate, an enaminol, comes after the deprotonation of the pre-catalyst acid precursor and the subsequent reaction with an aldehyde. The polarity of the aldehyde is changed from an electrophilic molecule to a nucleophilic one and can react with other aldehydes (Benzoin condensation, a^1-d^1), or α,β-unsaturated aldehydes (Stetter reaction, a^3-d^1), Scheme 1.9a. However, the most interesting part of using NHCs as asymmetric organocatalysts comes by exploding the use of enals, affording a conjugated Breslow intermediate which can react as a nucleophile in its position γ (β if is referred to the enal), which is also called *homoenolate chemistry,* Scheme 1.9b.

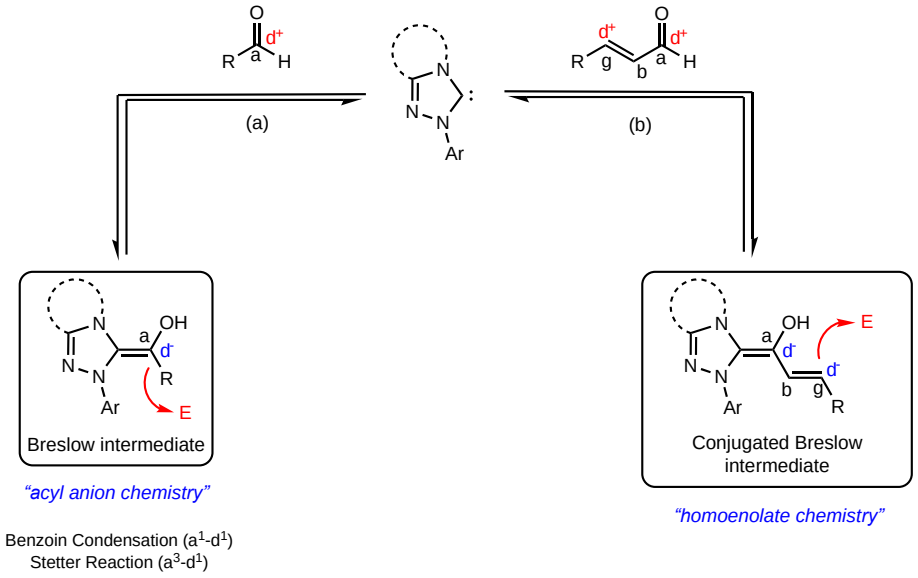

Scheme 1.9: Homoenolate formation.

The proton migration from α-position to γ-position in the *homoenolate* provides the formation of an *azolium enolate,*[41] a nucleophilic catalytic specie in β position (d^2), Scheme 1.10a. These intermediates can be achieved when suitably substituted aldehydes,[42] acid derivatives[43] or

[39] *Reviews:* (a) X. -Y. Chen, Z. -H. Gao, S. Ye *Acc. Chem. Res.* **2020**, *53*, 690–702, (b) S. Mondal, S. R. Yetra, S. Mukherjee, A. T. Biju *Acc. Chem. Res.* **2019**, *52*, 425–436, (c) X. -Y. Chen, Q. Liu, P. Chauhan, D. Enders *Angew. Chem. Int. Ed.* **2018**, *57*, 3862–3873, (d) X. -Y. Chen, S. Li, F. Vetica, M. Kumar, D. Enders *iScience* **2018**, *2*, 1–26, (e) C. Zhang, J. F. Hooper, D. W. Lupton *ACS Catal.* **2017**, *7*, 2583–2596, (f) M. N. Hopkinson, C. Richter, M. Schedler, F. Glorius *Nature*, **2014**, *510*, 485–496, (g) D. Enders, O. Niemeier, A. Henseler *Chem. Rev.* **2007**, *107*, 5606–5655.

[40] R. Breslow *J. Am. Chem. Soc.* **1958**, *80*, 3719–3726.

[41] S. Mondal, A. Ghosh, A. T. Biju *Chem. Rec.* **2022**, *22*, e202200054.

[42] *Some examples:* (a) A. B. Viveki, M. D. Pol, P. Halder, S. R. Sonavane, S. B. Mhaske *J. Org. Chem.* **2021**, *86*, 9466−9477, (b) M. He, G. J. Uc, J. W. Bode *J. Am. Chem. Soc.* **2006**, *128*, 15088–15089.

[43] *Some examples:* (a) N. Attaba, A. D. Smith *Tetrahedron* **2020**, *76*, 130835−130843, (b) A. Lee, A. Younai, C. K. Price, J. Izquierdo, R. K. Mishra, K. A. Scheidt *J. Am. Chem. Soc.* **2014**, *136*, 10589−10592.

ketenes[44] are used. In contrast, if the *homoenolate* is oxidized, an *α,β-unsaturated acyl azolium* is generated, Scheme 1.10b, which will act as a 1,3-bielectrophilic synthon (a^1 or a^3 – no *umpolung*). Some ways for obtaining acyl azolium intermediates come by using α-bromoenals,[45] ynals[46] or the combination of enals with an oxidant as reagents.[47] Moreover, if this oxidized homoenolate eliminates a proton, an *azolium dienolate*[48] is formed (d^2 or d^4), Scheme 1.10c.

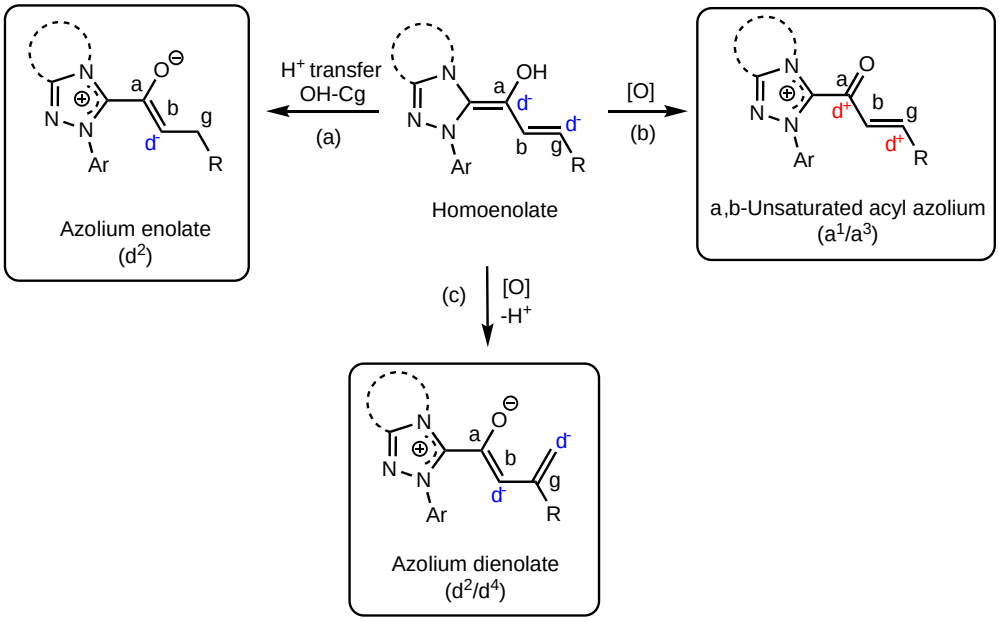

Scheme 1.10: Formation of different catalytic species from homoenolate: *azolium enolate* (a), *α,β-unsaturated acyl azolium* (b) and *azolium dienolate* (c).

In general, these NHC-catalyzed transformations are operationally simple reactions that proceed at room temperature without the generation of reaction by-products. If the NHC precursor/base combination is properly selected, it is possible to prepare structurally complex molecules from easy starting materials. In addition, high diastereo- and enantioselectivity levels are possible using chiral NHCs.

[44] *Some examples:* (a) X. N. Wang, H. Lv, X. -L. Huang, S. Ye *Org. Biomol. Chem.* **2009**, *7*, 346–350, (b) Y. -R. Zhang, H. Lv, D. Zhou, S. Ye *Chem. Eur. J.* **2008**, *14*, 8473–8476, (c) Y. -R. Zhang, L. He, X. Wu, P. -L. Shao, S. Ye *Org. Lett.* **2008**, *10*, 277–280.

[45] *Some examples:* (a) J. Wang, Y. Li, J. Sun, H. Wang, Z. Jin, Y. R. Chi *ACS Catal.* **2018**, *8*, 9859–9864, (b) C. Fang, T. Lu, J. Zhu, K. Sun, D. Du *Org. Lett.* **2017**, *19*, 3470–3473, (c) S. Mondal, S. R. Yetra, A. Patra, S. S. Kunte, R. G. Gonnade, A. T. Biju *Chem. Commun.* **2014**, *50*, 14539–14542.

[46] *Some examples:* (a) K. Dzieszkowski, M. Słotwiński, K. Rafińska, T. M. Muzioła, Z. Rafiński *Chem. Commun.* **2021**, *57*, 9999–10002, (b) J. Mahatthananchai, J. Kaeobamrung, J. W. Bode *ACS Catal.* **2012**, *2*, 494–503.

[47] *Some examples:* (a) X. Wu, B. Liu, Y. Zhang, M. Jeret, H. Wang, P. Zheng, S. Yang, B. A. Song, Y. R. Chi *Angew. Chem. Int. Ed*. **2016**, *55*, 12280–12284, (b) A. Biswas, S. De Sarkar, L. Tebben, A. Studer *Chem. Commun.* **2012**, *48*, 5190–5192.

[48] *Some examples:* (a) L. Liu, D. Guo, J. Wang *Org. Lett.* **2020**, *22*, 7025−7029, (b) J. Mo, X. Chen, Y. R. Chi *J. Am. Chem. Soc.* **2012**, *134*, 8810–8813.

1.4 Thioureas and squaramides

Hydrogen bond catalysis is known as a useful tool for the formation of new C-C bonds. Among all the possible structures which could allow this type of catalysis, thioureas[49] and squaramides[50] can be found. Squaramides present five significant differences with thioureas: (i) duality in binding, (ii) length between hydrogen atoms, (iii) rigidity, (iv) angle bond between hydrogen atoms and (v) pKa value, Figure 1.5.

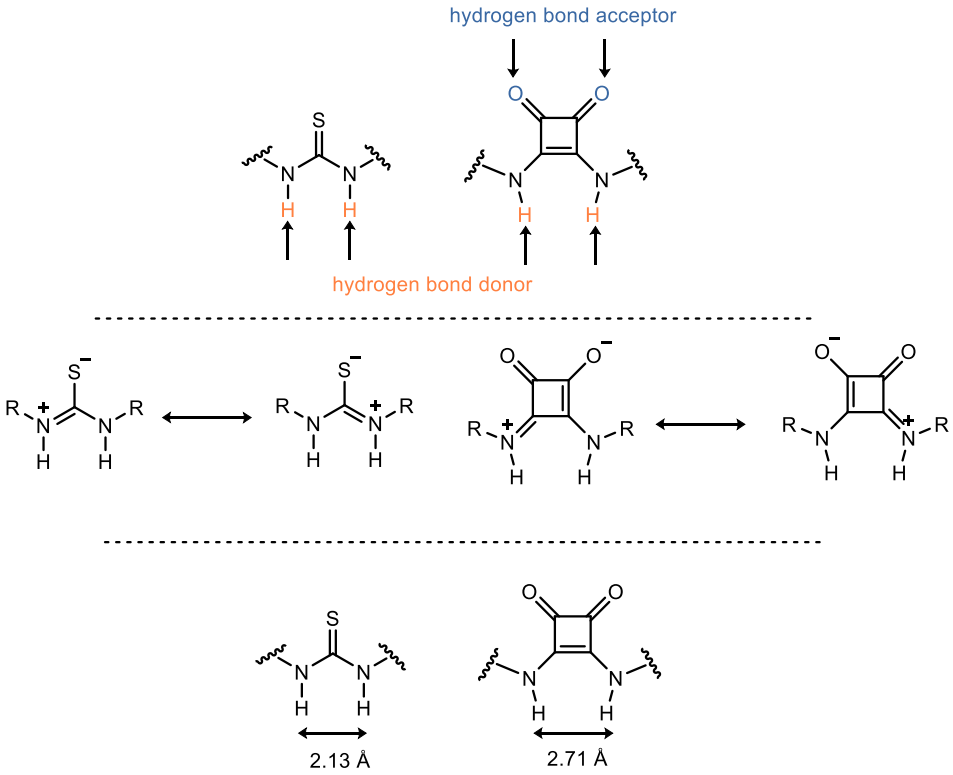

Figure 1.5: Some features of thioureas and squaramides.

The first difference is the possibility of squaramides to develop a double binding activation: donor groups (N-H) and acceptor groups (C=O). In both cases, thioureas and squaramides, delocalization is present in the structure, which restricts the C-N rotation, but in the squaramide, further delocalization is extended over the cyclobutadienone unit and more conformational restriction may arise. The distance between the two N-H groups of a squaramide is

[49] *Reviews:* (a) X. Fanga, C. -J. Wang *Chem. Commun*. **2015**, *51*, 1185−1197, (b) O. V. Serdyuk, C. M. Heckel, S. B. Tsogoeva *Org. Biomol. Chem*. **2013**, *11*, 7051−7071, (c) W. -Y. Siau, J. Wang *Catal. Sci. Technol*. **2011**, *1*, 1298−1310.
[50] *Reviews:* (a) E. A. Popova, Y. A. Pronina, A. V. Davtian, G. D. Nepochatyi, M. L. Petrov, V. M. Boitsov, A. V. Stepakov *Russ. J. Gen. Chem.* **2022**, *92*, 287−347, (b) B. L. Zhao, J. H. Li, D. M. Du *Chem. Rec.* **2017**, *17*, 994−1018, (c) P. Chauhan, S. Mahajan, U. Kaya, D. Hack, D. Enders *Adv. Synth. Catal.* **2015**, *357*, 253−281, (d) R. I. Storer, C. Aciroa, L. H. Jones *Chem. Soc. Rec.* **2011**, *40*, 2330−2346, (e) J. Alemán, A. Parra, H. Jiang, K. A. Jørgensen *Chem. Eur. J.* **2011**, *17*, 6890−6899.

approximately one third larger (2.72 Å) than that in a thiourea (2.13 Å). In addition, due to the "square geometric" structure of the cyclobutadienone, there is a convergent orientation of the N-H groups, tilting each by approximately six degrees. Proton acidity of N-H groups of squaramides[51] is also bigger than the corresponding one in thioureas,[52] due to their vinylogous amide nature. The pKa values of different squaramide derivatives in DMSO, including some commonly used bifunctional squaramides, are shown in the Figure 1.6.

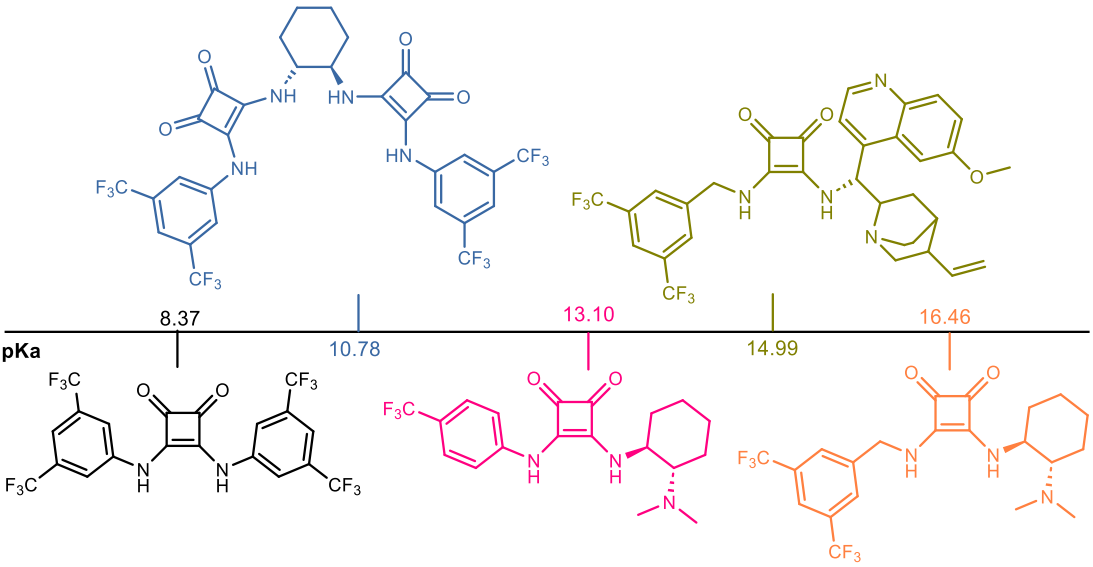

Figure 1.6: pKa values of different squaramides in DMSO as solvent.

Generally, squaramides stablish stronger hydrogen bonds with the substrates bearing nitro, carbonyl, imine and nitrile groups. The squaramide unit has often incorporated a chiral scaffold bearing a basic moiety, thus resulting in an effective bifunctional hydrogen bonding catalyst for promoting a wide variety of useful asymmetric reactions. Catalyst performance is highly dependent on the acidity of the N-H bond, high acidity will lead to higher rate constants, while enantioselectivity depends on the chiral scaffold carrying a basic moiety. Bifunctional squaramide-derived catalysts are expected to efficiently activate pyrazolone ketimines through hydrogen bonding in their reactions with different nucleophiles, Figure 1.7.

[51] X. Ni, X. Li, Z. Wang, J. P. Chen *Org Lett* **2014**, *16*, 1786–1789.
[52] G. Jakab, C. Tancon, Z. Zhang, K. M. Lippert, P. R. Schreiner *Org Lett* **2012**, *14*, 1724–1727.

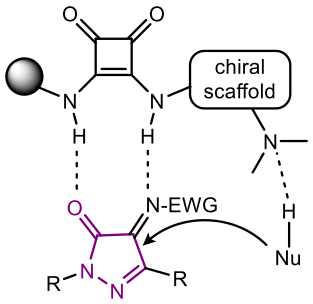

Figure 1.7: Proposed squaramide-activation mode for pyrazolone ketimines.

1.5 Thesis aims and outline

Several strategies that combine the generation of a chiral spiropyrazolone derivative with the formation of a quaternary center bearing a heteroatom have been depicted in the literature. However, the preparation of this type of spiropyrazolones from pyrazole-4,5-diones or pyrazolinone ketimines is a poorly developed area, with few examples reported in the literature. The main objective of the work described in this thesis was the development of new protocols of organocatalyzed asymmetric synthesis of spiropyrazolones from pyrazole-4,5-diones and their *N*-Boc-ketimine derivatives, Figure 1.8, promoted by *N*-Heterocyclic carbenes (NHCs) or by bifunctional hydrogen bonding catalysts.

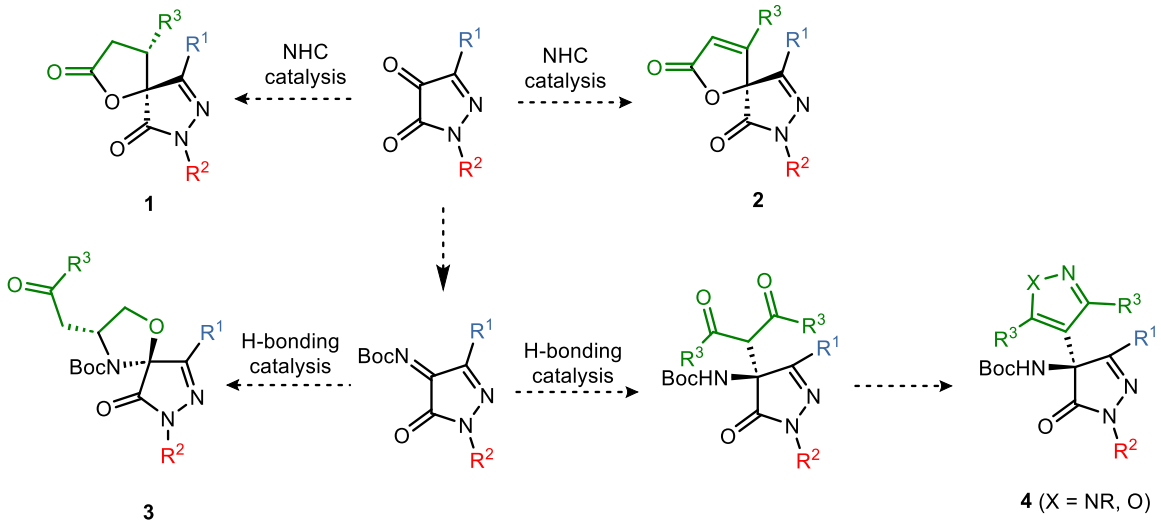

Figure 1.8: Proposed outline for this doctoral thesis.

More specifically, the fully diastereo- and highly enantioselective synthesis of novel spirocyclic pyrazolone γ-butyrolactones (**1**) *via* NHC-catalyzed [3+2] annulation reaction of enals and 1*H*-

pyrazolin-4,5-diones, was conducted in **Chapter II**. To understand the catalytic mechanism and origin of stereoselectivity, electronic structure calculations were carried out. Furthermore, the NHC-catalyzed [3+2] asymmetric annulation of β-bromo enals and 1*H*-pyrazol-4,5-diones was also examined, obtaining enantioenriched chiral spiropyrazolone-butenolides (**2**) (**Chapter III**).

There still exist a need to develop protocols for the synthesis of pyrazolones with *N,N*- or *N,O*-ketal motif. Therefore, in **Chapter IV**, efforts were made to develop the bifunctional squaramide-catalyzed asymmetric synthesis of pyrazolinone embedded oxazolidines (**3**) *via N,O*-acetalization/aza-Michael addition domino reaction between *N*-Boc pyrazolinone ketimines and γ-hydroxyenones. Additionally, the squaramide-catalyzed asymmetric Mannich reaction between 1,3-dicarbonyl compounds and pyrazolinone ketimines was studied, which constitutes a pathway for the preparation of enantioenriched 4-pyrazolyl- and 4-isoxazolyl-4-aminopyrazolone derivatives (**4**) (**Chapter V**).

Finally, **Chapter VI** contains part of the results of the work performed during the three-month stay at Aarhus University under the supervision of Prof. Karl Anker Jørgensen about the enantioselective synthesis of quaternary isochromanes through oxidative aminocatalysis and gold catalysis.

1.6 References

1. (a) P. K. Mykhailiuk *Chem. Rev.* **2021**, *121*, 1670–1715, (b) T. -F. Wang, S. R. Kosuru, S. -C. Yu, Y. -C. Chang, H. -Y. Lai, Y. -L. Chang, K. -H. Wu, S. Dingad, H. -Y. Chen *RSC Adv.* **2020**, *10*, 40690–40696, (c) M. J. Naim, O. Alam, F. Nawaz, M. J. Alam, P. Alam *J. Pharm. Bioallied Sci.* **2016**, *8*, 2-17, (d) S. Fustero, M. Sánchez-Roselló, P. Barrio, A. Simón-Fuentes *Chem. Rev.* **2011**, *111*, 6984–7034.
2. *Some examples:* (a) O. Barreiro-Costa, G. Morales-Noboa, P. Rojas-Silva, E. Lara-Barba, J. Santamaría-Aguirre, N. Bailón-Moscoso, J. C. Romero-Benavides, A. Herrera, C. Cueva, L. Ron-Garrido, A. Poveda, J. Heredia-Moya *Molecules* **2021**, *26*, 4960, (b) J. Zaiter, A. Hibot, A. Hafid, M. Khouili, C. M. B. Neves, M. M. Q. Simoes, M. G. P. M. S. Neves, M. A. F. Faustino, T. Dagci, L. Saso, G. Armagan *Eur. J. Med. Chem*. **2021**, *213*, 113140, (c) Y. Zhang, C. Wang, W. Huang, P. Haruehanroengra, C. Peng, J. Sheng, B. Han, G. He *Org. Chem. Front.* **2018**, *5*, 2229–2233, (d) S. Wu, Y. Li, G. Xu, S. Chen, Y. Zhang, N. Liu, G. Dong, C. Miao, H. Su, W. Zhang, C. Sheng *Eur. J. Med. Chem.* **2016**, *115*, 141–147, (e) Y. Zhang, S. Wu, S. Wang, K. Fang, G. Dong, N. Liu, Z. Miao, J. Yao, J. Li, W. Zhang, C. Sheng, W. Wang *Eur. J. Org. Chem.* **2015**, *9*, 2030–2037.
3. *Selected recent examples:* (a) B. Mao, J. Xu, W. Shi, W. Wang, Y. Wu, Y. Xiao, H. Guo *Org. Biomol. Chem.* **2022**, *20*, 4086–4090, (b) J. -M. Guo, X. -Z. Fan, H. -H. Wu, Z. Tang, X. -F.

Bi, H. Zhang, L. -Y. Cai, H. -W. Zhao, Q. -D. Zhong *J. Org. Chem.* **2021**, *86*, 1712−1720, (c). K. Shukla, S. Shah, N. K. Rana, V. K. Sin *Tetrahedron Letters* **2019**, *60*, 92–97.

4. Prof. B. List and Prof. D. W. C. MacMillan were awarded the Nobel Prize in Chemistry 2021 for their contributions to asymmetric organocatalysis.
5. *Review:* Y. Yang, X. Wang, X. Ye, B. Wang, X. Bao, H. Wang *Org. Biomol. Chem*. **2021**, *19*, 4610–4621.
6. *For reviews see:* (a) X. Bao, X. Wang, J. -M. Tian, X. Ye, B. Wang, H. Wang *Org. Biomol. Chem.* **2022**, *20*, 2370−2386, (b) L. Carceller-Ferrer, G. Blay, J.R. Pedro, C. Vila *Synthesis* **2021**, *53*, 215−237, (c). X. Xie, L. Xiang, C. Peng, B. Han *Chem. Rec.* **2019**, *19*, 2209–2235.
7. *Some examples:* (a) B. Wu, J. Chen, M. -Q. Li, J. -X. Zhang, X. -P. Xu, S. -J. Ji, X. -W. Wang *Eur. J. Org. Chem.* **2012**, 1318–1327, (b) A. -N. R. Alba, A. Zea, G. Valero, T. Calbet, M. Font-Bardía, A. Mazzanti, A. Moyano, R. Rios *Eur. J. Org. Chem.* **2011**, 1318–1325, (c) A. Zea, A. -N. R. Alba, A. Mazzanti, A. Moyano, R. Rios *Org. Biomol. Chem.* **2011**, *9*, 6519–6523.
8. *Some examples:* (a) S. Meninno, A. Mazzanti, A. Lattanzi *Adv. Synth. Catal.* **2019**, *361*, 79–84, (b) Y. Lin, B. -L. Zhao, D. -M. Du *J. Org. Chem.* **2019**, *84*, 10209−10220, (c) J. -Y. Liu, J. Zhao, J. -L. Zhang, P. -F. Xu *Org. Lett.* **2017**, *19*, 1846–1849, (d) J. -H. Li, T. -F. Feng, D. -M. Du *J. Org. Chem.* **2015**, *80*, 11369–11377.
9. *Some examples:* (a) C. Zhao, K. Shi, G. He, Q. Gu, Z. Ru, L. Yang, G. Zhong *Org. Lett*. **2019**, *21*, 7943−7947, (b) S. R. Yetra, S. Mondal, S. Mukherjee, R. G. Gonnade, A. T. Biju *Angew. Chem. Int. Ed*. **2016**, *55*, 268−272, (c) L. Wang, S. Li, P. Chauhan, D. Hack, A. R. Philipps, R. Puttreddy, K. Rissanen, G. Raabe, D. Enders *Chem. Eur. J.* **2016**, *22*, 5123−5127.
10. C. -K. Tang, Z. -Y. Zhou, A. -B. Xia, L. Bai, J. Liu, D. -Q. Xu, Z. -Y. Xu *Org. Lett.* **2018**, *20*, 5840−5844.
11. H. Lu, H. -X. Zhang, C. -Y. Tan, J. -Y. Liu, H. Wei, P. -F. Xu *J. Org. Chem.* **2019**, *84*, 10292-10305.
12. J. Zhou, W. J. Huang, G. F. Jiang *Org. Lett*. **2018**, *20*, 1158–1161.
13. M. -M. Chu, S. -S. Qi, Y. -F. Wang, B. Wang, Z. -H. Jiang, D. -Q. Xu, Z. -Y. Xu *Org. Chem. Front.* **2019**, *6*, 1977–1982.
14. S. Meninno, A. Roselli, A. Capobianco, J. Overgaard, A. Lattanzi *Org. Lett.* **2017**, *19*, 5030–5033.
15. A. B. Xia, X. L. Zhang, C. K. Tang, K. X. Feng, X. H. Du, D. Q. Xu *Org. Biomol. Chem*. **2017**, *15*, 5709–5718.
16. X. L. Zhang, C. K. Tang, A. B. Xia, K. X. Feng, X. H. Du, D. Q. Xu *Eur. J. Org. Chem.* **2017**, *2017*, 3152–3160.
17. P. K. Warghude, A. S. Sabale, R. G. Bhat *Org. Biomol. Chem*. **2020**, *18*, 1794–1799.
18. W. -R. Zhu, Q. Su, N. Lin, Q. Chen, Z. -W. Zhang, J. Weng, G. Lu *Org. Chem. Front*. **2020**, *7*, 3452–3458.
19. R. Qin, T. -T. Yu, S.-J. Liu, Y. -C. Wang, M. -Lan Luo, B. -H. Chen, Q. Zhao, W. Huang *J. Org. Chem.* **2022**, *87*, 5358−5370.
20. X. Bao, S. Wei, X. Qian, J. Qu, B. Wang, L. Zou, G. Ge *Org. Lett.* **2018**, *20*, 3394–3398.
21. W. Wang, S. Wei, X. Bao, S. Nawaz, J. Qu, B. Wang *Org. Biomol. Chem*. **2021**, *19*, 1145-1154.

22. W. Wang, X. Bao, S. Wei, S. Nawaz, J. Qu, B. Wang *Chem. Commun*. **2021**, *57*, 363–366.
23. W. Gong, X. Du, W. Wang, W. Zhang, B. Wang *Tetrahedron Letters* **2021**, *78*, 153259.
24. J. Tang, Z. -H. Yan, G. Zhan, Q. -Q. Yang, Y. -Y. Cheng, X. Li, W. Huang *Org. Chem. Front.* **2022**, *9*, 4341–4346.
25. Z. Zhao, X. Dai, C. Li, X. Wang, J. Tian, Y. Feng, J. Xie, C. Ma, Z. Nie, P. Fan, M. Qian, X. He, S. Wu, Y. Zhang, X. Zheng *Eur. J. Med. Chem.* **2020**, *186*, 11189.
26. (a) A. Hager, N. Vrielink, D. Hager, J. Lefranc, D. Trauner *Nat. Prod. Rep*. **2016**, *33*, 491–522, (b) P. Chauhan, S. Mahajan, D. Enders *Chem. Commun.* **2015**, *51*, 12890–12907.
27. M. Bae, J. Oh, E. S. Bae, J. Oh, J. Hur, Y. -G. Suh, S. K. Lee, J. Shin, D. -C. Oh *Org. Lett.* **2018**, *20*, 1999 —2002.
28. Z. Yang, Z. Wang, S. Bai, X. Liu, L. Lin, X. Feng *Org. Lett.* **2011**, *13*, 596–599.
29. (a) B. Formánek, V. Šeferna, M. Meazza, R. Rios, M. Patil, J. Veselý *Eur. J. Org. Chem.* **2021**, *2021*, 2362–2366, (b) M. Šimek, M. Remeš, J. Veselý, R. Rios *Asian J. Org. Chem.* **2013**, *2*, 64–68.
30. P. Chauhan, S. Mahajan, U. Kaya, A. Peuronen, K. Rissanen, D. Enders *J. Org. Chem.* **2017**, *82*, 7050−7058.
31. S. Mahajan, P. Chauhan, U. Kaya, K. Deckers, K. Rissanen, D. Enders *Chem. Commun.* **2017**, *53*, 6633—6636.
32. U. Kaya, P. Chauhan, S. Mahajan, K. Deckers, A. Valkonen, K. Rissanen, D. Enders *Angew. Chem. Int. Ed.* **2017**, *56*, 15358–15362.
33. Z. -T. Yang, W. -L. Yang, L. Chen, H. Sun, W. -P. Deng *Adv. Synth. Catal.* **2018**, *360*, 2049–2054.
34. T. Kang, W. Cao, L. Hou, Q. Tang, S. Zou, X. Liu, X. Feng *Angew. Chem.* **2019**, *131*, 2486–2490.
35. G. -Y. Ran, C. Chen, X. -X. Yang, Z. Zhao, W. Du, Y. -C. Chen *Org. Lett*. **2020**, *22*, 4732–4736.
36. A. -Q. Miao, M. Zhou, J. -L, Chen, S. -C. Wang, W. -J. Hao, S. -J. Tu, B. Jiang *Adv. Synth. Catal*. **2021**, *363*, 5162–5166.
37. Seebach's terminology to describe *umpolung* reactivity, D. Seebach *Angew. Chem. Int. Ed. Engl.* **1979**, *18*, 239–258.
38. J. Sheehan, D. H. Hunneman *J. Am. Chem. Soc.* **1966,** *88*, 3666−3667.
39. *Recent reviews:* (a) X. -Y. Chen, Z. -H. Gao, S. Ye *Acc. Chem. Res.* **2020**, *53*, 690–702, (b) S. Mondal, S. R. Yetra, S. Mukherjee, A. T. Biju *Acc. Chem. Res.* **2019**, *52*, 425–436, (c) X. -Y. Chen, Q. Liu, P. Chauhan, D. Enders *Angew. Chem. Int. Ed.* **2018**, *57*, 3862–3873, (d) X. -Y. Chen, S. Li, F. Vetica, M. Kumar, D. Enders *iScience* **2018**, *2*, 1–26, (e) C. Zhang, J. F. Hooper, D. W. Lupton *ACS Catal.* **2017**, *7*, 2583–2596, (f) M. N. Hopkinson, C. Richter, M. Schedler, F. Glorius *Nature*, **2014**, *51*0, 485–496, (g) D. Enders, O. Niemeier, A. Henseler *Chem. Rev.* **2007**, *107*, 5606–5655.
40. R. Breslow *J. Am. Chem. Soc.* **1958**, *80*, 3719–3726.
41. S. Mondal, A. Ghosh, A. T. Biju *Chem. Rec.* **2022**, *22*, e202200054.
42. *Some examples:* (a) A. B. Viveki, M. D. Pol, P. Halder, S. R. Sonavane, S. B. Mhaske *J. Org. Chem.* **2021**, *86*, 9466−9477, (b) M. He, G. J. Uc, J. W. Bode *J. Am. Chem. Soc.* **2006**, *128*, 15088–15089.

43. *Some examples:* (a) N. Attaba, A. D. Smith *Tetrahedron* **2020**, *76*, 130835−130843, (b) A. Lee, A. Younai, C. K. Price, J. Izquierdo, R. K. Mishra, K. A. Scheidt *J. Am. Chem. Soc.* **2014**, *136*, 10589−10592.
44. *Some examples:* (a) X. N. Wang, H. Lv, X. -L. Huang, S. Ye *Org. Biomol. Chem.* **2009**, *7*, 346–350, (b) Y. -R. Zhang, H. Lv, D. Zhou, S. Ye *Chem. Eur. J.* **2008**, *14*, 8473–8476, (c) Y. -R. Zhang, L. He, X. Wu, P. -L. Shao, S. Ye *Org. Lett.* **2008**, *10*, 277–280.
45. *Some examples:* (a) J. Wang, Y. Li, J. Sun, H. Wang, Z. Jin, Y. R. Chi *ACS Catal.* **2018**, *8*, 9859–9864, (b) C. Fang, T. Lu, J. Zhu, K. Sun, D. Du *Org. Lett.* **2017**, *19*, 3470–3473, (c) S. Mondal, S. R. Yetra, A. Patra, S. S. Kunte, R. G. Gonnade, A. T. Biju *Chem. Commun.* **2014**, *50*, 14539–14542.
46. *Some examples:* (a) K. Dzieszkowski, M. Słotwiński, K. Rafińska, T. M. Muzioła, Z. Rafiński *Chem. Commun.* **2021**, *57*, 9999–10002, (b) J. Mahatthananchai, J. Kaeobamrung, J. W. Bode *ACS Catal.* **2012**, *2*, 494–503.
47. *Some examples:* (a) X. Wu, B. Liu, Y. Zhang, M. Jeret, H. Wang, P. Zheng, S. Yang, B. A. Song, Y. R. Chi *Angew. Chem. Int. Ed*. **2016**, *55*, 12280–12284, (b) A. Biswas, S. De Sarkar, L. Tebben, A. Studer *Chem. Commun.* **2012**, *48*, 5190–5192.
48. *Some examples:* (a) L. Liu, D. Guo, J. Wang *Org. Lett.* **2020**, *22*, 7025−7029, (b) J. Mo, X. Chen, Y. R. Chi *J. Am. Chem. Soc.* **2012**, *134*, 8810–8813.
49. *Reviews:* (a) X. Fanga, C. -J. Wang *Chem. Commun*. **2015**, *51*, 1185−1197, (b) O. V. Serdyuk, C. M. Heckel, S. B. Tsogoeva *Org. Biomol. Chem*. **2013**, *11*, 7051−7071, (c) W. -Y. Siau, J. Wang *Catal. Sci. Technol*. **2011**, *1*, 1298−1310.
50. *Reviews:* (a) E. A. Popova, Y. A. Pronina, A. V. Davtian, G. D. Nepochatyi, M. L. Petrov, V. M. Boitsov, A. V. Stepakov *Russ. J. Gen. Chem.* **2022**, *92*, 287−347, (b) B. L. Zhao, J. H. Li, D. M. Du *Chem. Rec.* **2017**, *17*, 994−1018, (c) P. Chauhan, S. Mahajan, U. Kaya, D. Hack, D. Enders *Adv. Synth. Catal.* **2015**, *357*, 253−281, (d) R. I. Storer, C. Aciroa, L. H. Jones *Chem. Soc. Rec.* **2011**, *40*, 2330−2346, (e) J. Alemán, A. Parra, H. Jiang, K. A. Jørgensen *Chem. Eur. J.* **2011**, *17*, 6890−6899.
51. X. Ni, X. Li, Z. Wang, J. P. Chen *Org Lett* **2014**, *16*, 1786−1789.
52. G. Jakab, C. Tancon, Z. Zhang, K. M. Lippert, P. R. Schreiner *Org Lett* **2012**, *14*, 1724-1727.

Chapter II: Chiral NHCs as organocatalysts for the synthesis of spirocyclic pyrazolone γ-butyrolactones from pyrazolin-4,5-diones.

This work was published as:

"NHC-catalysed [3+2]-asymmetric annulation between pyrazolin-4,5-diones and enals: synthesis of novel spirocyclic pyrazolone γ-butyrolactones and computational study of mechanism and stereoselectivity"

Marta Gil-Ordóñez, Alicia Maestro, Pablo Ortega, Pablo G. Jambrina, José M. Andrés *Org. Chem. Front*. **2022**, *9*, 420-427.

2.1 Introduction and background

As previously indicated, there are some precedents in the literature on the preparation of chiral spirocyclic pyrazolones bearing an oxygen atom incorporated at the spirocyclic carbon using pyrazolones, α, β-unsaturated pyrazolones or pyrazolin-4,5-diones as starting materials. However, to the best of our knowledge there are no examples describing the preparation of spiropyrazolone γ-butyrolactones despite the interest of this cyclic ester unit as a chiral building block of diverse biological active compounds and complex molecules, Figure 2.1.[1,2]

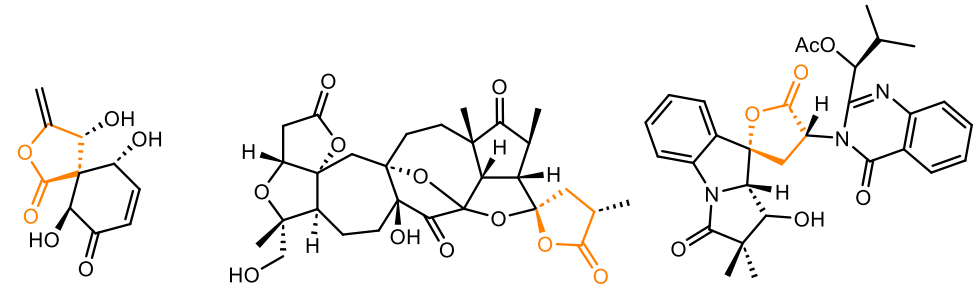

Figure 2.1: Representative bioactive compounds containing a spirobutyrolactone skeleton.

Instead, various organometallic[3] and organocatalytic[4] approaches have been described for the synthesis of spirooxindole γ-lactones as they possess a wide range of proven biological activities.[5] These methods use 3-hydroxy oxoindoles[3,4a] or their Boc derivatives as starting materials,[4c] Scheme 2.1.

[1] A. Quintavalla *Curr. Med. Chem*. **2018**, *25*, 917–962.
[2] J. Yang, B. -W. Pan, L. Chen, Y. Zhou, X. -L. Liu *Chem. Synth.* **2023**, *3*, 7–61.
[3] B. M. Trost, K. Hirano *Org. Lett*. **2012**, *14*, 2446–2449.
[4] (a) Z. -T. Yang, J. Zhao, W. -L. Yang, W. -P. Deng *Org. Lett.* **2019**, *21*, 1015–1020, (b) L. Chen, Z. -J. Wu, M. -L. Zhang, D. -F. Yue, X. -M. Zhang, X. -Y. Xu, W. -C. Yuan *J. Org. Chem.* **2015**, *80*, 12668–12675, (c) S. Jayakumar, S. Muthusamy, M. Prakash, V. Kesavan *Eur. J. Org. Chem.* **2014**, 1893–1898, (d) Q. -L. Wang, L. Peng, F. -Y. Wang, M. -L. Zhang, L. -N. Jia, F. Tian, X. -Y. Xu, L. -X. Wang *Chem. Commun.* **2013**, *49*, 9422–9424.
[5] (a) S. Rana, E. C. Blowers, C. Tebbe, J. I. Contreras, P. Radhakrishnan, S. Kizhake, T. Zhou, R. N. Rajule, J. L. Arnst, A. R. Munkarah, R. Rattan, A. Natarajan *J. Med. Chem*. **2016**, *59*, 5121–5127, (b) B. Yu, D. -Q. Yu, H. -M. Liu *Eur. J. Med. Chem*. **2015**, *97*, 673–698, (c) S. -S. Ma, W. -L. Mei, Z. -K. Guo, S. -B. Liu, Y. -S. Zhao, D. -L. Yang, Y. -B. Zeng, B. Jiang, H. -F. Dai *Org. Lett*. **2013**, *15*, 1492–1495.

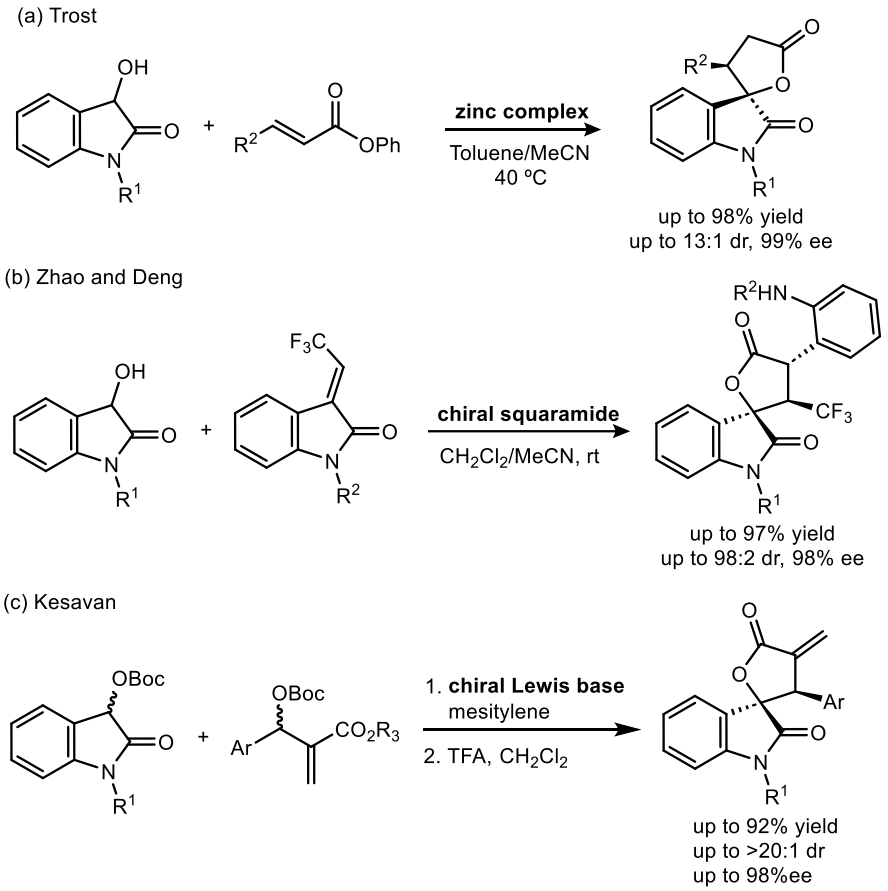

Scheme 2.1: Organometallic and organocatalytic approaches for the synthesis of spirooxindole γ-lactones.

Chiral *N*-heterocyclic carbenes have been also used as a powerful tool for the preparation of these spirooxindole γ-lactones.[6] For example, Sun and Ye group described the NHC-catalyzed oxidative [3+2] annulation of dioxindoles and enals[7] giving the desired spiro compounds in good yields with high to excellent diastereo- and enantioselectivities, Scheme 2.2a. The HOBt-assisted [3+2] annulation of carboxylic esters with isatins *via* acyl azolium intermediate,[8] or the enantioselective addition of homoenolates generated from enals to isatins by cooperative NHC/Lewis acid catalysis,[9] Scheme 2.2b and c, are some of the reported alternative approaches.

[6] Y. Liu, X. Zhang, R. Zeng, Y. Zhang, Q. -S. Dai, H. -J. Leng, X. -J. Gou, J. -L. Li *Molecules* **2017**, *22*, 1882–1904.
[7] X. -Y. Chen, K. -Q. Chen, D. -Q. Sun, S. Ye *Chem. Sci.* **2017**, *8*, 1936–1941.
[8] J. Xu, S. Yuan, M. Miao, Z. Chen *J. Org. Chem.* **2016**, *81*, 11454–11460.
[9] (a) Y. Reddi, R. B. Sunoj *ACS Catal.* **2017**, *7*, 530–537, (b) J. -L. Li, B. Sahoo, C. -G. Daniliuc, F. Glorius *Angew. Chem. Int. Ed. Engl.* **2014**, *53*, 10515–10519, (c) J. Dugal-Tessier, E. A. O'Bryan, T. B. H. Schroeder, D. T. Cohen. K. A. Scheidt *Angew. Chem. Int. Ed.* **2012**, *51*, 4963–4967.

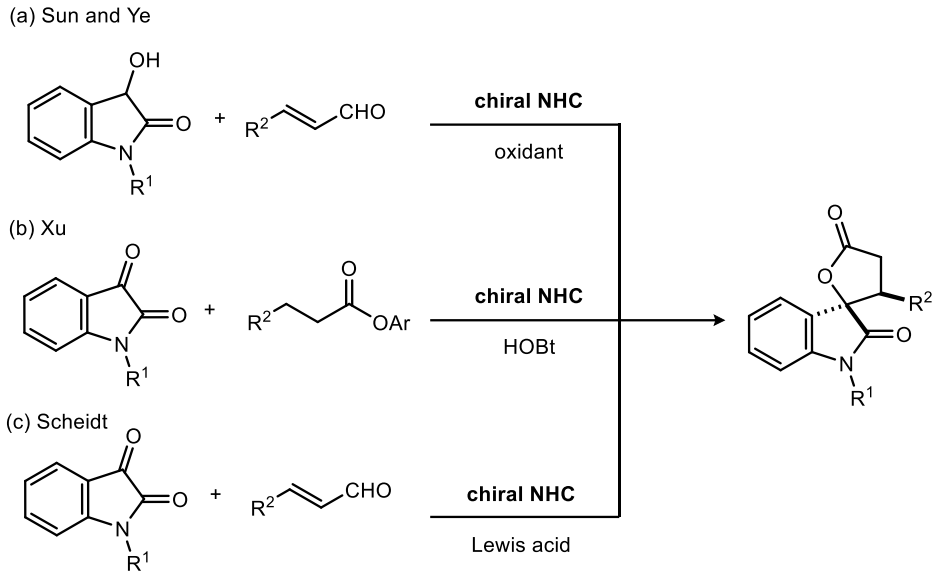

Scheme 2.2: Some examples of the preparation of spirooxindole γ-lactones by NHC catalysis.

After reviewing the existing literature, we have only found three examples of NHC-catalyzed asymmetric synthesis of spirocyclic pyrazolones with an all-carbon quaternary stereocenter. Biju's group reported the preparation of pyrazolone-fused spirocyclohexadienones from α, β-unsaturated aldehydes and α-arylidene pyrazolones under oxidative *N*-heterocyclic carbene catalysis,[10] Scheme 2.3. This [3+3] annulation reaction proceeds through a vinylogous Michael addition/spiroannulation/dehydrogenation cascade to afford spirocyclic compounds in moderate to good yields and excellent enantiomeric ratios.

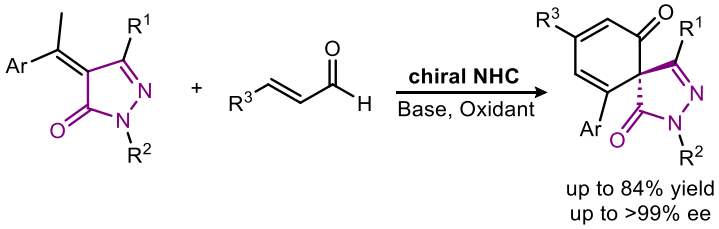

Scheme 2.3: Spirocyclohexadienones synthesis *via* oxidative NHC-catalyzed [3+2] annulation of enals reported by Biju.

Some years later, Yang and Zhong[11] group described the NHC-catalyzed [4+2] annulation of γ-chloroenals and α-arylidene pyrazolones, Scheme 2.4. In this case, the starting enal reacts with the catalyst affording a vinyl enolate intermediate after the C-Cl bond cleavage in the absence of expensive oxidants. The reaction finishes by the cycloaddition of vinyl enolate with the

[10] S. R. Yetra, S. Mondal, S. Mukherjee, R. G. Gonnade, A. T. Biju *Angew. Chem. Int. Ed.* **2016**, *55*, 268–272.
[11] C. Zhao, K. Shi, G. He, Q. Gu, Z. Ru, L. Yang, G. Zhong *Org. Lett.* **2019**, *21*, 7943–7947.

pyrazolone derivative, generating the enantioenriched spiropyrazolones and releasing the catalyst.

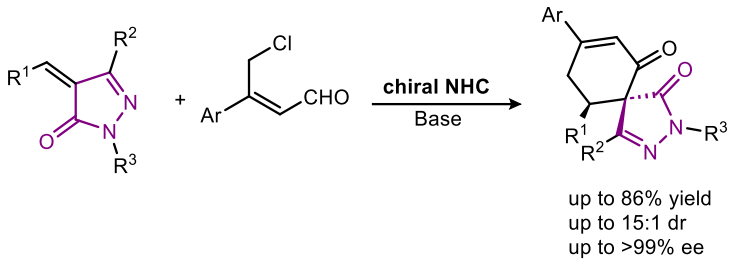

Scheme 2.4: Asymmetric [4+2] annulation of γ-chloroenals and α-arylidene pyrazolones described by Yang and Zhong.

On the other hand, Enders group[12] developed a three-component one-pot synthesis of spirocyclopentane pyrazolones through the aldol condensation of an enal with the pyrazolone to generate a Michael acceptor, followed by a NHC-catalyzed [3+2] annulation reaction with a second equivalent of enal, Scheme 2.5. The reaction sequence proceeds *via* an azolium homoenolate intermediate and with excellent diastereo- and enantioselectivity.

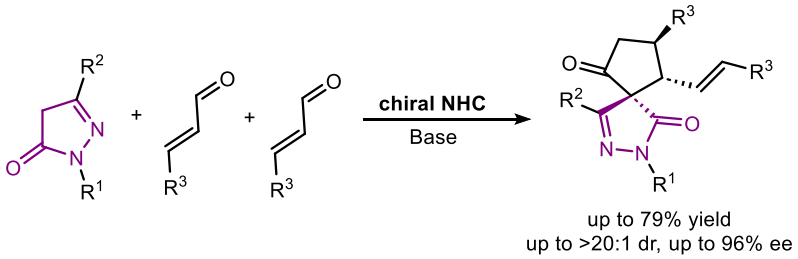

Scheme 2.5: Enders' synthesis of spirocyclopentane pyrazolones from pyrazolones and enals.

Due to their interest, in this chapter we describe the fully diastereo- and highly enantioselective synthesis of novel spiropyrazolone γ-butyrolactones *via* NHC-catalyzed [3+2] annulation reaction of enals and 1*H*-pyrazol-4,5-diones. Moreover, we carry out electronic structure calculations to elucidate the catalytic mechanism and the origin of the stereoselectivity.

[12] L. Wang, S. Li, P. Chauhan, D. Hack, A. R. Philipps, R. Puttreddy, K. Rissanen, G. Raabe, D. Enders *Chem. Eur. J.* **2016**, *22*, 5123–5127.

2.2 Results and discussion

As starting point for the study of the [3+2] annulation, we investigated the reaction of pyrazolin-4,5-dione **1a** and cinnamaldehyde **2a** in the presence of different pre-catalysts **A-E**, DABCO as base and toluene as solvent at room temperature (Table 1). In all the cases the diastereoselectivity was excellent (dr >99:<1) (Table 1, entries 2-5 and 7). The best results were obtained when *N*-mesityl triazolium salt **B** was used (Bode catalyst), yielding 72% and 86:14 er (entry 3).

Table 1. Screening of pre-catalysts **A-E**[a]

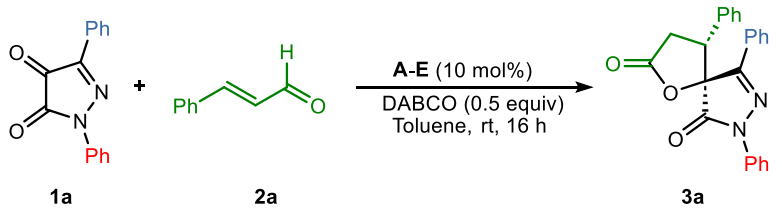

1a **2a** **3a**

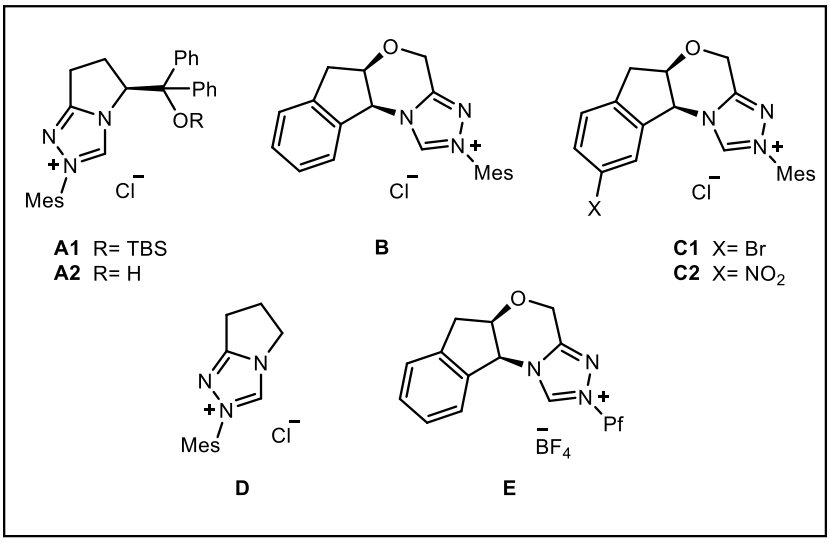

Entry	*pre-NHC*	*Yield (%)*[b]	*dr*[c]	*er*[d]
1	**A1**	n.r.	-	-
2	**A2**	41	>99:<1	37:63
3	**B**	72	>99:<1	86:14
4	**C1**	38	>99:<1	79:21
5	**C2**	45	>99:<1	86:14
6	**D**	<10	n.d.	n.d.
7	**E**	31	>99:<1	50:50

[a] Reaction conditions: **1a** (0.06 mmol), **2a** (0.06 mmol), **A**-**E** (10 mol%), DABCO (0.5 equiv), toluene (1 mL), at rt for 16 h. [b] Yield of **3a** determined after column chromatography. [c] Dr values determined by ^{1}H NMR. [d] Er values determined *via* chiral HPLC analysis.

When a strong electron-withdrawing group was introduced on the indanol ring (pre-catalyst **C2**) no change in the enantioselectivity was produced but the yield decreased dramatically (entry 5). A total loss of enantiodiscrimination was observed when catalyst **E** with a pentafluorophenyl group (Rovis catalyst) was used (entry 7). Triazolium salts derived from (*S*)-pyroglutamic acid were also tested. No reaction was observed when pre-carbene **A1** was used (entry 1). The absence of silyl ether substituent, triazolium salt **A2**, hoping hydrogen bond interactions by the free hydroxyl group[13] and as consequence better results in terms of yield and stereoselectivity, resulted in low yield and enantioselectivity (entry 2).

With pre-catalyst **B** as the most suitable one for performing the catalytic reaction, solvent screening was carried out. More polar solvents like 1,4-dioxane and tetrahydrofuran led to erosion of yield and enantiomeric ratio (Table 2, entries 5 and 8). Mesitylene maintained the level of enantioselectivity but a slightly loss in the yield was observed (Table 2, entry 2). Other solvents led to worse results in yield and enantioselectivity (Table 2, entries 3-4 and 6-7).

[13] X. -Y. Chen, Z. -H. Gao, S. Ye *Acc. Chem. Res.* **2020**, *53*, 690–702.

Table 2. Optimization of reaction conditions[a]

Entry	*pre-NHC*	*Base*	*Solvent*	*Yield (%)*[b]	*dr*[c]	*er*[d]
1	**B**	DABCO	Toluene	72	>99:<1	86:14
2	**B**	DABCO	Mesitylene	65	>99:<1	87:13
3	**B**	DABCO	Xilene	15	>99:<1	75:25
4	**B**	DABCO	Et_2O	66	>99:<1	71:29
5	**B**	DABCO	1,4-dioxane	39	>99:<1	70:30
6	**B**	DABCO	DCM	50	>99:<1	77:23
7	**B**	DABCO	$CHCl_3$	35	>99:<1	74:26
8	**B**	DABCO	THF	34	>99:<1	74:26
9	**B**	DMAP	Toluene	62	>99:<1	79:21
10	**B**	TBD	Toluene	25	>99:<1	82:18
11	**B**	Cs_2CO_3	Toluene	8	>99:<1	87:13
12	**B**	DBU	Toluene	n.r.	-	-
13	**B**	DIPEA	Toluene	52	>99:<1	84:16
14	**B**	KO*t*-Bu	Toluene	29	>99:<1	88:12
15	**B**	KHMDS	Toluene	n.r.	-	-
16	**B**	NaOAc	Toluene	73	>99:<1	74:26
17	**B**	TMEDA	Toluene	23	>99:<1	82:18
18[e]	**B**	DABCO	Toluene	22	>99:<1	86:14
19[f]	**B**	DABCO	Toluene	62	>99:<1	79:21
20[g]	**B**	DABCO	Toluene	58	>99:<1	80:20
21[h]	**B**	DABCO	Toluene	45	>99:<1	78:22
22[i]	**B**	DABCO	Toluene	34	>99:<1	82:18

[a] Reaction conditions: **1a** (0.06 mmol), **2a** (0.06 mmol), **B** (10 mol%), base (0.5 equiv), solvent (1 mL), at rt for 16 h. [b] Yield of **3a** determined after column chromatography. [c] Dr values determined by ^{1}H NMR. [d] Er values determined *via* chiral HPLC analysis. [e] Molar ratio **1a**:**2a** 1:2. [f] Molar ratio **1a**:**2a** 1.2:1. [g] 0 ^{o}C. [h] LiCl as additive. [i] 1,3-Diphenylurea as additive.

After solvent optimization, base screening was performed using pre-catalyst **B** and toluene. Among the different bases tested, DABCO remained as the optimal base. While bases like cesium carbonate and potassium *tert*-butoxide maintained the level of enantioselectivity but not the yield (Table 2, entries 11 and 14), sodium acetate kept the yield but not the

enantiomeric ratio (Table 2, entry 16). When DBU or KHMDS were used, no reaction was observed (Table 2, entries 12 and 15).

Finally, other parameters were evaluated (Table 2, entries 18-22). However, neither lower temperature nor changes in pyrazolin-4,5-dione/enal molar ratio, nor the presence of additives as lithium chloride[9] or 1,3-diphenyl urea as hydrogen-bond donor, led to an improvement in the previous enantiomeric ratios and yields.

Once the reaction conditions were optimized, the scope of the reaction was investigated. First, we modified the substituents of the pyrazolin-4,5-dione, Table 3. The diastereoselectivity remained excellent (>99:<1) except in the case of substrates having a non-bulky alkyl substituent (R^1), such as a methyl group (**3b**) (Table 3, entry 2).

Table 3. Substrate scope for pyrazolin-4,5-diones **1a-e**[a]

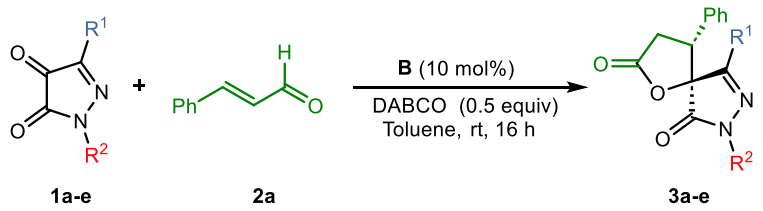

1a-e 2a 3a-e

Entry	*R^1, R^2, **3***	*Yield (%)*[b]	*dr*[c]	*er*[d]
1	Ph, Ph, **3a**	72	>99:<1	86:14
2	Me, Ph, **3b**	49	77:23	81:19[e]
3	Naph, Ph, **3c**	45	>99:<1	81:19
4	*t*-Bu, Ph, **3d**	73	>99:<1	73:27
5	Ph, Me, **3e**	65	>99:<1	80:20

[a] Reaction conditions: **1a-e** (0.06 mmol), **2a** (0.06 mmol), **B** (10 mol%), DABCO (0.5 equiv), toluene (1 mL), at rt for 16 h. [b] Yield of **3a-e** determined after column chromatography. [c] Dr values determined by ^{1}H NMR. [d] Er values determined *via* chiral HPLC analysis. [e] Er for major diastereomer.

When the reaction was performed with the 3-*tert*-butyl-substituted pyrazolin-4,5-dione **1d**, erosion in the enantioselectivity was observed. An additional optimization process was carried out to solve it using **1d** as substrate (Table 4). First, several bases were examined (Table 4, entries 1-8). Although cesium carbonate, potassium *tert*-butoxide or *N*,*N*-diisopropylethylamine worked well (Table 4, entries 3, 6-7), TBD was chosen as the optimal base (Table 4, entry 8) as afforded the best yield/enantiomeric ratio balance.

Table 4. Optimization of reaction conditions with pyrazolin-4,5-dione **1d**[a]

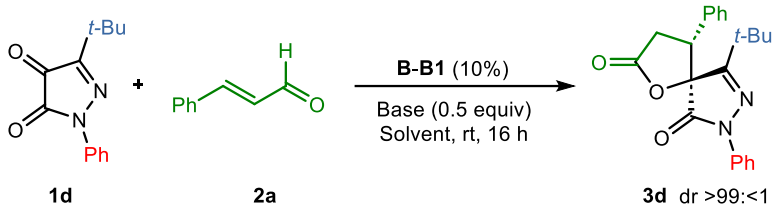

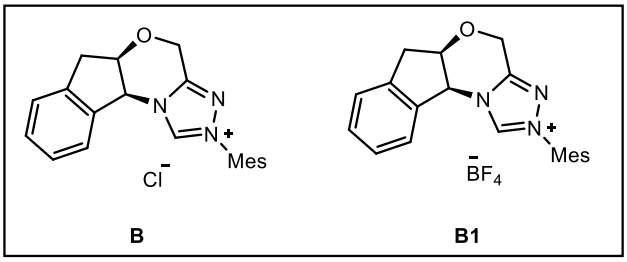

Entry	*pre-NHC*	*Base*	*Solvent*	*Yield (%)*[b]	*Er*[c]
1	**B**	DABCO	Toluene	73	73:27
2	**B**	DMAP	Toluene	46	72:28
3	**B**	KO*t*-Bu	Toluene	69	85:15
4[d]	**B**	KO*t*-Bu	Toluene	51	81:19
5	**B**	NaOAc	Toluene	55	75:25
6	**B**	Cs_2CO_3	Toluene	38	86:14
7	**B**	DIPEA	Toluene	69	84:16
8	**B**	TBD	Toluene	63	87:13
9	**B**	TBD	Benzene	39	89:11
10	**B**	TBD	Et_2O	49	79:21
11	**B**	TBD	THF	12	79:21
12	**B**	TBD	DCM	71	84:16
13	**B**	TBD	Hexane	64	84:16
14[e]	**B**	TBD	Toluene	15	70:30
15	**B1**	TBD	Toluene	42	88:12

[a] Reaction conditions: **1d** (0.06 mmol), **2a** (0.06 mmol), **B-B1** (10 mol%), base (0.5 equiv), solvent (1 mL), at rt for 16 h. [b] Yield of **3d** determined after column chromatography. [c] Er values determined *via* chiral HPLC analysis. [d] 0 °C. [e] LiCl as additive.

Then, combination of TBD with other solvents (Table 4, entries 8-14) was evaluated. Benzene maintained the enantiodiscrimination but led to lower yield of **3d** (Table 4, entry 9). Diethyl ether or THF gave lower yields and enantioselectivities (Table 4, entries 10 and 11). On contrast, good yields but worse enantiomeric ratios were obtained when dichloromethane or hexane were used (Table 4, entries 12 and 13). Finally, we tested the use of lithium chloride as

additive (Table 4, entry 14) and the activity of pre-catalyst **B1**, with a tetrafluoroborate anion instead of a chloride anion (Table 4, entry 15). In both cases, no improvement was detected.

So, the most suitable combination for the annulation reaction of 3-*tert*-butyl substituted pyrazolin-4,5-diones with enals was TBD as base and toluene as solvent (Table 4, entry 8). With this optimized conditions, *tert*-butyl-derived pyrazolin-4,5-dione **1f**, with a methyl group directly attached to the nitrogen atom, was reacted with **2a** giving rise to **3f** in moderate yield and good enantiomeric ratio (58% yield, dr >99:<1, er 84:16).

Next, we studied the influence of the enal by using different aromatic and aliphatic α, β-unsaturated aldehydes (Table 5).

Table 5. Substrate scope for enals **2b-g**[a,b,c,d]

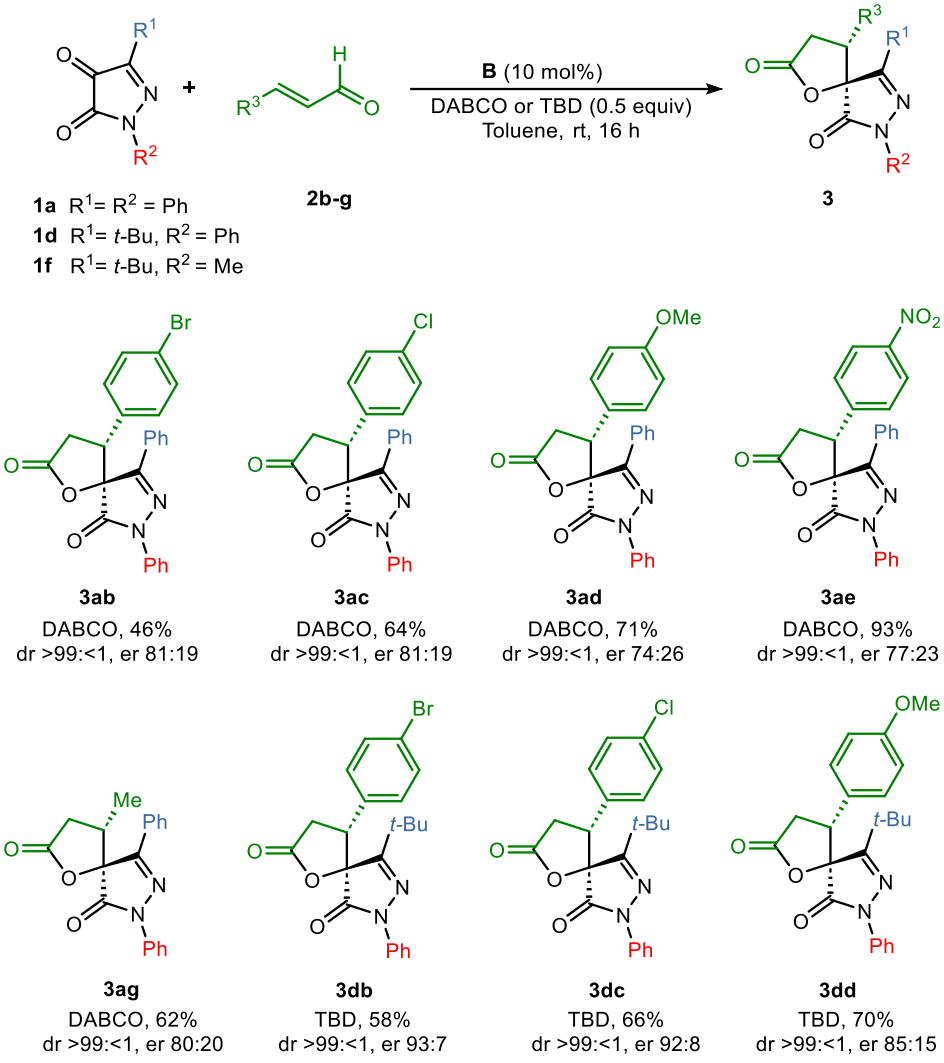

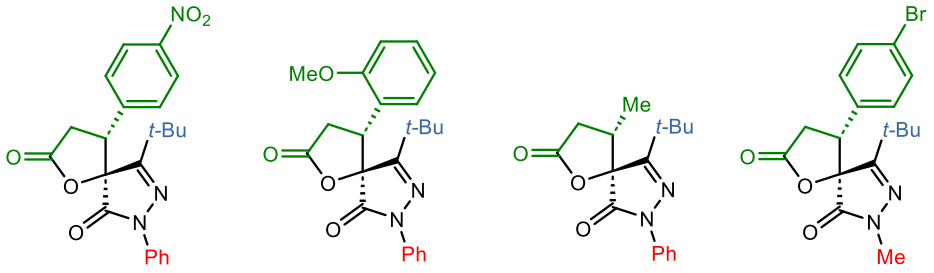

3de
TBD, 51%
dr >99:<1, er 94:6

3df
TBD, 51%
dr >99:<1, er 77:23

3dg
TBD, 58%
dr >99:<1, er 92:8

3fb
TBD, 71%
dr >99:<1, er 90:10

[a] Reaction conditions: **1a,d,f** (0.06 mmol), **2b-g** (0.06 mmol), **B** (10 mol%), DABCO or TBD (0.5 equiv), toluene (1 mL), at rt for 16 h. [b] Yield of **3** determined after column chromatography. [c] Dr values determined by ^{1}H NMR. [d] Er values determined *via* chiral HPLC analysis.

The reaction of pyrazolin-4,5-dione **1a** with *para*-halo substituted cinnamaldehydes worked well, furnishing the desired spiro compounds **3ab** and **3ac** in good yields with total diastereoselectivity and good enantioselectivity. As can be seen, the presence of strongly electron-withdrawing (NO_2) and electron-donating (MeO) groups in this position of enal led to the lactones **3ad** and **3ae** in good yields but with lower enantioselectivity. However, C-3 *tert*-butyl substituted pyrazolin-4,5-dione **3d** reacted with different *p*-substituted cinnamaldehydes affording adducts **3db–3de** with better enantiomeric ratios independently of the electronic properties of the substituent present in the aromatic ring. The introduction of a methoxy group at the *ortho*-position of the aryl ring resulted in a significant decrease in both yield and enantioselectivity (**3df**). The reaction also tolerated an *N*-methyl group to provide, in a diastereoselective way, the desired product **3fb** in 71% yield with good er value (90:10). Interestingly, the reaction also worked with enals bearing a β-methyl substituent giving the corresponding products (**3ag** and **3dg**) with good yields, very high diastereoselectivity (>99:<1), and moderate to good enantioselectivities (er 80:20 and 92:8).

In order to determinate the absolute configuration of products, optically pure (4*R*,5*S*)-4-(4-chlorophenyl)-7,9-diphenyl-1-oxa-7,8-diazaspiro[4.4]non-8-ene-2,6-dione, (–)-**3ac** was isolated after recrystallization from chloroform.[14] X-ray crystallographic analysis of a single-crystal confirmed the absolute configuration as (4*R*,5*S*) for the spiro compound, Figure 2.2.

[14] Er >99: <1 was confirmed *via* chiral HPLC analysis.

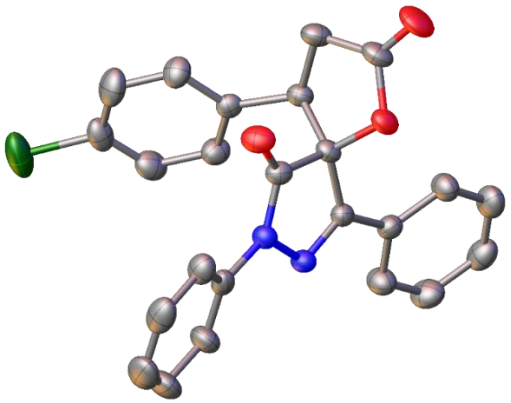

Figure 2.2: X-ray crystallographic analysis of **3ac**.

To demonstrate the synthetic utility of this method, a gram-scale synthesis of spiro derivative **3db** was carried out, Scheme 2.6. A slightly decreased in the yield was observed, but both the diastereoselectivity and enantioselectivity remained excellent.

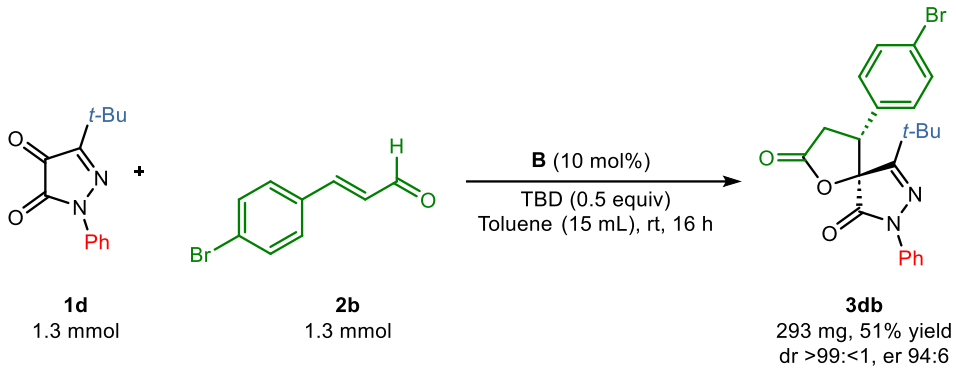

Scheme 2.6: Scale-up reaction for spiropyrazolone **3db**.

Computational methods and model reaction

To elucidate the mechanism of the NHC-catalyzed [3+2] asymmetric annulation and rationalize the origin of the diastereo- and enantioselectivity observed, electronic structure calculations were carried out. The stationary points (minima and saddle points) were optimized at the M06-2X/6-31G(d,p)[15] level of theory using Gaussian16.[16] Solvation effects were included using the SMD continuum solvation model,[17] with the default parameters for toluene.

[15] Y. Zhao, D. G. Truhlar *Theor. Chem. Acc.* **2008**, *120*, 215–241.
[16] M. J. Frisch, G. W. Trucks, H. B. Schlegel, G. E. Scuseria, M. A. Robb, J. R. Cheeseman, *et al.*, Gaussian-16 Revision A.03, Gaussian Inc., Wallingford, CT, **2016**.
[17] A. V. Marenich, C. J. Cramer, D. G. Truhlar *J. Phys. Chem. B*, **2009**, *113*, 6378–6396.

Frequencies were calculated to ensure the convergence and intrinsic reaction coordinate (IRC) calculations were carried out to confirm that the transition states obtained connect reactants and products.[18] Subsequently, single-point calculations of the stationary points were computed at a M062X/maug-cc-pVTZ level, and the free-energies reported were obtained by adding the electronic energy at the M062X/maug-cc-pVTZ level of theory with the thermal free energies computed at the M062X/6-31G(d, p) level. This selection of functional and basis set was done according to recent benchmarks,[19] and the overall procedure is similar to those followed in the literature for the study of other NHC-catalyzed [3+2] asymmetric annulations.[9a,20]

To carry out the electronic structure calculations, we chose as a model the reaction for which the best enantiomeric excess was experimentally observed (**3de**): the reaction between **R2**(**1d**) and **R1**(**2e**), Scheme 2.7.

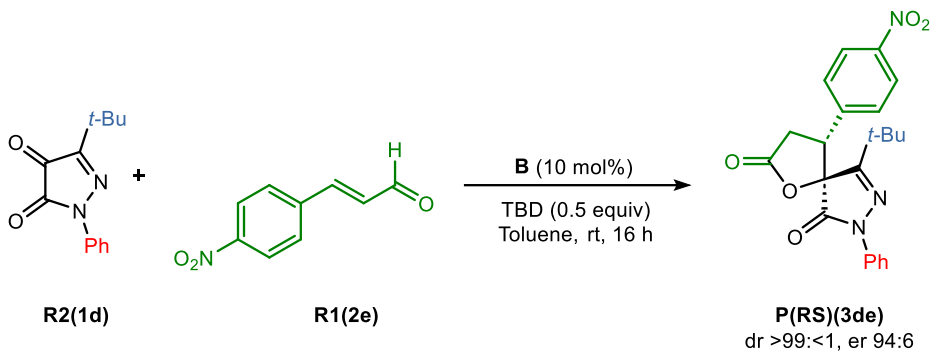

Scheme 2.7: NHC-catalyzed [3+2] annulation chosen as model for the calculations.

The mechanism that emerges from our calculations is depicted in Scheme 2.8. In it, we can differentiate two different stages. In the first stage, the NHC catalyst reacts with the aldehyde moiety of **R1(2e)**, forming a new C-C bond in **IM1**, and finally leading to the **IM2**.

[18] A. Hollwarth, M. Bohme, S. Dapprich, A. W. Ehlers, A. Gobbi, V. Jonas, K. F. Kohler, R. Stegmann, A. Veldkamp, G. Frenking *Chem. Phys. Lett.* **1993**, *208*, 237–240.

[19] (a) S. Rayne, K. Forest *J. Comput. Theor. Chem.* **2016**, *1090*, 147–152, (a) E. Papajak, D. G. Truhlar *J. Chem. Theory Comput.* **2010**, *6*, 597–601.

[20] (a) Y. Li, Z. Li, Z. Zhang *Mol. Catal.* **2020**, *496*, 111183–111192, (b) Y. Li, Z. Zhang *Eur. J. Org. Chem.* **2019**, *2019*, 2989–2997, (c) J. Gao, Y. Wang *Org. Biomol. Chem.* **2019**, *17*, 7442–7447, (d) Y. Li, Z. Zhang, C. Liang *Org. Biomol. Chem.* **2018**, *16*, 9251–9258.

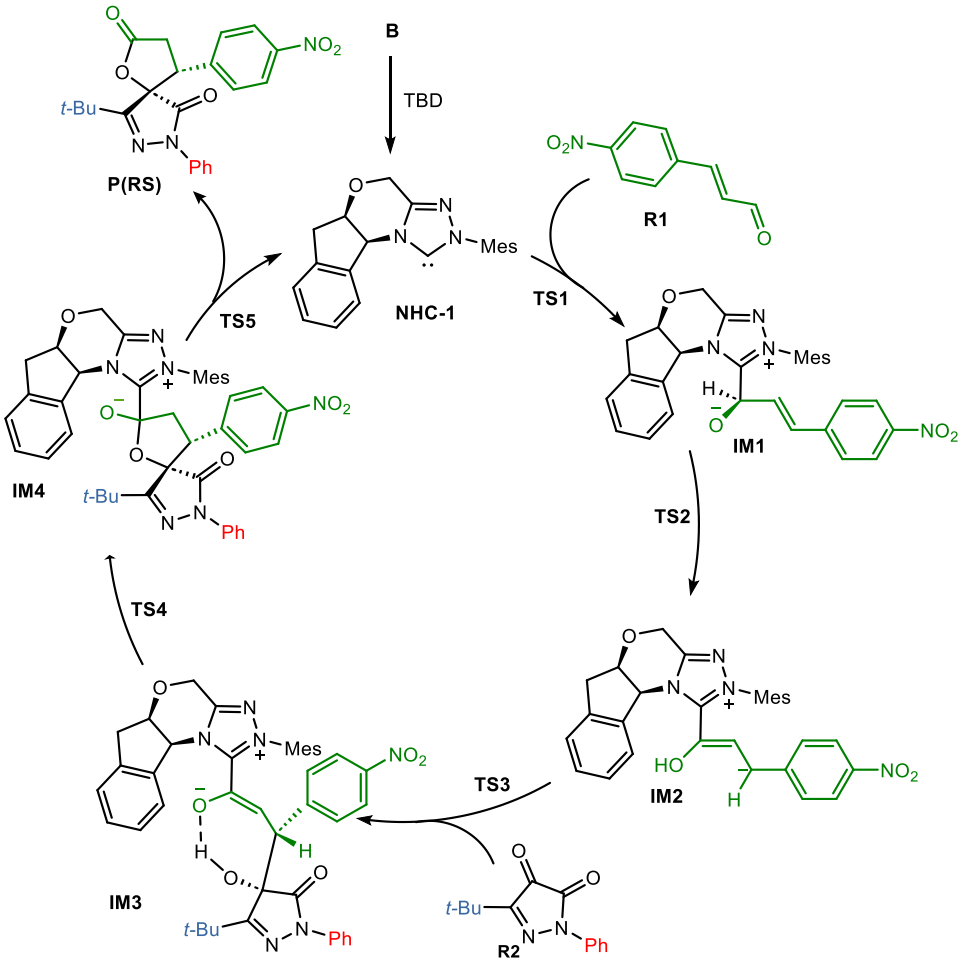

Scheme 2.8: Catalytic cycle of [3+2] annulation reaction.

The free energy profile for the first stage is shown in Scheme 2.9. According to our calculations, the rate-limiting step in this stage is the hydrogen migration and formation of Breslow intermediate. The free energy barrier for the intramolecular hydrogen migration is too high (> 50 kcal·mol^{-1}). However, this energy barrier shrinks to 27.56 kcal·mol^{-1} if assisted by two water molecules that could be present in catalytic concentrations in the bulk, and to 22.92 kcal·mol^{-1} if hydrogen migration is assisted by TBD.[21] Depending on the side of the carbene attack with respect to the aldehyde, the reaction can proceed *via* a *Re*/*Si* path. As it is shown in Scheme 2.9, the barrier for the *Si* mechanism is larger, regardless of whether the reaction is assisted by water or TBD. Accordingly, from this step, we only focused on the *Re* mechanism.

[21] M. J. Ajitha, C. H. Suresh *Tetrahedron Lett.* **2013**, *54*, 7144–7146.

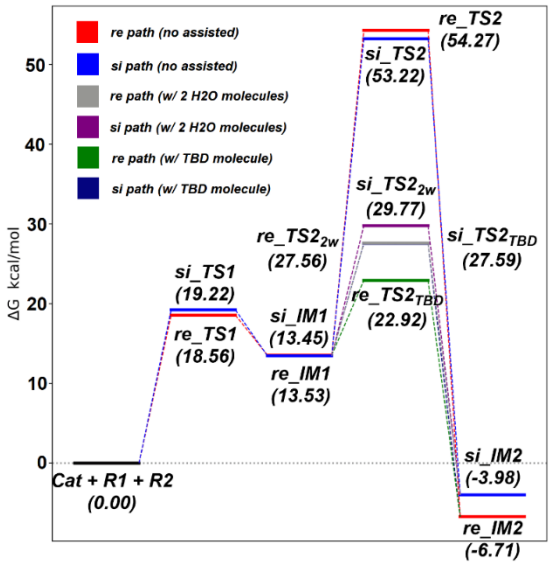

Scheme 2.9: Free-energy profile of the first stage of the reaction. The solvation-corrected relative free-energies at the SMD(toluene)/M06-2X/maug-cc-pVTZ level are given in kcal·mol^{-1}.

In the second stage, whose energy profile is depicted in Scheme 2.10, **R2(1d)** reacts with the activated aldehyde (***Re*_IM2**), leading to the formation of **P(3de)** and the release of the NHC catalyst. This stage consists of three further steps: addition of the pyrazolin-4,5-dione (third step), lactonization (fourth step) and release of NHC (fifth step). Of these steps, the 4th step is the rate-limiting step and also will determine the enantiomeric and diastereomeric ratios.

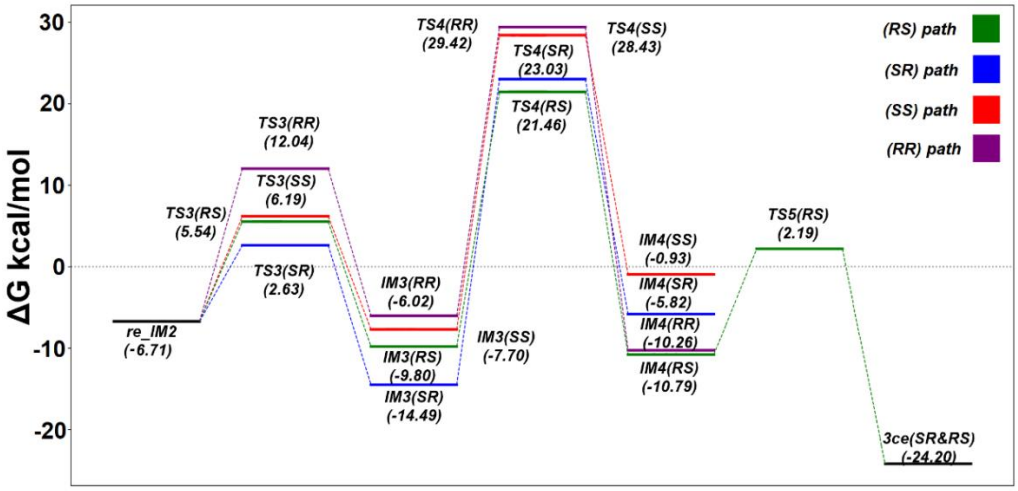

Scheme 2.10: Free-energy profile of the second stage of the reaction. The solvation-corrected relative free-energies at the SMD(toluene)/M06-2X/maug-cc-pVTZ level are given in kcal·mol^{-1}.

As it is depicted in Figure 2.3, depending on the mode of attack of the pyrazoldione **R2(1d)** in the third step, and as a consequence of two proquiral faces in both **R2** as Breslow intermediate ***Re*_IM2**, we could find four different mechanisms that will produce four different stereoisomers (*SS*), (*SR*), (*RR*) and (*RS*).

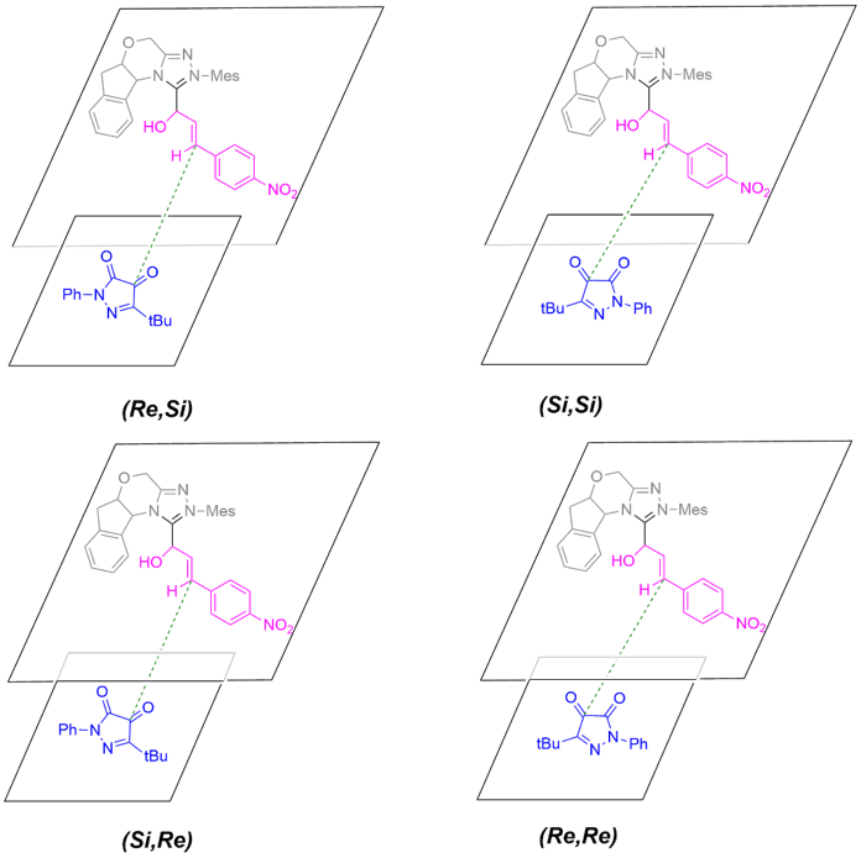

Figure 2.3: Diagram of the four possible modes of attack of **R2(1d)** on ***Re*_IM2**. The energies of the transition states originated from these modes of attack are shown in Scheme 2.10 (**TS3**).

The formation of rotational conformers associated with the *Z*-configuration of the C=C bond was not feasible due to the high energy barrier associated with C=C torsion (above 30 kcal·mol^{-1}). Although the free-energy barrier for the four pathways is considerably different ranging from 2.63 to 12.04 kcal·mol^{-1}, all barriers are well below those obtained in the 4th step. In this step, formation of the lactone proceeds with basis assistance. First, a proton transfer from the hydroxyl group at C4-position of the pyrazoldione moiety to the α-carbon atom of the homoenolate intermediate *via* protonation of the basis (TBD), Figure 2.4. Then, TBD dissociates and spontaneous rearrangement occurs affording **IM4**. Our calculations predict that the free energy barrier is lower for the (*RS*) mechanism, which after NHC release that

proceeds with almost no barrier, will produce the **P(*RS*)(3de)** product. This is also the main product obtained experimentally (with an er of 94:6).

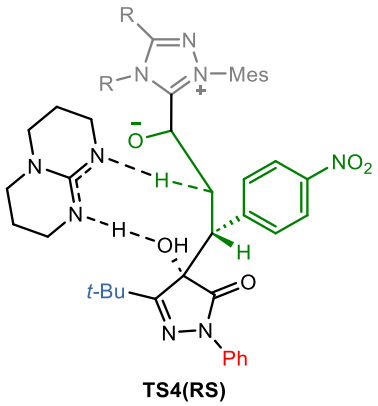

TS4(RS)

Figure 2.4: Transition state determining the stereoselectivity of the process.

To rationalize the origin of the enantioselectivity, we analyse the structure of the four **TS4**, Figure 2.5. According to **TS4** structures, there is a good correlation between the degree of synchronicity of the two proton transfer steps at the saddle point and the energy barrier, as it was previously observed for Diels–Alder reactions.[22] For the **TS4**(*SR*) and **TS4**(*RS*) structures, both protons are located between **IM3** and TBD at the TS, while for **TS4**(*SS*) the OH group of pyrazoldione has not been deprotonated, and for **TS4** (*RR*) this proton has already been transferred to TBD. To quantify the origin of the differences, we combine the distortion-interaction analysis (following the analysis carried out for other NHC-catalysis articles[20a,d,23]) with the energy decomposition analysis (carried out using QChem 5.2[24,25]) and a 6–31G basis set. Leaving aside the entropic contribution, stabilization of the **TS4**(*RS*) is traced back from a more favourable interaction, which is induced by the relaxation of the molecular orbitals of the fragments (lower polarization energy).

[22] P. Vermeeren, T. A. Hamlin, F. M. Bickelhaupt *Phys. Chem. Chem. Phys.* **2021**, *23*, 20095–20106.
[23] Y. Lin, Z. Zhang *RSC Adv.* **2019**, *9*, 7635–7644.
[24] R. Z. Khaliullin, E. A. Cobar, R. C. Lochan, A. T. Bell, M. Head-Gordon *J. Phys. Chem. A* **2007**, *111*, 8753–8765.
[25] Y. Shao, Z. Gan, E. Epifanovsky, A. T. B. Gilbert, M. Wormit, J. Kussmann, *et al. Mol. Phys.* **2015**, *113*, 184.

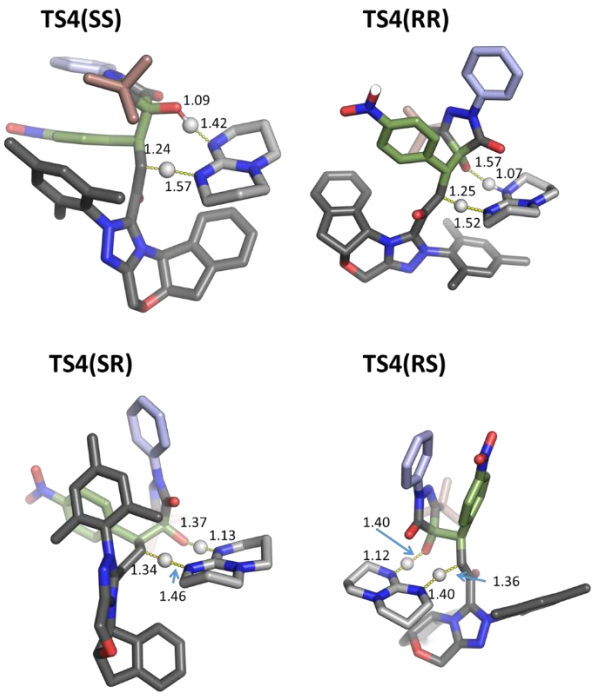

Figure 2.5: Structure of the four **TS4.** The relevant rOH, rCH and rNH distances are shown. Colour scheme corresponds to that used. Hydrogens other than those transferred in the reaction are not shown.

2.3 Conclusions

In this chapter, we have described the first asymmetric synthesis of spiropyrazolone γ-butyrolactones from 1*H*-pyrazol-4,5-diones and enals by an NHC-catalyzed [3+2] annulation process. The developed protocol is mild and tolerates a wide range of substituents on both substrates. The use of Bode catalyst in this cascade reaction provided the enantioenriched spirocyclic compounds containing two contiguous stereogenic centers in good yields (up to 93%) with excellent diastereoselectivity (dr> 99:<1) and good enantioselectivity (up to er 94:6). To understand the catalytic mechanism and origin of stereoselectivity, electronic structure calculations were carried out. These indicate that the Brϕnsted base used to generate the carbene NHC also assists the hydrogen migration for the generation of homoenolate. Furthermore, the formation of the lactone that proceeds after the pyrazolin-4,5-dione attack on the Breslow intermediate is the rate-limiting step and determining of the enantio- and diastereomeric ratios. The pathway responsible for the *RS*-configuration of spirocyclic pyrazolones has been identified to be the most favorable one.

2.4 References

1. A. Quintavalla *Curr. Med. Chem*. **2018**, *25*, 917–962.
2. J. Yang, B. -W. Pan, L. Chen, Y. Zhou, X. -L. Liu *Chem. Synth.* **2023**, *3*, 7–61.
3. B. M. Trost, K. Hirano *Org. Lett*. **2012**, *14*, 2446–2449.
4. (a) Z. -T. Yang, J. Zhao, W. -L. Yang, W. -P. Deng *Org. Lett.* **2019**, *21*, 1015–1020, (b) L. Chen, Z. -J. Wu, M. -L. Zhang, D. -F. Yue, X. -M. Zhang, X. -Y. Xu, W. -C. Yuan *J. Org. Chem.* **2015**, *80*, 12668–12675, (c) S. Jayakumar, S. Muthusamy, M. Prakash, V. Kesavan *Eur. J. Org. Chem.* **2014**, 1893–1898, (d) Q. -L. Wang, L. Peng, F. -Y. Wang, M. -L. Zhang, L. -N. Jia, F. Tian, X. -Y. Xu, L. -X. Wang *Chem. Commun.* **2013**, *49*, 9422–9424.
5. (a) S. Rana, E. C. Blowers, C. Tebbe, J. I. Contreras, P. Radhakrishnan, S. Kizhake, T. Zhou, R. N. Rajule, J. L. Arnst, A. R. Munkarah, R. Rattan, A. Natarajan *J. Med. Chem*. **2016**, *59*, 5121–5127, (b) B. Yu, D. -Q. Yu, H. -M. Liu *Eur. J. Med. Chem*. **2015**, *97*, 673–698, (c) S. -S. Ma, W. -L. Mei, Z. -K. Guo, S. -B. Liu, Y. -S. Zhao, D. -L. Yang, Y. -B. Zeng, B. Jiang, H. -F. Dai *Org. Lett*. **2013**, *15*, 1492–1495.
6. Y. Liu, X. Zhang, R. Zeng, Y. Zhang, Q. -S. Dai, H. -J. Leng, X. -J. Gou, J. -L. Li *Molecules* **2017**, *22*, 1882–1904.
7. X. -Y. Chen, K. -Q. Chen, D. -Q. Sun, S. Ye *Chem. Sci.* **2017**, *8*, 1936–1941.
8. J. Xu, S. Yuan, M. Miao, Z. Chen *J. Org. Chem.* **2016**, *81*, 11454–11460.
9. (a) Y. Reddi, R. B. Sunoj *ACS Catal.* **2017**, *7*, 530–537, (b) J. -L. Li, B. Sahoo, C. -G. Daniliuc, F. Glorius *Angew. Chem. Int. Ed. Engl.* **2014**, *53*, 10515–10519, (c) J. Dugal-Tessier, E. A. O'Bryan, T. B. H. Schroeder, D. T. Cohen. K. A. Scheidt *Angew. Chem. Int. Ed.* **2012**, *51*, 4963–4967.
10. S. R. Yetra, S. Mondal, S. Mukherjee, R. G. Gonnade, A. T. Biju *Angew. Chem. Int. Ed.* **2016**, *55*, 268–272.
11. C. Zhao, K. Shi, G. He, Q. Gu, Z. Ru, L. Yang, G. Zhong *Org. Lett.* **2019**, *21*, 7943–7947.
12. L. Wang, S. Li, P. Chauhan, D. Hack, A. R. Philipps, R. Puttreddy, K. Rissanen, G. Raabe, D. Enders *Chem. Eur. J.* **2016**, *22*, 5123–5127.
13. X. -Y. Chen, Z. -H. Gao, S. Ye *Acc. Chem. Res.* **2020**, *53*, 690–702.
14. Er >99: <1 was confirmed *via* chiral HPLC analysis.
15. Y. Zhao, D. G. Truhlar *Theor. Chem. Acc.* **2008**, *120*, 215–241.
16. M. J. Frisch, G. W. Trucks, H. B. Schlegel, G. E. Scuseria, M. A. Robb, J. R. Cheeseman, *et al.*, Gaussian-16 Revision A.03, Gaussian Inc., Wallingford, CT, **2016**.
17. A. V. Marenich, C. J. Cramer, D. G. Truhlar *J. Phys. Chem. B*, **2009**, *113*, 6378–6396.
18. A. Hollwarth, M. Bohme, S. Dapprich, A. W. Ehlers, A. Gobbi, V. Jonas, K. F. Kohler, R. Stegmann, A. Veldkamp, G. Frenking *Chem. Phys. Lett.* **1993**, *208*, 237–240.
19. (a) S. Rayne, K. Forest *J. Comput. Theor. Chem.* **2016**, *1090*, 147–152, (a) E. Papajak, D. G. Truhlar *J. Chem. Theory Comput.* **2010**, *6*, 597–601.
20. (*a*) Y. Li, Z. Li, Z. Zhang *Mol. Catal.* **2020**, *496*, 111183–111192, (*b*) Y. Li, Z. Zhang *Eur. J. Org. Chem.* **2019**, *2019*, 2989–2997, (*c*) J. Gao, Y. Wang *Org. Biomol. Chem.* **2019**, *17*, 7442–7447, (*d*) Y. Li, Z. Zhang, C. Liang *Org. Biomol. Chem.* **2018**, *16*, 9251–9258.
21. M. J. Ajitha, C. H. Suresh *Tetrahedron Lett.* **2013**, *54*, 7144–7146.

22. P. Vermeeren, T. A. Hamlin, F. M. Bickelhaupt *Phys. Chem. Chem. Phys.* **2021**, *23*, 20095–20106.
23. Y. Lin, Z. Zhang *RSC Adv.* **2019**, *9*, 7635–7644.
24. R. Z. Khaliullin, E. A. Cobar, R. C. Lochan, A. T. Bell, M. Head-Gordon *J. Phys. Chem. A* **2007**, *111*, 8753–8765.
25. Y. Shao, Z. Gan, E. Epifanovsky, A. T. B. Gilbert, M. Wormit, J. Kussmann, *et al. Mol. Phys.* **2015**, *113*, 184.

2.5 Experimental section

2.5.1 General Procedure for Spirocyclic Pyrazolone γ-Butyrolactones.

In a dried 5 mL heat gun-dried flask equipped with a magnetic stirring bar the pre-catalyst **A-E** (0.006 mmol, 0.1 equiv) was weighed. Then pyrazolin-4,5-dione **1a–f** (0.06 mmol) and enal **2a–g** (0.06 mmol, 1.0 equiv) were added under a N_2 atmosphere. Dry toluene (1 mL) was added and the mixture was stirred several minutes. Finally, the base (0.03 mmol, 0.5 equiv) was introduced to the flask. After 16 h, the solvent was straight removed under reduced pressure and the residue was purified by column chromatography (hexane/ethyl acetate, 10/1) to give the desired compound.

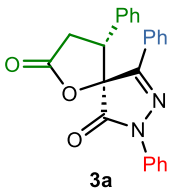

3a

(4*R*,5*S*)-4,7,9-Triphenyl-1-oxa-7,8-diazaspiro[4.4]non-8-ene-2,6-dione (3a). Yellow oil (16.5 mg, 72% yield). $[\alpha]^{25}_{D}$= -101.6 (c= 0.1, $CHCl_3$, er 86:14). ^{1}H NMR (500 MHz, $CDCl_3$) δ 2.93 (dd, *J*= 17.1, 8.2 Hz, 1H), 3.82 (dd, *J*= 14.0, 13.8 Hz, 1H), 4.15 (dd, *J*= 13.8, 8.2 Hz, 1H), 7.11-7.13 (m, 2H), 7.14-7.18 (m, 1H), 7.22-7.31 (m, 5H), 7.43-7.45 (m, 2H), 7.54-7.59 (m, 3H), 7.98-8.00 (m, 2H). ^{13}C NMR (126 MHz, $CDCl_3$) δ 30.3, 49.0, 87.8, 119.5, 126.1, 126.8, 127.6, 128.6, 128.7, 128.8, 129.1, 129.4, 130.5, 131.5, 136.5, 153.2, 168.7, 173.5. IR ν_{max}/cm^{-1} 751, 919, 1076, 1160, 1291, 1308, 1324, 1398, 1452, 1492, 1596, 1720, 1804, 2859, 2927. HRMS (ESI-TOF) m/z: calcd for $C_{24}H_{18}N_2NaO_3$ $[M+Na]^+$ 405.1210. Found 405.1220. HPLC (Lux Amylose-1, n-hexane/2-propanol 70:30, λ= 254 nm, 0.8 mL/min): t_R (minor)= 8.2 min, t_R (major)= 9.8 min, (er 86:14).

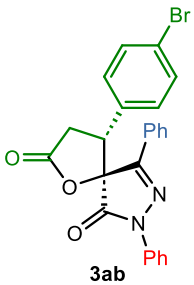

3ab

(4*R*,5*S*)-4-(4-Bromophenyl)-7,9-diphenyl-1-oxa-7,8-diazaspiro[4.4]non-8-ene-2,6-dione (3ab). Yellow oil (12.7 mg, 46% yield). $[\alpha]^{25}_{D}$= -29.2 (c= 0.2, $CHCl_3$, er 81:19). ^{1}H NMR (500 MHz, $CDCl_3$) δ 2.93 (dd, *J*= 17.0, 8.2 Hz, 1H), 3.75 (dd, *J*= 17.0, 13.8 Hz, 1H), 4.11 (dd, *J*= 13.7, 8.1 Hz, 1H), 6.97- 7.00 (m, 2H), 7.18-7.22 (m, 1H), 7.32-7.39 (m, 4H), 7.47-7.49 (m, 2H), 7.53-7.59 (m, 3H), 7.95- 7.97 (m, 2H). ^{13}C NMR (126 MHz, $CDCl_3$) δ 30.4, 48.4, 87.4, 119.4, 123.3, 126.3, 126.8, 128.6, 128.9, 129.3, 129.5, 129.6, 131.6, 132.0, 136.4, 153.1, 168.4, 173.0. IR ν_{max}/cm^{-1} 1023, 1010, 1047, 1077, 1157, 1328, 1395,

1445, 1492, 1596, 1724, 1807, 2853, 29323, 2957, 3065. HRMS (ESI-TOF) m/z: calcd for $C_{24}H_{17}BrN_2NaO_3$ $[M+Na]^+$ 483.0315. Found 483.0324. HPLC (Lux Amylose-1, n-hexane/2-propanol 90:10, λ= 210 nm, 1 mL/min): t_R (minor)= 15.0 min, t_R (major)= 26.6 min, (er 81:19).

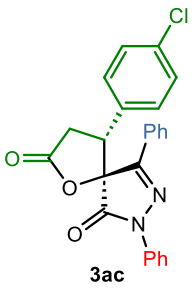

3ac

(4*R*,5*S*)-4-(4-Chlorophenyl)-7,9-diphenyl-1-oxa-7,8-diazaspiro[4.4]non-8-ene-2,6-dione (3ac). White solid (16.9 mg, 64% yield). Mp 188-190°C (from chloroform). $[\alpha]^{25}_D$= -43.0 (c= 0.4, $CHCl_3$, er 81:19). ^{1}H NMR (500 MHz, $CDCl_3$) δ 2.94 (dd, *J*= 16.9, 8.1 Hz, 1H), 3.76 (dd, *J*= 16.9, 13.7 Hz, 1H), 4.12 (dd, *J*= 13.8, 8.2 Hz, 1H), 7.05 (d, *J*= 8.5, 2H), 7.18-7.24 (m, 3H), 7.34 (t, *J*= 7.6 Hz, 2H), 7.49 (d, *J*= 7.7 Hz, 2H), 7.53-7.59 (m, 3H), 7.97 (dd, *J*= 3.3, 1.6 Hz, 2H). ^{13}C NMR (126 MHz, $CDCl_3$) δ 30.5, 48.3, 87.5, 119.4, 126.3, 126.8, 128.6, 128.9, 129.0, 129.1, 129.2, 129.5, 131.6, 135.1, 136.4, 153.1, 168.5, 173.0. IR ν_{max}/cm^{-1} 1157, 1298, 1399, 1445, 1486, 1596, 1720, 1807, 2856, 2923, 2954, 3064. HRMS (ESI-TOF) m/z: calcd for $C_{24}H_{17}ClN_2NaO_3$ $[M+Na]^+$ 439.0820. Found 439.0834. HPLC (Lux i-Cellulose-5, n-hexane/2-propanol 85:15, λ= 210 nm, 1 mL/min): t_R (minor)= 10.8 min, t_R (major)= 16.7 min, (er 81:19).

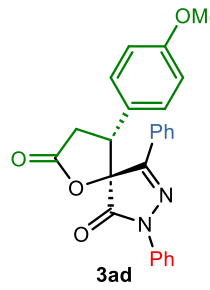

3ad

(4*R*,5*S*)-4-(4-Methoxyphenyl)-7,9-diphenyl-1-oxa-7,8-diazaspiro[4.4]non-8-ene-2,6-dione (3ad). Pale yellow oil (17.6 mg, 71% yield). $[\alpha]^{25}_D$= -5.9 (c= 0.1, $CHCl_3$, er 74:26). ^{1} H NMR (500 MHz, $CDCl_3$) δ 2.89 (dd, *J*= 17.0, 8.1 Hz, 1H), 3.68 (s, 3H), 3.74 (dd, *J*= 16.8, 13.9 Hz, 1H), 4.09 (dd, *J*= 13.7, 8.0 Hz, 1H), 6.74 (d, *J*= 8.7 Hz, 2H), 7.02 (d, *J*= 8.6 Hz, 2H), 7.15 (t, *J*= 7.3 Hz, 1H), 7.30 (t, *J*= 7.7 Hz, 2H), 7.48 (d, *J*= 8.2 Hz, 2H), 7.55-7.53 (m, 3H), 7.96 (d, *J*= 7.8 Hz, 2H). ^{13}C NMR (126 MHz, $CDCl_3$) δ 29.7, 48.4, 55.2, 87.9, 114.2, 119.4, 122.2, 126.1, 126.8, 128.7, 128.8, 128.9, 129.4, 129.5, 131.4, 136.6, 153.3, 159.9, 173.5. IR ν_{max}/cm^{-1} 802, 953, 1063, 1399, 1462, 1496, 1516, 1593, 1613, 1727, 1811, 2859, 2924, 2954. HRMS (ESI-TOF) m/z: calcd for $C_{25}H_{20}KN_2O_4$ $[M+K]^+$ 451.1055. Found 451.1058. HPLC (Lux Amylose-1, n-hexane/2-propanol 90:10, λ= 254 nm, 1 mL/min): t_R (minor)= 18.1 min, t_R (major)= 29.9 min, (er 74:26).

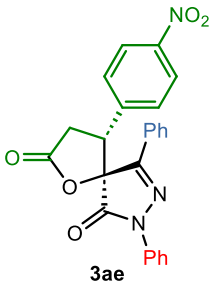

3ae

(4*R*,5*S*)-4-(4-Nitrophenyl)-7,9-diphenyl-1-oxa-7,8-diazaspiro[4.4]non-8-ene-2,6-dione (3ae). Yellow oil (23.9 mg, 93% yield). $[\alpha]^{25}_D$= -45.8 (c= 0.2, $CHCl_3$, er 77:23). ^{1}H NMR (500 MHz, $CDCl_3$) δ 3.01 (dd, *J*= 16.9, 8.4 Hz, 1H), 3.83 (dd, *J*= 16.9, 13.5 Hz, 1H), 4.24 (dd, *J*= 13.6, 8.1 Hz, 1H), 7.17 (t, *J*= 7.9 Hz, 1H), 7.28-7.33 (m, 4H), 7.48 (d, *J*= 8.1 Hz, 2H), 7.56-7.61 (m, 3H), 7.98 (dd, *J*= 7.1, 1.0 Hz, 2H), 8.11 (d, *J*= 8.6 Hz, 2H). ^{13}C NMR (126 MHz, $CDCl_3$) δ 30.4, 48.4, 87.1, 119.0, 124.0, 126.4, 126.7, 128.4, 128.8, 129.0, 129.6, 131.9, 136.2, 137.9, 148.2, 152.9, 168.0, 172.3. IR ν_{max}/cm^{-1} 760, 840, 1071, 1164, 1307, 1324, 1344, 1398, 1491, 1524, 1598, 1644, 1725, 1814, 2872, 2946, 3009, 3059. HRMS (ESI-TOF) m/z: calcd for $C_{24}H_{17}N_3NaO_5$ $[M+Na]^+$ 450.1060. Found 450.1068. HPLC (Lux Amylose-1, n-hexane/2-propanol 90:10, λ= 210 nm, 1 mL/min): t_R (minor)= 32.5 min, t_R (major)= 51.1 min, (er 77:23).

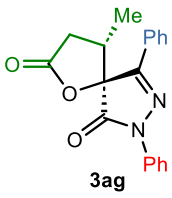

3ag

(4*S*,5*S*)-4-Methyl-7,9-diphenyl-1-oxa-7,8-diazaspiro[4.4]non-8-ene-2,6-dione (3ag). Pale yellow oil (11.9 mg, 62% yield). $[\alpha]^{25}_{D}$= -70.5 (c= 0.1, $CHCl_3$, er 80:20). ^{1}H NMR (500 MHz, $CDCl_3$) δ 1.12 (d, *J*= 5.8 Hz, 3H), 2.75 (dd, *J*= 22.7, 14.1 Hz, 1H), 3.02-2.96 (m, 2H), 7.27 (t, *J*= 7.6 Hz, 1H), 7.44- 7.52 (m, 5H), 7.91 (d, *J*= 6.9 Hz, 2H), 7.95 (d, *J*= 8.6 Hz, 2H). ^{13}C NMR (126 MHz, $CDCl_3$) δ 12.6, 33.1, 38.7, 87.6, 118.9, 126.0, 126.7, 128.5, 129.1, 129.2, 131.4, 137.2, 153.9, 169.0, 174.0. IR ν_{max}/cm^{-1} 1338, 1409, 1452, 1492, 1596, 1714, 1811, 2850, 2927, 2967. HRMS (ESI-TOF) m/z: calcd for $C_{19}H_{16}N_2NaO_3$ $[M+Na]^+$ 343.1053. Found 343.1059. HPLC (Lux i-Cellulose-5, n-hexane/2- propanol 95:5, λ= 210 nm, 0.8 mL/min): t_R (minor)= 48.0 min, t_R (major)= 54.1 min, (er 80:20).

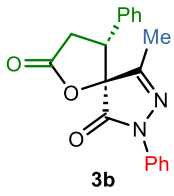

3b

(4*R*,5*S*)-9-Methyl-4,7-diphenyl-1-oxa-7,8-diazaspiro[4.4]non-8-ene-2,6-dione (3b). Yellow oil (9.4 mg, 49% yield). Major diastereomer: $[\alpha]^{25}_{D}$= -161.5 (c= 0.2, EtOAc, er 81:19). ^{1}H NMR (500 MHz, $CDCl_3$) δ 2.37 (s, 3H), 2.90 (dd, *J*= 16.8, 7.9 Hz, 1H), 3.76 (dd, *J*= 16.8, 13.7 Hz, 1H), 3.98 (dd, *J*= 13.6, 7.8 Hz, 1H), 7.12 (tt, *J*= 7.3, 1.2 Hz, 1H), 7.22-7.32 (m, 7H), 7.37 (dd, *J*= 8.8, 1.3 Hz, 2H). ^{13}C NMR (126 MHz, $CDCl_3$) δ 12.9, 30.6, 47.3, 87.3, 119.1, 125.8, 127.4, 128.7, 129.0, 129.1, 130.6, 136.5, 155.7, 168.3, 173.4. IR ν_{max}/cm^{-1} 1120, 1157, 1371, 1408, 1455, 1499, 1596, 1726, 1804, 2853, 2920, 2957, 2997, 3031, 3054. HRMS (ESI-TOF) m/z: calcd for$C_{19}H_{16}N_2NaO_3$ $[M+Na]^+$ 343.1053. Found 343.1061. HPLC (Lux Amylose-1, n-hexane/2-propanol 80:20, λ= 254 nm, 0.6 mL/min): t_R (minor)= 15.9 min, t_R (major)= 19.2 min, (er 81:19).

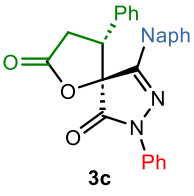

3c

(4*R*,5*S*)-9-(Naphthalen-2-yl)-4,7-diphenyl-1-oxa-7,8-diazaspiro[4.4]non-8-ene-2,6-dione (3c). Yellow oil (11.7 mg, 45% yield). $[\alpha]^{25}_{D}$= -33.9 (c= 0.2, $CHCl_3$, er 81:19). ^{1}H NMR (500 MHz, $CDCl_3$) δ 2.99 (dd, *J*= 17.1, 8.1 Hz, 1H), 3.86 (dd, *J*= 17.0, 13.8 Hz, 1H), 4.26 (dd, *J*= 11.9, 6.6 Hz, 1H), 7.11- 7.13 (m, 2H), 7.18 (t, *J*= 7.4 Hz, 1H), 7.23-7.26 (m, 2H), 7.32 (t, *J*= 1.3 Hz, 3H), 7.47 (dd, *J*= 8.8, 1.2 Hz, 2H), 7.59-7.65 (m, 2H), 7.92-7.94 (m, 1H), 7.98-8.02 (m, 2H), 8.12 (dd, *J*= 8.6, 1.7 Hz, 1H), 8.38 (br, 1H). ^{13}C NMR (126 MHz, $CDCl_3$) δ 30.3, 49.4, 88.0, 119.6, 123.1, 126.1, 126.2, 127.2, 127.3, 127.6, 128.0, 128.1, 128.8, 128.9, 129.0, 129.1, 129.5, 130.4, 133.0, 134.5, 136.5, 153.1, 168.7, 173.6. IR ν_{max}/cm^{-1} 755, 775, 1164, 1362, 1459, 1502, 1600, 1723, 1804, 2927, 2947. HRMS (ESI-TOF) m/z: calcd for $C_{28}H_{20}N_2NaO_3$ $[M+Na]^+$ 455.1366. Found 455.1360. HPLC (Lux iCellulose-5, n-hexane/2-propanol 80:20, λ= 254 nm, 0.6 mL/min): t_R (major)= 35.0 min, t_R (minor)= 47.1 min, (er 81:19).

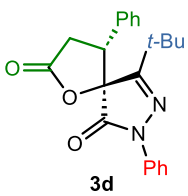

3d

(4*R*,5*S*)-9-(tert-Butyl)-4,7-diphenyl-1-oxa-7,8-diazaspiro[4.4]non-8-ene-2,6-dione (3d). Yellow oil (13.7 mg, 63% yield). $[\alpha]^{25}_{D}$= -150.5 (c= 0.2, $CHCl_3$, er 87:13). ^{1}H NMR (500 MHz, $CDCl_3$) δ 1.52 (s, 9H), 2.86 (dd, *J*= 17.0, 8.4 Hz, 1H), 3.73 (dd, *J*= 17.0, 13.4 Hz, 1H), 4.40 (dd, *J*= 13.4, 8.4 Hz, 1H), 7.10 (m, 1H), 7.21-7.23 (m, 2H), 7.24-7.26 (m, 5H), 7.32-7.36 (m, 2H). ^{13}C NMR (126 MHz, $CDCl_3$) δ 29.3, 30.1, 36.6, 47.2, 89.1, 119.0, 125.6, 127.3, 128.6, 128.8, 128.9, 131.2, 136.5, 163.7, 168.8, 173.4. IR ν_{max}/cm^{-1} 684, 757, 890, 1087, 1107, 1381, 1494, 1598,

1718, 1761, 1805, 2925, 2969, 3029. HRMS (ESI-TOF) m/z: calcd for $C_{22}H_{23}N_2O_3$ $[M+H]^+$ 363.1703. Found 363.1709. HPLC (Lux i-Cellulose-5, n-hexane/2-propanol 80:20, λ= 254 nm, 0.8 mL/min): t_R (minor)= 16.6 min, t_R (major)= 21.5 min, (er 87:13).

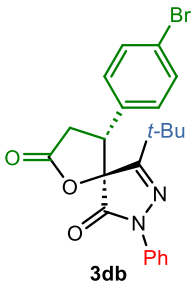

3db

(4*R*,5*S*)-4-(4-Bromophenyl)-9-(tert-butyl)-7-phenyl-1-oxa-7,8-diazaspiro[4.4]non-8-ene-2,6- dione (3db). White solid (15.4 mg, 58% yield). Mp > 300°C (from hexane). $[\alpha]^{25}_D$= -93.6 (c= 0.1, $CHCl_3$, er 93:7). ^{1}H NMR (500 MHz, $CDCl_3$) δ 1.49 (s, 9H), 2.86 (dd, *J*= 16.9, 8.3 Hz, 1H), 3.66 (dd, *J*= 16.8, 13.2 Hz, 1H), 4.34 (dd, *J*= 13.6, 8.6 Hz, 1H), 7.16-7.10 (m, 3H), 7.31-7.27 (m, 2H), 7.41- 7.36 (m, 4H). ^{13}C NMR (126 MHz, $CDCl_3$) δ 29.3, 30.2, 36.7, 46.7, 88.7, 119.0, 123.1, 125.9, 128.8, 129.0, 130.3, 132.0, 136.4, 163.7, 168.6, 172.9. IR ν_{max}/cm^{-1} 896, 1010, 1083, 1114, 1187, 1382, 1496, 1596, 1724, 1811, 2860, 2874, 2931, 2968. HRMS (ESI-TOF) m/z: calcd for $C_{22}H_{21}BrN_2NaO_3$ [M+Na]+ 463.0628. Found 463.0638. HPLC (Lux i-Cellulose-5, n-hexane/2-propanol 80:20, λ= 254 nm, 0.8 mL/min): t_R (minor)= 16.5 min, t_R (major)= 23.7 min, (er 93:7).

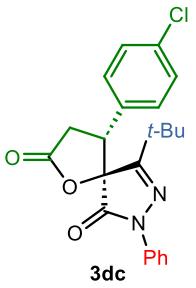

3dc

(4*R*,5*S*)-9-(tert-Butyl)-4-(4-chlorophenyl)-7-phenyl-1-oxa-7,8-diazaspiro[4.4]non-8-ene-2,6- dione (3dc). Yellow oil (15.7 mg, 66% yield). $[\alpha]^{25}_D$= -99.4 (c= 0.3, $CHCl_3$, er 92:8). ^{1}H NMR (500 MHz, $CDCl_3$) δ 1.49 (s, 9H), 2.87 (dd, *J*= 17.1, 8.5 Hz, 1H), 3.67 (dd, *J*= 16.9, 13.4 Hz, 1H), 4.36 (dd, *J*= 13.4, 8.4 Hz, 1H), 7.12-7.18 (m, 3H), 7.24-7.30 (m, 4H), 7.36-7.39 (m, 2H). ^{13}C NMR (126 MHz, $CDCl_3$) δ 29.3, 30.3, 36.7, 46.7, 88.8, 118.9, 125.8, 128.8, 129.0, 129.8, 135.0, 136.4, 163.7, 168.7, 173.0. IR ν_{max}/cm^{-1} 691, 899, 1020, 1114, 1187, 1385, 1499, 1596, 1720, 1808, 2870, 2931, 2967. HRMS (ESI-TOF) m/z: calcd for $C_{22}H_{21}ClN_2NaO_3$ $[M+Na]^+$ 419.1133. Found 419.1139. HPLC (Lux i-Cellulose-5, n-hexane/2-propanol 90:10, λ= 254 nm, 0.8 mL/min): t_R (minor)= 24.5 min, t_R (major)= 36.4 min, (er 92:8).

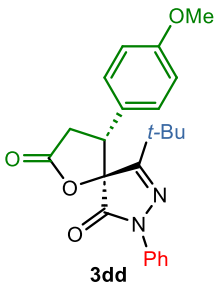

3dd

(4*R*,5*S*)-9-(tert-Butyl)-4-(4-methoxyphenyl)-7-phenyl-1-oxa-7,8-diazaspiro[4.4]non-8-ene-2,6- dione (3dd). Pale yellow oil (16.5 mg, 70% yield). $[\alpha]^{25}_D$= -56.2 (c= 0.4, $CHCl_3$, er 85:15). ^{1}H NMR (500 MHz, $CDCl_3$) δ 1.49 (s, 9H), 2.83 (dd, *J*= 16.9, 8.3 Hz, 1H), 3.67 (dd, *J*= 17.0, 13.5 Hz, 1H), 3.68 (s, 3H), 4.35 (dd, *J*= 13.3, 8.5 Hz, 1H), 6.75-6.79 (m, 2H), 7.11 (tt, *J*= 7.4, 1.1 Hz, 1H), 7.15-7.18 (m, 2H), 7.23-7.28 (m, 2H), 7.37-7.39 (m, 2H). ^{13}C NMR (126 MHz, $CDCl_3$) δ 29.3, 30.4, 36.6, 46.8, 55.2, 89.2, 114.2, 119.0, 123.0, 125.6, 128.6, 128.7, 136.6, 159.9, 163.8, 169.0, 173.5. IR ν_{max}/cm^{-1} 757, 894, 1111, 1187, 1237, 1271, 1384, 1494, 1594, 1611, 1721, 1805, 2872, 2932, 2966, 3083. HRMS (ESI-TOF) m/z: calcd for $C_{23}H_{24}N_2NaO_4$ $[M+Na]^+$ 415.1628. Found 415.1630. HPLC (Lux i-Cellulose-5, n-hexane/2-propanol 95:5, λ= 254 nm, 1 mL/min): t_R (minor)= 53.7 min, t_R (major)= 79.2 min, (er 85:15).

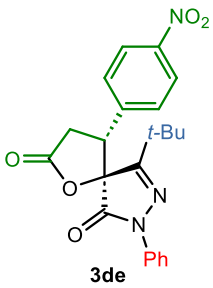

3de

(4*R*,5*S*)-9-(tert-Butyl)-4-(4-nitrophenyl)-7-phenyl-1-oxa-7,8-diazaspiro[4.4]non-8-ene-2,6-dione (3de). Yellow oil (12.5 mg, 51% yield). $[\alpha]^{25}_{D}$= -194.3 (c= 0.3, $CHCl_3$, er 94:6). ^{1}H NMR (500 MHz, $CDCl_3$) δ 1.52 (s, 9H), 2.95 (dd, *J*= 16.8, 8.5 Hz, 1H), 3.74 (dd, *J*= 17.1, 13.6 Hz, 1H), 4.47 (dd, *J*= 13.3, 8.5 Hz, 1H), 7.10-7.14 (m, 1H), 7.24-7.27 (m, 2H), 7.37-7.43 (m, 5H), 8.12-8.14 (m, 2H). ^{13}C NMR (126 MHz, $CDCl_3$) δ 29.2, 30.1, 36.8, 46.8, 88.4, 118.5, 123.9, 126.0, 128.5, 128.8, 138.2, 138.7, 148.0, 163.6, 168.2, 172.2. IR ν_{max}/cm^{-1} 754, 894, 1111, 1184, 1348, 1494, 1517, 1494, 1517, 1594, 1721, 1811, 2869, 2929, 2962, 3079. HRMS (ESI-TOF) m/z: calcd for $C_{22}H_{20}N_3O_5$ $[M+H]^+$ 406.1408. Found 406.1411. HPLC (Lux i-Cellulose-5, n-hexane/2-propanol 80:20, λ= 254 nm, 0.8 mL/min): t_R (minor)= 30.9 min, t_R (major)= 42.2 min, (er 94:6).

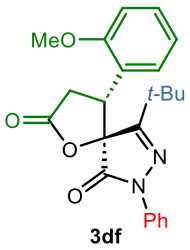

3df

(4*R*,5*S*)-9-(tert-Butyl)-4-(2-methoxyphenyl)-7-phenyl-1-oxa-7,8-diazaspiro[4.4]non-8-ene-2,6- dione (3df). Pale yellow oil (5.4 mg, 23% yield). $[\alpha]^{25}_{D}$= -204.9 (c= 0.1, $CHCl_3$, er 77:23). ^{1}H NMR (500 MHz, $CDCl_3$) δ 1.46 (s, 9H), 2.79 (dd, *J*= 17.2, 8.6 Hz, 1H), 3.64 (dd, *J*= 17.2, 13.5 Hz, 1H), 3.79 (s, 3H), 4.91 (dd, *J*= 13.6, 8.6 Hz, 1H), 6.78 (dd, *J*= 9.2, 0.8 Hz, 1H), 6.90 (dt, *J*= 7.7, 1 Hz, 1H), 7.08 (tt, *J*= 7.1, 1.1 Hz, 1H), 7.18 (td, *J*= 7.6, 1.6 Hz, 1H), 7.21-7.25 (m, 2H), 7.32-7-34 (m, 2H), 7.42 (d, *J*= 7.8, 1.6 Hz, 1H). ^{13}C NMR (126 MHz, $CDCl_3$) δ 28.4, 30.5, 36.7, 40.4, 55.1, 89.1, 110.4, 119.0, 119.6, 120.7, 125.4, 127.8, 128.6, 129.8, 137.0, 157.6, 165.5, 169.5, 174.0. IR ν_{max}/cm^{-1} 745, 899, 1020, 1083, 1114, 1187, 1244, 1288, 1358, 1382, 1462, 1496, 1600, 1720, 1808, 2850, 2964. HRMS (ESI-TOF) m/z: calcd for $C_{23}H_{24}N_2NaO_4$ $[M+Na]^+$ 415.1628. Found 415.1628. HPLC (Lux i-Cellulose-5, n-hexane/2-propanol 80:20, λ= 254 nm, 0.8 mL/min): t_R (minor)= 19.5 min, t_R (major)= 23.7 min, (er 77:23).

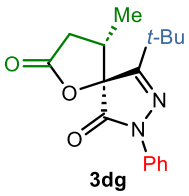

3dg

(4*S*,5*S*)-9-(tert-Butyl)-4-methyl-7-phenyl-1-oxa-7,8-diazaspiro[4.4]non-8-ene-2,6-dione (3dg). Pale yellow oil (10.5 mg, 58% yield). $[\alpha]^{25}_{D}$= -123.8 (c= 0.3, $CHCl_3$, er 92:8). ^{1}H NMR (500 MHz, $CDCl_3$) δ 1.14 (d, *J*= 7.3 Hz, 9H), 2.66 (dd, *J*= 16.9, 8.0 Hz, 1H), 2.99 (dd, *J*= 17.0, 12.0 Hz, 1H), 3.14- 3.25 (m, 1H), 7.22 (t, *J*= 8.5 Hz, 1H), 7.41 (t, *J*= 8.3 Hz, 2H), 7.85 (d, *J*= 9.8 Hz, 2H). ^{13}C NMR (126 MHz, $CDCl_3$) δ 12.5, 29.0, 32.7, 36.3, 37.3, 88.7, 118.6, 125.6, 129.0, 137.2, 164.0, 169.0, 174.0. IR ν_{max}/cm^{-1} 1305, 1382, 1499, 1596, 1720, 1804, 2877, 2907, 2934, 2974. HRMS (ESI-TOF) m/z: calcd for $C_{17}H_{20}N_2NaO_3$ $[M+Na]^+$ 323.1366. Found 323.1371. HPLC (Lux i-Cellulose-5, n-hexane/2- propanol 98:2, λ= 210 nm, 1 mL/min): t_R (major)= 45.4 min, t_R (minor)= 51.2 min, (er 92:8).

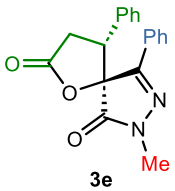

3e

(4*R*,5*S*)-7-Methyl-4,9-diphenyl-1-oxa-7,8-diazaspiro[4.4]non-8-ene-2,6-dione (3e). Pale yellow oil (12.5 mg, 65% yield). $[\alpha]^{25}_{D}$= -81.1 (c= 0.3, $CHCl_3$, er 80:20). ^{1}H NMR (500 MHz, $CDCl_3$) δ 2.86 (dd, *J*= 16.9, 8.0 Hz, 1H), 2.96 (s, 1H), 3.75 (dd, *J*= 16.9, 13.9 Hz, 1H), 4.05 (dd, *J*= 13.8, 8.0 Hz, 1H), 7.04-7.06 (m, 2H), 7.27-7.31 (m, 3H), 7.50-7.53 (m, 3H), 7.86- 7.88 (m, 2H). ^{13}C NMR (126 MHz, $CDCl_3$) δ 30.3, 31.2, 48.6, 87.1, 126.5, 127.6, 128.7, 128.9, 129.0, 129.3, 130.8, 131.1, 152.6, 170.1, 173.6. IR ν_{max}/cm^{-1} 758, 859, 973, 1036, 1164, 1395, 1452, 1496,

1717, 1801, 2931, 2994, 3031, 3068. HRMS (ESI-TOF) m/z: calcd for$C_{19}H_{16}N_2NaO_3$ $[M+Na]^+$ 343.1053. Found 343.1059. HPLC (Lux Amylose-1, n-hexane/2-propanol 90:10, λ= 254 nm, 0.8 mL/min): t_R (minor)= 14.6 min, t_R (major)= 18.1 min, (er 80:20).

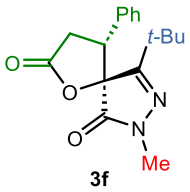

3f

(4*R*,5*S*)-9-(tert-Butyl)-7-methyl-4-phenyl-1-oxa-7,8-diazaspiro[4.4]non-8-ene-2,6-dione (3f). Pale yellow oil (10.5 mg, 58% yield). $[\alpha]^{25}_D$= -122.8 (c= 0.2, $CHCl_3$, er 84:16). ^{1}H NMR (500 MHz, $CDCl_3$) δ 1.42 (s, 9H), 2.80 (s, 3H), 2.81 (dd, *J*= 16.8, 8.3 Hz, 1H), 3.67 (dd, *J*= 16.8, 13.6 Hz, 1H), 4.30 (dd, *J*= 13.6, 8.2 Hz, 1H), 7.18-7.20 (m, 2H), 7.31-7.33 (m, 3H). ^{13}C NMR (126 MHz, $CDCl_3$) δ 29.2, 30.1, 30.7, 36.3, 46.9, 88.4, 127.4, 128.7, 128.8, 131.6, 163.0, 170.3, 173.6. IR ν_{max}/cm^{-1} 1047, 1117, 1184, 1221, 1281, 1365, 1409, 1459, 1707, 1808, 2860, 2961. HRMS (ESI-TOF) m/z: calcd for $C_{17}H_{20}N_2NaO_3$ $[M+Na]^+$ 323.1366. Found 323.1371. HPLC (Lux i-Cellulose-5, n-hexane/2- propanol 80:20, λ= 210 nm, 0.8 mL/min): t_R (minor)= 24.8 min, t_R (major)= 74.8 min, (er 84:16).

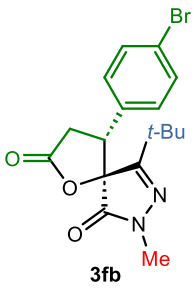

3fb

(4*R*,5*S*)-4-(4-Bromophenyl)-9-(tert-butyl)-7-methyl-1-oxa-7,8-diazaspiro[4.4]non-8-ene-2,6- dione (3fb). Yellow oil (16.2 mg, 71% yield). $[\alpha]^{25}_D$= -108.6 (c= 0.4, $CHCl_3$, er 90:10). ^{1}H NMR (500 MHz, $CDCl_3$) δ 1.40 (s, 9H), 2.79 (dd, *J*= 15.7, 8.1 Hz, 1H), 2.85 (s, 3H), 3.60 (dd, *J*= 15.8, 11.2 Hz, 1H), 4.24 (dd, *J*= 16.3, 8.6 Hz, 1H), 7.07 (d, *J*= 8.2 Hz, 2H), 7.46 (d, *J*= 8.5 Hz, 2H). ^{13}C NMR (126 MHz, $CDCl_3$) δ 29.2, 30.2, 30.9, 36.3, 46.3, 88.0, 122.9, 129., 130.7, 131.9, 162.9, 170.2, 173.0. IR ν_{max}/cm^{-1} 1047, 1114, 1181, 1211, 1419, 1462, 1492, 1720, 1801, 2870, 2921, 2967. HRMS (ESI-TOF) m/z: calcd for $C_{17}H_{19}BrN_2NaO_3$ $[M+Na]^+$ 401.0471. Found 401.0480. HPLC (Lux i-Cellulose-5, n-hexane/2-propanol 80:20, λ= 210 nm, 0.8 mL/min): t_R (minor)= 23.1 min, t_R (major)= 66.1 min, (er 90:10).

2.5.2 Crystallographic data of spirocycle 3ac.

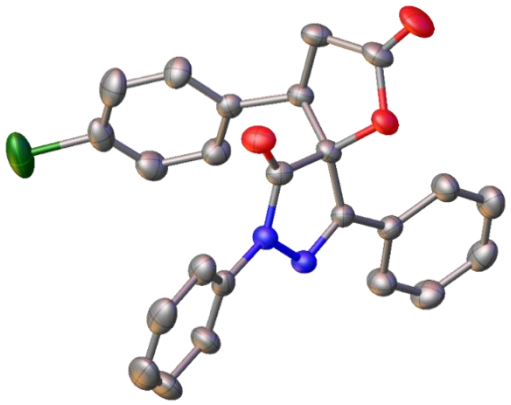

Crystal data and structure refinement for 3ac

Empirical formula	$C_{24}H_{17}ClN_2O_3$
Formula weight	416.84
Temperature/K	293(2)

Crystal system	orthorhombic
Space group	$P2_12_12_1$
a/Å	10.0795(6)
b/Å	13.8030(9)
c/Å	14.5673(11)
α/°	90
β/°	90
γ/°	90
Volume/Å^3	2026.7(2)
Z	4
ρcalcg/cm^3	1.366
μ/mm^{-1}	1.908
F(000)	864.0
Crystal size/mm^3	1.401 × 1.214 × 0.9
Radiation	CuKα (λ = 1.54184)
2Θ range for data collection/°	8.826 to 149.654
Index ranges	-10 ≤ h ≤ 12, -16 ≤ k ≤ 12, -18 ≤ l ≤ 15
Reflections collected	6218
Independent reflections	3944 [R_{int} = 0.0533, R_{sigma} = 0.0550]
Data/restraints/parameters	3944/0/271
Goodness-of-fit on F^2	1.040
Final R indexes [I>=2σ (I)]	R_1 = 0.0735, wR_2 = 0.1866
Final R indexes [all data]	R_1 = 0.0806, wR_2 = 0.1984
Largest diff. peak/hole / e Å^{-3}	0.34/-0.43
Flack parameter	-0.05(3)

Chapter III: Synthesis of Spirocyclic Pyrazolone-Butenolides through *N*-Heterocyclic Carbene catalysis.

"Access to spiropyrazolone-butenolides through NHC-catalyzed [3+2]-asymmetric annulation of 3-bromoenals and 1H-pyrazol-4,5-diones"

Marta Gil-Ordóñez, Alicia Maestro, José M. Andrés *Manuscript submitted and under revision*

3.1 Introduction and background

Butenolides are unsaturated γ-lactones which represent a wide range of natural products with medical and biological importance[1] as they involve interesting activities including anti-inflammatory,[2] antifungal[3] or antimicrobial,[4] among others,[5] Figure 3.1a.

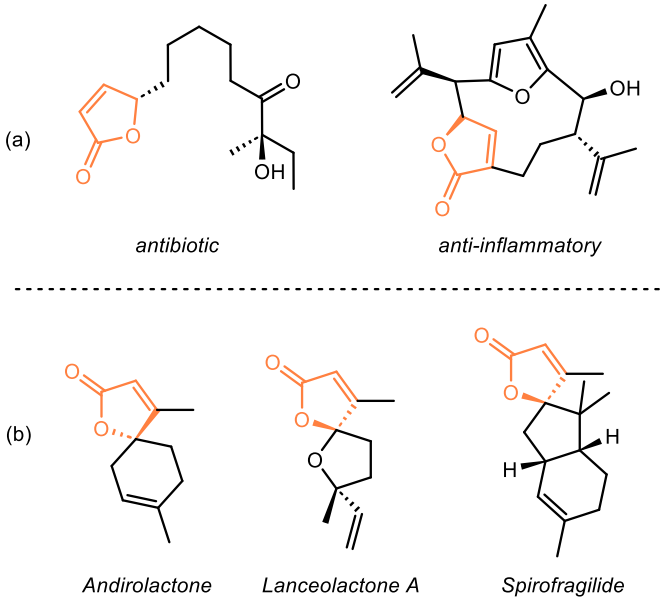

Figure 3.1: Some examples of biologically active butenolide derivatives.

γ-Spirobutenolides are an important subclass within spiro lactones. Biological activity of natural spirocyclic butenolides, Figure 3.1b, has attracted significant efforts towards their synthesis.[6] Among all the strategies reported for the stereoselective synthesis of these challenging spirocycles, few of them are organocatalyzed methods despite their current relevance in asymmetric synthesis. An example is shown in Scheme 3.1, where chiral γ,γ-disubstituted butenolides are prepared *via* trienamine-mediated [4+2] cycloaddition,[7] using diphenylprolinol trimethylsilyl ether as catalyst.

---

[1] (a) K. Tadiparthi, S. Venkatesh *J Heterocyclic Chem.* **2022**, *59*, 1285–1307, (b) S. Chatterjee, R. Sahoo, S. Nanda *Org. Biomol. Chem.* **2021**, *19*, 7298–7332, (c) T. Montagnon, M. Tofi, G. Vassilikogiannakis *Acc. Chem. Res.* **2008**, *41*, 1001–1011, (d) F. Q. Alali, X. -X. Liu, J. L. McLaughlin *J. Nat. Prod.* **1999**, *62*, 504–540.

[2] S. Padakanti, M. Pal, K. R. Yeleswarapu *Tetrahedron* **2003**, *59*, 7915−7920.

[3] M. Pour, M. Spulak, V. Balsanek, J. Kunes, P. Kubanova, V. Buchta *Bioorg. Med. Chem.* **2003**, *11*, 2843−2866.

[4] G. Grossmann, M. Poncioni, M. Bornand, B. Jolivet, M. Neuburger, U. Sequin *Tetrahedron* **2003**, *59*, 3237−3251.

[5] T. R. Hoye, L. Tan *Tetrahedron Lett.* **1995**, *36*, 1981−1984.

[6] *For reviews see:* (a) B. Mandal, B. Thirupathi *Org. Biomol. Chem.* **2020**, *18*, 5287–5314, (b) P. Yadav, R. Pratap, V. J. Ram *Asian J. Org.Chem*. **2020**, *9*, 1377–1409. *Some examples:* (a) D. Dar'in, G. Kantin, E. Chupakhin, V. Sharoyko, M. Krasavin *Chem. Eur. J.* **2021**, *27*, 8221–8227, (b) A. Elagamy, R. Shaw, R. Panwar, Shally, V. J. Ram, R. Pratap *J. Org. Chem.* **2019**, *84,* 1154−1161, (c) U. Albrecht, P. Langer *Tetrahedron* **2007**, *63*, 4648–4654.

[7] (a) A. Skrzynska, P. Drelich, S. Frankowski, Ł. Albrecht *Chem. Eur. J.* **2018**, *24*, 16543–16547, (b) J. Hejmanowska, M. Dzięgielewski, D. Kowalczyk, Ł. Albrecht *Synlett* **2014**, *25*, 2957–2961.

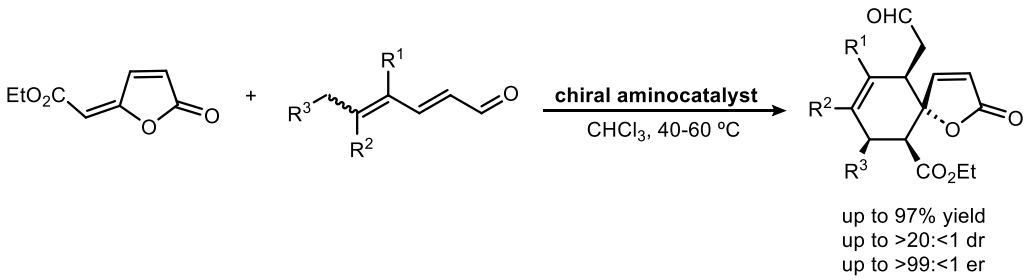

Scheme 3.1: γ,γ-Disubstituted butenolides synthesized through aminocatalysis.

Since *N*-heterocyclic carbenes began to be used as a powerful tool in asymmetric organocatalysis, the scientific community has dedicated effort to elucidate different intermediates and mechanisms that can be involved when NHCs are used. When a carbene reacts with an α, β-unsaturated aldehyde, an *homoenolate* is formed, which will be responsible for the catalytic performance. The presence of halogen atoms at α or β-position of the aldehyde allows other different species to be responsible of the catalytic activity. An *α, β-unsaturated acyl azolium* is formed when α-bromo enals are used in the reaction, Scheme 3.2a. This methodology was employed for the preparation of spirocyclic oxindolo-γ-lactams,[8] 3,4-dihydropyrano[3,2-b]indol-2(5*H*)-ones[9] or 5-disubstituted dihydropyranones.[10] However, when α-chloroaldehydes are used, the catalytic specie is an *azolium enolate*, Scheme 3.2b, as reported by Ye[11] for the synthesis of dihydropyranopyrazolones from pyrazolone-derived oxodienes.

[8] K. -Q. Chen, Y. Li, C. -L. Zhang, D. -Q. Sun, S. Ye *Org. Biomol. Chem* **2016**, *14*, 2007–2014.
[9] Q. Ni, X. Song, G. Raabe, D. Enders *Chem. Asian J.* **2014**, *9*, 1535–1538.
[10] S. R. Yetra, T. Kaicharla, S. S. Kunte, R. G. Gonnade, A. T. Biju *Org. Lett.* **2013**, *15*, 5202–5205.
[11] H. -M. Zhang, H. Ly, S. Ye *Org. Biomol. Chem.* **2013**, *11*, 6255–6257.

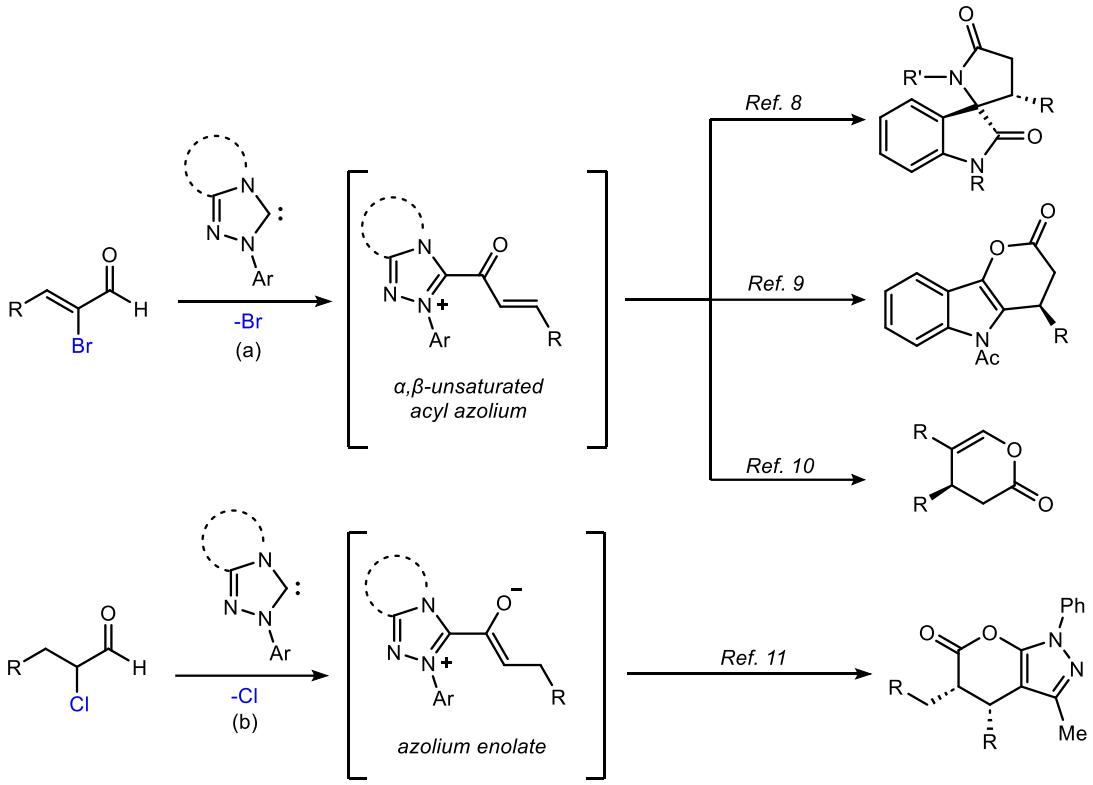

Scheme 3.2: Different catalytic species formed after the reaction of NHCs with halogenated aldehydes at α-position.

In another way, when β-bromo enals react with NHCs, several pathways should also be considered, Scheme 3.3. Ma group[12] showed how the presence of an external oxidant affects to the final result of the reaction. Under oxidizing conditions, an *α, β-unsaturated acyl azolium* intermediate (**I**) with a bromine atom at 3-position will be formed, Scheme 3.3a. But, if there is not an external oxidant, the *homoenolate* will evolve to a classical *α, β-unsaturated acyl azolium* (**II**) with loss of the bromine atom, Scheme 3.3b.

[12] G. Wang, X. Chen, G. Miao, W. Yao, C. Ma *J. Org. Chem.* **2013**, *78*, 12, 6223–6232.

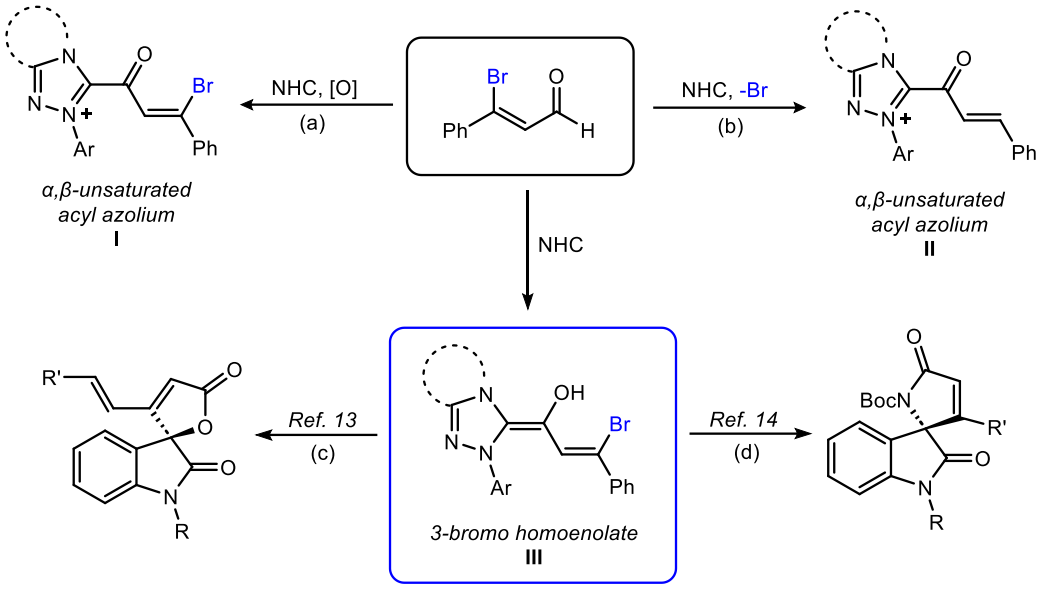

Scheme 3.3: Possible catalytic species formed with β-haloenals.

However, it is also possible to work with the *3-bromo homoenolate* intermediate **III**, formed from the 3-bromoenal and the *N*-heterocyclic carbene, which enables an addition/dehalogenation/lactonization cascade process. This strategy was first used by Ma group[13] for the synthesis of spirooxindole butenolides, Scheme 3.3c. In another approximation, Hui group[14] used the same *3-bromo homoenolate* to synthesize spiro[indoline-3,2'-pyrroles] from isatin-derived ketimines, Scheme 3.3d.

As far as we concerned, there are no examples of the synthesis of spiropyrazolone-butenolides in literature despite the challenging properties that the combination of these motifs could have. In this chapter, we study the [3+2] asymmetric annulation reaction of pyrazolin-4,5-diones and 3-bromoenals through NHC catalysis providing enantioenriched spiropyrazolone-butenolides.

[13] C. Zheng, W. Yao, Y. Zhang, C. Ma *Org. Lett.* **2014**, *16*, 5028–503.
[14] C. Wang, S. Zhu, G. Wang, Z. Li, X. -P. Hui *Eur. J. Org. Chem.* **2016**, 5653–5658.

3.2 Results and discussion

We started the study of the reaction combining pyrazolin-4,5-dione **1a** with 3-bromo cinnamaldehyde **2a** in the presence of pre-catalysts **A**-**C**, DBU as base in THF as solvent at room temperature, Table 1.

Table 1. Screening of pre-catalysts **A-C**[a]

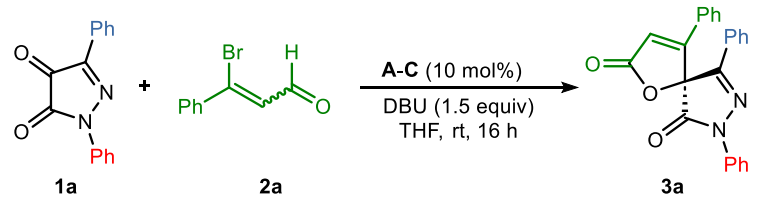

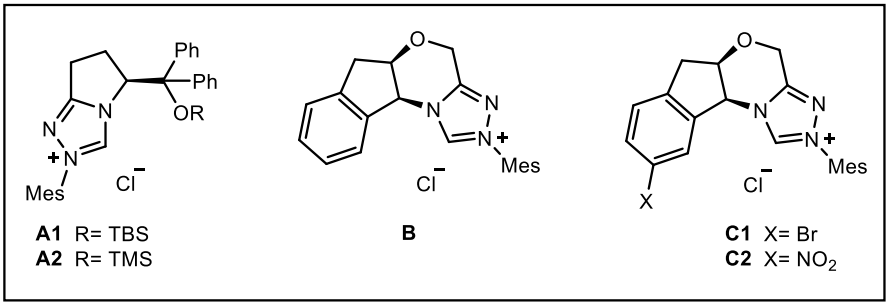

Entry	*pre-NHC*	*Base*	*Yield (%)*[b]	*er*[c]
1	**A1**	DBU	n.r.	-
2	**A2**	DBU	27	96:4
3	**B**	DBU	56	81:19
4	**C1**	DBU	<5	32:68
5	**C2**	DBU	57	92:8

[a] Reaction conditions: **1a** (0.06 mmol), **2a** (0.09 mmol), **A**-**C** (10 mol%), DBU (1.5 equiv), THF (1 mL) at rt for 16 h. [b] Yield of **3a** determined after column chromatography. [c] Er values determined *via* chiral HPLC analysis.

Initially (*S*)-pyroglutamic acid-derived pre-catalysts were evaluated. When **A2** with a silyl ether substituent was used, good enantiomeric ratio but low yield was achieved, (entry 2). Bulkier silyl ether substituents, as occurred in **A1**, derived in no reaction (entry 1). On the other hand, when Bode catalyst **B** was used, spirobutenolide **3a** was isolated with moderate yield and enantiomeric ratio (entry 3). Introduction of an electron-withdrawing group on the indanol ring, such as a bromine atom, **C1**, resulted in very low yield and enantiodiscrimination, (entry

4). If a stronger electron-withdrawing group (-NO_2) is in the structure of the triazolium salt, **C2**, the enantiomeric ratio for **3a** increased up to 92:8, entry 5. With these results, we decided to follow the optimization process using two pre-catalysts: **A2** due to the good enantiomeric ratio achieved and **C2** as it provided good yield-enantiomeric ratio balance.

Different bases were tested in the presence of pre-catalyst **A2** in THF as solvent (Table 2). Whereas TBD and KO*t*-Bu maintained the enantiomeric ratio (Table 2, entries 3 and 6) but not the yield, other bases such as DMAP and DIPEA afforded higher yield but led to a loss in the enantioselectivity (Table 2, entries 4 and 7). Both yield and enantioselectivity decreased using DABCO or NaOAc (Table 2, entries 2 and 5) while cesium carbonate improved the yield (71%) despite a slight loss in the enantiomeric ratio, 88:12 (Table 2, entry 9). Efforts to improve the yield using DBU as base were unsuccessful. Switching from THF to chloroform, acetonitrile, 1,4-dioxane or a mixture THF/*t*-BuOH (10:1) was ineffective (Table 2, entries 10-13). In other solvents such as hexane, diethyl ether or THF/MeCN (1:1) the reaction did not happen at all (entries 14-16). Different molar ratios between pyrazolin-4,5-dione **1a** and 3-bromo cinnamaldehyde **2a** were also tested but afforded lower yields (Table 2, entries 17 and 18).
To improve the annulation results using cesium carbonate and the triazolium salt **A2**, other solvent changes were performed. Yet neither with acetonitrile, chloroform and diethyl ether improvements were achieved (Table 2, entries 19-21). Also, the mixture of DBU and Cs_2CO_3 was not effective as it provided high enantioselectivity but only 20% yield (Table 2, entry 22).

Table 2. Screening of reaction conditions with pre-catalyst **A2**[a]

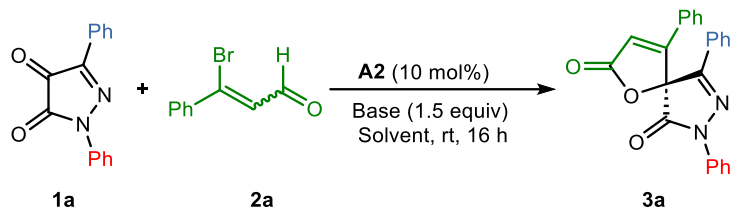

1a **2a** **3a**

Entry	*Base*	*Solvent*	*Yield (%)*[b]	*er*[c]
1	DBU	THF	27	96:4
2	DABCO	THF	5	71:29
3	TBD	THF	20	95:5
4	DMAP	THF	47	86:14
5	NaOAc	THF	15	76:24
6	KO*t*-Bu	THF	16	91:9
7	DIPEA	THF	47	86:14
8	TMG	THF	n. r.	-
9	Cs_2CO_3	THF	71	88:12
10	DBU	$CHCl_3$	14	88:12
11	DBU	MeCN	22	99:1
12	DBU	Dioxane	9	95:5
13	DBU	THF/*t*-BuOH (10:1)	33	88:12
14	DBU	Hexane	n. r.	-
15	DBU	Et_2O	n. r.	-
16	DBU	THF/MeCN (1:1)	n.r.	-
17[d]	DBU	THF	14	98:2
18[e]	DBU	THF	10	98:2
19	Cs_2CO_3	MeCN	39	94:6
20	Cs_2CO_3	$CHCl_3$	32	73:27
21	Cs_2CO_3	Et_2O	n. r.	-
22	DBU+Cs_2CO_3 (1:1)	THF	20	96:4

[a] Reaction conditions: **1a** (0.06 mmol), **2a** (0.09 mmol), **A2** (10 mol%), base (1.5 equiv), solvent (1 mL) at rt for 16 h. [b] Yield of **3a** determined after column chromatography. [c] Er values determined *via* chiral HPLC analysis. [d] Molar ratio **1a**:**2a** 1:1. [e] Molar ratio **1a**:**2a** 1.2:1.

Combination of **1a** with **2a** in the presence of triazolium salt **C2** with DBU as base and chloroform as solvent improved slightly the enantiomeric ratio (Table 3, entry 2). Lowering the temperature led to the same enantiomeric ratio although a slightly decrease in the yield was observed (Table 3, entry 3). Other solvents provided the pyrazolone-butenolide **3a** in better yields but the enantioselectivity decreased (Table 3, entries 4-6). Again, a good yield for spiropyrazolone was obtained when the catalyst was formed from **C2** using cesium carbonate in $CHCl_3$ (Table 3, entry 7) but the enantioselectivity was worse. Other solvents did not involve any improvement (Table 3, entries 8-10). Finally, TBD and DMAP (Table 3, entries 11 and 12) gave lower yields and enantiomeric ratios. After having a look at the complete screening, the best balance between yield and enantiomeric ratio was achieved by using a combination of **C2**/DBU/chloroform (Table 3, entry 2).

Table 3. Screening of reaction conditions with pre-catalyst **C2.**[a]

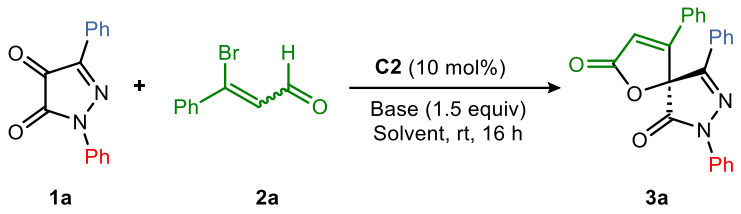

1a **2a** **3a**

Entry	*pre-NHC*	*Base*	*Solvent*	*Yield (%)*[b]	*er*[c]
1	**C2**	DBU	THF	57	92:8
2	**C2**	DBU	$CHCl_3$	54	94:6
3[d]	**C2**	DBU	$CHCl_3$	52	94:6
4	**C2**	DBU	DCE	74	83:17
5	**C2**	DBU	Dioxane	74	79:21
6	**C2**	DBU	MeTHF	55	88:12
7	**C2**	Cs_2CO_3	$CHCl_3$	70	90:10
8	**C2**	Cs_2CO_3	THF	41	88:12
9	**C2**	Cs_2CO_3	DCM	49	82:18
10	**C2**	Cs_2CO_3	MeCN	20	60:40
11	**C2**	TBD	$CHCl_3$	29	86:14
12	**C2**	DMAP	$CHCl_3$	14	50:50

[a] Reaction conditions: **1a** (0.06 mmol), **2a** (0.09 mmol), **C2** (10 mol%), base (1.5 equiv), solvent (1 mL) at rt for 16 h. [b] Yield of **3a** determined after column chromatography. [c] Er values determined *via* chiral HPLC analysis. [d] Reaction performed at 0 ºC.

With the optimized conditions in hand, we proceeded to study the scope of the reaction of the 3-bromo cinnamaldehyde **2a** with different pyrazolin-4,5-diones **1a-i** (Table 4). In all cases, the yields ranged from moderate to good and the enantioselectivities were high no matter whether an alkyl or an aryl group was located at C-3 position of the pyrazolone (Table 4, **3a-3f**). ^{1}H-NMR analysis of the crude reaction indicated total conversion of the starting pyrazole-4,5-dione, so the decrease in the yield is probably due to the formation of non-identifiable by-products. On the other hand, the influence of the *N*-substituent has also been considered and a slight drop of performance was detected when an *N*-methyl group was present in the butenolide (Table 4, **3g** and **3h**). Similar result was observed for compound **3i**, with a *p*-chlorophenyl group at the *N*-1 position, which, nevertheless, gave a good enantiomeric ratio, 90:10.[15]

Table 4. Substrate scope for pyrazolin-4,5-diones **1a-i.**[a, b, c]

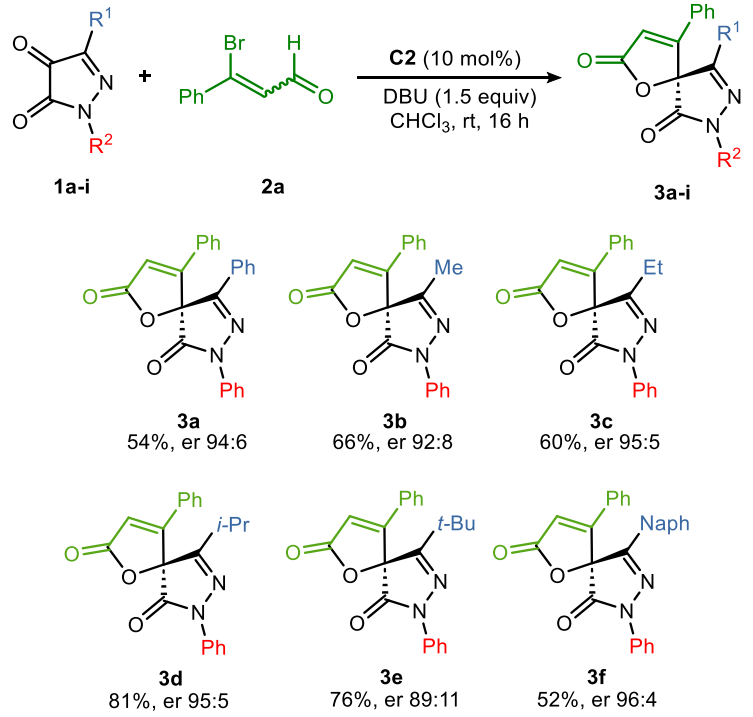

[15] The spiro butenolide **3i** is not described in the Experimental Section because it has not been possible to separate it from a minor impurity.

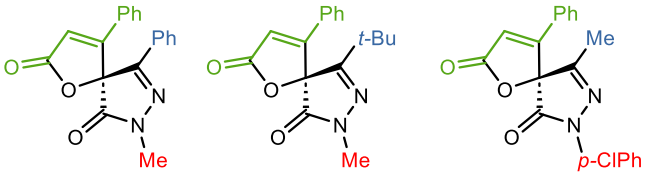

3g
46%, er 90:10

3h
50%, er 88:12

3i (impure mixture)
er 90:10

[a] Reaction conditions: **1a-i** (0.06 mmol), **2a** (0.09 mmol), **C2** (10 mol%), DBU (1.5 equiv), $CHCl_3$ (1 mL) at rt for 16 h. [b] Yield of **3a-h** determined after column chromatography. [c] Er values determined *via* chiral HPLC analysis.

Next, we studied the influence of the β-bromoenal in the annulation reaction so that both aryl and heteroaryl β-bromo-α,β-unsaturated aldehydes **2b-l** were tested (Table 5). The process worked well when the pyrazolin-4,5-dione **1a** was reacted with *p*-substituted cinnamyl aldehydes, affording the corresponding spiropyrazolones (**3ab-3ac** and **3ae**-**3ah**) with excellent enantioselectivities irrespective of the presence of electron-withdrawing or donating groups in the enal, except for compound **3ac** that gave a slightly lower enantiomeric ratio. However, a quasi-racemic mixture and poor yield were obtained in the reaction of the methoxy *ortho*-substituted enal, **3ad**. On the other hand, the *meta*-substitution of the phenyl group of the enal led to no significant change in both the yield and the enantioselectivity (**3ah** and **3ai**). Interestingly, heteroaromatic-substituted enals, with 2-furyl or 2-thiophenyl groups, worked equally well providing good yields and enantioselectivities (**3aj** and **3ak**). Again, and regardless of the enal substitution, the enantiomeric ratios remained high when the pyrazolin-4,5-dione had an ethyl or isopropyl group at C-3 position (**3ce**, **3db** and **3df**). Finally, the reaction using β-bromo benzylidene crotonaldehyde afforded the expected spirocyclic butenolide **3al** in low yield and moderate enantioselectivity (18%, er 78:22).

Table 5. Substrate scope for 3-bromo enals **2b-l.**[a,b,c]

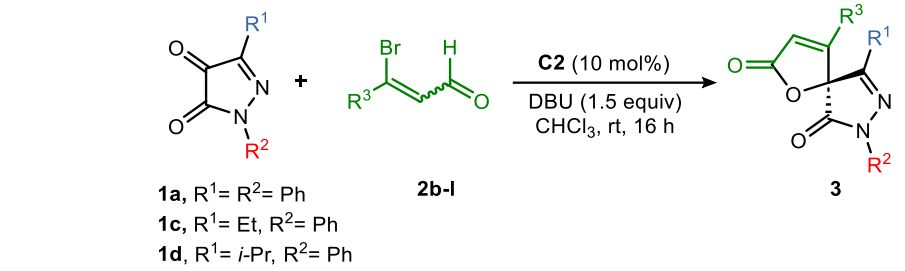

1a, R^1= R^2= Ph
1c, R^1= Et, R^2= Ph
1d, R^1= *i*-Pr, R^2= Ph

2b-l

3

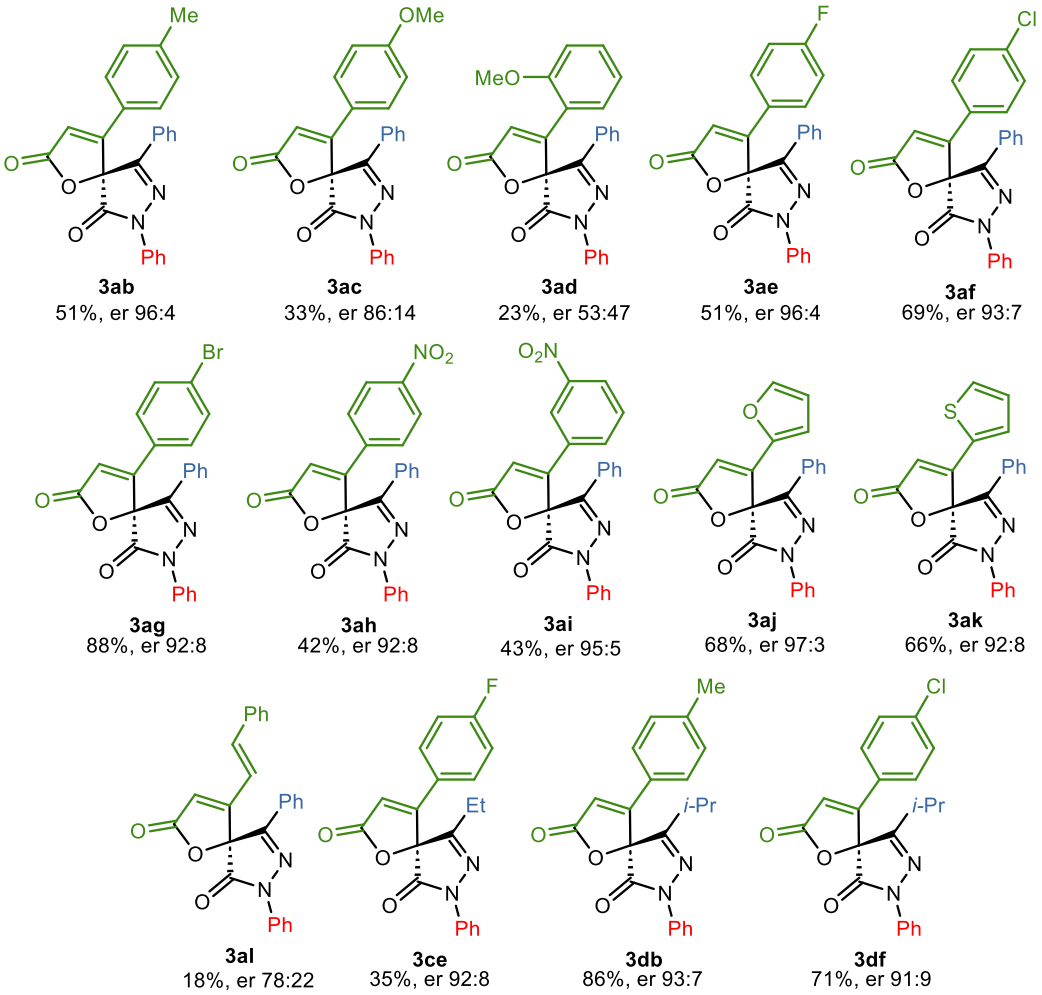

3ab 51%, er 96:4
3ac 33%, er 86:14
3ad 23%, er 53:47
3ae 51%, er 96:4
3af 69%, er 93:7
3ag 88%, er 92:8
3ah 42%, er 92:8
3ai 43%, er 95:5
3aj 68%, er 97:3
3ak 66%, er 92:8
3al 18%, er 78:22
3ce 35%, er 92:8
3db 86%, er 93:7
3df 71%, er 91:9

[a] Reaction conditions: **1a,c,d** (0.06 mmol), **2b-l** (0.09 mmol), **C2** (10 mol%), DBU (1.5 equiv), $CHCl_3$ (1 mL) at rt for 16 h. [b] Yield of **3** determined after column chromatography. [c] Er values determined *via* chiral HPLC analysis.

Attempts to obtain a single crystal of some spiro butenolides **3** were unsuccessful. Therefore, the stereochemistry of the major enantiomer of **3a** was established by chemical correlation with the spirocyclic pyrazolone γ-butyrolactone **4**,[16] obtained by catalytic hydrogenation of **3a**,

[16] M. Gil-Ordóñez, A. Maestro, P. Ortega, P. G. Jambrina, J. M. Andrés *Org. Chem. Front.* **2022**, 9, 420–427.

Scheme 3.4. The absolute configuration of the other butenolides is expected to be the same, (4*R*,5*S*), by analogy.

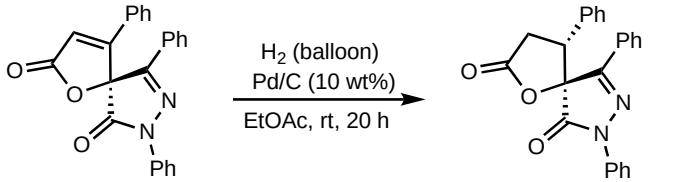

3a er 94:6 (4*R*,5*S*)-**4** 45%, er 94:6

Scheme 3.4: Catalytic hydrogenation of spirocyclic butenolide **3a**.

The reaction worked equally well when using 1 mmol of starting material demonstrating the feasibility of our protocol. When pyrazolin-4,5-dione **1a** was reacted with 3-bromo enal **2g** the same level of enantioselectivity (er 91:9) and good yield (367 mg, 80% yield) were achieved, Scheme 3.5.

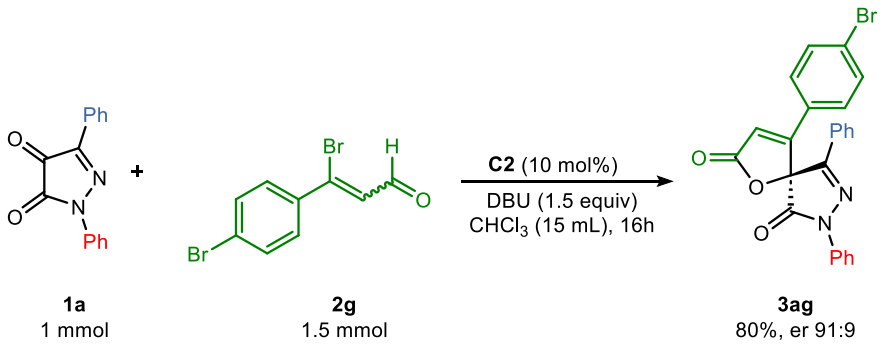

1a
1 mmol

2g
1.5 mmol

3ag
80%, er 91:9

Scheme 3.5: Scale-up reaction for spiropyrazolone butenolide **3ag**.

The synthetic utility of our method was demonstrated by the treatment of *p*-bromophenyl-substituted butenolide **3ag** with phenylboronic acid under Suzuki conditions. After heating at 70 °C for eight hours the cross-coupling product **5** was obtained with no erosion of the enantiomeric purity and excellent yield, Scheme 3.6.

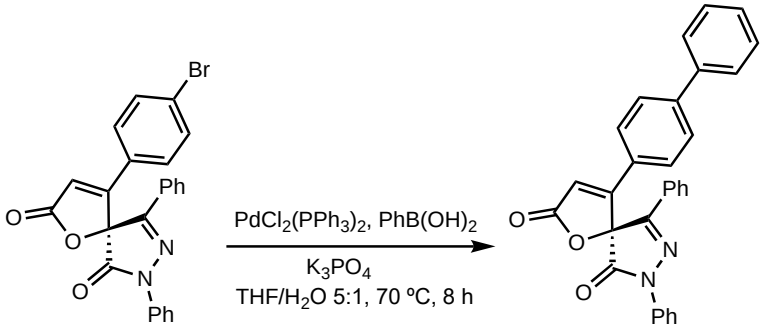

3ag er 95:5 **5** 96%, er 95:5

Scheme 3.6: Transformation of spiropyrazolone butenolide **3ag**.

Finally, although the objective of this work was the preparation of spiropyrazolone butenolides, we also wanted to know our method's synthetic compatibility when other ketones were used. Thus, the reaction of *N*-benzyl isatin **6** with **2a** was accomplished in the previously established conditions. The spirooxindole butenolide **7**[13] was obtained in 75% yield and good enantioselectivity, revealing the reliability of our method.

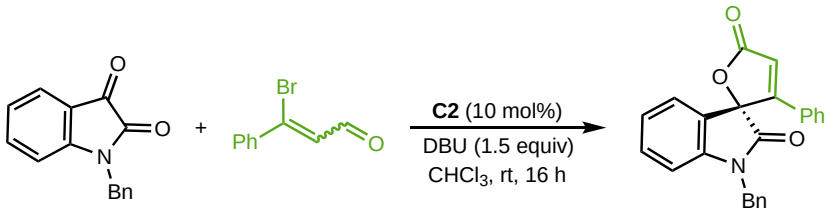

6 **2a** **7** 75%, er 93:7

Scheme 3.7: Reaction of *N*-benzyl isatin with 3-bromo cynnamaldehyde.

A plausible mechanism for the NHC-catalyzed [3+2] annulation reaction is depicted in Scheme 3.8. In the first step, the chiral carbene reacts with the bromoenal **2**, giving rise to the intermediate **IM1.** It evolves to the Breslow homoenolate **IM2** after base-assisted 1,2-hydrogen migration. Previously, we proved[16] that the Brønsted base used have a dual role. Firstly, it generates the carbene catalyst and, on the other hand, it assists the [1,2]-proton transfer for the generation of homoenolate. Subsequently, the attack of the *Re* face of pyrazole-dione **1** on the *Re* face of homoenolate would be possible, giving rise to the formation of the intermediate **IM3**. Then, the butenolide unit in **IM4** is formed by cyclization and release of the bromide anion which was found to be the stereoselectivity-determining step. In addition, the free energy barrier was lower for the stereoisomer with the (*S*) spiro

center. Finally, the catalytic cycle is completed with the formation of the butenolide product **3** and the regeneration of the NHC catalyst.

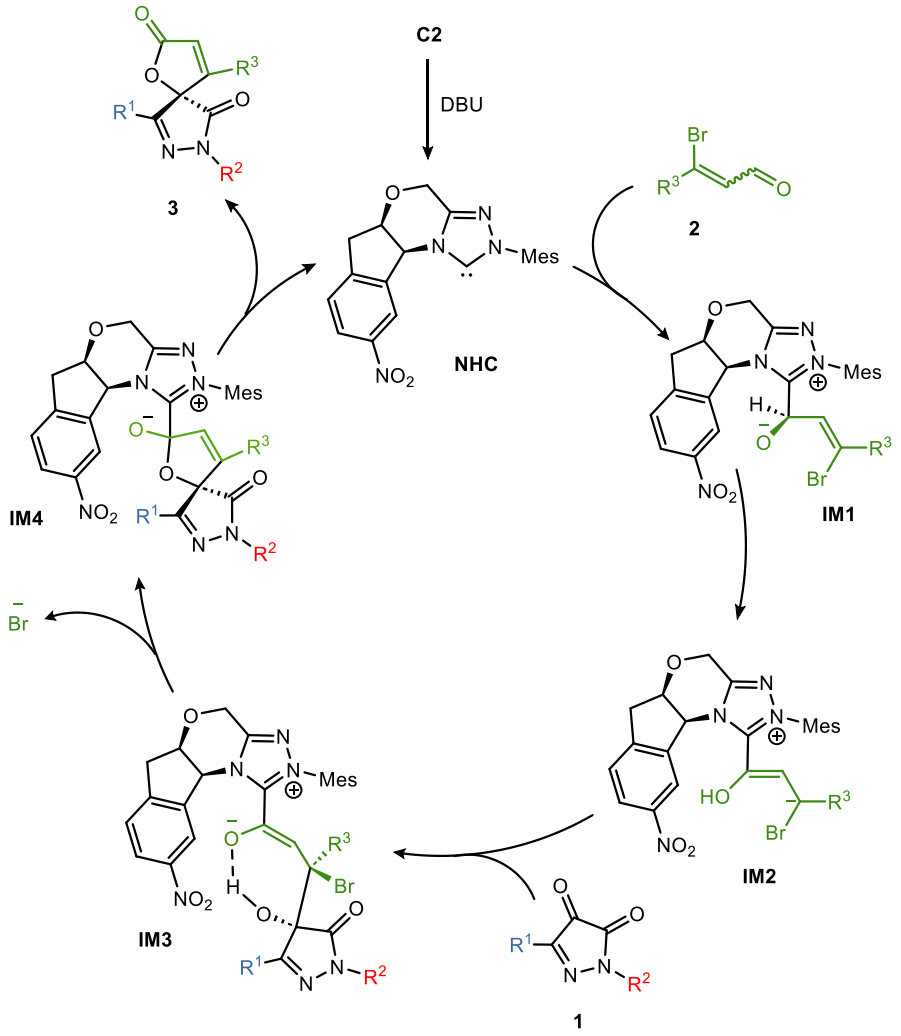

Scheme 3.8: Proposed mechanism for the [3+2] annulation of pyrazolin-4,5-diones and 3-bromo enals through NHC catalysis.

3.3 Conclusions

In this chapter, we describe the unprecedented [3+2] asymmetric annulation reaction of 3-bromoenals and 1*H*-pyrazol-4,5-diones *via N*-heterocyclic carbene catalysis for the synthesis of novel chiral spiropyrazolone-butenolides. The key step consists of the use of *3-bromo homoenolates* prepared from 3-bromoenals and a *meta*-nitro substituted Bode catalyst. Then, these intermediates act as nucleophiles on the pyrazolin-4,5-diones triggering an addition/dehalogenation/lactonization cascade reaction. The process tolerates a wide range of substituents on both pyrazolin-4,5-dione and 3-bromoenal. In addition, the experimental

procedure is very simple and the optimal reaction conditions are extremely mild. The new quaternary stereocenter created at the C-4 position of the pyrazolone is (*S*). This agrees with our previous computational studies performed on the mechanism for the preparation of spiropyrazolone-γ-butyrolactones.

3.4 References

1. (a) K. Tadiparthi, S. Venkatesh *J Heterocyclic Chem.* **2022**, *59*, 1285–1307, (b) S. Chatterjee, R. Sahoo, S. Nanda *Org. Biomol. Chem.* **2021**, *19*, 7298–7332, (c) T. Montagnon, M. Tofi, G. Vassilikogiannakis *Acc. Chem. Res.* **2008**, *41*, 1001–1011, (d) F. Q. Alali, X. -X. Liu, J. L. McLaughlin *J. Nat. Prod.* **1999**, *62*, 504–540.
2. S. Padakanti, M. Pal, K. R. Yeleswarapu *Tetrahedron* **2003**, *59*, 7915−7920.
3. M. Pour, M. Spulak, V. Balsanek, J. Kunes, P. Kubanova, V. Buchta *Bioorg. Med. Chem.* **2003**, *11*, 2843−2866.
4. G. Grossmann, M. Poncioni, M. Bornand, B. Jolivet, M. Neuburger, U. Sequin *Tetrahedron* **2003**, *59*, 3237−3251.
5. T. R. Hoye, L. Tan *Tetrahedron Lett.* **1995**, *36*, 1981−1984.
6. *For reviews see:* (a) B. Mandal, B. Thirupathi *Org. Biomol. Chem.* **2020**, *18*, 5287–5314, (b) P. Yadav, R. Pratap, V. J. Ram *Asian J. Org.Chem*. **2020**, *9*, 1377–1409. *Some examples:* (a) D. Dar'in, G. Kantin, E. Chupakhin, V. Sharoyko, M. Krasavin *Chem. Eur. J.* **2021**, *27*, 8221–8227, (b) A. Elagamy, R. Shaw, R. Panwar, Shally, V. J. Ram, R. Pratap *J. Org. Chem.* **2019**, *84,* 1154−1161, (c) U. Albrecht, P. Langer *Tetrahedron* **2007**, *63*, 4648–4654.
7. (a) A. Skrzynska, P. Drelich, S. Frankowski, Ł. Albrecht *Chem. Eur. J.* **2018**, *24*, 16543–16547, (b) J. Hejmanowska, M. Dzięgielewski, D. Kowalczyk, Ł. Albrecht *Synlett* **2014**, *25*, 2957–2961.
8. K. -Q. Chen, Y. Li, C. -L. Zhang, D. -Q. Sun, S. Ye *Org. Biomol. Chem* **2016**, *14*, 2007–2014.
9. Q. Ni, X. Song, G. Raabe, D. Enders *Chem. Asian J*. **2014**, *9*, 1535–1538.
10. S. R. Yetra, T. Kaicharla, S. S. Kunte, R. G. Gonnade, A. T. Biju *Org. Lett.* **2013**, *15*, 5202–5205.
11. H. -M. Zhang, H. Ly, S. Ye *Org. Biomol. Chem.* **2013**, *11*, 6255–6257.
12. G. Wang, X. Chen, G. Miao, W. Yao, C. Ma *J. Org. Chem.* **2013**, *78*, 12, 6223–6232.
13. C. Zheng, W. Yao, Y. Zhang, C. Ma *Org. Lett.* **2014**, *16*, 5028–503.
14. C. Wang, S. Zhu, G. Wang, Z. Li, X. -P. Hui *Eur. J. Org. Chem.* **2016**, 5653–5658.
15. The spiro butenolide **3i** is not described in the Experimental Section because it has not been possible to separate it from a minor impurity.
16. M. Gil-Ordóñez, A. Maestro, P. Ortega, P. G. Jambrina, J. M. Andrés *Org. Chem. Front.* **2022**, 9, 420–427.

3.5 Experimental section

3.5.1 General Procedure for Spiropyrazolone-Butenolides.

In a 5 mL heat gun-dried flask equipped with a magnetic stirring bar the pre-catalyst **C2** (6 μmol, 0.1 equiv) and the pyrazolin-4,5-dione **1a-i** (0.06 mmol) were weighed. Then β-bromoenal **2a-l** (0.09 mmol, 1.5 equiv) was added under a N_2 atmosphere. Dry chloroform (1 mL) was added before the mixture was stirred. Several minutes later, the base (0.09 mmol, 1.5 equiv) was introduced to the flask. After 16 h, the solvent was straight removed under reduced pressure and the residue was subjected to column chromatography over silica gel using a mixture of hexane and ethyl acetate as eluent to give the desired compound.

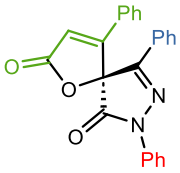

3a

(S)-4,7,9-triphenyl-1-oxa-7,8-diazaspiro[4.4]nona-3,8-diene-2,6-dione (**3a**). Following the general procedure and after column chromatography using hexane/ethyl acetate 10:1 as eluent, **3a** was isolated as white solid (12.1 mg, 54% yield). Mp 137-139 °C (from hexane). $[\alpha]^{25}_{D}$= -94.5 (*c*= 0.2, $CHCl_3$, er 94:6). ^{1}H NMR (500 MHz, $CDCl_3$) δ 7.97 (d, *J*= 9.8 Hz, 2H), 7.73 (d, *J*= 9.7 Hz, 2H), 7.50-7.42 (m, 4H), 7.41-7.38 (m, 4H), 7.37-7.33 (m, 2H), 7.30 (tt, *J*= 7.5, 1.1 Hz, 1H), 6.77 (s, 1H). ^{13}C {^{1}H} NMR (126 MHz, $CDCl_3$) δ 170.3, 165.4, 162.3, 153.3, 137.2, 132.3, 131.7, 129.7, 129.2, 129.0, 128.1, 126.7, 124.4, 126.2, 119.2, 116.8, 87.3. IR ν_{max}/cm^{-1} 3114, 3059, 2917, 1808, 1779, 1727, 1596, 1497, 1449, 1321, 1175, 1085. HRMS (ESI-TOF) m/z: calcd for $C_{24}H_{16}N_2NaO_3$ $[M+Na]^+$ 403.1053. Found 403.1062. HPLC (Chiralcel OD, n-hexane/2-propanol 80:20, λ= 254 nm, 0.6 mL/min). t_R (major)= 16.2 min, t_R (minor)= 27.7 min (er 94:6).

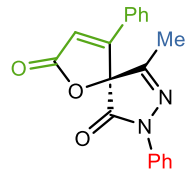

3b

(S)-9-methyl-4,7-diphenyl-1-oxa-7,8-diazaspiro[4.4]nona-3,8-diene-2,6-dione (**3b**). Following the general procedure and after column chromatography using hexane/ethyl acetate 10:1 as eluent, **3b** was isolated as yellow oil (16.7 mg, 66% yield). $[\alpha]^{25}_{D}$= -78.1 (*c*= 0.3, $CHCl_3$, er 92:8). ^{1}H NMR (500 MHz, $CDCl_3$) δ 7.88 (d, *J*= 9.8 Hz, 2H), 7.51-7.40 (m, 5H), 7.38-7.36 (m, 2H), 7.27 (tt, *J*= 7.4, 1.1 Hz, 1H), 6.67 (s, 1H), 2.08 (s, 3H). ^{13}C {^{1}H} NMR (126 MHz, $CDCl_3$) δ 170.1, 165.2, 160.1, 156.2, 137.2, 132.4, 129.9, 129.2, 128.0, 126.5, 126.1, 118.9, 116.9, 87.5, 13.3. IR ν_{max}/cm^{-1} 3109, 3062, 2961, 2921, 2849, 1806, 1770, 1727, 1597, 1481, 1366, 1294, 1182, 1121, 1063, 926, 901. HRMS (ESI-TOF) m/z: calcd for $C_{19}H_{15}N_2O_3$ $[M+H]^+$ 319.1077. Found 319.1083. HPLC (Chiralcel OD, n-hexane/2-propanol 80:20, λ= 254 nm, 0.6 mL/min). t_R (major)= 17.7 min, t_R (minor)= 27.6 min (er 92:8).

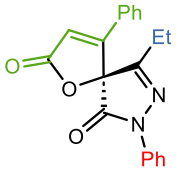

3c

(S)-9-ethyl-4,7-diphenyl-1-oxa-7,8-diazaspiro[4.4]nona-3,8-diene-2,6-dione (**3c**). Following the general procedure and after column chromatography using hexane/ethyl acetate 10:1 as eluent, **3c** was isolated as yellow oil (14.6 mg, 60% yield). $[\alpha]^{25}_{D}$= -10.7 (*c*= 0.4, $CHCl_3$, er 95:5). ^{1}H NMR (500 MHz, $CDCl_3$) δ 7.90 (d, *J*= 8.1 Hz, 2H), 7.50-7.35 (m, 7H), 7.27 (t, *J*= 8.0 Hz, 1H), 6.67 (s, 1H), 2.54-2.44 (m, 1H), 2.33-2.23 (m, 1H), 1.22 (t, *J*= 7.8 Hz, 3H). ^{13}C {^{1}H} NMR (126 MHz, $CDCl_3$) δ 170.2, 165.4, 160.3, 160.2, 137.3, 132.4, 129.8, 129.1, 128.1, 126.5, 126.1, 118.9, 116.7, 87.6, 21.3, 9.3. IR ν_{max}/cm^{-1} 3109, 3062, 2957, 1803, 1781, 1730, 1590, 1575, 1489, 1453, 1348, 1258, 1182, 1124, 1038, 753. HRMS (ESI-TOF) m/z: calcd for $C_{20}H_{16}KN_2O_3$

$[M+K]^+$ 371.0793. Found 371.0799. HPLC (Chiralcel OD, n-hexane/2-propanol 85:15, λ= 210 nm, 1 mL/min). t_R (major)= 10.7 min, t_R (minor)= 18.6 min (er 95:5).

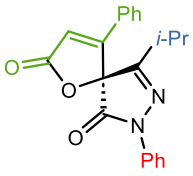

3d

(S)-9-isopropyl-4,7-diphenyl-1-oxa-7,8-diazaspiro[4.4]nona-3,8-diene-2,6-dione (**3d**). Following the general procedure and after column chromatography using hexane/ethyl acetate 10:1 as eluent, **3d** was isolated as yellow oil (17.1 mg, 81% yield). $[\alpha]^{25}_D$= -74.8 (*c*= 0.3, $CHCl_3$, er 95:5). ^{1}H NMR (500 MHz, $CDCl_3$) δ 7.91 (d, *J*= 8.8 Hz, 2H), 7.49-7.35 (m, 7H), 7.27 (t, *J*= 8.0 Hz, 1H), 6.69 (s, 1H), 2.70-2.60 (m, 1H), 1.26 (d, *J*= 6.9 Hz, 3H), 1.10 (d, *J*= 7.0 Hz, 3H). ^{13}C {^{1}H} NMR (126 MHz, $CDCl_3$) δ 170.3, 165.5, 163.3, 160.1, 137.3, 132.4, 129.8, 129.1, 128.3, 126.5, 126.1, 119.0, 116.5, 87.8, 29.2, 20.2. IR ν_{max}/cm^{-1} 3058, 2964, 2928, 1808, 1774, 1730, 1597, 1500, 1377, 1344, 1328, 1240, 1186, 1124, 1045. HRMS (ESI-TOF) m/z: calcd for $C_{21}H_{18}N_2NaO_3$ $[M+Na]^+$ 369.1210. Found 369.1216. HPLC (Chiralcel OD, n-hexane/2-propanol 90:10, 0.8 mL/min, λ= 210 nm). t_R (major)= 13.3 min, t_R (minor)= 29.9 min (er 95:5).

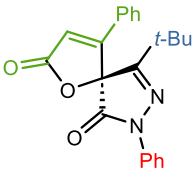

3e

(S)-9-(tert-butyl)-4,7-diphenyl-1-oxa-7,8-diazaspiro[4.4]nona-3,8-diene-2,6-dione (**3e**). Following the general procedure and after column chromatography using hexane/ethyl acetate 10:1 as eluent, **3e** was isolated as yellow oil (17.8 mg, 76% yield). $[\alpha]^{25}_D$= -103.7 (*c*= 0.4, $CHCl_3$, er 89:11). ^{1}H NMR (500 MHz, $CDCl_3$) δ 7.88 (d, *J*= 8.6 Hz, 2H), 7.49-7.35 (m, 7H), 7.27 (t, *J*= 8.7 Hz, 1H), 6.69 (s, 1H), 1.20 (s, 9H). ^{13}C {^{1}H} NMR (126 MHz, $CDCl_3$) δ 170.3, 165.6, 164.6, 162.0, 137.3, 132.3, 129.7, 129.1, 128.6, 126.5, 126.1, 118.9, 116.2, 88.1, 36.9, 28.6. IR ν_{max}/cm^{-1} 3098, 2972, 2932, 1817, 1770, 1723, 1601, 1500, 1362, 1294, 1207, 1175, 1067, 1023, 955. HRMS (ESI-TOF) m/z: calcd for $C_{22}H_{20}N_2NaO_3$ $[M+Na]^+$ 383.1366. Found 383.1372. HPLC (Chiralcel OD, n-hexane/2-propanol 80:20, λ= 254 nm, 0.6 mL/min). t_R (major)= 11.6 min, t_R (minor)= 22.9 min (er 89:11).

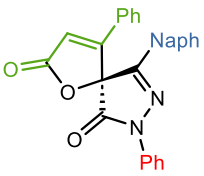

3f

(S)-9-(naphthalen-2-yl)-4,7-diphenyl-1-oxa-7,8-diazaspiro[4.4]nona-3,8-diene-2,6-dione (**3f**). Following the general procedure and after column chromatography using hexane/ethyl acetate 10:1 as eluent, **3f** was isolated as pale yellow oil (11.2 mg, 52% yield). $[\alpha]^{25}_D$= -70.1 (*c*= 0.2, $CHCl_3$, er 96:4). ^{1}H NMR (500 MHz, $CDCl_3$) δ 8.01-7.98 (m, 4H), 7.87 (d, *J*= 8.6 Hz, 1H), 7.81 (t, *J*= 8.5 Hz, 2H), 7.56-7.48 (m, 4H), 7.42-7.38 (m, 3H), 7.35-7.30 (m, 3H), 6.8 (s, 1H). ^{13}C {^{1}H} NMR (126 MHz, $CDCl_3$) δ 170.3, 165.4, 162.6, 153.1, 137.2, 134.6, 132.8, 132.3, 129.7, 129.2, 129.2, 129.0, 128.2, 128.1, 127.8, 127.0, 126.8, 126.7, 126.5, 126.4, 122.5, 119.2, 116.8, 87.4. IR ν_{max}/cm^{-1} 3066, 2954, 2925, 2860, 1803, 1770, 1730, 1597, 1453, 1308, 1175, 1128, 1059, 966. HRMS (ESI-TOF) m/z: calcd for$C_{28}H_{18}N_2NaO_3$ $[M+Na]^+$ 453.1210. Found 453.1222. HPLC (Chiralcel OD, n-hexane/2-propanol 80:20, λ= 254 nm, 0.6 mL/min). t_R (major)= 18.3 min, t_R (minor)= 32.3 min (er 96:4).

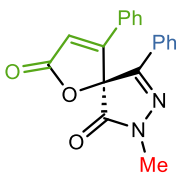

3g

(S)-7-methyl-4,9-diphenyl-1-oxa-7,8-diazaspiro[4.4]nona-3,8-diene-2,6-dione (**3g**). Following the general procedure and after column chromatography using hexane/ethyl acetate 10:1 as eluent, **3g** was isolated as yellow oil (11.6 mg, 46% yield). $[\alpha]^{25}_D$= -72.0 (*c*= 0.2, $CHCl_3$, er 90:10). ^{1}H NMR (500 MHz, $CDCl_3$) δ 7.60 (d, *J*= 9.8 Hz, 2H), 7.45-7.33 (m, 8H), 6.70 (s, 1H), 3.51 (s, 3H). ^{13}C {^{1}H} NMR (126 MHz, $CDCl_3$) δ 170.4, 167.3, 162.4, 151.6, 132.2, 131.3,

129.6, 129.1, 128.2, 126.7, 125.9, 116.7, 86.2, 32.5. IR ν_{max}/cm^{-1} 3109, 3069, 2925, 2853, 1808, 1770, 1727, 1604, 1445, 1391, 1341, 1229, 1095, 1063, 864. HRMS (ESI-TOF) m/z: calcd for $C_{19}H_{14}N_2NaO_3$ 1579, $[M+Na]^+$ 341.0897. Found 341.0907. HPLC (Lux Amylose-1, n-hexane/2-propanol 80:20, λ= 254 nm, 0.6 mL/min). t_R (minor)= 25.1 min, t_R (major)= 39.0 min (er 90:10).

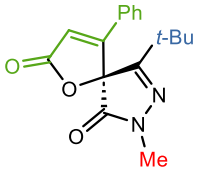

3h

(S)-9-(tert-butyl)-7-methyl-4-phenyl-1-oxa-7,8-diazaspiro[4.4]nona-3,8-diene-2,6-dione (**3h**). Following the general procedure and after column chromatography using hexane/ethyl acetate 10:1 as eluent, **3h** was isolated as pale yellow oil (13.3 mg, 50% yield). $[\alpha]^{25}_D$= -14.3 (*c*= 0.3, $CHCl_3$, er 88:12). ^{1}H NMR (500 MHz, $CDCl_3$) δ 7.50-7.40 (m, 3H), 7.33 (d, *J*= 9.7 Hz, 2H), 6.63 (s, 1H), 3.43 (s, 3H), 1.12 (s, 9H). ^{13}C {^{1}H} NMR (126 MHz, $CDCl_3$) δ 170.5, 167.7, 163.9, 162.0, 132.2, 129.6, 128.7, 126.5, 116.0, 87.0, 36.6, 32.2, 28.6. IR ν_{max}/cm^{-1} 3120, 2972, 2936, 2878, 1803, 1777, 1727, 1611, 1500, 1449, 1399, 1283, 1204, 1164, 1121, 1045. HRMS (ESI-TOF) m/z: calcd for $C_{17}H_{18}N_2NaO_3$ $[M+Na]^+$ 321.1210. Found 321.1216. HPLC (Chiralpak AD-H, n-hexane/2-propanol 90:10, λ= 254 nm, 0.7 mL/min). t_R (minor)= 17.2 min, t_R (major)= 20.3 min (er 88:12).

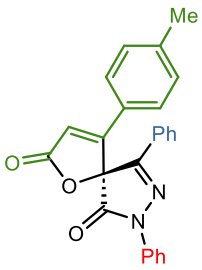

3ab

(S)-7,9-diphenyl-4-(p-tolyl)-1-oxa-7,8-diazaspiro[4.4]nona-3,8-diene-2,6-dione (**3ab**). Following the general procedure and after column chromatography using hexane/ethyl acetate 10:1 as eluent, **3ab** was isolated as pale yellow oil (11.9 mg, 51% yield). $[\alpha]^{25}_D$= -134.9 (*c*= 0.2, $CHCl_3$, er 96:4). ^{1}H NMR (500 MHz, $CDCl_3$) δ 7.97 (d, *J*= 7.1 Hz, 2H), 7.72 (d, *J*= 8.1 Hz, 2H), 7.50-7.43 (m, 4H), 7.40-7.36 (m, 2H), 7.32-7.29 (m, 2H), 7.15 (d, *J*= 7.8 Hz, 2H), 6.73 (s, 1H), 2.30 (s, 3H). ^{13}C {^{1}H} NMR (126 MHz, $CDCl_3$) δ 170.5, 165.5, 162.2, 153.5, 143.3, 137.3, 131.7, 130.5, 129.2, 129.1, 129.0, 126.6, 126.3, 126.2, 125.3, 119.1, 115.6, 87.2, 21.5. IR ν_{max}/cm^{-1} 3065, 2953, 2921, 2856, 1803, 1774, 1737, 1593, 1492, 1384, 1319, 1182, 1142, 1063. HRMS (ESI-TOF) m/z: calcd for$C_{25}H_{18}N_2NaO_3$ $[M+Na]^+$ 417.1210. Found 417.1224. HPLC (Chiralcel OD, n-hexane/2-propanol 95:5, λ= 254 nm, 0.8 mL/min). t_R (major)= 25.7 min, t_R (minor)= 30.5 min (er 96:4).

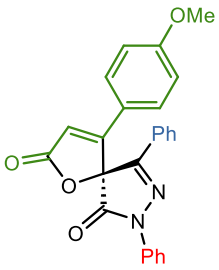

3ac

(S)-4-(4-methoxyphenyl)-7,9-diphenyl-1-oxa-7,8-diazaspiro[4.4]nona-3,8-diene-2,6-dione (**3ac**). Following the general procedure and after column chromatography using hexane/ethyl acetate 10:1 as eluent, **3ac** was isolated as pale pink solid (8.1 mg, 33% yield). Mp 67-69 °C (from hexane). $[\alpha]^{25}_D$= -120.9 (*c*= 0.2, $CHCl_3$, er 86:14). ^{1}H NMR (500 MHz, $CDCl_3$) δ 7.98 (d, *J*= 8.8 Hz, 2H), 7.72 (d, *J*= 8.4 Hz, 2H), 7.51-7.43 (m, 3H), 7.40-7.36 (m, 4H), 7.30 (t, *J*= 7.5 Hz, 1H), 6.84 (d, *J*= 8.0 Hz, 2H), 6.65 (s, 1H), 3.76 (s, 3H). ^{13}C {^{1}H} NMR (126 MHz, $CDCl_3$) δ 170.6, 165.6, 162.8, 161.6, 153.8, 137.3, 131.7, 129.2, 129.0, 128.6, 126.1, 120.6, 119.1, 115.2, 114.0, 87.0, 55.5. IR ν_{max}/cm^{-1} 3105, 3062, 2961, 2918, 2853, 1803, 1781, 1727, 1597, 1496, 1316, 1240, 1063, 901. HRMS (ESI-TOF) m/z: calcd for$C_{25}H_{18}N_2NaO_3$ $[M+Na]^+$ 433.1159. Found 433.1169. HPLC (Lux i-Cellulose-5, n-hexane/2-propanol 70:30, λ= 254 nm, 0.6 mL/min). t_R (minor)= 47.9 min, t_R (major)= 81.0 min (er 86:14).

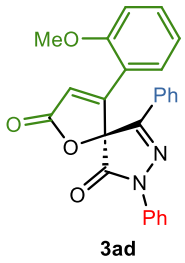

3ad

(S)-4-(2-methoxyphenyl)-7,9-diphenyl-1-oxa-7,8-diazaspiro[4.4]nona-3,8-diene-2,6-dione (**3ad**). Following the general procedure and after column chromatography using hexane/ethyl acetate 10:1 as eluent, **3ad** was isolated as white solid (5.6 mg, 23% yield). Mp 38-40 °C (from hexane). ^{1}H NMR (500 MHz, $CDCl_3$) δ 8.01 (d, *J*= 7.7 Hz, 2H), 7.68 (d, *J*= 9.7 Hz, 2H), 7.48 (t, *J*= 7.6 Hz, 1H), 7.42-7.32 (m, 5H), 7.28 (t, *J*= 8.5 Hz, 1H), 7.03 (s, 1H), 6.89 (d, *J*= 8.1 Hz, 2H), 3.71 (s, 3H). ^{13}C {^{1}H} NMR (126 MHz, $CDCl_3$) δ 170.8, 165.8, 158.3, 157.9, 153.2, 137.6, 133.5, 131.3, 129.2, 129.0, 128.5, 126.2, 125.9, 121.4, 119.7, 118.8, 117.6, 111.8, 83.0, 55.1. IR ν_{max}/cm^{-1} 3077, 2956, 2923, 1861, 1806, 1780, 1725, 1600, 1491, 1465, 1384, 1263, 1139, 1025, 941, 754. HRMS (ESI-TOF) m/z: calcd for$C_{25}H_{18}N_2NaO_3$ $[M+Na]^+$ 433.1159. Found 433.1163. HPLC (Lux i-Cellulose-5, n-hexane/2-propanol 70:30, λ= 254 nm, 0.6 mL/min). t_R= 57.8 min, 63.9 min (er 53:47).

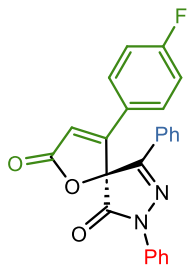

3ae

(S)-4-(4-fluorophenyl)-7,9-diphenyl-1-oxa-7,8-diazaspiro[4.4]nona-3,8-diene-2,6-dione (**3ae**). Following the general procedure and after column chromatography using hexane/ethyl acetate 10:1 as eluent, **3ae** was isolated as yellow oil (11.9 mg, 51% yield). $[\alpha]^{25}_D$= -13.8 (*c*= 0.1, $CHCl_3$, er 96:4). ^{1}H NMR (500 MHz, $CDCl_3$) δ 7.95 (d, *J*= 9.8 Hz, 2H), 7.71 (d, *J*= 7.2 Hz, 2H), 7.50-7.45 (m, 3H), 7.45-7.38 (m, 4H), 7.31 (t, *J*= 7.4 Hz, 1H), 7.05 (t, *J*= 8.4 Hz, 2H), 6.71 (s, 1H). ^{13}C {^{1}H} NMR (126 MHz, $CDCl_3$) δ 170.0, 165.5 (d, *J*= 177.2 Hz), 165.2, 163.8, 153.2, 137.1, 131.8, 129.3, 129.2, 129.0, 128.9, 128.8, 126.5, 126.2, 124.4, 119.1, 117.2, 117.1, 116.7, 87.2. ^{19}F NMR (470 MHz, $CDCl_3$) δ -106.3. IR ν_{max}/cm^{-1} 3069, 2957, 2925, 2853, 1777, 1734, 1604, 1492, 1445, 1387, 1319, 1294, 1233, 1164, 1142. HRMS (ESI-TOF) m/z: calcd for$C_{24}H_{16}FN_2O_3$ $[M+H]^+$ 399.1139. Found 399.1147. HPLC (Lux i-Cellulose-5, n-hexane/2-propanol 80:20, λ= 230 nm, 0.6 mL/min). t_R (minor)= 36.7 min, t_R (major)= 56.2 min (er 96:4).

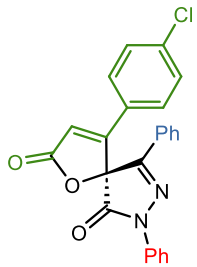

3af

(S)-4-(4-chlorophenyl)-7,9-diphenyl-1-oxa-7,8-diazaspiro[4.4]nona-3,8-diene-2,6-dione (**3af**). Following the general procedure and after column chromatography using hexane/ethyl acetate 10:1 as eluent, **3af** was isolated as white solid (17 mg, 69% yield). Mp 52-54 °C (from hexane). $[\alpha]^{25}_D$= -157.7 (*c*= 0.1, $CHCl_3$, er 93:7). ^{1}H NMR (500 MHz, $CDCl_3$) δ 7.95 (d, *J*= 9.6 Hz, 2H), 7.70 (d, *J*= 9.7 Hz, 2H), 7.50-7.45 (m, 3H), 7.40 (t, *J*= 6.6 Hz, 1H), 7.35-7.29 (m, 5H), 6.75 (s, 1H). ^{13}C {^{1}H} NMR (126 MHz, $CDCl_3$) δ 169.9, 165.1, 161.0, 153.1, 138.7, 137.1, 131.9, 130.1, 129.3, 129.2, 128.8, 127.9, 126.6, 126.5, 126.2, 119.1, 117.3, 87.1. IR ν_{max}/cm^{-1} 2968, 2925, 2860, 1806, 1774, 1734, 1591, 1489, 1388, 1323, 1301, 1178, 1142. HRMS (ESI-TOF) m/z: calcd for $C_{24}H_{15}ClN_2NaO_3$ $[M+Na]^+$ 437.0663. Found 437.0674. HPLC (Chiralcel OD, n-hexane/2-propanol 95:5, λ= 254 nm, 0.8 mL/min,). t_R (minor)= 26.0 min, t_R (major)= 32.9 min (er 93:7).

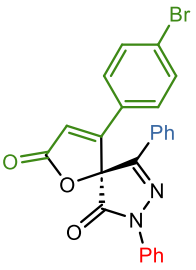

3ag

(S)-4-(4-bromophenyl)-7,9-diphenyl-1-oxa-7,8-diazaspiro[4.4]nona-3,8-diene-2,6-dione (**3ag**). Following the general procedure and after column chromatography using hexane/ethyl acetate 10:1 as eluent, **3ag** was isolated as yellow oil (23.9 mg, 88% yield). $[\alpha]^{25}_{D}$= -52.7 (*c*= 0.5, $CHCl_3$, er 92:8). ^{1}H NMR (500 MHz, $CDCl_3$) δ 7.95 (d, *J*= 7.9 Hz, 2H), 7.70 (d, *J*= 9.0 Hz, 2H), 7.51-7.42 (m, 5H), 7.40-7.38 (m, 2H), 7.31 (t, *J*= 7.5 Hz, 1H), 7.24-7.23 (m, 1H), 6.76 (s, 1H). ^{13}C {^{1}H} NMR (126 MHz, $CDCl_3$) δ 169.9, 165.1, 161.1, 153.0, 137.1, 133.1, 131.9, 129.3, 129.2, 128.8, 128.0, 127.2, 127.0, 126.5, 126.1, 119.1, 117.3, 87.1. IR ν_{max}/cm^{-1} 3063, 2960, 2923, 2857, 1806, 1777, 1733, 1593, 1494, 1387, 1299, 1178, 1141, 1071, 1009. HRMS (ESI-TOF) m/z: calcd for$C_{24}H_{15}BrN_2NaO_3$ $[M+Na]^+$ 481.0158. Found 481.0169. HPLC (Chiralcel OD, n-hexane/2-propanol 85:15, λ= 254 nm, 0.8 mL/min). t_R (minor)= 23.8 min, t_R (major)= 32.4 min (er 92:8).

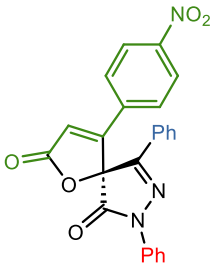

3ah

(S)-4-(4-nitrophenyl)-7,9-diphenyl-1-oxa-7,8-diazaspiro[4.4]nona-3,8-diene-2,6-dione (**3ah**). Following the general procedure and after column chromatography using hexane/ethyl acetate 10:1 as eluent, **3ah** was isolated as white solid (10.6 mg, 42% yield). Mp 48-50 °C (from hexane). $[\alpha]^{25}_{D}$= -30.7 (*c*= 0.2, $CHCl_3$, er 92:8). ^{1}H NMR (500 MHz, $CDCl_3$) δ 8.02 (d, *J*= 8.8 Hz, 2H), 7.94 (d, *J*= 9.7 Hz, 2H), 7.71 (d, *J*= 9.5 Hz, 2H), 7.53 (d, *J*= 8.3 Hz, 2H), 7.49 (t, *J*= 7.3 Hz, 3H), 7.42 (t, *J*= 7.7 Hz, 2H), 7.32 (d, *J*= 7.4 Hz, 1H), 6.89 (s, 1H). ^{13}C {^{1}H} NMR (126 MHz, $CDCl_3$) δ 169.1, 164.7, 159.8, 152.4, 149.5, 136.9, 133.8, 132.1, 129.4, 129.3, 128.6, 127.8, 126.7, 126.1, 124.8, 120.4, 119.0, 87.3. IR ν_{max}/cm^{-1} 3109, 1815, 1779, 1717, 1598, 1525, 1489, 1348, 1323, 1178, 1138, 1058, 909. HRMS (ESI-TOF) m/z: calcd for $C_{24}H_{15}N_3NaO_5$ $[M+Na]^+$ 448.0904. Found 448.0915. HPLC (Chiralcel OD, n-hexane/2-propanol 80:20, λ= 254 nm, 0.6 mL/min). t_R (minor)= 33.6 min, t_R (major)= 50.4 min (er 92:8).

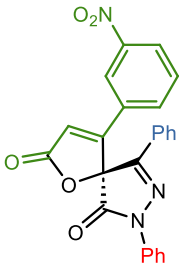

3ai

(S)-4-(3-nitrophenyl)-7,9-diphenyl-1-oxa-7,8-diazaspiro[4.4]nona-3,8-diene-2,6-dione **(3ai)**. Following the general procedure and after column chromatography using hexane/ethyl acetate 10:1 as eluent, **3ai** was isolated as white solid (13.4 mg, 43% yield). Mp 184-186 °C (from hexane/acetate). $[\alpha]^{25}_{D}$= -35.8 (*c*= 0.2, $CHCl_3$, er 95:5). ^{1}H NMR (500 MHz, $CDCl_3$) δ 8.29-8.27 (m, 2H), 7.75-7.73 (m, 2H), 7.70-7.67 (m, 1H), 7.61-7.58 (m, 1H), 7.58-7.52 (m, 4H), 7.45-7.42 (m, 3H), 7.31 (tt, *J*= 7.1, 1.2 Hz, 1H), 6.90 (s, 1H). ^{13}C {^{1}H} NMR (126 MHz, $CDCl_3$) δ 169.2, 164.8, 159.6, 152.6, 148.8, 136.9, 132.1, 131.0, 130.6, 129.6, 129.4, 129.1, 128.7, 128.7, 126.8, 126.5, 121.7, 119.5, 119.4, 119.2, 87.2. IR ν_{max}/cm^{-1} 2971, 2923, 2846, 1776, 1732, 1597, 1538, 1487, 1381, 1381, 1351, 1326, 1139, 1069, 956. HRMS (ESI-TOF) m/z: calcd for $C_{24}H_{15}N_3NaO_5$ $[M+Na]^+$ 448.0904. Found 448.0899. HPLC (Chiralcel OD, n-hexane/2-propanol 75:25, λ= 254 nm, 1 mL/min). t_R (major)= 17.0 min, t_R (minor)= 20.3 min (er 95:5).

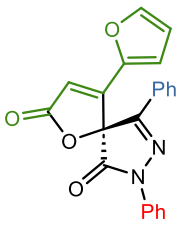

3aj

(S)-4-(furan-2-yl)-7,9-diphenyl-1-oxa-7,8-diazaspiro[4.4]nona-3,8-diene-2,6-dione (**3aj**). Following the general procedure and after column chromatography using hexane/ethyl acetate 10:1 as eluent, **3aj** was isolated as white solid (14.8 mg, 68% yield). Mp 155-157 °C (from hexane). $[\alpha]^{25}_{D}$= -84.5 (*c*= 0.2, $CHCl_3$, er 97:3). ^{1}H NMR (500 MHz, $CDCl_3$) δ 7.98 (d, *J*= 8.5 Hz, 2H), 7.71 (d, *J*= 7.9 Hz, 2H), 7.53-7.44 (m, 4H), 7.42-7.38 (m, 2H), 7.31 (t, *J*= 6.5 Hz, 1H), 6.70 (s, 1H), 6.60 (s, 1H), 6.43 (s, 1H). ^{13}C {^{1}H} NMR (126 MHz, $CDCl_3$) δ 170.5, 165.4, 153.4, 150.2, 147.1, 143.6, 131.7, 131.2, 129.2, 129.1, 128.8, 126.3, 126.2, 119.1, 115.1, 113.3, 112.0, 85.6. IR ν_{max}/cm^{-1} 3148, 3115, 3075, 2957, 2932, 2862, 1797, 1775, 1735, 1628, 1592, 1500, 1383, 1316, 1170, 1070, 1026, 905. HRMS (ESI-TOF) m/z: calcd for $C_{22}H_{15}N_2O_4$ $[M+Na]^+$ 371.1026. Found 371.1030. HPLC (Chiralcel IA, n-hexane/2-propanol 90:10, λ= 254 nm, 0.5 mL/min). t_R (major)= 42.9 min, t_R (minor)= 147.7 min (er 97:3).

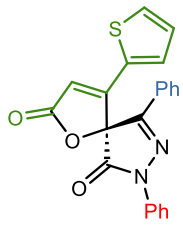

3ak

(S)-7,9-diphenyl-4-(thiophen-2-yl)-1-oxa-7,8-diazaspiro[4.4]nona-3,8-diene-2,6-dione (**3ak**). Following the general procedure and after column chromatography using hexane/ethyl acetate 10:1 as eluent, **3ak** was isolated as white solid (15.0 mg, 66% yield). Mp 130-132 °C (from hexane). $[\alpha]^{25}_{D}$= -150.7 (*c*= 0.3, $CHCl_3$, er 92:8). ^{1}H NMR (500 MHz, $CDCl_3$) δ 7.98 (d, *J*= 9.3 Hz, 2H), 7.74 (d, *J*= 8.8 Hz, 2H), 7.52-7.45 (m, 4H), 7.24-7.38 (m, 2H), 7.31 (t, *J*= 7.3 Hz, 1H), 7.23 (d, *J*= 3.8 Hz, 1H), 7.01 (dd, *J*= 4.7, 3.9 Hz, 1H), 6.57 (s, 1H). ^{13}C {^{1}H} NMR (126 MHz, $CDCl_3$) δ 170.2, 165.3, 155.2, 153.6, 137.2, 132.0, 131.8, 130.6, 129.4, 129.3, 129.2, 129.1, 128.8, 126.4, 126.2, 119.1, 113.6, 86.7. IR ν_{max}/cm^{-1} 3115, 2965, 2921, 2851, 1801, 1768, 1742, 1592, 1482, 1386, 1173, 1148, 1085, 1067, 946. HRMS (ESI-TOF) m/z: calcd for $C_{22}H_{14}N_2NaO_3S$ $[M+Na]^+$ 409.0617. Found 409.0624. HPLC (Chiralcel OD, n-hexane/2-propanol 95:5, λ= 254 nm, 0.5 mL/min). t_R (major)= 56.3 min, t_R (minor)= 63.2 min (er 92:8).

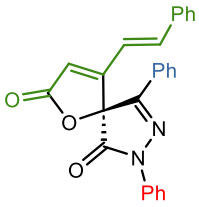

3al

(S)-7,9-diphenyl-4-styryl-1-oxa-7,8-diazaspiro[4.4]nona-3,8-diene-2,6-dione (**3al**). Following the general procedure and after column chromatography using hexane/ethyl acetate 10:1 as eluent, **3al** was isolated as pale yellow oil (8.5 mg, 18% yield). $[\alpha]^{25}_{D}$= -75.7 (*c*= 0.2, $CHCl_3$, er 78:22). ^{1}H NMR (500 MHz, $CDCl_3$) δ 8.00 (d, *J*= 9.8 Hz, 2H), 7.73 (d, *J*= 9.7 Hz, 2H), 7.52-7.46 (m, 3H), 7.42 (t, *J*= 8.3 Hz, 2H), 7.33-7.30 (m, 6H), 6.94 (d, *J*= 16.5 Hz, 1H), 6.77 (dd, *J*= 16.5, 0.7 Hz, 1H), 6.48 (s, 1H). ^{13}C {^{1}H} NMR (126 MHz, $CDCl_3$) δ 170.7, 165.5, 159.5, 153.6, 140.0, 137.2, 134.3, 131.8, 130.6, 129.3, 129.2, 129.0, 128.8, 127.8, 126.4, 126.2, 119.2, 116.3, 115.8, 87.0. IR ν_{max}/cm^{-1} 2924, 2854, 1804, 1774, 1727, 1621, 1588, 1494, 1315, 1293, 1169, 1143, 1070, 899. HRMS (ESI-TOF) m/z: calcd for $C_{26}H_{18}N_2NaO_3$ $[M+H]^+$ 429.1210. Found 429.1219. HPLC (Chiralcel OD, n-hexane/2-propanol 90:10, λ= 220 nm, 0.5 mL/min). t_R (major)= 36.3 min, t_R (minor)= 28.7 min (er 78:22).

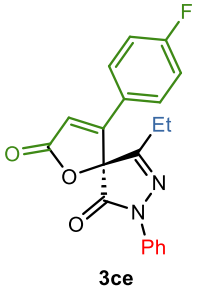

3ce

(S)-9-ethyl-4-(4-fluorophenyl)-7-phenyl-1-oxa-7,8-diazaspiro[4.4]nona-3,8-diene-2,6-dione (**3ce**). Following the general procedure and after column chromatography using hexane/ethyl acetate 10:1 as eluent, **3ce** was isolated as yellow oil (9.2 mg, 35% yield). $[\alpha]^{25}_{D}$= -45.7 (*c*= 0.2, $CHCl_3$, er 92:8). ^{1}H NMR (500 MHz, $CDCl_3$) δ 7.90 (d, *J*= 8.8 Hz, 2H), 7.46 (t, *J*= 7.7 Hz, 2H), 7.39-7.36 (m, 2H), 7.28 (t, *J*= 7.3 Hz, 1H), 7.11 (t, *J*= 8.2 Hz, 2H), 6.61 (s, 1H), 2.54-2.44 (m, 1H), 2.31-2.23 (m, 1H), 1.22 (t, *J*= 7.5 Hz, 3H). ^{13}C {^{1}H}

NMR (126 MHz, $CDCl_3$) δ 170.0, 166.2, 164.5 (d, *J*= 177.2 Hz), 160.2, 159.1, 137.2, 129.2, 128.9, 128.8, 126.2, 124.4, 118.9, 117.4, 117.1, 116.5, 87.5, 21.3, 9.3. ^{19}F NMR (470 MHz, $CDCl_3$) δ -106.4. IR ν_{max}/cm^{-1} 2986, 2913, 2855, 1808, 1783, 1728, 1598, 1500, 1457, 1391, 1348, 1239, 1181, 1163, 1120, 1051. HRMS (ESI-TOF) m/z: calcd for $C_{20}H_{15}FN_2NaO_3$ $[M+Na]^+$ 373.0959. Found 373.0961. HPLC (Chiralcel OD, n-hexane/2-propanol 95:5, λ= 254 nm, 1 mL/min). t_R (minor)= 21.3 min, t_R (major)= 24.6 min (er 92:8).

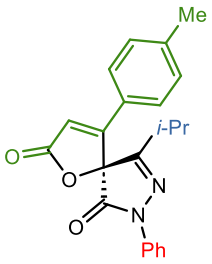

3db

(S)-9-isopropyl-7-phenyl-4-(p-tolyl)-1-oxa-7,8-diazaspiro[4.4]nona-3,8-diene-2,6-dione (**3db**). Following the general procedure and after column chromatography using hexane/ethyl acetate 10:1 as eluent, **3db** was isolated as yellow oil (18.8 mg, 86% yield). $[\alpha]^{25}_D$= -93.0 (*c*= 0.4, $CHCl_3$, er 93:7). ^1H NMR (500 MHz, $CDCl_3$) δ 7.90 (d, *J*= 9.8 Hz, 2H), 7.46 (t, *J*= 7.4 Hz, 2H), 7.29-7.25 (m, 3H), 7.21-7.19 (m, 2H), 6.63 (s, 1H), 2.70-2.61 (m, 1H), 2.35 (s, 3H), 1.26 (d, *J*= 6.9 Hz, 3H), 1.10 (d, *J*= 7.0 Hz, 3H). ^{13}C $\{^1H\}$ NMR (126 MHz, $CDCl_3$) δ 170.5, 165.3, 163.5, 160.8, 143.3, 137.4, 130.5, 129.1, 126.5, 126.0, 125.5, 118.9, 115.3, 87.7, 29.1, 21.5, 20.2. IR ν_{max}/cm^{-1} 2975, 2874, 1803, 1774, 1727, 1597, 1500, 1380, 1326, 1182, 1128, 1049, 904. HRMS (ESI-TOF) m/z: calcd for $C_{22}H_{20}N_2NaO_3$ $[M+Na]^+$ 383.1366. Found 383.1378. HPLC (Lux i-Cellulose-5, n-hexane/2-propanol 80:20, λ= 210 nm, 0.8 mL/min). t_R (minor)= 28.1 min, t_R (major)= 38.9 min (er 93:7).

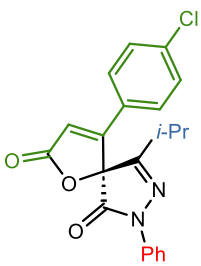

3df

(S)-4-(4-chlorophenyl)-9-isopropyl-7-phenyl-1-oxa-7,8-diazaspiro[4.4]nona-3,8-diene-2,6-dione (**3df**). Following the general procedure and after column chromatography using hexane/ethyl acetate 10:1 as eluent, **3df** was isolated as yellow oil (16.6 mg, 71% yield). $[\alpha]^{25}_D$= -65.1 (*c*= 0.3, $CHCl_3$, er 91:9). ^1H NMR (500 MHz, $CDCl_3$) δ 7.89 (d, *J*= 9.5 Hz, 2H), 7.46 (t, *J*= 7.6 Hz, 2H), 7.40-7.38 (m, 2H), 7.30-7.28 (m, 3H), 6.67 (s, 1H), 2.70-2.60 (m, 1H), 1.26 (d, *J*= 6.9 Hz, 3H), 1.11 (d, *J*= 6.9 Hz, 3H). ^{13}C $\{^1H\}$ NMR (126 MHz, $CDCl_3$) δ 170.0, 165.3, 163.1, 159.4, 138.8, 137.2, 130.2, 129.2, 127.8, 126.7, 126.2, 118.9, 116.9, 87.7, 29.2, 20.2. IR ν_{max}/cm^{-1} 3108, 2979, 2939, 2880, 1808, 1772, 1731, 1588, 1489, 1375, 1342, 1181, 1093, 927. HRMS (ESI-TOF) m/z: calcd for $C_{21}H_{17}ClN_2NaO_3$ $[M+Na]^+$ 403.0820. Found 403.0821. HPLC (Lux i-Cellulose-5, n-hexane/2-propanol 80:20, λ= 210 nm, 0.6 mL/min). t_R (minor)= 31.9 min, t_R (major)= 47.8 min (er 91:9).

3.5.2 Catalytic Hydrogenation of Spiropyrazolone-Butenolide 3a.

To a solution of spirocyclic butenolide **3a** (34.8 mg, 0.091 mmol) in ethyl acetate (2 mL), Pd/C (10 wt%) was added. The mixture was stirred under hydrogen atmospheric pressure for 20 h. After removal of the palladium on carbon, the solvent was removed and the crude product was purified by column chromatography (hexane/ethyl acetate 10:1) affording compound **4** as a single diastereomer (15.7 mg, 45% yield).

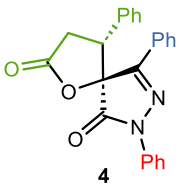

4

(4R,5S)-4,7,9-Triphenyl-1-oxa-7,8-diazaspiro[4.4]non-8-ene-2,6-dione (**4**).[16] ^1H NMR (500 MHz, $CDCl_3$) δ 7.98-8.00 (m, 2H), 7.54-7.59 (m, 3H), 7.43-7.45 (m, 2H), 7.22-7.31 (m, 5H), 7.14-7.18 (m, 1H), 7.11-7.13 (m, 2H), 4.15 (dd, *J*= 13.8, 8.2 Hz, 1H), 3.82 (dd, *J*= 14.0, 13.8 Hz, 1H), 2.93 (dd, *J*= 17.1, 8.2 Hz, 1H). ^{13}C $\{^1H\}$ NMR (126 MHz, $CDCl_3$) δ 173.5, 168.7, 153.2, 136.5, 131.5, 130.5, 129.4,

129.1, 128.8, 128.7, 128.6, 127.6, 126.8, 126.1, 119.5, 87.8, 49.0, 30.3. HPLC (Lux Amylose-1, n-hexane/2-propanol 70:30, λ= 254 nm, 0.8 mL/min): t_R (minor)= 6.4 min, t_R (major)= 7.8 min (er 94:6).

3.5.3 Transformation of spiropyrazolone-butenolide 3ag.

To a solution of spirocyclic butenolide **3ag** (38.3 mg, 0.083 mmol), phenylboronic acid (15.3 mg, 0.125 mmol) and K_3PO_4 (35.3 mg, 0.166 mmol) in THF/H_2O 5:1 (1.2 mL) under a N_2 atmosphere, $PdCl_2(PPh_3)_2$ (10 mol%) was added. After refluxing for 8 h, the solvent was removed under reduced pressure. The crude mixture was purified by column chromatography (hexane/ethyl acetate 10:1) affording **5** as a white solid (36.8 mg, 96% yield).

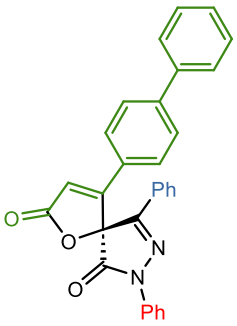

5

(S)-4-([1,1'-biphenyl]-4-yl)-7,9-diphenyl-1-oxa-7,8-diazaspiro[4.4]nona-3,8-diene-2,6-dione (**5**). Mp 66-68 °C (from hexane/acetate). $[\alpha]^{25}_D$= -116.0 (*c*= 0.4, $CHCl_3$, er 95:5). ^{1}H NMR (500 MHz, $CDCl_3$) δ 7.99 (d, *J*= 8.8 Hz, 2H), 7.75 (d, *J*= 8.1 Hz, 2H), 7.58 (d, *J*= 8.3 Hz, 2H), 7.52-7.48 (m, 5H), 7.47-7.46 (m, 2H), 7.44-7.37 (m, 5H), 7.31 (t, *J*= 8.0 Hz, 1H), 6.80 (s, 1H). ^{13}C {^{1}H} NMR (126 MHz, $CDCl_3$) δ 170.3, 165.4, 161.7, 153.5, 145.2, 139.1, 137.3, 133.1, 131.8, 129.2, 129.0, 128.4, 128.3, 127.0, 126.8, 126.4, 126.3, 119.2, 116.3, 81.2. IR ν_{max}/cm^{-1} 3073, 3030, 2927, 2851, 1804, 1774, 1723, 1599, 1559, 1442, 1384, 1180, 1143, 1070, 1005. HRMS (ESI-TOF) m/z: calcd for $C_{30}H_{21}N_2O_3$ $[M+H]^+$ 457.1547. Found 457,1528. HPLC (Lux i-Cellulose 5, n-hexane/2-propanol 85:15, λ= 254 nm, 0.8 mL/min). t_R (minor)= 56.4 min, t_R (major)= 85.4 min (er 95:5).

3.5.4 Procedure for Spirooxindole-Butenolide 7.

In a 5 mL heat gun-dried flask equipped with a magnetic stirring bar pre-catalyst **C2** (6 μmol, 0.1 equiv) and *N*-benzyl isatin **6** (0.06 mmol) were weighed. Then β-bromoenal **2a** (0.09 mmol, 1.5 equiv) was added under a N_2 atmosphere. Dry chloroform (1 mL) was added before the mixture was stirred. Several minutes later, DBU (0.09 mmol, 1.5 equiv) was introduced to the flask. After 16 h, the solvent was straight removed under reduced pressure and the residue was purified by column chromatography (hexane/ethyl acetate, 10:1) affording compound **7** as a white solid (16.6 mg, 75%).

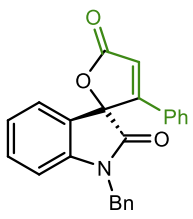

7

(S)-1'-benzyl-3-phenyl-5H-spiro[furan-2,3'-indoline]-2',5-dione (**7**).[13] $[\alpha]^{25}_D$= +15.0 (*c*= 0.4, $CHCl_3$, er 93:7). ^{1}H NMR (500 MHz, $CDCl_3$) δ 7.37-7.33 (m, 2H), 7.30-7.28 (m, 3H), 7.24-7.22 (m, 2H), 7.20-7.17 (m, 3H), 7-09-7.04 (m, 3H), 6.88 (d, *J*= 7.9 Hz, 1H), 6.67 (s, 1H), 5.13 (d, *J*= 15.4 Hz, 1H), 4.76 (d, *J*= 15.5 Hz, 1H). ^{13}C {^{1}H} NMR (126 MHz, $CDCl_3$) δ 171.3, 170.0, 163.0, 143.5, 134.7, 131.8, 131.4, 129.1, 129.0, 128.8, 128.1, 127.6, 127.2, 125.1, 124.0, 123.8, 117.0, 110.4, 86.5, 44.6. HPLC (Chiralcel OD, n-hexane/2-propanol 85:15, λ= 254 nm, 0.4 mL/min). t_R (major)= 77.7 min, t_R (minor)= 87.8 min (er 93:7).

Chapter IV: Squaramide-catalyzed Asymmetric Synthesis of Spiropyrazolone-Oxazolidines from *N*-Boc pyrazolinone ketimines and γ-hydroxyenones.

This work was published as:

"Organocatalytic Asymmetric Synthesis of Oxazolidino Spiropyrazolinones via N,O-acetalization/aza Michael addition domino reaction between N-Boc pyrazolinone ketimines and γ-hydroxyenones"

Marta Gil-Ordóñez, Laura Martín, Alicia Maestro, José M. Andrés. *Org. Biomol. Chem*. **2023**, *21*, 2361-2369.

4.1 Introduction and background

The stereoselective construction of heterocyclic spiropyrazolone molecules is currently considered an arduous challenge due to difficulties in controlling diastereo- and enantioselectivities. Although the formation of enantioenriched 4-spiropyrazolones with one heteroatom-incorporated spirocenter is a growing field, the asymmetric synthesis of spiropyrazolones with two heteroatoms attached (*N*,O; *N*,*N*') at the C-4 position has hardly been studied despite the fact that *N,N'*[1] and *N,O*-acetal[2] frameworks are privileged structures of biologically active compounds. Recently, Yang and Huang[3] described the palladium-catalyzed asymmetric [4+2] annulation of vinyl benzoxazinanones with pyrazolin-4,5-diones to access spirobenzoxazine derivatives. In contrast, in the literature, *N,N* and *N,O*-acetals derived from isatin have been prepared through addition of arylamines[4] and alcohols[5] to isatin-derived ketimines in the presence of a quinine-based bifunctional catalyst.

Chiral oxazolidines are important motifs as they involve interesting biological properties in natural products,[6] Figure 4.1.

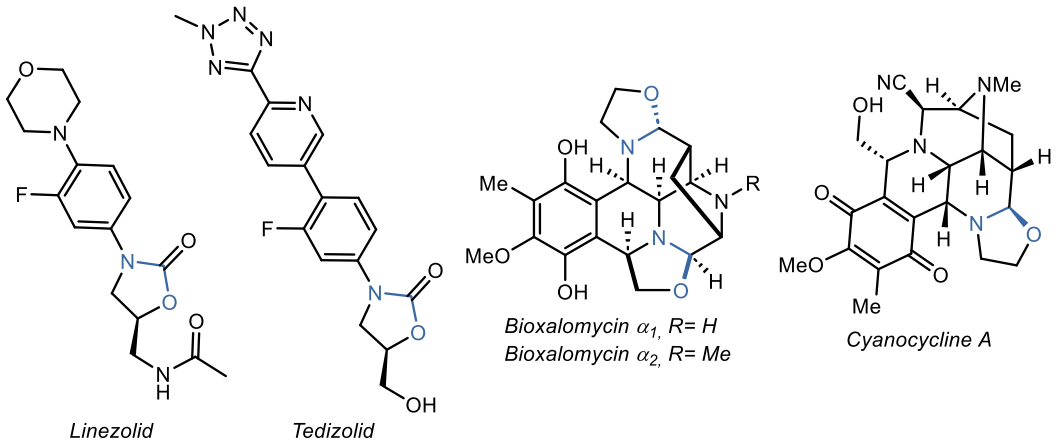

Figure 4.1: Some antibiotics containing chiral oxazolidinones and oxazolidines.

[1] (a) A. Kapil, D. Anshu *Lett. Org. Chem.* **2007**, *4*, 378−383, (b) S. Y. Hwang, D. A. Berges, J. J. Taggart, C. Gilvart *J. Med. Chem.* **1989**, *32,* 694698.
[2] (a) W. -L. Wang, T. -J. Zhu, H. -W. Tao, Z. -Y. Lu, Y. -C. Fang, Q. -Q. Gu, W. -M. Zhu *Chem. Biodiversit*y **2007**, *4*, 2913, (b) A. B. Smith, I. G. Safanov, R. M. Corbett *J. Am. Chem. Soc.* **2001**, *123*, 12426−12427.
[3] B. -H. Chen, S. -J. Liu, Q. Zhao, Q. Hou, J. -L. Yuan, G. Zhan, Q. -Q. Yang, W. Huang *Chem. Commun.* **2023**, 59, 1233–1236.
[4] Y. Liu, J. Wang, Z. Wei, J. Cao, D. Liang, Y. Lin, H. Duan *Org. Lett*. **2019**, *21*, 5719−5724.
[5] (a) J. Liu, F. -M. Zhu, Y. -B. Chu, L. -H. Huang, Y. -F. Zhou *Tetrahedron Asymmetry* **2015**, *26*, 1130−1137, (b) T. -Z. Li, X. -B. Wang, F. Sha, X. -Y. Wu *Tetrahedron* **2013**, *69*, 7314−7319.
[6] (a) C. Foti, A. Piperno, A. Scala, O. Giuffrè *Molecules*, **2021**, *26*, 4280, (b) J. F. Branco-Junior, D. R. C. Teixeira, M. C. Pereira, I. R. Pitta, M. R. Galdino-Pitta *Curr. Bioact. Compd*. **2017**, *13*, 292-304, (c) P. Siengalewicz, U. Rinner, J. Mulzer *Chem. Soc. Rev*. **2008**, *37*, 2676–2690, (d) J. D. Scott, R. M. Williams *Chem. Rev.* **2002**, *102*, 1669−1730.

Despite their interest, the organocatalytic asymmetric synthesis of oxazolidines has been little studied. Matsubara[7] first developed the synthesis of 2,4-disubstituted chiral oxazolidines *via* formal [3+2] cycloaddition of γ-hydroxyenones with *N*-tosylaldimines, but the enantioselectivity was moderate, Scheme 4.1a. Later, Terada[8] described the [3+2] cycloaddition of β,γ-epoxysulfones and *N*-Boc aldimines, for the synthesis of 2,4,5-trisubstituted 1,3-oxazolidines in a highly diastereo- and enantioselective manner, Scheme 4.1b. Next, Pan[9] prepared 2,5-disubstituted oxazolidines *via* hemiaminal formation/Michael reaction between simple alkyl aldehydes and *N*-tosyl aminomethyl enones with excellent diastero- and enantioselectivity, Scheme 4.1c.

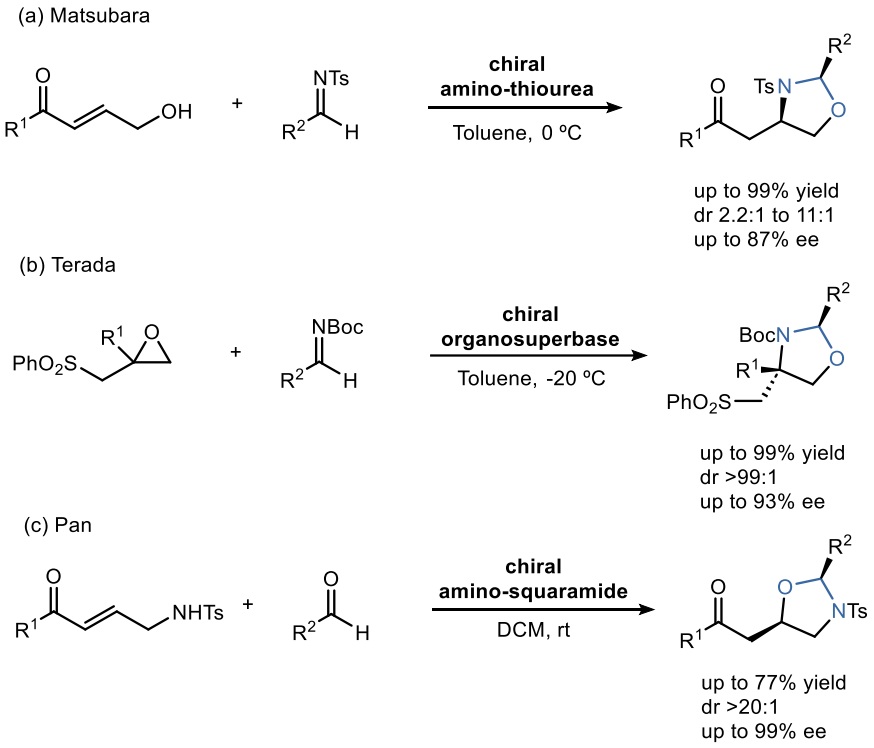

Scheme 4.1: Representative examples of organocatalytic asymmetric synthesis of oxazolidines.

Recently, the same author reported the synthesis of spirooxindole embedded oxazolidines *via* a domino reaction involving hemiaminal formation, followed by an aza-Michael reaction between isatin derived *N*-Boc ketimines and γ-hydroxyenones, promoted by a quinine-derived bifunctional squaramide catalyst,[10] Scheme 4.2.

[7] Y. Fukata, K. Asano, S. Matsubara *Chem. Lett.* **2013**, *42*, 355–357.
[8] A. Kondoh, S. Akahira, M. Oishi, M. Terada *Angew. Chem. Int. Ed.* **2018**, *57*, 6299–6303.
[9] S. Mukhopadhyayaand, S. C. Pan *Adv. Synth. Catal.* **2019**, *361*, 1028–1032.
[10] C. Parida, B. Mondal, A. Ghosh, S. C. Pan *J. Org. Chem.* **2021**, *86*, 13082–13091.

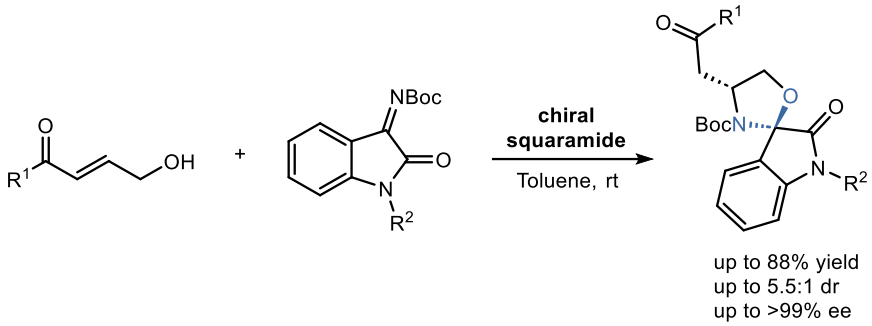

Scheme 4.2: Synthesis of spirooxindole embedded oxazolidines reported by Pan.

When involving the pyrazole core, there is only one example in literature of the synthesis of oxazolidino-spiropyrazolinones. Li[11] reported the synthesis of trispirocyclic *N,O*-ketal from pyrazole-derived ketimines *via* organic-base/Au(I)-catalyzed sequential asymmetric 1,2-addition/hydroamination/hetero Diels-Alder (HAD)/debutylation reactions, Scheme 4.3.

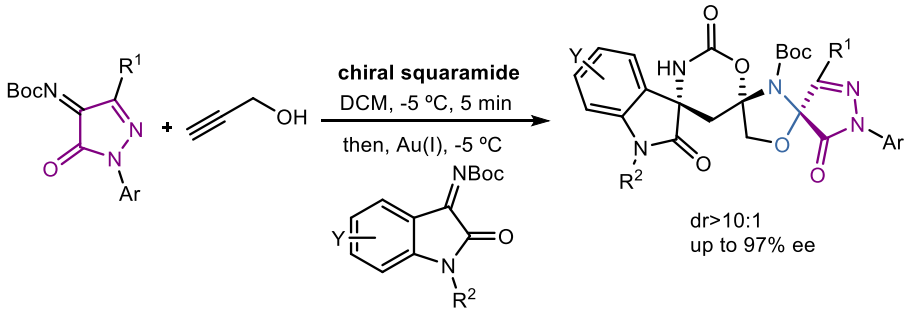

Scheme 4.3: Synthesis of oxazolidino-spiropyrazolones displayed by Li.

However, apart from this example, there are no examples in literature for the synthesis of spiropyrazolone-derived oxazolidines. Consequently, in this chapter, we study the synthesis of spiropyrazolones with a *N,O*-acetal directly attached to the spirocyclic center through hydrogen bond catalysis.

[11] W. Guo, L. Li, Q. Ding, X. Lin, X. Liu, K. Wang, Y. Liu, H. Fan, C. Li *ACS Catal*. **2018**, *8*, 10180–10189.

4.2 Results and discussion

First, we started the study of the reaction combining phenyl-derived *N*-Boc ketimine **1a** with hydroxyenone **2a**. Different catalysts **C1**-**C8** were evaluated in toluene as solvent at room temperature. When quinine-derived thiourea **C1** was used in the reaction, **3aa** was isolated in good yield (89%), low diastereomeric ratio (1:1.2 dr) and 62% ee for the major diastereomer and that of the minor 94% ee (entry 1). Switching the thiourea scaffold to a squaramide motif, **C2**, supposed an improvement of the diastereometic ratio (2.7:1 dr) accompanied with excellent enantioselectivity of the major diastereomer (99% ee) despite the moderate enantiomeric excess in the minor diastereomer (46% ee, entry 2).

Next, the influence of the hydrogen bonding donor group was analyzed by comparing squaramide **C2** (bearing a phenethyl group) with **C3** (a (bis(trifluoromethyl)benzyl derivative) and **C4** (a bis(trifluoromethyl)phenyl derivative) (entries 2-4). When catalyst **C3** was used in the reaction, the diastereomeric ratio remained the same and both diastereomers were obtained with good to excellent enantiomeric ratios (98% and 80% ee, respectively). Moreover, when squaramide **C4** was used as catalyst, the enantiomeric excess of both diastereomers became excellent (>99 and 94%) but the diastereomeric ratio dropped to 1:1.2, entry 4. To improve the diastereo- and enantioselectivity, additional attempts with bifunctional squaramides **C5** and **C6** having bis(trifluoromethyl)benzyl groups were performed (entries 5 and 6). Cinchonidine-derived squaramide **C5** did not involve any improvement and **3aa** yielded 19% after 12 h, probably due to the lower solubility of the catalyst in toluene (entry 5). Delightfully, hydroquinine-derived catalyst **C6** provided spiropyrazolone derivative in 97% yield, the highest diastereomeric ratio so far (2.8:1 dr) and 98 and 90% ee, respectively (entry 6).

Further attempts to improve diastereoselectivity were carried out with *L*-valine and *L*-*tert*-leucine-derived squaramides, **C7** and **C8**, providing no better results (entries 7-8). Both catalysts led to a change in the diastereoselection.

Table 1. Screening of catalysts **C1-C8**.[a]

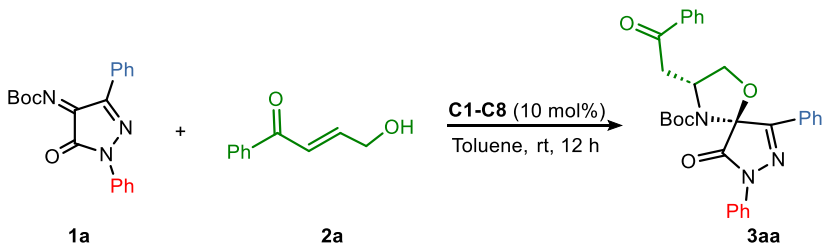

1a **2a** **3aa**

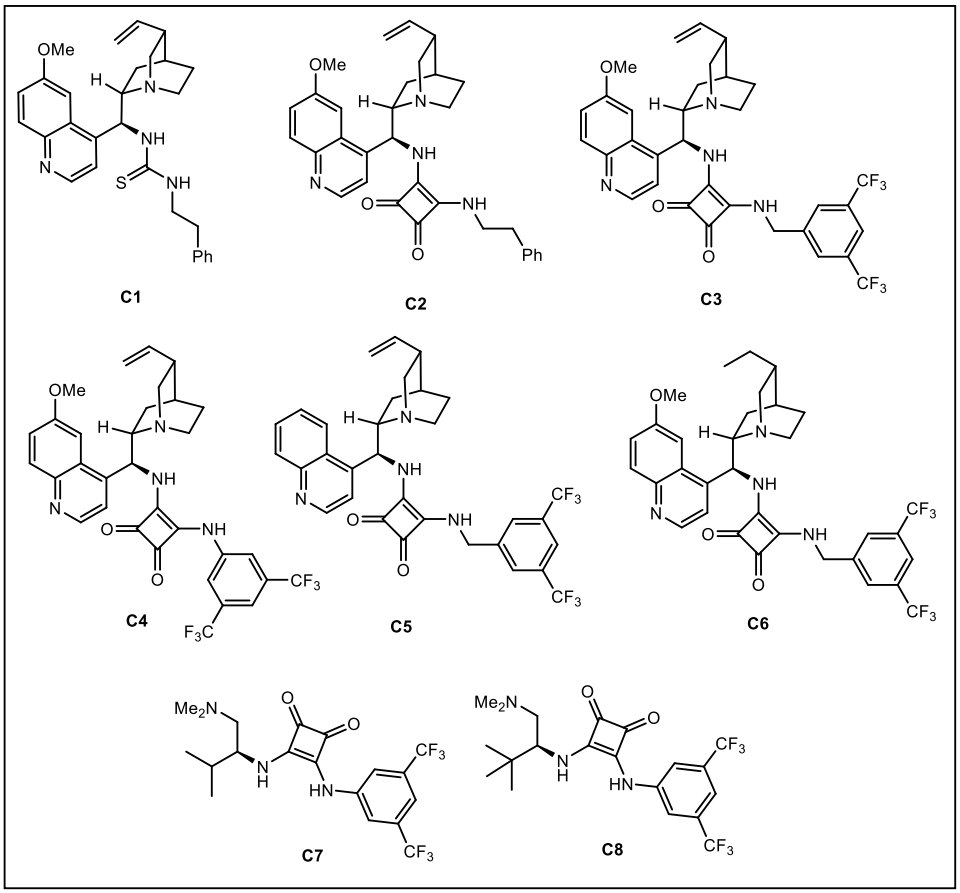

Entry	Catalyst	Yield (%)[b]	dr (**3aa**:epi-**3aa**)[c]	ee (**3aa**)[c]	ee (epi-**3aa**)[c]
1	**C1**	89	1:1.2	94	62
2	**C2**	83	2.7:1	>99	46
3	**C3**	78	2.7:1	98	80
4	**C4**	79	1:1.2	>99	94
5	**C5**	19	1:1.5	>99	54
6	**C6**	97	2.8:1	98	90
7	**C7**	88	1:1.6	92	78
8	**C8**	87	1:1.6	98	88

[a] Reaction conditions: **1a** (0.1 mmol), **2a** (0.15 mmol), **C1**-**C8** (10 mol%), toluene (1 mL) at rt for 12 h. [b] Yield of **3aa** determined after column chromatography. [c] Dr and ee values determined *via* chiral HPLC analysis.

With hydroquinine-derived squaramide **C6** as the best catalyst for performing the [3+2] annulation, reaction conditions optimization was carried out, Table 2. Different solvents were tested (Table 2, entries 1-5), but no better results were found. In all the cases, the enantioselectivity observed for **3aa** was better, but the diastereocontrol was inferior, with the exception of diethyl ether, which provided similar results to toluene. Interestingly, the enantioselectivities obtained for *epi*-**3aa** depended strongly on the solvent, and another case of solvent-induced reversal of enantioselectivity was found with acetonitrile.[12] The reaction also worked nicely when 5 mol% of catalyst **C6** was used, but a considerable increase in reaction time was required (48 h, Table 2, entry 6). The reaction carried out at 0 ^{o}C led to the same results as the one performed at room temperature although the yield decreased to 80% (Table 2, entry 7).

[12] Some cases of solvent-induced reversal of enantioselectivity in organocatalyzed transformations have been previously reported: (a) C. -H. Chang, N. Sathishkumar, Y. -T. Liao, H. -T. Chen, J. -L. Han *Adv. Synth. Catal*. **2020**, *362*, 903–912, (b) J. Flores-Ferrándiz, B. Fiser, E. Gómez-Bengoa, R. Chinchilla *Eur. J. Org. Chem*. **2015**, 1218–1225.

Table 2. Optimization of reaction conditions.[a]

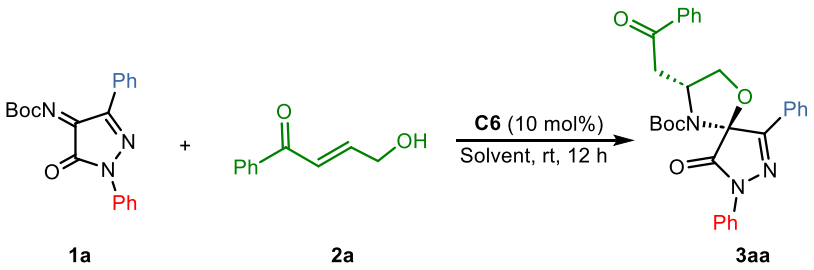

1a **2a** **3aa**

Entry	*Solvent*	*Yield (%)*[b]	*dr (**3aa**:epi-**3aa**)*[c]	*ee (**3aa**)*[c]	*ee (epi-**3aa**)*[c]
1	Toluene	97	2.8:1	98	90
2	Et_2O	92	2.8:1	>99	78
3	THF	72	1.1:1	>99	36
4	CH_2Cl_2	90	1.6:1	>99	56
5	MeCN	99	1:1.9	>99	-20
6[d]	Toluene	92	2.8:1	98	88
7[e]	Toluene	80	2.7:1	98	90

[a] Reaction conditions: **1a** (0.1 mmol), **2a** (0.15 mmol), **C6** (10 mol%), solvent (1 mL) at rt for 12 h. [b] Yield of **3aa** determined after column chromatography. [c] Dr and ee values determined *via* chiral HPLC analysis. [d] Reaction performed with 5 mol% of catalyst for 48 h. [e] Reaction performed at 0 °C.

Having established the optimal reaction conditions (10 mol% of **C6** and toluene as solvent at room temperature), substrate scope was then examined. Initially, different *para*-substituted phenyl γ-hydroxyenones (**2a**-**e**) were screened (Table 3), and gratifyingly, good results were achieved for the products **3aa**-**3ae** after 12 h reaction time. 4-Halo-substituted γ-hydroxyenones were well tolerated in the reaction, providing adducts **3ab** and **3ac** with moderate diastereoselectivity (up to 3:1 dr) and high enantioselectivities for the major diastereomer (98% ee). The reaction also worked with similar diastereo- and excellent enantioselectivity with γ-hydroxyenones having a *p*-tolyl or anisole motif to deliver products **3ad** and **3ae** (99% and >99% ee).

Table 3. Scope of the reaction with differently substituted γ-hydroxyenones.[a,b,c]

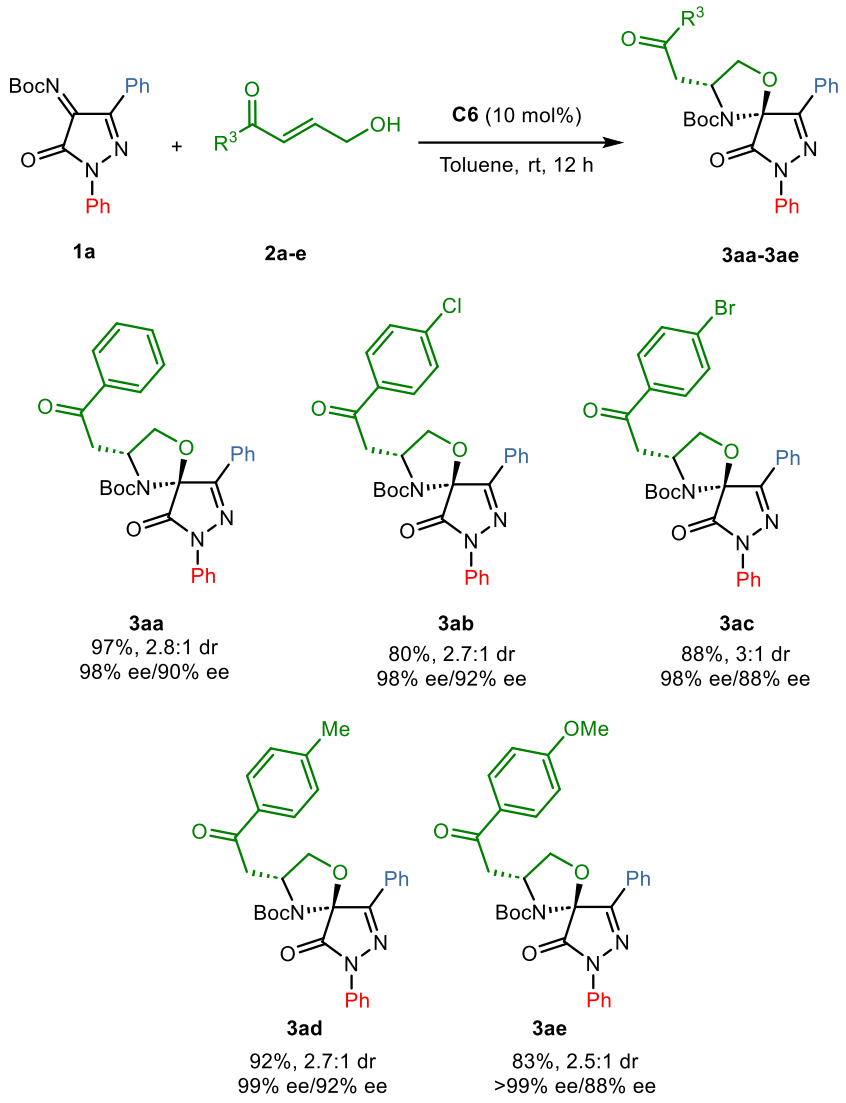

3aa
97%, 2.8:1 dr
98% ee/90% ee

3ab
80%, 2.7:1 dr
98% ee/92% ee

3ac
88%, 3:1 dr
98% ee/88% ee

3ad
92%, 2.7:1 dr
99% ee/92% ee

3ae
83%, 2.5:1 dr
>99% ee/88% ee

[a] Reaction conditions: **1a** (0.1 mmol), **2a-e** (0.15 mmol), **C6** (10 mol%), toluene (1 mL) at rt for 12 h. [b] Yield of **3aa-3ae** determined after column chromatography. [c] Dr and ee values determined *via* chiral HPLC analysis.

Next, the effect of substitution in the pyrazolone ring of the *N*-Boc ketimine was tested (Table 4). Ketimines **1b**-**d**, with different alkyl substituents at the C-3 position (R^1) were reacted with γ-hydroxyenone **2a** to produce the corresponding adducts **3ba**-**3da** in good yields. In particular, methyl-substituted imine **1b** afforded the desired product **3ba** with good diastereo- and enantioselectivity (3.3:1 dr, 92% ee). Imines **1c** and **1d** bearing bulkier groups attached at C-3, like an ethyl or an isopropyl group, also worked well in the reaction albeit with somewhat diminished diastereoselectivity (1.9:1 and 2:1 dr). A *tert*-butyl group directly attached at C-3 position blocked the reaction and no product was observed after several days, **3ea**.

Moreover, our methodology is also suitable for *N*-Boc ketimines with a methyl group at the *N*-1 position (R^2), affording adduct **3fa** in 98% yield, moderate diastereomeric ratio and excellent enantiomeric excess for both diastereomers (94% and >99%, respectively). However, when the nitrogen atom had a *para*-substituted phenyl group, the corresponding products, **3ga** and **3ha**, were obtained in good yield but low diastereoselectivity and, surprisingly, with a loss of enantioselectivity in the major diastereomer (82% and 76% ee, respectively).

Table 4. Scope of the reaction with differently substituted *N*-Boc pyrazolinone ketimines.[a,b,c]

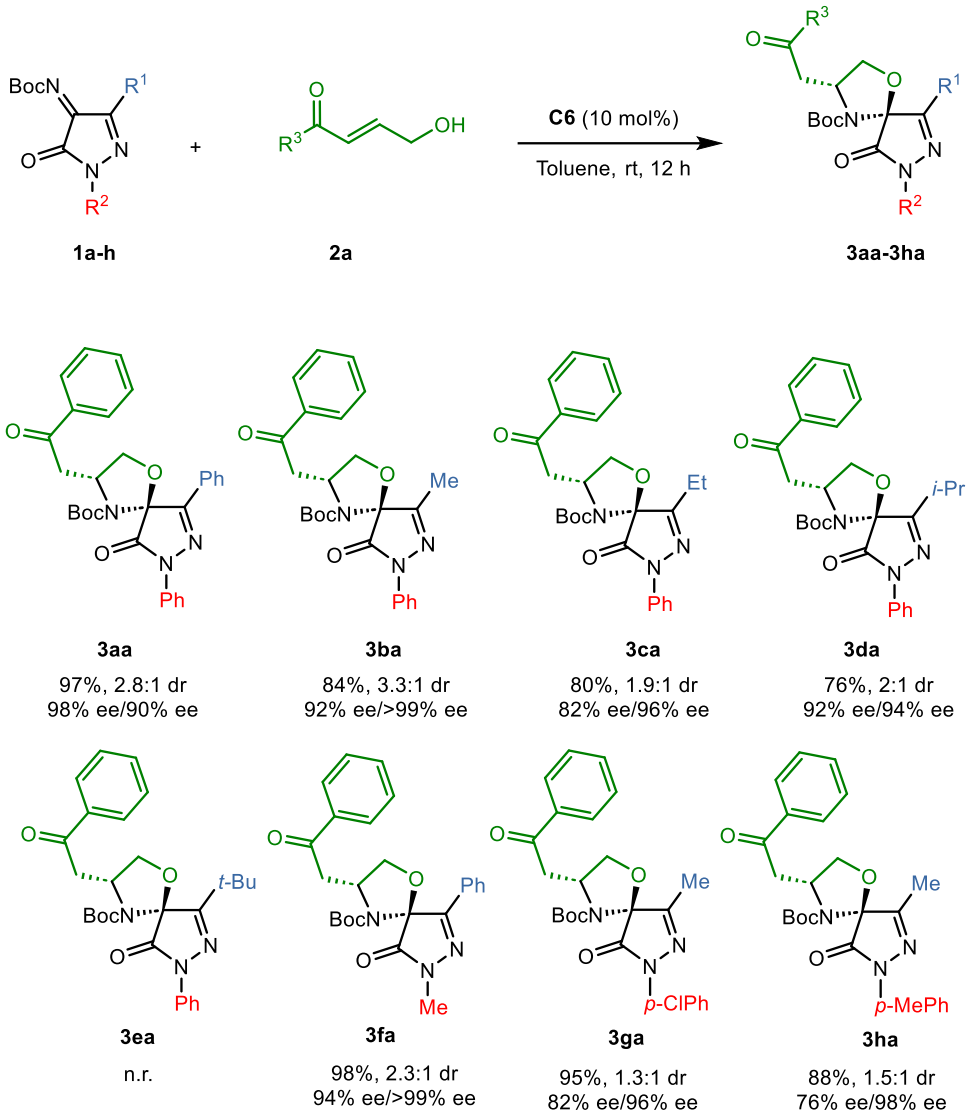

[a] Reaction conditions: **1a-h** (0.1 mmol), **2a** (0.15 mmol), **C6** (10 mol%), toluene (1 mL) at rt for 12 h. [b] Yield of **3aa-3ha** determined after column chromatography. [c] Dr and ee values determined *via* chiral HPLC analysis.

The reaction can be scaled-up using 0.5 mmol of **1a** as shown in Scheme 4.4. The formation of spirocyclic oxazolidine **3ac** proceeded with high yield, a slightly improvement in the diastereomeric ratio and no erosion in the enantioselectivity.

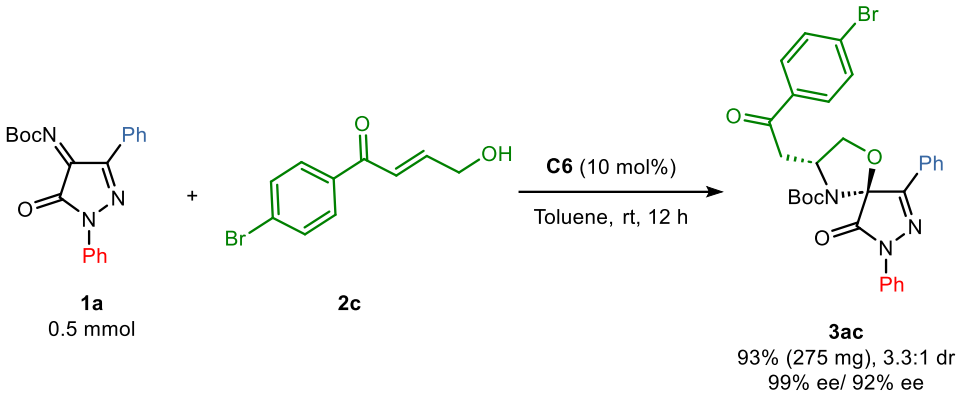

Scheme 4.4: Scale-up reaction of ketimine **1a** and hydroxyenone **2c**.

The absolute configuration of spirocyclic oxazolidines **3** was assigned by X-ray diffraction of a single crystal of **3ab** after recrystallization from dichloromethane. Product **3ab** was determined to be (3*R*,5*S*), Figure 4.2. For the other spirocycles, it is expected to be the same by analogy.

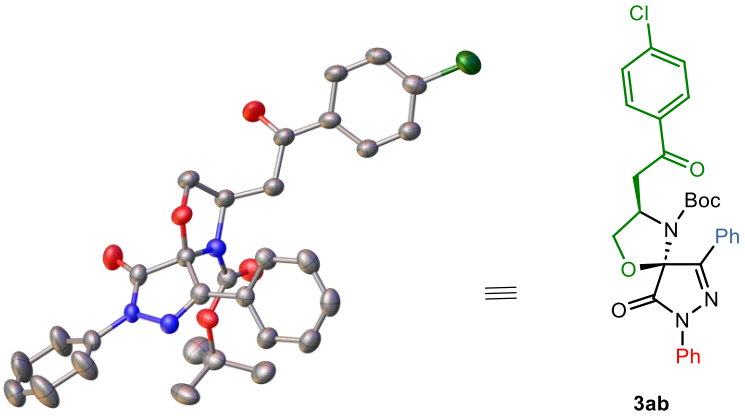

Figure 4.2: Absolute configuration (3*R*,5*S*) for spirocycle **3ab**.

To elucidate more precisely the reaction time, kinetic experiments were carried out performing the reaction between *N*-Boc ketimine **1a** and hydroxyenone **2a** inside an NMR tube. The reaction was monitored for two days through ^{1}H-NMR spectroscopy. The profile is shown in Figure 4.3.

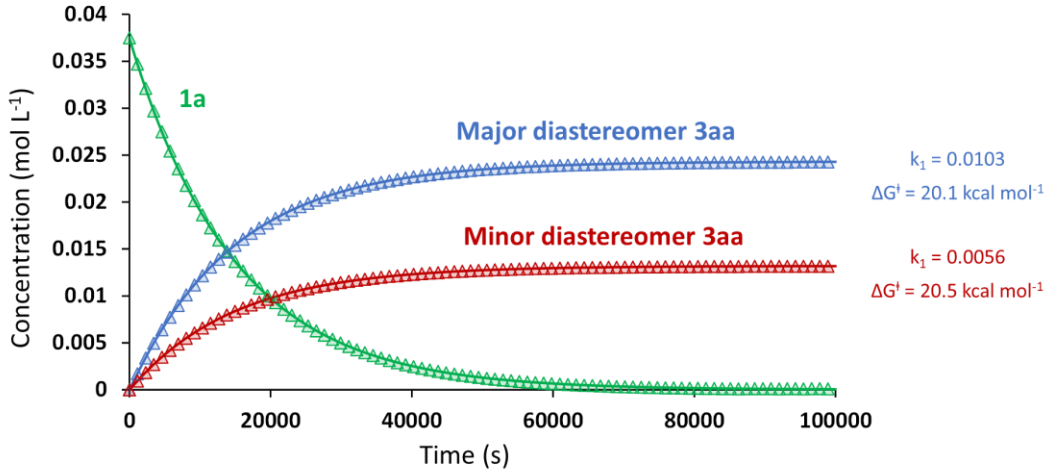

Figure 4.3: ^{1}H-NMR monitoring of the reaction between *N*-Boc ketimine **1a** and hydroxyenone **2a**. Lines represent kinetic fitting of data using COPASI software.[13]

As it is depicted in the profile, in the first hours the reaction rapidly evolves as **1a** is consumed and then, the reaction proceeds slower until it becomes steady after full conversion. Major diastereomer is formed faster than the minor one (rate constants: k_{major} = 0.0103, k_{minor} = 0.0056) until diastereomers reach a ratio of 2.8:1. From the NMR study, we can extract that after approximately twelve hours, the conversion is high enough to conclude the reaction is over.

To illustrate the synthetic utility of this reaction, the preparation of biphenyl derivative **4** was studied, Scheme 4.5. A 2.7:1 mixture of diastereomers of **3ac** was reacted with phenyl boronic acid under Suzuki conditions affording spirocyclic pyrazolone **4** with excellent yield, retention of the diastereomeric ratio and excellent enantiomeric ratio for both diastereomers (98 and 96% ee, respectively).

[13]S. Hoops, S. Sahle, R. Gauges, C. Lee, J. Pahle, N. Simus, M. Singhal, L. Xu, P. Mendes, U. Kummer *Bioinformatics*, **2 006**, *22*, 3067–3074.

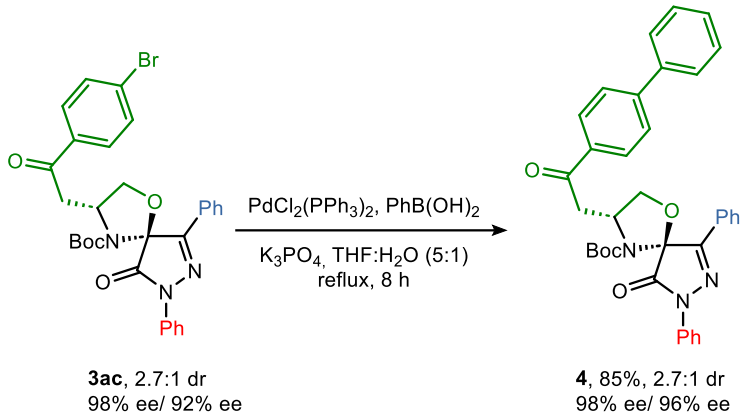

Scheme 4.5: Synthesis of spirocyclic oxazolidine **4**.

To investigate the stereochemical outcome of the reaction, control experiments were carried out, Table 5. *N*-Boc ketimine **1a** was reacted with allyl alcohol **5** in presence of catalyst **C6** under the optimized reaction conditions and pyrazolone-derived *N,O*-aminal **6a** was isolated in 80% yield and 74:26 er. In the same way, reaction of ketimine **1g** with allyl alcohol under the same reaction conditions gave adduct **6g** in 91% yield and 58:42 er. The enantiomeric ratio observed for products **6a** and **6g** matches with the diastereomeric ratio of products **3aa** and **3ga**. These results indicated that since the hemiaminal center is stable, the diastereoselectivity of this reaction might be due to the *N,O*-acetalization step.

Table 5. Enantioselective addition of allyl alcohol to *N*-Boc pyrazolinone ketimines **1a,g**.[a,b,c]

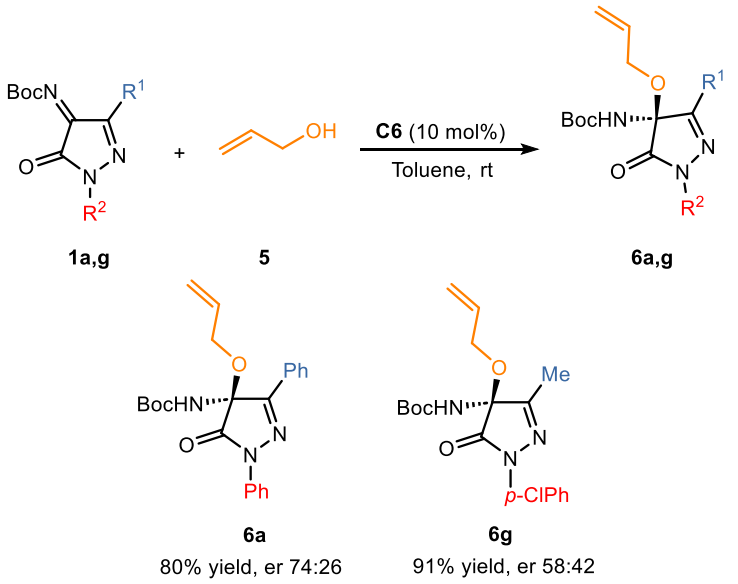

[a] Reaction conditions: **1** (0.17 mmol), **5** (0.25 mmol), **C6** (10 mol%), toluene (2.5 mL) at rt. [b] Yield of **6** determined after column chromatography. [c] Er values determined *via* chiral HPLC analysis.

On the basis of the control experiments results, the absolute configuration of the adducts assigned by X-ray diffraction and previous works,[10] a plausible mechanism is shown in Scheme 4.6, in which a bifunctional mode of activation operates. It is expected that the keto and imine groups of **1a** are activated by the squaramide moiety of the catalyst **C6**, whereas the OH group of **2a** is deprotonated by the quinuclidine motif of **C6**. The addition of the hydroxyenone **2a** takes place from the *Si*-face to provide hemiaminal **I**. The enone part of hemiaminal **I** is again activated by the squaramide moiety of **C6** and an intramolecular aza-Michael reaction, with Boc-carbamate as the nucleophile, proceeds from the *Si*-face of the enone to generate product **3aa**.

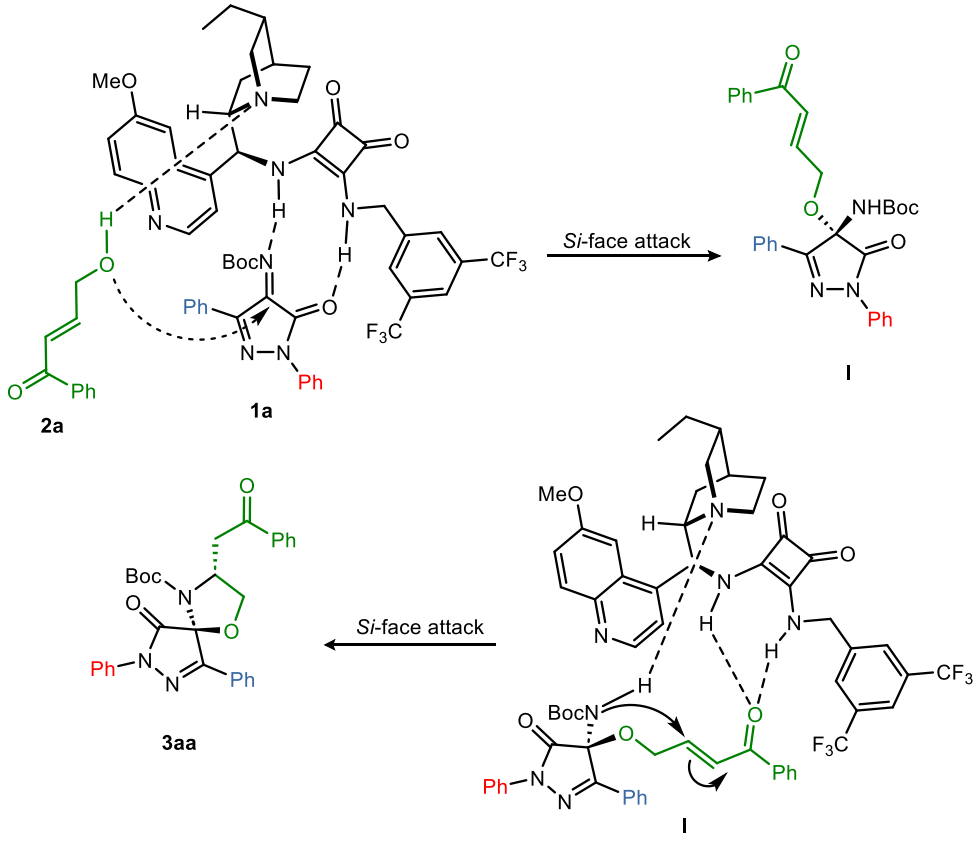

Scheme 4.6: Proposed mechanism.

4.3 Conclusions

In this chapter we have studied the first organocatalyzed reaction between *N*-Boc ketimines and γ-hydroxyenones affording pyrazolinone embedded oxazolidines. The reaction proceeds under mild conditions with 10 mol% of a hydroquinine-derived squaramide. Kinetic experiments confirm that twelve hours are enough to complete the reaction (or that the reaction is fast enough to achieve a high conversion in 12 h). Spirocyclic oxazolidines are

obtained in good to excellent yields, moderate to good diastereoselectivity and high enantioselectivity for a wide range of substrates *via* a domino reaction envolving hemiaminal formation, followed by an aza-Michael reaction between pyrazolinone ketimines and γ-hydroxyenones.

4.4 References

1. (a) A. Kapil, D. Anshu *Lett. Org. Chem.* **2007**, *4*, 378–383, (b) S. Y. Hwang, D. A. Berges, J. J. Taggart, C. Gilvart *J. Med. Chem.* **1989**, *32,* 694–698.
2. (a) W. -L. Wang, T. -J. Zhu, H. -W. Tao, Z. -Y. Lu, Y. -C. Fang, Q. -Q. Gu, W. -M. Zhu *Chem. Biodiversit*y **2007**, *4*, 2913. (b) A. B. Smith, I. G. Safanov, R. M. Corbett *J. Am. Chem. Soc.* **2001**, *123*, 12426–12427.
3. B. -H. Chen, S. -J. Liu, Q. Zhao, Q. Hou, J. -L. Yuan, G. Zhan, Q. -Q. Yang, W. Huang *Chem. Commun.* **2023**, 59, 1233–1236.
4. Y. Liu, J. Wang, Z. Wei, J. Cao, D. Liang, Y. Lin, H. Duan *Org. Lett*. **2019**, *21*, 5719–5724.
5. (a) J. Liu, F. -M. Zhu, Y. -B. Chu, L. -H. Huang, Y. -F. Zhou *Tetrahedron Asymmetry* **2015**, *26*, 1130–1137, (b) T. -Z. Li, X. -B. Wang, F. Sha, X. -Y. Wu *Tetrahedron* **2013**, *69*, 7314–7319.
6. (a) C. Foti, A. Piperno, A. Scala, O. Giuffrè *Molecules*, **2021**, *26*, 4280, (b) J. F. Branco-Junior, D. R. C. Teixeira, M. C. Pereira, I. R. Pitta, M. R. Galdino-Pitta *Curr. Bioact. Compd*. **2017**, *13*, 292–304, (c) P. Siengalewicz, U. Rinner, J. Mulzer *Chem. Soc. Rev*. **2008**, *37*, 2676–2690, (d) J. D. Scott, R. M. Williams *Chem. Rev.* **2002**, *102*, 1669−1730.
7. Y. Fukata, K. Asano, S. Matsubara *Chem. Lett.* **2013**, *42*, 355–357.
8. A. Kondoh, S. Akahira, M. Oishi, M. Terada *Angew. Chem. Int. Ed.* **2018**, *57*, 6299–6303.
9. S. Mukhopadhyayaand, S. C. Pan *Adv. Synth. Catal.* **2019**, *361*, 1028–1032.
10. C. Parida, B. Mondal, A. Ghosh, S. C. Pan *J. Org. Chem.* **2021**, *86*, 13082–13091.
11. W. Guo, L. Li, Q. Ding, X. Lin, X. Liu, K. Wang, Y. Liu, H. Fan, C. Li *ACS Catal*. **2018**, *8*, 10180–10189.
12. Some cases of solvent-induced reversal of enantioselectivity in organocatalysed transformations have been previously reported: (a) C. -H. Chang, N. Sathishkumar, Y. -T. Liao, H. -T. Chen, J. -L. Han *Adv. Synth. Catal*. **2020**, *362*, 903–912, (b) J. Flores-Ferrándiz, B. Fiser, E. Gómez-Bengoa, R. Chinchilla *Eur. J. Org. Chem*. **2015**, 1218–1225.
13. S. Hoops, S. Sahle, R. Gauges, C. Lee, J. Pahle, N. Simus, M. Singhal, L. Xu, P. Mendes, U. Kummer *Bioinformatics*, **2006**, *22*, 3067–3074.

4.5 Experimental section

4.5.1 General Procedure for Spirocyclic Oxazolidine Pyrazolones.

In a Wheaton vial equipped with a magnetic stirring bar the catalyst **C6** (0.1 equiv) and the *N*-Boc ketimine **1a-h** (0.1 mmol) were weighed. Then toluene (1 mL) was added before the mixture was stirred. Several minutes later, hydroxyenone **2a-e** (0.15 mmol, 1.5 equiv) was

introduced to the flask. After 12 h, the solvent was straight removed under reduced pressure and the residue was purified by column chromatography (hexane/ethyl acetate 10:1) to give the desired compound.

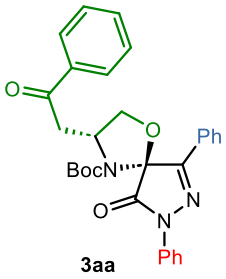

3aa

***tert*-Butyl (3*R*,5*S*)-9-oxo-3-(2-oxo-2-phenylethyl)-6,8-diphenyl-1-oxa-4,7,8-triazaspiro[4.4]non-6-ene-4-carboxylate (3aa).** 49.6 mg (97% combined yield). Mixture of diastereomers, 2.8:1 dr. Major diastereomer (3*R*,5*S*). White solid. Mp 138-140 °C (from hexane). $[\alpha]^{25}_{D}$= -93.2 (c= 0.3, $CHCl_3$, 98% ee). ^{1}H NMR (500 MHz, $CDCl_3$) δ 1.24 (s, 9H), 3.17 (dd, *J*= 16.9, 10.9 Hz, 1H), 3.92 (d, *J*= 18.6 Hz, 1H), 4.22 (dd, *J*= 9.1, 2.0 Hz, 1H), 4.91 (t, *J*= 8.5 Hz, 1H), 5.03 (t, *J*= 8.2 Hz, 1H), 7.23 (t, *J*= 15.5, 1H), 7.43-7.56 (m, 7H), 7.59 (t, *J*= 7.4 Hz, 1H), 7.89-7.91 (m, 2H), 7.96 (dd, *J*= 10.9, 8.0 Hz, 4H). ^{13}C NMR (126 MHz, $CDCl_3$) δ 27.9, 42.6, 54.0, 71.2, 83.2, 91.1, 118.2, 125.3, 127.2, 128.1, 128.7, 129.0, 129.8, 130.9, 133.6, 136.2, 137.8, 151.3, 154.1, 168.8, 197.9. IR ν_{max}/cm^{-1} 512, 687, 760, 986, 1151, 1300, 1369, 1497, 1599, 1679, 1705, 1723, 2847, 2927, 2975. HRMS (ESI-TOF) m/z: calcd for $C_{30}H_{29}N_3NaO_5$ $[M+Na]^+$ 534.1999. Found 534.2008. HPLC (Lux i-Cellulose-5, n-hexane/2-propanol 90:10, λ= 210 nm, 0.8 mL/min): t_R (minor)= 33.3 min, t_R (major)= 40.4 min, (98% ee). Minor diastereomer: Pale yellow oil. $[\alpha]^{25}_{D}$= +0.3 (c= 0.1, $CHCl_3$, 90% ee). ^{1}H NMR (500 MHz, $CDCl_3$) δ 1.15 (s, 9H), 3.59 (dd, *J*= 19.6, 10.5 Hz, 1H), 4.31-4.37 (m, 2H), 4.82-4.86 (m, 2H), 7.24 (t, *J*= 6.5, 1H), 7.44-7.50 (m, 7H), 7.59 (t, *J*= 8.1 Hz, 1H), 7.87 (d, *J*= 10.8 Hz, 2H), 7.98 (d, *J*= 7.8 Hz, 2H), 8.03 (d, *J*= 7.4 Hz, 2H). ^{13}C NMR (126 MHz, $CDCl_3$) δ 27.7, 41.8, 53.6, 73.1, 83.2, 90.6, 113.8, 118.5, 125.4, 126.4, 128.2, 128.7, 128.9, 129.0, 130.5, 131.1, 133.5, 136.3, 137.8, 150.2, 154.4, 168.7, 198.5. HPLC (Lux i-Cellulose-5, n-hexane/2-propanol 90:10, λ= 210 nm, 0.8 mL/min): t_R (minor)= 9.9 min, t_R (major)= 11.3 min, (90% ee).

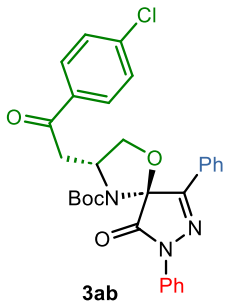

3ab

***tert*-Butyl (3*R*,5*S*)-3-(2-(4-chlorophenyl)-2-oxoethyl)-9-oxo-6,8-diphenyl-1-oxa-4,7,8-triazaspiro[4.4]non-6-ene-4-carboxylate (3ab).** 43.2 mg (80% combined yield). Mixture of diastereomers, 2.7:1 dr. ^{1}H NMR (500 MHz, $CDCl_3$) δ 1.15 (s, 2.7H, minor), 1.24 (s, 6.3H, major), 3.11 (dd, *J*= 16.8, 10.9 Hz, 0.7H, major), 3.54 (dd, *J*= 18.1, 9.7 Hz, 0.3H, minor), 3.88 (dd, *J*= 16.7, 1.8 Hz, 0.7H, major), 4.21 (dd, *J*= 9.1, 2.0 Hz, 0.7H, major), 4.28-4.33 (m, 0.6H, minor), 4.83-4.86 (m, 0.6H, minor), 4.86-4.89 (m, 0.7H, major), 5.02 (t, *J*= 8.1 Hz, 0.7H, major), 7.21-7.24 (1H), 7.43-7.57 (m, 7.2H), 7.85-7.90 (m, 3.3H), 7.96-7.98 (2.5H). ^{13}C NMR (126 MHz, $CDCl_3$) δ 27.7, 27.9, 41.2, 42.6, 53.5, 53.9, 71.1, 73.0, 81.9, 83.3, 90.9, 91.1, 118.2, 118.5, 125.3, 126.4, 127.2, 128.7, 128.9, 129.0, 129.5, 129.6, 130.9, 131.1, 134.5, 134.6, 137.7, 140.0, 140.1, 150.2, 154.4, 168.7, 196.8, 197.3. IR ν_{max}/cm^{-1} 986, 1085, 1143, 1300, 1366, 1490, 1588, 1682, 1705, 1729, 2898, 2971. HRMS (ESI-TOF) m/z: calcd for $C_{30}H_{28}ClN_3NaO_5$ $[M+Na]^+$ 568.1610. Found 568.1618. HPLC (Lux i-cellulose 5, n-hexane/2-propanol 92:8, λ= 220 nm, 0.5 mL/min): major diastereomer: t_R (minor)= 51.4 min, t_R (major)= 59.1 min (98% ee); minor diastereomer: t_R (minor)= 14.7 min, t_R (major)= 17.9 min (92% ee).

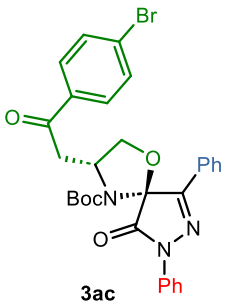

3ac

***tert*-Butyl (3*R*,5*S*)-3-(2-(4-bromophenyl)-2-oxoethyl)-9-oxo-6,8-diphenyl-1-oxa-4,7,8-triazaspiro[4.4]non-6-ene-4-carboxylate (3ac).** 51.8 mg (88% combined yield). Mixture of diastereomers, 3:1 dr. ^{1}H NMR (500 MHz, $CDCl_3$) δ 1.15 (s, 2.7H, minor), 1.24 (s, 6.3H, major), 3.11 (dd, *J*= 16.8, 10.8 Hz, 0.7H, major), 3.54 (dd, *J*= 18.1, 9.7 Hz, 0.3H, minor), 3.88 (dd, *J*= 16.9, 2.0 Hz, 0.7H, major), 4.21 (dd, *J*= 9.1, 1.9 Hz, 0.7H, major), 4.27-4.33 (m, 0.6H, minor), 4.75-4.86 (m, 0.6H, minor), 4.84-4.90 (m, 0.7H, major), 5.02 (t, *J*= 8.1 Hz, 0.7H, major), 7.21-7.24 (0.9H), 7.43-7.57 (m, 7.2H), 7.85-7.90 (m, 3.9H), 7.96-7.98 (2.0H). ^{13}C NMR (126 MHz, $CDCl_3$) δ 27.7, 27.9, 41.8, 42.5, 53.5, 53.9, 71.1, 73.0, 83.3, 90.9, 91.1, 1128.2, 118.5, 125.3, 125.5, 126.4, 127.2, 128.7, 128.9, 129.0, 129.6, 129.7, 129.8, 130.9, 131.1, 131.9, 132.1, 134.9, 135.0, 137.7, 150.2, 151.3, 153.9, 154.4, 168.7, 168.8, 196.9, 197.5. IR ν_{max}/cm^{-1} 512, 694, 753, 822, 983, 1067, 1140, 1297, 1366, 1486, 1585, 1680, 1709, 1727, 2847, 2920, 2975. HRMS (ESI-TOF) m/z: calcd for $C_{30}H_{28}BrN_3NaO_5$ $[M+Na]^+$ 612.1105. Found 612.1116. HPLC (Lux i-cellulose 5, n-hexane/2-propanol 92:8, λ= 220 nm, 0.5 mL/min): major diastereomer: t_R (minor)= 55.0 min, t_R (major)= 62.1 min (98% ee); minor diastereomer: t_R (minor)= 15.4 min, t_R (major)= 19.0 min (88% ee).

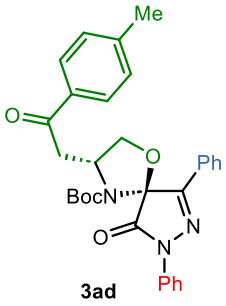

3ad

***tert*-Butyl (3*R*,5*S*)-9-oxo-3-(2-oxo-2-(p-tolyl)ethyl)-6,8-diphenyl-1-oxa-4,7,8-triazaspiro[4.4]non-6-ene-4-carboxylate (3ad).** 46.2 mg (88% combined yield). Mixture of diastereomers, 2.7:1 dr. Major diastereomer (3*R*,5*S*). White solid. Mp 167-169 °C (from hexane). $[\alpha]^{25}_{D}$= -50.0 (c= 0.2, $CHCl_3$, 99% ee). ^{1}H NMR (500 MHz, $CDCl_3$) δ 1.24 (s, 9H), 2.43 (s, 3H), 3.15 (dd, *J*= 16.8, 11.0 Hz, 1H), 3.89 (d, *J*= 16.8 Hz, 1H), 4.22 (dd, *J*= 9.1, 2.0 Hz, 1H), 4.89 (t, *J*= 10.5 Hz, 1H), 5.02 (t, *J*= 8.2 Hz, 1H), 7.23 (t, *J*= 7.4, 1H), 7.27 (d, *J*= 7.9 Hz, 2H), 7.44 (t, *J*= 8.3 Hz, 2H), 7.49-7.56 (m, 3H), 7.85 (d, *J*= 8.2 Hz, 1H), 7.88-7.90 (m, 2H), 7.97 (d, *J*= 8.6 Hz, 2H). ^{13}C NMR (126 MHz, $CDCl_3$) δ 27.9, 42.4, 54.1, 71.2, 83.2, 91.1, 118.2, 125.3, 127.2, 128.2, 128.7, 129.0, 129.4, 129.8, 130.9, 133.8, 136.2, 137.8, 144.5, 151.3, 154.1, 168.9, 197.6. IR ν_{max}/cm^{-1} 754, 974, 1164, 1300, 1365, 1384, 1487, 1604, 1674, 1710, 2861, 2930, 2978, 3070, 3348. HRMS (ESI-TOF) m/z: calcd for $C_{31}H_{31}N_3NaO_5$ $[M+Na]^+$ 548.2156. Found 548.2161. HPLC (Lux i-Cellulose-5, n-hexane/2-propanol 92:8, λ= 220 nm, 0.5 mL/min): t_R (minor)= 79.5 min, t_R (major)= 98.1 min, (99% ee).

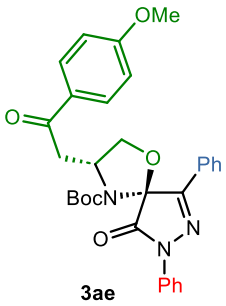

3ae

***tert*-Butyl (3*R*,5*S*)-3-(2-(4-methoxyphenyl)-2-oxoethyl)-9-oxo-6,8-diphenyl-1-oxa-4,7,8-triazaspiro[4.4]non-6-ene-4-carboxylate (3ae).** 45.0 mg (83% combined yield). Mixture of diastereomers, 2.5:1 dr. ^{1}H NMR (500 MHz, $CDCl_3$) δ 1.15 (s, 2.7H, minor), 1.24 (s, 6.3H, major), 3.10 (dd, *J*= 16.5, 11.1 Hz, 0.7H, major), 3.52 (dd, *J*= 17.9, 9.7 Hz, 0.3H, minor), 3.86-3.87 (m, 0.7H, major), 3.88 (s, 3H, minor and major), 4.23 (dd, *J*= 9.1, 2.0 Hz, 0.7H, major), 4.31-4.35 (m, 0.6H, minor), 4.81-4.84 (m, 0.6H, minor), 4.86-4.90 (m, 0.7H, major), 5.01 (t, *J*= 8.2 Hz, 0.7H, major), 6.95 (2H), 7.21-7.24 (m, 0.9H), 7.42-7.54 (m, 5.1H), 7.86- 8.00 (m, 6H). ^{13}C NMR (126 MHz, $CDCl_3$) δ 27.7, 27.9, 41.4, 42.3, 53.7, 54.2, 55.5, 71.2, 73.2, 83.1, 83.2, 90.9, 91.1, 113.8, 113.9, 118.2,

118.5, 118.8, 125.3, 125.4, 126.4, 126.5, 127.2, 128.7, 128.9, 129.0, 129.1, 129.4, 129.5, 129.8, 130.5, 130.9, 131.0, 137.8, 150.2, 151.3, 154.1, 154.5, 163.8, 163.9, 168.8, 168.9, 196.5, 197.0. IR ν_{max}/cm^{-1} 761, 835, 1029, 1069, 1142, 1164, 1219, 1296, 1395, 1461, 1505, 1574, 1670, 1714, 1725, 2853, 2923, 2960, 3062. HRMS (ESI-TOF) m/z: calcd for $C_{31}H_{31}N_3NaO_6$ $[M+Na]^+$ 564.2105. Found 564.2113. HPLC (Lux i-cellulose 5, n-hexane/2-propanol 92:8, λ= 254 nm, 0.5 mL/min): major diastereomer: t_R (minor)= 145.6 min, t_R (major)= 161.5 min (>99% ee); minor diastereomer: t_R (minor)= 35.0 min, t_R (major)= 42.3 min (88% ee).

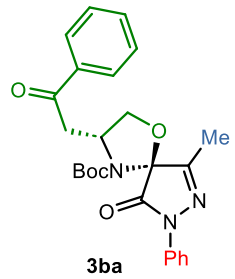

3ba

***tert*-Butyl (3*R*,5*S*)-6-methyl-9-oxo-3-(2-oxo-2-phenylethyl)-8-phenyl-1-oxa-4,7,8-triazaspiro[4.4]non-6-ene-4-carboxylate (3ba).** 37.8 mg (84% combined yield). Mixture of diastereomers, 3.3:1 dr. ^{1}H NMR (500 MHz, $CDCl_3$) δ 1.28 (s, 2.7H, minor), 1.30 (s, 6.3H, major), 2.15 (s, 0.9H, minor), 2.16 (s, 2.1H, major), 3.13 (dd, *J*= 16.6, 10.2 Hz, 0.7H, minor), 3.63 (dd, *J*= 18.2, 10.5 Hz, 0.3H, minor), 3.85 (dd, *J*= 16.2, 2.2 Hz, 0.7H, major), 4.06 (dd, *J*= 18.2, 2.9 Hz, 0.3H, minor), 4.13 (d, *J*= 7.6 Hz, 0.3H, minor), 4.26 (t, *J*= 9.1, 3.2 Hz, 0.7H, major), 4.54 (t, *J*= 8.9 Hz, 0.7H, major), 4.72-4.77 (m, 1H, minor and major), 4.82-4.85 (m, 0.3H, minor), 7.16-7.21 (1H), 7.38-7.42 (m, 2.1H), 7.46-7.52 (m, 2.1H), 7.57-7.61 (m, 1H). ^{13}C NMR (126 MHz, $CDCl_3$) δ 12.3, 12.8, 27.9, 40.8, 42.0, 53.8, 71.1, 73.3, 83.1, 83.2, 90.0, 90.5, 117.9, 118.1, 124.9, 125.1, 128.2, 128.6, 128.8, 128.9, 133.5, 133.6, 136.1, 136.3, 137.7, 137.8, 150.1, 150.8, 156.3, 157.6, 167.9, 168.6, 197.8, 198.7. IR ν_{max}/cm^{-1} 688, 750, 1142, 1370, 1490, 1583, 1676, 1714, 1725, 2916, 2961. HRMS (ESI-TOF) m/z: calcd for $C_{25}H_{27}N_3NaO_5$ $[M+Na]^+$ 472.1843. Found 472.1855. HPLC (Lux i-cellulose 5, n-hexane/2-propanol 95:5, λ= 210 nm, 1 mL/min): minor diastereomer: t_R (minor)= 32.3 min, t_R (major)= 43.2 min (>99% ee); major diastereomer: t_R (major)= 17.3 min, t_R (minor)= 19.2 min (92% ee).

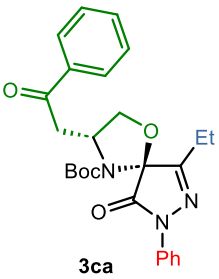

3ca

***tert*-Butyl (3*R*,5*S*)-6-ethyl-9-oxo-3-(2-oxo-2-phenylethyl)-8-phenyl-1-oxa-4,7,8-triazaspiro[4.4]non-6-ene-4-carboxylate (3ca).** 37.1 mg (80% combined yield). Mixture of diastereomers, 1.9:1 dr. ^{1}H NMR (500 MHz, $CDCl_3$) δ 1.27 (s, 3.6H, minor), 1.29 (s, 5.4H, major), 1.35-1.39 (m, 3H, minor and major), 2.41-2.58 (m, 2H, minor and major), 3.12 (dd, *J*= 16.7, 10.4 Hz, 0.6H, major), 3.63 (dd, *J*= 18.2, 10.5 Hz, 0.4H, minor), 3.85 (d, *J*= 16.9 Hz, 0.6H, major), 4.05 (d, *J*= 18.2 Hz, 0.4H, minor), 4.11 (d, *J*= 7.3 Hz, 0.6H, major), 4.26 (dd, *J*= 9.0, 3.0 Hz, 0.6H, major), 4.53 (t, *J*= 8.0 Hz, 0.4H, minor), 4.71-4.76 (m, 0.4H, minor), 4.83-4.86 (m, 1H, minor and major), 7.16-7.20 (m, 1H), 7.38-7.42 (m, 2H), 7.46-7.51 (m, 2H), 7.57-7.61 (m, 1H), 7.89-7.93 (m, 2H), 8.00-8.05 (m, 2H). ^{13}C NMR (126 MHz, $CDCl_3$) δ 9.2, 9.5, 20.1, 20.6, 27.9, 28.0, 28.2, 29.7, 40.8, 42.0, 53.9, 71.0, 73.3, 82.9, 83.0, 90.2, 90.6, 117.9, 118.1, 118.6, 118.7, 124.9, 125.0, 128.1, 128.2, 128.6, 128.7, 128.9, 133.5, 133.6, 136.2, 136.3, 137.7, 138.0, 150.1, 150.9, 159.9, 161.3, 168.2, 168.8, 197.8, 198.7. IR ν_{max}/cm^{-1} 985, 1051, 1164, 1216, 1278, 1373, 1454, 1498, 1600, 1718, 2916, 2934, 2978, 3066. HRMS (ESI-TOF) m/z: calcd for $C_{26}H_{29}N_3NaO_5$ $[M+Na]^+$ 486.1999. Found 486.1999. HPLC (Chiralpak AD-H, n-hexane/2-propanol 98:2, λ= 254 nm, 0.7 mL/min): major

diastereomer: t_R (major)= 44.2 min, t_R (minor)= 51.7 min (82% ee); minor diastereomer: t_R (minor)= 27.2 min, t_R (major)= 59.6 min (96% ee).

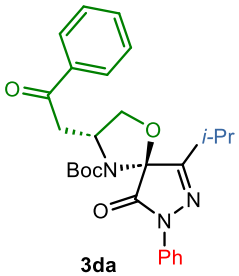

3da

***tert*-Butyl (3*R*,5*S*)-6-isopropyl-9-oxo-3-(2-oxo-2-phenylethyl)-8-phenyl-1-oxa-4,7,8-triazaspiro[4.4]non-6-ene-4-carboxylate (3da).** 36.3 mg (76% combined yield). Mixture of diastereomers, 2:1 dr. Major diastereomer (3*R*,5*S*). Pale yellow oil. $[\alpha]^{25}_D$= -7.0 (c= 0.1, $CHCl_3$, 92% ee). ^{1}H NMR (500 MHz, $CDCl_3$) δ 1.28 (s, 9H), 1.34 (dd, *J*= 6.7, 4.2 Hz, 6H), 2.75-2.81 (m, 1H), 3.64 (dd, *J*= 18.1, 10.5 Hz, 1H), 4.10 (dd, *J*= 18.1, 2.8 Hz, 1H), 4.26 (dd, *J*= 9.0, 3.0 Hz, 1H), 4.57 (dd, *J*= 8.5, 5.8 Hz, 1H), 4.72-4.76 (m, 1H), 7.19 (t, *J*= 8.2 Hz, 1H), 7.41 (t, *J*= 7.8 Hz, 2H), 7.48 (t, *J*= 7.7 Hz, 2H), 7.58 (t, *J*= 7.7 Hz, 1H), 7.92 (d, *J*= 8.7 Hz, 2H), 8.03 (d, *J*= 7.6 Hz, 2H). ^{13}C NMR (126 MHz, $CDCl_3$) δ 9.2, 9.5, 20.1, 20.6, 27.9, 28.0, 28.2, 29.7, 40.8, 42.0, 53.9, 71.0, 73.3, 82.9, 83.0, 90.2, 90.6, 117.9, 118.1, 118.6, 118.7, 124.9, 125.0, 128.1, 128.2, 128.6, 128.7, 128.9, 133.5, 133.6, 136.2, 136.3, 137.7, 138.0, 150.1, 150.9, 159.9, 161.3, 168.2, 168.8, 197.8, 198.7. IR v_{max}/cm^{-1} 992, 1047, 1146, 1366. 1392, 1498, 1600, 1677, 1714, 1725, 2934, 2978. HRMS (ESI-TOF) m/z: calcd for $C_{27}H_{31}N_3NaO_5$ $[M+Na]^+$ 500.2156. Found 500.2164. HPLC (Chiralpak AD-H, n-hexane/2-propanol 95:5, λ= 210 nm, 0.8 mL/min): t_R (minor)= 10.1 min, t_R (major)= 22.4 min (92% ee).

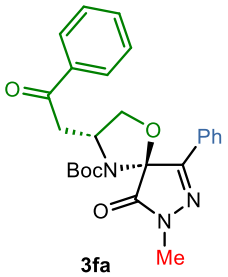

3fa

***tert*-Butyl (3*R*,5*S*)-8-methyl-9-oxo-3-(2-oxo-2-phenylethyl)-6-phenyl-1-oxa-4,7,8-triazaspiro[4.4]non-6-ene-4-carboxylate (3fa).** 44.2 mg (98% combined yield). Mixture of diastereomers, 2.3:1 dr. ^{1}H NMR (500 MHz, $CDCl_3$) δ 1.20 (s, 2.7H, minor), 1.33 (s, 6.3H, major), 3.14 (dd, *J*= 17.0, 11.1 Hz, 0.7H, major), 3.40 (s, 2.1H, major), 3.41 (s, 0.9H, minor), 3.53 (dd, *J*= 15.1, 4.4 Hz, 0.3H, minor), 3.90 (d, *J*= 18.3 Hz, 0.7H, major), 4.16 (d, *J*= 10.7 Hz, 0.7H, major), 4.25-4.32 (m, 0.6H, minor), 4.73-4.80 (m, 0.6H, minor), 4.83 (t, *J*= 10.6 Hz, 0.7H, major), 4.96 (t, *J*= 7.9 Hz, 0.7H, major), 7.43-7.52 (m, 5.2H), 7.59 (1H), 7.75 (0.6H), 7.79 (1.4H), 7.94 (1.1H), 8.01 (0.7H). ^{13}C NMR (126 MHz, $CDCl_3$) δ 27.7, 28.0, 28.2, 29.7, 31.7, 31.8, 41.9, 42.4, 53.5, 53.9, 70.8, 72.8, 82.9, 89.7, 90.0, 126.0, 126.1, 126.8, 127.2, 128.1, 128.2, 128.6, 128.7, 128.8, 128.9, 129.2, 129.9, 130.6, 130.7, 133.5, 133.6, 136.2, 136.3, 150.2, 151.2, 153.3, 153.7, 169.8, 170.1, 198.0, 198.5. IR v_{max}/cm^{-1} 681, 769, 860, 981, 1044, 1142, 1212, 1366, 1388, 1447, 1578, 1681, 1703, 1721, 2908, 2934, 2982. HRMS (ESI-TOF) m/z: calcd for $C_{25}H_{27}N_3NaO_5$ $[M+Na]^+$ 472.1843. Found 472.1852. HPLC (Chiralpak OD, n-hexane/2-propanol 93:7, λ= 210 nm, 0.5 mL/min): major diastereomer: t_R (minor)= 21.7 min, t_R (major)= 25.3 min (94% ee); minor diastereomer: t_R (minor)= 15.8 min, t_R (minor)= 17.5 min (>99% ee).

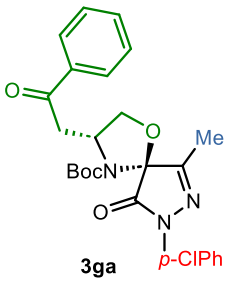

***tert*-Butyl (3*R*,5*S*)-8-(4-chlorophenyl)-6-methyl-9-oxo-3-(2-oxo-2-phenylethyl)-1-oxa-4,7,8-triazaspiro[4.4]non-6-ene-4-carboxylate (3ga).** 37.8 mg (78% combined yield). Mixture of diastereomers, 1.3:1 dr. ^{1}H NMR (500 MHz, $CDCl_3$) δ 1.26 (s, 3.6H, minor), 1.28 (s, 5.4H, major), 2.14 (s, 1.2H, minor), 2.15 (s, 1.8H, major), 3.12 (dd, *J*= 16.5, 10.4 Hz, 0.6H, major), 3.59 (dd, *J*= 18.1, 1.9 Hz, 0.4H, minor), 3.83 (d, *J*= 16.5 Hz, 0.6H, minor), 4.05 (dd, *J*= 18.1, 10.6 Hz, 0.4H, minor), 4.13 (d, *J*= 7.6 Hz, 0.4H, minor), 4.25 (dd, *J*= 12.0, 9.0 Hz, 0.6H, major), 4.54 (td, *J*= 9.0, 1.7 Hz, 0.6H, major), 4.72-4.76 (m, 1H, minor and major), 4.82-4.85 (m, 0.4H, minor), 7.35-7.38 (m, 1.8H), 7.46-7.51 (2.1H), 7.57-7.61 (m, 1H), 7.84-7.89 (m, 2H), 7.99-8.02 (m, 2.1H). ^{13}C NMR (126 MHz, $CDCl_3$) δ 12.3, 12.8, 27.9, 40.8, 42.0, 53.8, 53.9, 71.2, 73.4, 83.1, 83.2, 89.9, 90.4, 118.9, 119.1, 1196.6, 119.7, 128.2, 128.7, 128.8, 129.0, 130.0, 130.2, 133.6, 133.7, 136.3, 136.4, 150.0, 150.7, 156.6, 157.9, 167.9, 168.5, 197.7, 198.6. IR ν_{max}/cm^{-1} 512, 597, 765, 832, 979, 1113, 1294, 1360, 1494, 1591, 1676, 1720, 1738, 2915, 2978. HRMS (ESI-TOF) m/z: calcd for $C_{25}H_{26}ClN_3NaO_5$ $[M+Na]^+$ 506.1453. Found 506.1462. HPLC (Chiralpak IA, n-hexane/2-propanol 98:2, λ= 254 nm, 0.5 mL/min): major diastereomer: t_R (minor)= 51.9 min, t_R (major)= 72.9 min (82% ee); minor diastereomer: t_R (major)= 36.0 min, t_R (minor)= 61.3 min (96% ee).

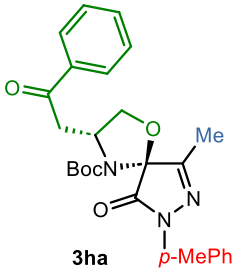

***tert*-Butyl (3*R*,5*S*)-6-methyl-9-oxo-3-(2-oxo-2-phenylethyl)-8-(p-tolyl)-1-oxa-4,7,8-triazaspiro[4.4]non-6-ene-4-carboxylate (3ha).** 40.7 mg (88% combined yield). Mixture of diastereomers, 1.5:1 dr. ^{1}H NMR (500 MHz, $CDCl_3$) δ 1.28 (s, 3.6H, minor), 1.30 (s, 5.4H, major), 2.14 (s, 1.2H, minor), 2.15 (s, 1.8H, major), 2.35 (s, 1.2H, minor), 2.36 (s, 1.8H, major), 3.12 (dd, *J*= 16.7, 10.4 Hz, 0.6H, major), 3.63 (dd, *J*= 18.2, 10.5 Hz, 0.4H, minor), 3.83 (dd, *J*= 17.0, 2.1 Hz, 0.6H, major), 4.05 (dd, *J*= 17.3, 3.0 Hz, 0.4H, minor), 4.12 (dd, *J*= 14.2, 6.9 Hz, 0.4H, minor), 4.25 (dd, *J*= 9.0, 3.1 Hz, 0.6H, major), 4.52-4.55 (m, 0.6H, major), 4.71-4.77 (m, 1H, minor and major), 4.82-4.84 (m, 0.4H, minor), 7.18-7.21 (m, 2H), 7.45-7.51 (2.2H), 7.56-7.62 (m, 1H), 7.72-7.78 (m, 1.9H), 7.99-8.05 (m, 1.9H). ^{13}C NMR (126 MHz, $CDCl_3$) δ 12.3, 12.8, 20.9, 27.8, 28.2, 40.8, 42.0, 53.8, 71.0, 73.3, 83.0, 83.1, 90.5, 118.0, 118.2, 128.2, 128.6, 128.8, 129.4, 133.5, 133.6, 134.6, 134.8, 135.4, 136.2, 136.3, 150.2, 150.9, 156.1, 157.4, 167.7, 168.3, 197.8, 198.7. IR ν_{max}/cm^{-1} 508, 690, 814, 979, 1143, 1294, 1365, 1512, 1685, 1716, 2925, 2978. HRMS (ESI-TOF) m/z: calcd for $C_{26}H_{29}N_3NaO_5$ $[M+Na]^+$ 486.1999. Found 486.1990. HPLC (Lux Cellulose 1, n-hexane/2-propanol 70:30, λ= 254 nm, 0.2 mL/min): major diastereomer: t_R (major)= 24.5 min, t_R (minor)= 29.3 min (76% ee); minor diastereomer: t_R (major)= 22.2 min, t_R (minor)= 26.2 min (98% ee).

*4.5.2 Transformation of spyrocyclic product **3ac**.*

To a solution of spyrocycle **3ac** (dr 2.7:1) (50 mg, 0.084 mmol), phenylboronic acid (15.5 mg, 0.127 mmol) and K_3PO_4 (35.7 mg, 0.168 mmol) in THF/H_2O 5:1 (1.5 mL) under a N_2 atmosphere, $PdCl_2(PPh_3)_2$ (0.008 mmol) was added. After refluxing for 8 h, the solvent was removed under reduced pressure. The crude mixture was purified by column chromatography (hexane/ethyl acetate 10:1) affording **4** as a pale yellow oil (41.8 mg, 85% yield).

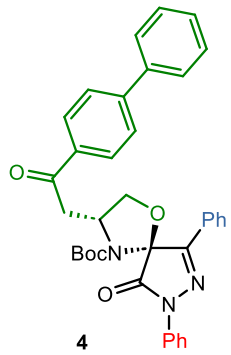

4

***tert*-Butyl (3*R*,5*S*)-3-(2-([1,1'-biphenyl]-4-yl)-2-oxoethyl)-9-oxo-6,8-diphenyl-1-oxa-4,7,8-triazaspiro[4.4]non-6-ene-4-carboxylate (4).** Mixture of diastereomers, 2.7:1 dr. Major diastereomer (3*R*,5*S*). Pale yellow oil. $[\alpha]^{25}_{D}$= -66.0 (c= 0.1, $CHCl_3$, 98% ee). ^{1}H NMR (500 MHz, $CDCl_3$) δ 1.25 (s, 9H), 3.19 (dd, *J*= 16.8, 11.0 Hz, 1H), 3.95 (d, *J*= 18.9 Hz, 1H), 4.24 (dd, *J*= 9.1 Hz, 1H), 4.92 (t, *J*= 8.4 Hz, 1H), 5.04 (t, *J*= 7.4 Hz, 1H), 7.23 (t, *J*= 8.5 Hz, 1H), 7.42-7.50 (m, 5H), 7.51-7.58 (m, 3H), 7.63 (d, *J*= 6.1 Hz, 2H), 7.70 (d, *J*= 9.2 Hz, 2H), 7.90 (d, *J*= 8.2 Hz, 2H), 7.98 (d, *J*= 8.1 Hz, 2H), 8.02 (d, *J*= 8.0 Hz, 2H). ^{13}C NMR (126 MHz, $CDCl_3$) δ 27.9, 29.5, 42.6, 54.1, 71.2, 83.3, 91.1, 115.3, 118.2, 125.3, 127.2, 127.3, 127.4, 128.3, 128.7, 128.9, 129.0, 129.6, 129.8, 130.9, 134.9, 137.8, 139.7, 146.3, 151.3, 154.1, 168.8, 197.6. IR ν_{max}/cm^{-1} 989, 1073, 1139, 1216, 1300, 1362, 1391, 1450, 1494, 1674, 1714, 2857, 2919, 2960. HRMS (ESI-TOF) m/z: calcd for $C_{36}H_{33}N_3NaO_5$ $[M+Na]^+$ 610.2312. Found 610.2318. HPLC (Lux i-cellulose 5, n-hexane/2-propanol 90:10, λ= 210 nm, 0.8 mL/min): t_R (minor)= 57.0 min, t_R (major)= 63.2 min (98% ee).

4.5.3 General Procedure for the enantioselective addition of allyl alcohol to N-Boc pyrazolinone ketimines 1a and 1g.

In a Wheaton vial equipped with a magnetic stirring bar the catalyst **C6** (0.1 equiv) and the *N*-Boc ketimine **1a,g** (0.17 mmol) were weighed. Then toluene (2.5 mL) was added before the mixture was stirred. Several minutes later, allylic alcohol (0.25 mmol, 1.5 equiv) was introduced to the flask and the reaction mixture was stirred until the reaction completed (monitoring by TLC). Then, the solvent was straight removed under reduced pressure and the residue was purified by column chromatography (hexane/ethyl acetate 10:1) to give the desired compound.

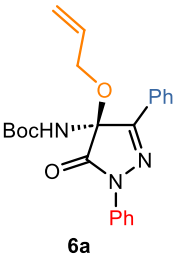

6a

***tert*-Butyl (*S*)-(4-(allyloxy)-5-oxo-1,3-diphenyl-4,5-dihydro-1H-pyrazol-4-yl)carbamate (6a).** Pale yellow oil (54.4 mg, 80% yield). $[\alpha]^{25}_{D}$= -19.8 (c= 1.1, $CHCl_3$, 74:26 er). ^{1}H NMR (500 MHz, $CDCl_3$) δ 1.24 (s, 9H), 4.05-4.15 (m, 2H), 5.15 (dd, *J*= 10.4, 1.3 Hz, 1H), 5.24 (dd, *J*= 17.2, 1.5 Hz, 1H), 5.77 (br, 1H), 5.78-5.87 (m, 1H), 7.24 (tt, *J*= 7.4, 1.1 Hz, 1H), 7.42-7.47 (m, 5H), 8.03-8.06 (m, 4H). ^{13}C NMR (126 MHz, $CDCl_3$) δ 27.9, 66.0, 86.3, 125.4, 126.6, 128.8, 129.0, 131.0, 132.4, 137.8, 152.3, 153.5, 167.7. IR ν_{max}/cm^{-1} 1154, 1260, 1366, 2395, 1464, 1597, 1703, 1729, 2857, 2923, 2971, 3300. HRMS (ESI-TOF) m/z: calcd for $C_{23}H_{25}N_3NaO_4$ $[M+Na]^+$ 430.1737. Found 430.1727. HPLC (Chiralpak AD-H, n-hexane/2-propanol 90:10, λ= 254 nm, 1 mL/min): t_R (major)= 10.1 min, t_R (minor)= 62.2 min (48% ee).

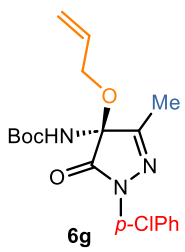

6g

***tert*-Butyl (*S*)-(4-(allyloxy)-1-(4-chlorophenyl)-3-methyl-5-oxo-4,5-dihydro-1*H*-pyrazol-4-yl)carbamate (6g).** Pale yellow oil (58.8 mg, 91% yield). $[\alpha]^{25}_{D}$ = -0.2 (c= 0.6, $CHCl_3$, 58:42 er). ^{1}H NMR (500 MHz, $CDCl_3$) δ 1.35 (s, 9H), 2.16 (s, 3H), 4.05-4.16 (m, 2H), 5.18 (dd, J= 10.4, 0.8 Hz, 1H), 5.26 (dd, J= 16.8, 1.5 Hz, 1H), 5.35 (br, 1H), 5.80-5.88 (m, 1H), 7.35 (d, J= 8.7 Hz, 1H), 7.88 (d, J= 8.7 Hz, 1H). ^{13}C NMR (126 MHz, $CDCl_3$) δ 12.9, 28.0, 65.3, 85.3, 118.2, 119.5, 128.9, 130.3, 132.7, 136.2, 152.4, 157.5, 167.1. IR $_{vmax}$/cm^{-1} 1150, 1234, 1359, 1494, 1593, 1703, 1729, 2985, 3128, 3231. HRMS (ESI-TOF) m/z: calcd for $C_{18}H_{22}ClN_3NaO_4$ $[M+Na]^+$ 402.1191. Found 402.1196. HPLC (Chiralpak AD-H, n-hexane/2-propanol 95:5, λ= 254 nm, 1 mL/min): t_R (minor)= 8.4 min, t_R (major)= 25.3 min (16% ee).

*4.5.4 Crystallographic data of spirocycle **3ab**.*

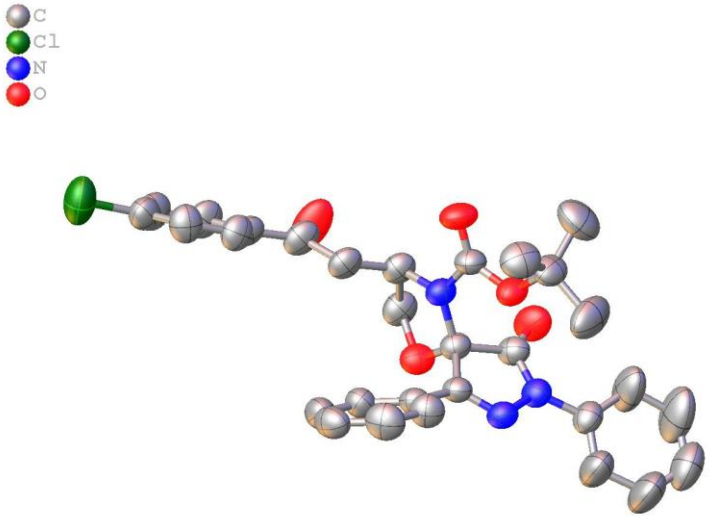

Crystal data and structure refinement for spirocycle 3ab.

Identification code	**3ab**
Empirical formula	$C_{30}H_{28}ClN_3O_5$
Formula weight	546.00
Temperature/K	298
Crystal system	orthorhombic
Space group	$P2_12_12_1$
a/Å	8.3506(2)
b/Å	11.0548(3)
c/Å	35.8931(9)
α/°	90
β/°	90
γ/°	90
Volume/Å^3	3313.44(15)
Z	4
ρ_{calc}g/cm^3	1.095
μ/mm^{-1}	1.327

F(000)	1144.0
Crystal size/mm^3	0.737 × 0.372 × 0.3
Radiation	Cu Kα (λ = 1.54184)
2Θ range for data collection/°	8.37 to 150.626
Index ranges	-10 ≤ h ≤ 10, -13 ≤ k ≤ 13, -44 ≤ l ≤ 44
Reflections collected	26672
Independent reflections	6729 [R_{int} = 0.0520, R_{sigma} = 0.0308]
Data/restraints/parameters	6729/0/355
Goodness-of-fit on F^2	1.140
Final R indexes [I>=2σ (I)]	R_1 = 0.0932, wR_2 = 0.2551
Final R indexes [all data]	R_1 = 0.1009, wR_2 = 0.2768
Largest diff. peak/hole / e Å^{-3}	1.30/-0.42
Flack parameter	0.004(12)

Chapter V: Synthesis of 4-pyrazolyl- and 4-isoxazolyl-4-amino-pyrazolone derivatives *via* squaramide-catalyzed asymmetric Mannich reaction between 1,3-dicarbonyl compounds and pyrazolinone ketimines.

This work was published as:

"*Squaramide-catalyzed asymmetric Mannich reaction between 1,3-dicarbonyl compounds and pyrazolinone ketimines: a pathway to enantioenriched 4-pyrazolyl and 4-isoxazolyl-4-aminopyrazolone derivatives"*

Marta Gil-Ordóñez, Camille Aubry, Cristopher Niño, Alicia Maestro, José M. Andrés *Molecules* **2022**, *27*, 6983.

5.1 Introduction and background

The asymmetric Mannich reaction is a crucial method for the formation of new C-C bonds which allows the preparation of β-aminocarbonyl compounds.[1] Recently, numerous examples of asymmetric Mannich reactions have been developed using as starting materials isatin-derived ketimines,[2] cyclic imines,[3] and straight-chain imines,[4] among others. In all these asymmetric catalytic reactions, organic squaramide-derived hydrogen bond catalysts are widely used due to their high efficiency, easy availability, mild reaction conditions and the low catalyst loading needed for the stereoselective formation of new C-C bonds.

As previously mentioned, pyrazolone derivatives are widely spread in pharmaceutical and natural products. Efforts have been devoted to develop new compounds containing pyrazolone scaffold, generally taking advantage of the nucleophilicity of the C-4 position of pyrazolone. In 2017, Enders firstly reported a new series of pyrazolone-derived ketimines which provides an electrophilic alternative to the classical reactivity, affording an easy route for synthesizing 4-aminopyrazolones bearing a quaternary stereocenter at C-4 position of pyrazolone, Scheme 5.1.

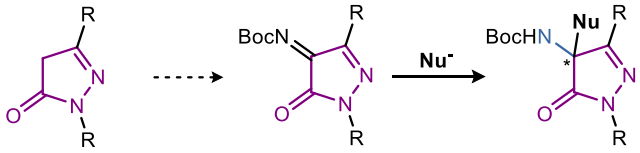

Scheme 5.1: New way for obtaining 4-aminopyrazolones bearing a tetra-substituted stereocenter.

Next, the new developed ketimines derived from pyrazole-4,5-diones were applied as new electrophiles in asymmetric Mannich reaction. Enders[5] reported the first asymmetric Mannich reaction using pyrazolone-derived ketimines in combination with nucleophilic pyrazolin-5-ones synthesizing a new series of different amino-bis-pyrazolone derivatives with excellent yields and stereoselectivities, Scheme 5.2a. Later, Yuan[6] described how pyrazolinone ketimines could undergo decarboxylative Mannich reaction with β-ketoacids providing β-amino ketone-

[1] X. -Q. Hou, D. -M. Du *Adv. Synth. Catal.* **2020**, *362*, 4487–4512.
[2] *Some selected examples with 1,3-dicarbonyl compounds:* (a) P. Rodríguez-Ferrer, M. Sanz-Novo, A. Maestro, J. M. Andrés, R. Pedrosa *Adv. Synth. Catal.* **2019**, *361,* 3645–3655, (b) D. İşibol, S. Karahan, C. Tanyeli *Tetrahedron Lett*. **2018**, *59*, 541–545, (c) S. Ričko, J. Svete, B. Štefane, A. Perdih, A. Golobič, A. Meden, U. Grošelj *Adv. Synth. Catal*. **2016**, *358*, 3786–3796, (d) K. S. Rao, P. Ramesh, L. R. Chowhan, R. Trivedi *RSC Adv*. **2016**, *6*, 84242–84247, (e) W. Yan, D. Wang, J. Feng, P. Li, D. Zhao, R. Wang *Org. Lett*. **2012**, *14*, 2512–2515.
[3] Y. Luo, K. Xie, D. Yue, X. Zhang, X. Xu, W. Yuan *Org. Biomol. Chem*. **2018**, *16*, 3372–3375.
[4] (a) L. Carceller-Ferrer, C. Vila, G. Blay, I. Fernández, M. C. Muñoz, J. R. Pedro *Org. Biomol. Chem*. **2019**, *17*, 9859–9863, (b) H. Y. Bae, M. J. Kim, J. H. Sim, C. -E. Song *Angew. Chem. Int. Ed.* **2016**, *55*, 10825–10829, (c) H. -X. He, D. -M. Du *RSC Adv*. **2013**, *3*, 16349–16358.
[5] P. Chauhan, S. Mahajan, U. Kaya, A. Peuronen, K. Rissanen, D. Enders *J. Org. Chem.* **2017**, *82*, 7050−7058.
[6] Y. Zhou, Y. You, Z. -H. Wang, X. -M. Zhang, X. -Y. Xu, W. -C. Yuan *Eur. J. Org. Chem.* **2019**, *2019*, 3112–3116.

pyrazolinone derivatives with excellent yields and good enantioselectivities, Scheme 5.2b. In both cases, a quinine-derived squaramide was used as organocatalyst.

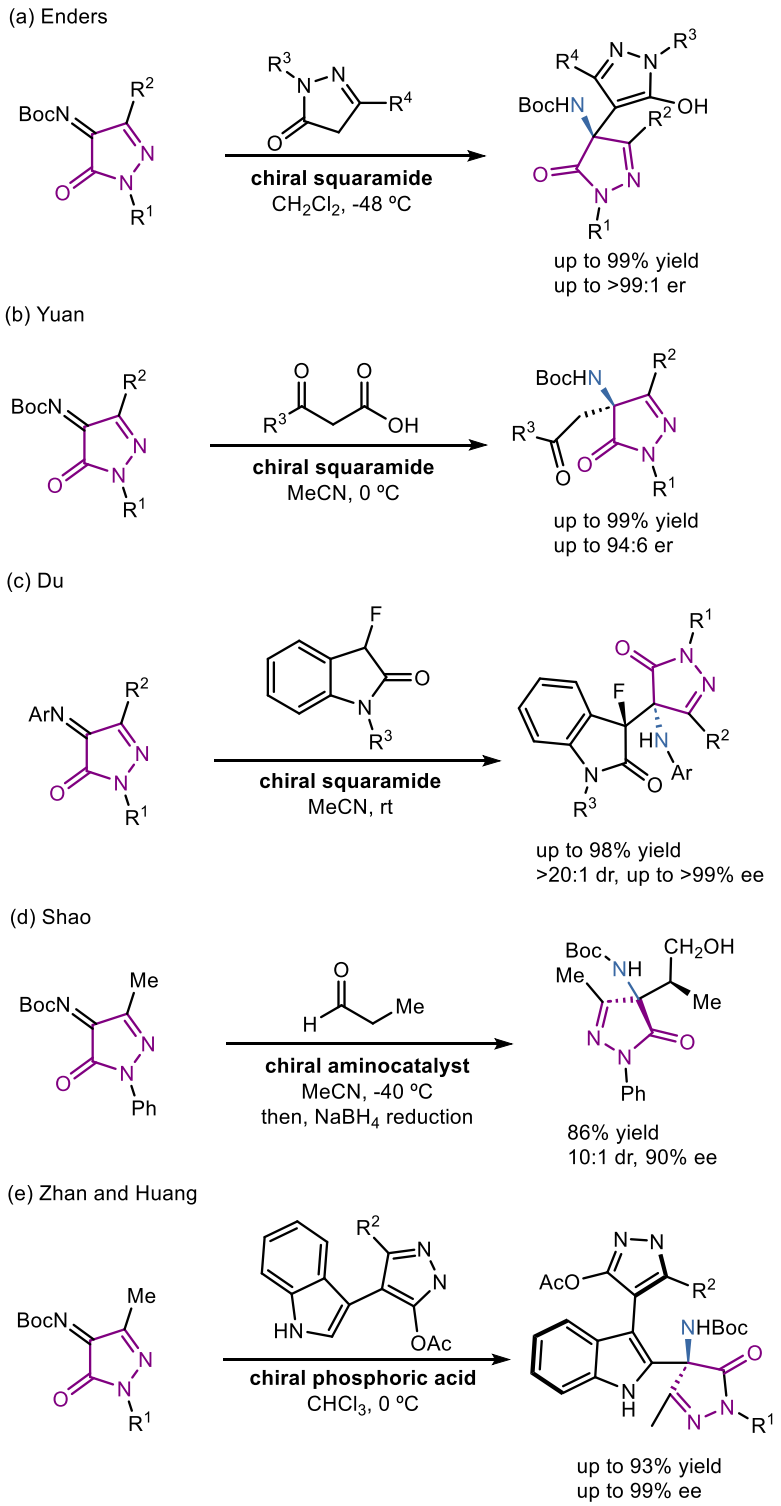

Scheme 5.2: Mannich reactions with pyrazolone-derived ketimines reported in literature.

Du[7] constructed amino-pyrazolone-oxindoles containing interesting stereogenic C–F units *via* asymmetric Mannich reaction of pyrazolinone ketimines with 3-fluorooxindoles using a hydroquinine-derived squaramide as catalyst, Scheme 5.2c. Excellent yields and both diastereo- and enantioselectivities were achieved with long reaction times using *N*-aryl pyrazole-4,5-dione-derived ketimines. When the *N*-Boc-protected ketimine was used, the enantiomeric excess dropped to 28% as well as the yield which shrunk to 36%. Shao[8] developed an enantiodivergent Mannich reaction between pyrazole-derived ketimines and propionaldehyde through aminocatalysis giving rise to the corresponding adducts in good yields with high diastereo- and enantioselectivity, Scheme 5.2d. Zhan and Huang[9] displayed the synthesis of 3,4'-indole-pyrazole derivatives featuring axially chiral bis-pentatomic heteroaryls from *N*-Boc-protected ketimines and 3-indolyl pyrazole derivatives through chiral phosphoric acid-catalyzed Mannich reaction, Scheme 5.2e. More recently, Wang[10] constructed β-fluoroamine derivatives from pyrazolinone ketimines and 2-fluoroindanones *via* asymmetric Mannich reaction catalyzed by a chiral cupper complex.

1,3-Dicarbonyl compounds as an important class of nucleophiles, can undergo various addition reactions with unsaturated bonds.[11] In this chapter, a new organocatalytic asymmetric Mannich reaction between 1,3-dicarbonyl compounds and ketimines derived from pyrazolin-5-one is studied. The reaction provides 4-amino-5-pyrazolone derivatives bearing a tetrasubstituted stereocenter and containing two privileged structure motifs, the pyrazole scaffold and a β-diketone, which could be used in further transformations.

5.2 Results and discussion

We started our study with the reaction between pyrazolinone ketimine **1a** and 2,4-pentanedione **2a** in the presence of catalysts **C1**-**C8** in toluene as solvent at room temperature (Table 1). Quinine-derived thiourea **C1** as catalyst gave rise to adduct **3a** with good yield and moderate enantioselectivity (74% yield and er 68:32) in short reaction time (entry 1). Interestingly, when a quinine-derived squaramide **C2** was used, the yield increased, 88%, and so did the enantiomeric ratio, 80:20 (entry 2). This result showed that squaramide catalysts

[7] Q. -D. Zhang, B. -L. Zhao, B. -Y. Li, D. -M. Du *Org. Biomol. Chem.* **2019**, *17*, 7182–7191.
[8] J. Dai, Z. Wang, Y. Deng, L. Zhu, F. Peng, Y. Lan, Z. Shao *Nat. Commun.* **2019**, *10*, 5182.
[9] C. Li, W. -F. Zuo, J. Zhou, W. -J. Zhou, M. Wang, X. Li, G. Zhan, W. Huang *Org. Chem. Front.* **2022**, *9*, 1808–1813.
[10] W. Gu, J. Li, K. Li, Q. Sun, T. Li, Z. Zha, Z. Wang *J. Org. Chem.* **2023** DOI: 10.1021/acs.joc.2c02040.
[11] *Review*: D. Bonne, Y. Coquerel, T. Constantieux, J. Rodriguez *Tetrahedron: Asymmetry*, **2010**, *21*, 1085–1109.

perform better than thioureas in this reaction and, due to this, we further studied the reaction screening with different bifunctional squaramides.

Before screening of catalysts, a wide variety of solvents (DCM, $CHCl_3$, DCE, Et_2O, THF, 1,4-dioxane and ethyl acetate) were examined in the presence of catalyst **C2**, but the enantioselectivity decreased (entry 2 vs. entries 3-9). In contrast, when acetonitrile was used, the opposite enantiomer was obtained with the same enantiomeric ratio (entry 10).[12]

Table 1. Screening of catalysts **C1**-**C8** and optimization of reaction conditions.[a]

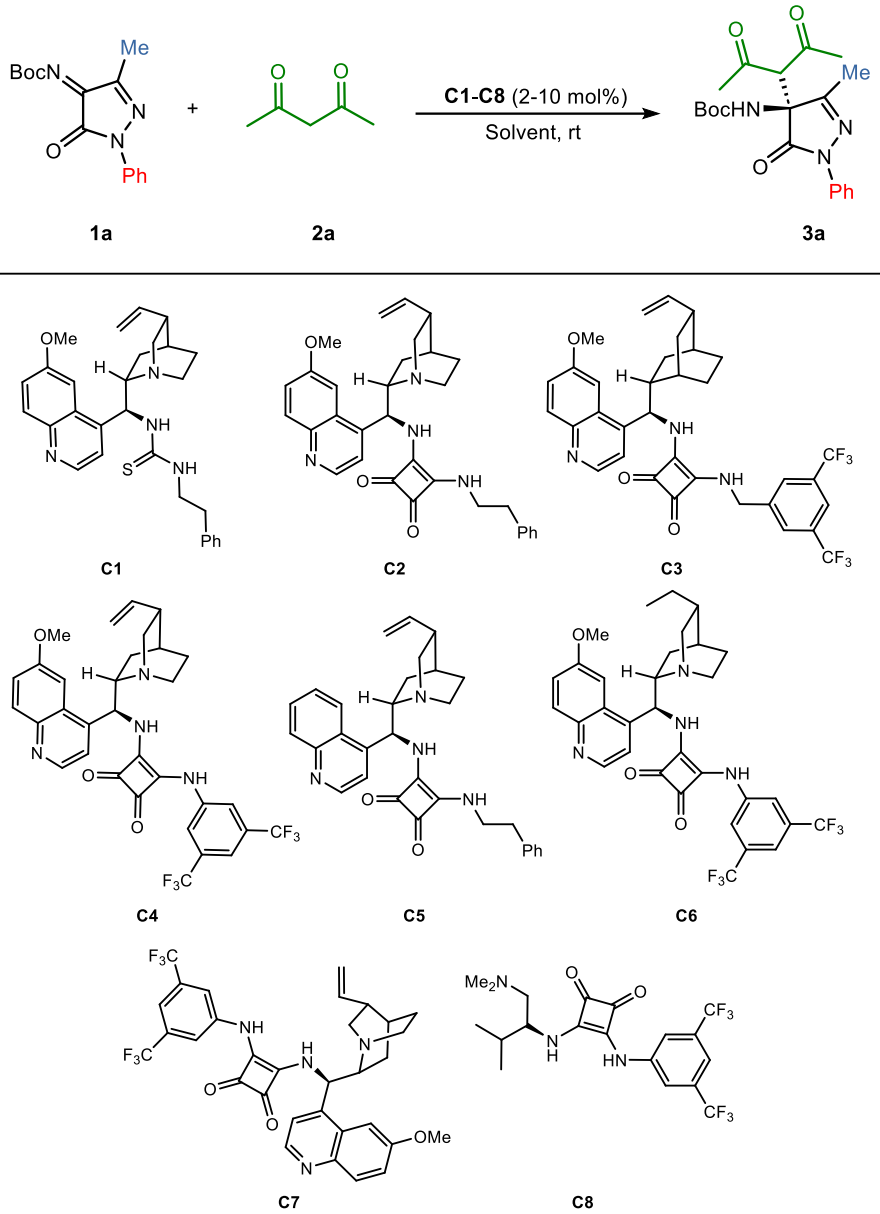

[12] Examples of solvent-induced reversal of enantioselectivity have been described in Chapter IV – Ref. 12.

Entry	*Catalyst*	*Solvent*	*t (h)*	*Yield (%)*[b]	*er*[c]
1	**C1**	Toluene	4	74	68:32
2	**C2**	Toluene	5	88	80:20
3	**C2**	DCM	1	85	60:40
4	**C2**	$CHCl_3$	1	83	78:22
5	**C2**	DCE	1	68	59:41
6	**C2**	Et_2O	6	90	73:27
7	**C2**	THF	6	82	58:42
8	**C2**	Dioxane	3	65	55:45
9	**C2**	EtOAc	2	85	60:40
10	**C2**	MeCN	2	73	20:80
11	**C3**	Toluene	1	80	78:22
12	**C4**	Toluene	1	84	84:16
13	**C5**	Toluene	1.5	68	84:16
14	**C6**	Toluene	2.5	80	80:20
15	**C7**	Toluene	1	76	29:71
16	**C8**	Toluene	4	82	64:36
17[d]	**C4**	Toluene	2	86	84:16
18[e]	**C4**	Toluene	2	92	85:15
19[f]	**C4**	Toluene	6	71	84:16
20[e,g]	**C4**	Toluene	2.5	92	85:15

[a] Reaction conditions: **1a** (0.1 mmol), **2a** (0.2 mmol), catalyst (10 mol%), solvent (1 mL) at rt. [b] Yield of **3a** determined after column chromatography. [c] Er values determined *via* chiral HPLC analysis. [d] 5 mol% of catalyst. [e] 2 mol% of catalyst. [f] Reaction at -18 ^{o}C. [g] Reaction performed with 1.1 equiv. of 2,4-pentanedione.

With toluene as the best choice to carry out the reaction, the influence of the H-bonding donor group was analyzed by comparing quinine-derived squaramides **C2** (phenethyl substituted), **C3** (bis(trifluoromethyl)benzyl substituted) and **C4** (bis(trifluoromethyl)phenyl substituted) (entries 2 and 11-12). Squaramide **C4** with an aromatic ring directly attached to the nitrogen atom afforded better enantiomeric ratio (er 84:16) than the other squaramides in shorter reaction time. Additional trials performed under the same reaction conditions using cinchonidine-derived squaramide **C5** and hydroquinine-derived squaramide **C6** did not lead to any increase in enantioselectivity (entries 13-14). Quinidine-derived squaramide **C7**, pseudoenantiomer of **C4**, catalyzed the reaction to afford the opposite enantiomer in similar yield but lower

enantioselectivity (entry 15). The enantiomeric ratio dropped to 64:36 when *L*-valine derived-squaramide **C8** was used (entry 16).

The reaction also worked effectively when 5 mol% of catalyst **C4** was used (entry 17) and even, 2 mol% could be used giving rise to pyrazolone derivative **3a** in 92% yield and er 85:15 after two hours (entry 18). Lowering the reaction temperature to -18 ^{o}C resulted in a longer reaction time but no improvement in the enantiomeric ratio was observed (entry 19). The equivalents of the nucleophile can be decreased from 2 to 1.1 without any remarkable change in the enantioselectivity (entry 20).

Once the optimized reaction conditions were fixed (molar ratio **1a**:**2a** 1:1.1, toluene, 2 mol% of **C4** and room temperature), the reaction between *N*-Boc pyrazolinone ketimines **1a-h** and different dicarbonyl compounds **2a-c** was studied, Table 2. First, 2,4-pentadione **2a** was reacted with *N*-Boc ketimines differently substituted at C-3 position. When an ethyl or an isopropyl group were present, **3b** and **3c** were obtained with moderate to good enantioselectivity (er 84:16 and 88:12). However, when *N*-Boc ketimine **1d** bearing a *tert*-butyl group was treated with **2a,** no reaction was observed (Table 2, **3d**), probably due to the bulky group. The reaction tolerates aromatic rings at C-3 position. So that the phenyl-substituted adduct **3e** was isolated with high yield and excellent enantiomeric ratio (er 94:6) after 48 hours of reaction although higher catalyst loading (5 mol%) was needed. Moreover, a methyl group can be attached to the nitrogen atom of the *N*-Boc ketimine, and **3f** was successfully isolated with only a slightly decrease in the enantioselectivity (Table 2, **3f**). Substituted aromatic rings can also be attached to the nitrogen atom. Regardless of whether an electron-withdrawing or electron-donating substituent was in the ring, the adducts were obtained with good enantiomeric ratio and moderate to good yields (Table 2, **3g** and **3h**).

It is important to note that recrystallization of Mannich adducts **3a** and **3g** from hexane/ethyl acetate allowed for obtaining enantioenriched **3a** and **3g** (er 95:5 and 96:4, respectively) from the mother liquor in 68% yield.

Table 2. Substrate scope for the asymmetric Mannich reaction.[a,b,c]

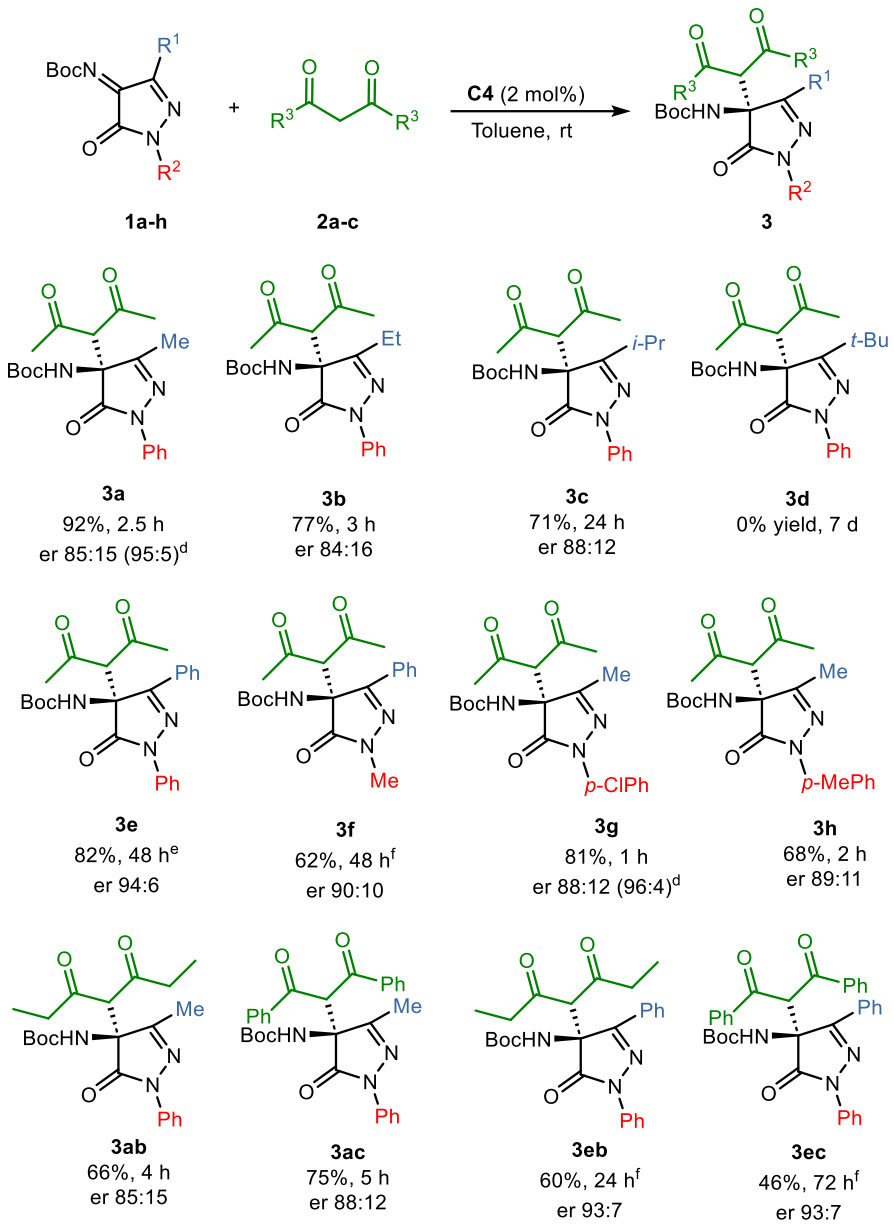

[a] Reaction conditions: **1** (0.1 mmol), **2** (0.11 mmol), **C4** (2 mol%), toluene (1 mL) at rt. [b] Yield of **3** determined after column chromatography. [c] Er values determined *via* chiral HPLC analysis. [d] Determined from the mother liquor after recrystallization from hexane/ethyl acetate. [e] 5 mol% catalyst was used. [f] 10 mol% catalyst was used.

Next, different β-diketones **2b-c** were evaluated. 3,5-Heptanedione (**2b**) reacted with ketimine **1a** leading to **3ab** in good yield and moderate enantioselectivity (er 85:15). On the contrary, the reaction of **1a** with dibenzoylmethane (**2c**) giving rise to **3ac** was slower and more enantioselective (er 88:12). Both diketones **2b** and **2c** reacted with the less reactive phenyl-substituted ketimine **1e** in the presence of 10 mol% catalyst **C4**, providing adducts **3eb** and **3ec**

in moderate yield but with good enantioselectivity (er 93:7), although longer reaction time was necessary to obtain high conversion.

To conclude the study of the scope, *N*-phenyl ketimine **1i** was treated with 2,4-pentadione in the presence of quinine-derived squaramide **C4**, but no reaction was observed after four days, probably due to the lower electrophilicity of *N*-phenyl ketimines, Scheme 5.3. Further efforts were made to prepare *N*-tosyl ketimines derived from pyrazolin-5-one, but the different methods[13] used for the preparation of these new *N*-protected ketimines were not successful.

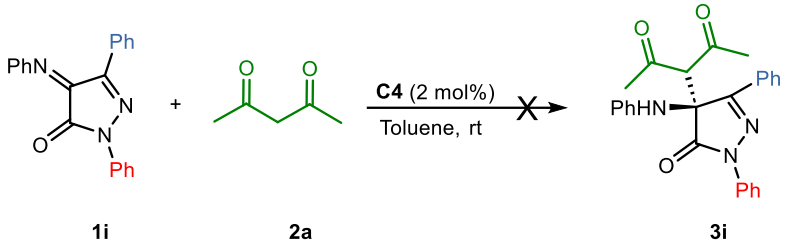

1i **2a** **3i**

Scheme 5.3: Unsuccessful Mannich reaction with *N*-phenyl ketimine **1i**.

To demonstrate the synthetic utility of the process, further transformation of Mannich products **3** into 4-pyrazolyl-pyrazolone derivatives **4** with potential pharmacological interest was carried out, Table 3. Condensation of adducts **3** with a two-fold excess of hydrazine monohydrate in methanol at room temperature gave rise to pyrazole derivatives **4** in moderate to good yield (60-82%) except when **3eb**, prepared from heptane-3,5-dione, was used, which yielded 40%. In all the cases, the pyrazole derivatives were obtained with no erosion in the enantiomeric ratio. 4-Pyrazolyl-pyrazolone **4a** was achieved as a single enantiomer after recrystallization from hexane/ethyl acetate.

[13] (a) J. Esquivias, R. Gómez Arrayás, J. C. Carretero *J. Org. Chem.* **2005**, *70,* 7451–7454, (b) J. L. García Ruano, J. Alemán, M. B. Cid, A. Parra *Org. Lett*. **2005**, *7*, 179–182, (c) B. E. Love, P. S. Raje, T. C. Williams *Synlett* **1994**, 493–494.

Table 3. Preparation of pyrazole derivatives.[a,b,c]

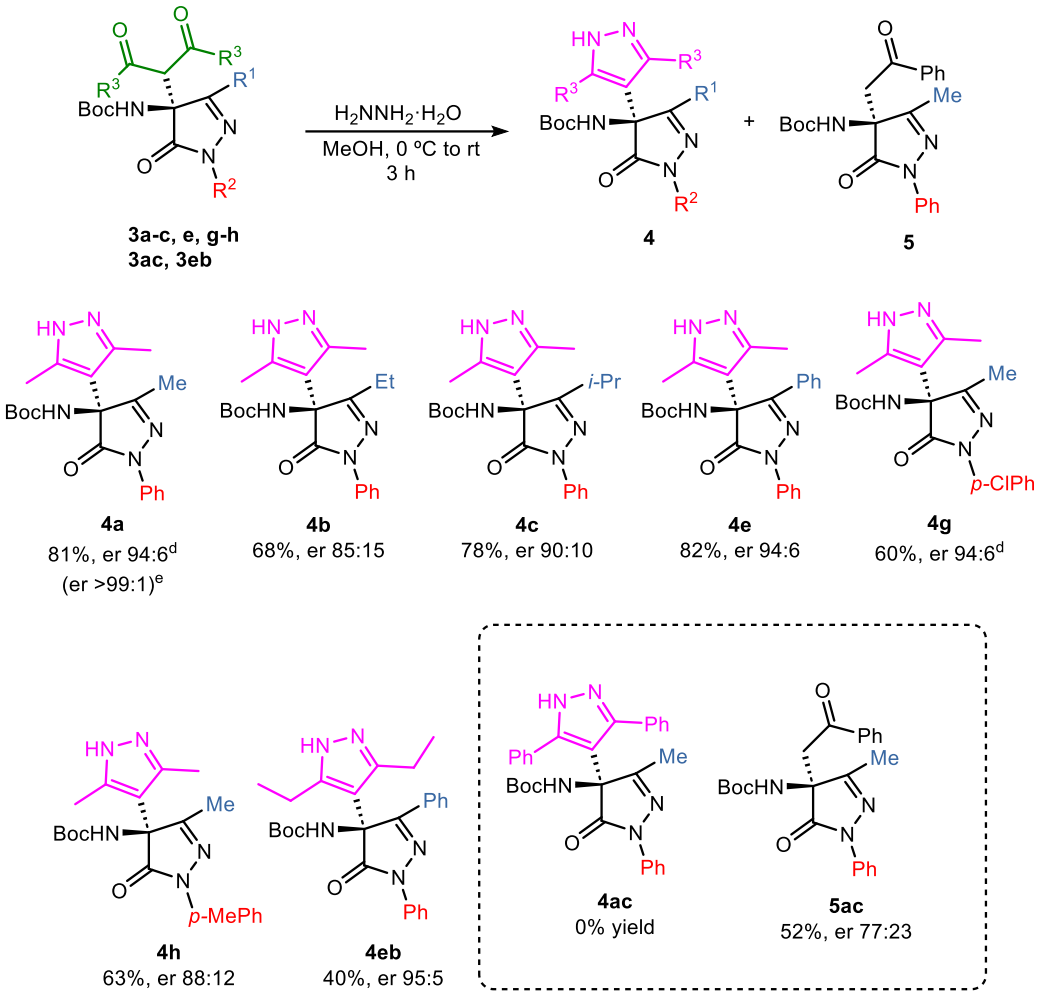

[a] Reactions were carried out with $H_2NNH_2 \cdot H_2O$ (2 equiv) in MeOH at 0 °C to rt. [b] Yield of **4** determined after column chromatography. [c] Er values determined *via* chiral HPLC analysis. [d] The reactions were performed with enantioenriched **3a** (er 95:5) and **3g** (er 96:4). [e] After recrystallization with hexane/ethyl acetate.

Surprisingly, when **3ac**, derived from dibenzoylmethane, was used in the condensation reaction with hydrazine monohydrate, product **4ac** was not observed; instead, β-amino ketone-pyrazolinone derivative **5ac** was isolated. This unwanted reaction has not been observed in the reactions of the adducts derived from pentane-2,4-dione and heptane-3,5-dione. Fortunately, the comparison of specific rotation and HPLC analysis of **5ac** with those described in literature[6] allowed us to determine the absolute configuration (*S*) of product **3ac** by chemical correlation. The absolute configuration of the other products **3** and **4** is expected to be the same by analogy assuming a common reaction pathway. A plausible mechanism for the debenzoylation process[14] is shown in Scheme 5.4. The nucleophilic attack of hydrazine hydrate on the carbonyl group of

[14] Q. Gao, Y. Zhu, M. Lian, M. Liu, J. Yuan, G. Yin, A. Wu *J. Org. Chem.* **2012**, *77*, 9865–9870.

3ac leads to intermediate **A**, which after debenzoylation process furnished β-amino ketone-pyrazolinone derivative **5ac**.

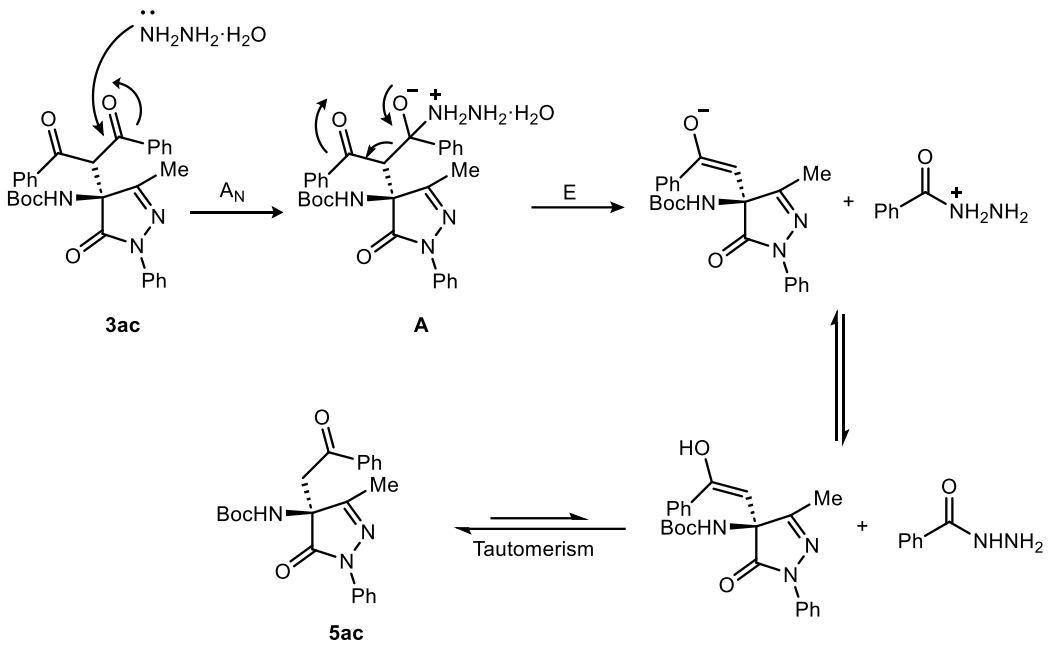

Scheme 5.4: Plausible mechanism of debenzoylation.

To further illustrate the utility of this process, Mannich adducts **3a** and **3e** were treated with 4-chlorophenylhydrazine in refluxing ethanol affording the corresponding 4-chlorophenyl pyrazoles **6a** and **6e** in moderate to good yields (40-75%) with retention of enantiomeric excess, Scheme 5.5.

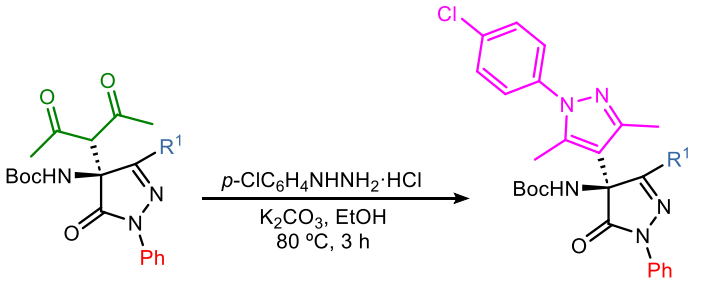

3a R^1= Me, er 85:15
3e R^1= Ph, er 94:6

6a R^1= Me, 75%, er 84:16
6e R^1= Ph, 40%, er 96:4

Scheme 5.5: Preparation of 4-chlorophenylpyrazol derivatives **6**.

Moreover, reaction of pyrazole derivatives **3a,e** with hydroxylamine hydrochloride worked well providing isoxazole derivatives **7a,e**, Scheme 5.6.

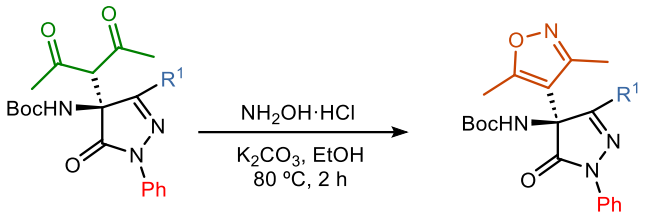

3a R^1= Me, er 85:15
3e R^1= Ph, er 94:6

7a R^1= Me, 44%, er 83:17
7e R^1= Ph, 80%, er 93:7

Scheme 5.6: Preparation of isoxazole derivatives **7**.

In addition, on the basis of our results and those previously reported,[5,6] a plausible ternary complex that rationalizes the absolute configuration of the Mannich adducts **3** is shown in Figure 5.1. The H-bonding activation of *N*-Boc ketimine **1** by the squaramide moiety of catalyst **C4** facilitates the nucleophilic attack of the diketone enolate from the *Re*-face of the imine group, providing the formation of adducts with (*S*) as absolute configuration.

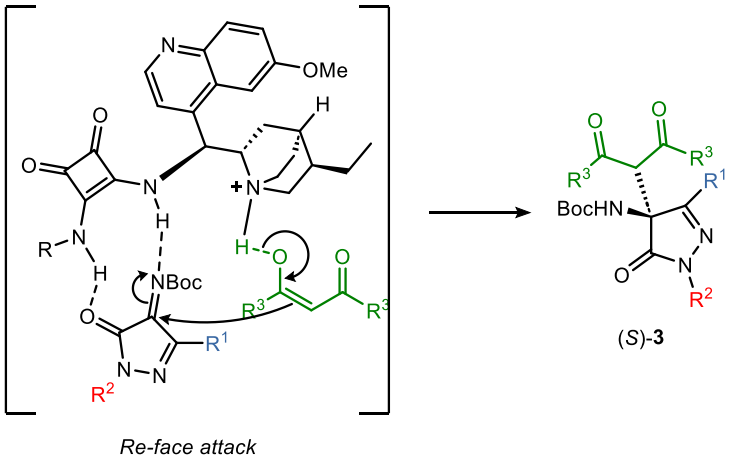

Figure 5.1: Proposed ternary complex which rationalizes the *(S)* configuration for the Mannich adducts.

5.3 Conclusions

In this chapter, we have developed the first asymmetric Mannich reaction between β-diketones and *N*-Boc ketimines derived from pyrazolin-5-one yielding 4-substituted-4-aminopyrazolones in good yields (46-90%) and enantioselectivities (er up to 94:6) by employing a very low loading of 2 mol% of organocatalyst for a wide range of substrates. Squaramide catalyst facilitates the nucleophilic attack of the β-dicarbonyl enolate to the *N*-Boc ketimine providing adducts with (*S*) configuration. Additionally, we achieved the transformation of the Mannich adducts into enantioenriched 4-pyrazolyl-pyrazolones and 4-isoxazolyl-pyrazolones through condensation

with hydrazines and hydroxylamine, opening a new way to the preparation of that kind of compounds.

5.4 References

1. X. -Q. Hou, D. -M. Du *Adv. Synth. Catal.* **2020**, *362*, 4487–4512.
2. *Some selected examples with 1,3-dicarbonyl compounds:* (a) P. Rodríguez-Ferrer, M. Sanz-Novo, A. Maestro, J. M. Andrés, R. Pedrosa *Adv. Synth. Catal.* **2019**, *361,* 3645–3655, (b) D. İşibol, S. Karahan, C. Tanyeli *Tetrahedron Lett*. **2018**, *59*, 541–545, (c) S. Ričko, J. Svete, B. Štefane, A. Perdih, A. Golobič, A. Meden, U. Grošelj *Adv. Synth. Catal*. **2016**, *358*, 3786–3796, (d) K. S. Rao, P. Ramesh, L. R. Chowhan, R. Trivedi *RSC Adv*. **2016**, *6*, 84242–84247, (e) W. Yan, D. Wang, J. Feng, P. Li, D. Zhao, R. Wang *Org. Lett*. **2012**, *14*, 2512–2515.
3. Y. Luo, K. Xie, D. Yue, X. Zhang, X. Xu, W. Yuan *Org. Biomol. Chem.* **2018**, *16*, 3372–3375.
4. (a) L. Carceller-Ferrer, C. Vila, G. Blay, I. Fernández, M. C. Muñoz, J. R. Pedro *Org. Biomol. Chem*. **2019**, *17*, 9859–9863, (b) H. Y. Bae, M. J. Kim, J. H. Sim, C. -E. Song *Angew. Chem. Int. Ed.* **2016**, *55*, 10825–10829, (c) H. -X. He, D. -M. Du *RSC Adv*. **2013**, *3*, 16349–16358.
5. P. Chauhan, S. Mahajan, U. Kaya, A. Peuronen, K. Rissanen, D. Enders *J. Org. Chem.* **2017**, *82*, 7050−7058.
6. Y. Zhou, Y. You, Z. -H. Wang, X. -M. Zhang, X. -Y. Xu, W. -C. Yuan *Eur. J. Org. Chem.* **2019**, *2019*, 3112–3116.
7. Q. -D. Zhang, B. -L. Zhao, B. -Y. Li, D. -M. Du *Org. Biomol. Chem.* **2019**, *17*, 7182–7191.
8. J. Dai, Z. Wang, Y. Deng, L. Zhu, F. Peng, Y. Lan, Z. Shao *Nat. Commun.* **2019**, *10*, 5182.
9. C. Li, W. -F. Zuo, J. Zhou, W. -J. Zhou, M. Wang, X. Li, G. Zhan, W. Huang *Org. Chem. Front.* **2022**, *9*, 1808–1813.
10. W. Gu, J. Li, K. Li, Q. Sun, T. Li, Z. Zha, Z. Wang *J. Org. Chem.* **2023,** DOI: 10.1021/acs.joc.2c02040.
11. *Review*: D. Bonne, Y. Coquerel, T. Constantieux, J. Rodriguez *Tetrahedron: Asymmetry*, **2010**, *21*, 1085–1109.
12. Examples of solvent-induced reversal of enantioselectivity have been described in Chapter IV – Ref. 12.
13. (a) J. Esquivias, R. Gómez Arrayás, J. C. Carretero *J. Org. Chem.* **2005***, 70,* 7451–7454, (b) J. L. García Ruano, J. Alemán, M. B. Cid, A. Parra *Org. Lett*. **2005**, *7*, 179–182, (c) B. E. Love, P. S. Raje, T. C. Williams *Synlett* **1994**, 493–494.
14. Q. Gao, Y. Zhu, M. Lian, M. Liu, J. Yuan, G. Yin, A. Wu *J. Org. Chem.* **2012**, *77*, 9865–9870.

5.5 Experimental section

5.5.1 *General Procedure for the Synthesis of Mannich Products by Enantioselective Mannich Reaction of N-Boc Ketimines with β-Diketones.*

To a mixture of *N*-Boc ketimine **1** (0.1 mmol) and catalyst **C4** (0.002 mmol, 0.02 equiv) in 1.0 mL of toluene, β-diketone **2a**–**c** (0.11 mmol, 1.1 equiv) was added at room temperature, and the reaction mixture was stirred in a Wheaton vial. The progress of the reaction was monitored by TLC analysis. After the completion of the reaction, the solvent was removed under reduced pressure. The crude reaction mixture was purified by flash column chromatography to afford the corresponding product **3**. The enantiomeric excess was determined by chiral-phase HPLC analysis using mixtures of hexane/isopropanol as eluent.

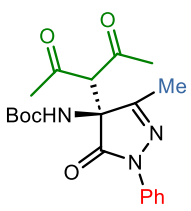

3a

***tert*-Butyl (*S*)-(4-(2,4-dioxopentan-3-yl)-3-methyl-5-oxo-1-phenyl-4,5-dihydro-1*H*-pyrazol-4-yl)carbamate (3a).** Product **3a** was obtained according to general procedure using pentane-2,4-dione (11 µL, 0.11 mmol, 1.1 equiv) as β-diketone and catalyst **C4** (1.3 mg, 0.002 mmol, 0.02 equiv). Chromatography on silica gel using hexane/EtOAc = 3:1 as eluent afforded compound **3a** as a colorless solid (35 mg, 0.09 mmol, 90% yield). Mp 140-141 ^{o}C (hexane-EtOAc). $[\alpha]_D^{25}$ = +18.9 (c= 0.9, $CHCl_3$). ^{1}H NMR (500 MHz, $CDCl_3$) δ 7.87 (dd, *J*= 8.6, 1.2 Hz, 2H), 7.39 (dd, *J*= 8.6, 7.4 Hz, 2H), 7.19 (tt, *J*= 7.4, 1.3 Hz, 1H), 6.38 (br, 1H), 4.08 (s, 1H), 2.31 (s, 3H), 2.30 (s, 3H), 2.08 (s, 3H), 1.36 (s, 9H). ^{13}C NMR (126 MHz, $CDCl_3$) δ 200.4, 169.9, 137.7, 128.9, 125.4, 118.9, 77.3, 66.9, 66.7, 32.1, 31.9, 28.1, 14.8. IR (ATR): 3403, 3356, 2974, 2931, 1707, 1596, 1496, 1375, 1254, 1154, 758, 688 cm^{-1}. HRMS (ESI-QTOF) m/z $[M+H]^+$ Calcd. For $C_{20}H_{26}N_3O_5$ 388.1867; Found 388.1868. Chiral HPLC analysis: Chiralpak AD-H column, hexane/*i*-PrOH 85:15, 0.7 mL/min, λ = 254 nm, major enantiomer (*S*) t_R = 11.5 min, minor enantiomer (*R*) t_R = 26.1 min. (er 85:15). A sample of **3a** (er 85:15) was recrystallized from MeOH to afford **3a** as white crystals (quasi-racemic mixture, er 58:42) and enantioenriched **3a** from the mother liquors (er 95:5). This last fraction was then used to prepare compound **4a**.

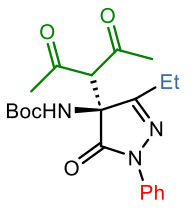

3b

***tert*-Butyl (*S*)-(4-(2,4-dioxopentan-3-yl)-3-ethyl-5-oxo-1-phenyl-4,5-dihydro-1*H*-pyrazol-4-yl)carbamate (3b).** Product **3b** was obtained according to general procedure using pentane-2,4-dione (11 µL, 0.11 mmol, 1.1 equiv) as β-diketone and catalyst **C4** (1.3 mg, 0.002 mmol, 0.02 equiv). Chromatography on silica gel using hexane/EtOAc = 3:1 as eluent afforded compound **3b** as a colorless oil (31 mg, 0.077 mmol, 77% yield). $[\alpha]_D^{25}$ = +10.7 (c= 0.5, $CHCl_3$). ^{1}H NMR (500 MHz, $CDCl_3$) δ 7.89 (dd, *J*= 8.7, 1.2 Hz, 2H), 7.38 (dd, *J*= 8.7, 7.4 Hz, 2H), 7.18 (tt, *J*= 7.4, 1.2 Hz, 1H, 6.40 (br, 1H), 4.05 (s, 1H), 2.41 (m, 1H), 2.34 (m, 1H), 2.30 (s, 3H), 2.29 (s, 3H), 1.34 (s, 9H), 1.27 (t, *J*= 7.3 Hz, 3H). ^{13}C NMR (126 MHz, $CDCl_3$) δ 200.7, 170.1, 137.9, 128.8, 125.3, 118.9, 77.3, 67.1, 66.9, 32.1, 31.9, 28.1, 22.2, 9.6. IR (ATR): 3388, 2985, 2942, 1707, 1596, 1493, 1453, 1351, 1279, 1152, 1054, 761, 692 cm^{-1}. HRMS (ESI-QTOF) m/z

[M+H]$^+$ Calcd. For $C_{21}H_{28}N_3O_5$ 402.2023; Found 402.2029. Chiral HPLC analysis: Chiralpak AD-H column, hexane/*i*-PrOH 85:15, 0.7 mL/min, λ = 254 nm, major enantiomer (*S*) t_R = 10.0 min, minor enantiomer (*R*) t_R = 20.0 min. (er 84:16).

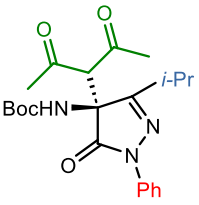

3c

***tert*-Butyl (*S*)-(4-(2,4-dioxopentan-3-yl)-3-isopropyl-5-oxo-1-phenyl-4,5-dihydro-1*H*-pyrazol-4-yl)carbamate (3c).** Product **3c** was obtained according to general procedure using pentane-2,4-dione (11 µL, 0.11 mmol, 1.1 equiv) as β-diketone and catalyst **C4** (1.3 mg, 0.002 mmol, 0.02 equiv). Chromatography on silica gel using hexane/EtOAc = 4:1 as eluent afforded compound **3c** as a colorless oil (30 mg, 0.071 mmol, 71% yield). $[\alpha]_D^{25}$ = +42.5 (c= 0.8, MeOH). ^{1}H NMR (500 MHz, $CDCl_3$) δ 7.89 (d, *J*= 8.1 Hz, 2H), 7.38 (dd, *J*= 8.7, 7.4 Hz, 2H), 7.17 (tt, *J*= 7.4, 1.2 Hz, 1H), 6.49 (br, 1H), 4.04 (s, 1H), 2.65 (sept, *J*= 6.9 Hz, 1H), 2.29 (s, 3H), 2.28 (s, 3H), 1.37 (s, 9H), 1.27 (d, *J*= 6.8 Hz, 6H), 1.24 (d, *J*= 7.0 Hz, 6H). ^{13}C NMR (126 MHz, $CDCl_3$) δ 201.1, 169.8, 138.0, 128.8, 125.2, 119.1, 77.3, 67.4, 67.0, 32.1, 31.7, 28.8, 28.1, 20.3. IR (ATR): 3413, 2975, 2935, 1710, 1598, 1493, 1457, 1359, 1283, 1156, 1083, 1054, 754, 688 cm^{-1}. HRMS (ESI-QTOF) m/z: [M+Na]$^+$ Calcd. For $C_{22}H_{29}N_3NaO_5$ 438.1999; Found 438.1999. Chiral HPLC analysis: Chiralpak AD-H column, hexane/*i*-PrOH 95:5, 0.7 mL/min, λ = 254 nm, major enantiomer (*S*) t_R = 18.6 min, minor enantiomer (*R*) t_R = 27.0 min. (er 88:12).

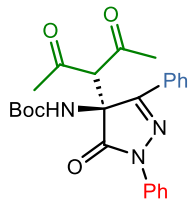

3e

***tert*-Butyl (*S*)-(4-(2,4-dioxopentan-3-yl)-5-oxo-1,3-diphenyl-4,5-dihydro-1*H*-pyrazol-4-yl)carbamate (3e).** Product **3e** was obtained according to general procedure using pentane-2,4-dione (11 µL, 0.11 mmol, 1.1 equiv) as β-diketone and catalyst **C4** (3.2 mg, 0.005 mmol, 0.05 equiv). Chromatography on silica gel using hexane/EtOAc = 4:1 as eluent afforded compound **3e** as a colorless oil (37 mg, 0.082 mmol, 82% yield). $[\alpha]_D^{25}$ = +56.3 (c= 0.6, $CHCl_3$). ^{1}H NMR (500 MHz, $CDCl_3$) δ 7.98 (dd, *J*= 8.4, 1.2 Hz, 2H), 7.90 (dd, *J*= 7.8, 2.0 Hz, 2H), 7.43 (m, 5H), 7.23 (tt, *J*= 7.4, 1.0 Hz, 1H), 6.82 (br, 1H), 3.97 (s, 1H), 2.11 (s, 3H), 2.03 (s, 3H), 1.31 (s, 9H). ^{13}C NMR (126 MHz, $CDCl_3$) δ 202.2, 200.5, 170.0, 137.9, 130.8, 129.0, 128.9, 126.7, 125.6, 119.2, 77.3, 66.3, 66.2, 32.3, 32.2, 28.1. IR (ATR): 3379, 2982, 1714, 1597, 1490, 1358, 1255, 1156, 751, 689 cm^{-1}. HRMS (ESI-QTOF) m/z [M+Na]$^+$ Calcd. For $C_{25}H_{27}N_3NaO_5$ 472.1843; Found 472.1842. Chiral HPLC analysis: Chiralpak AD-H column, hexane/*i*-PrOH 85:15, 0.7 mL/min, λ = 254 nm, major enantiomer (*S*) t_R = 12.7 min, minor enantiomer (*R*) t_R = 29.1 min. (er 94:6).

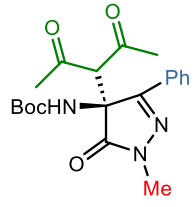

3f

***tert*-Butyl (*S*)-(4-(2,4-dioxopentan-3-yl)-1-methyl-5-oxo-3-phenyl-4,5-dihydro-1*H*-pyrazol-4-yl)carbamate (3f).** Product **3f** was obtained according to general procedure using pentane-2,4-dione (11 µL, 0.11 mmol, 1.1 equiv) as β-diketone and catalyst **C4** (6.4 mg, 0.01 mmol, 0.1 equiv). Chromatography on silica gel using hexane/EtOAc = 4:1 as eluent afforded compound **3f** as a colorless oil (24 mg, 0.062 mmol, 62% yield). $[\alpha]_D^{25}$ = +46.0 (c= 0.3, $CHCl_3$). ^{1}H NMR (500 MHz, $CDCl_3$) δ 7.77 (m, 2H), 7.40 (m, 3H), 6.76 (br, 1H), 3.86 (s, 1H), 3.45 (s, 1H), 2.07 (s, 3H), 2.03 (s, 3H), 1.36 (br, 9H). ^{13}C NMR (126 MHz,

$CDCl_3$) δ 202.4, 200.5, 171.4, 133.9, 130.4, 128.9, 126.4, 77.2, 66.0, 64.9, 32.2, 32.2, 28.1. IR (ATR): 3375, 2978, 2926, 1703, 1483, 1351, 1252, 1157, 765, 695 cm^{-1}. HRMS (ESI-QTOF) m/z: $[M+Na]^+$ Calcd. For $C_{20}H_{25}N_3NaO_5$ 410.1686; Found 410.1686. Chiral HPLC analysis: Chiralpak AD-H column, hexane/*i*-PrOH 95:5, 0.8 mL/min, λ = 254 nm, major enantiomer (*S*) t_R = 31.6 min, minor enantiomer (*R*) t_R = 43.1 min. (er 90:10).

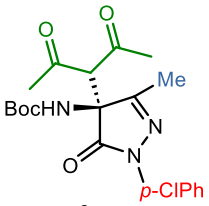

3g

***tert*-Butyl (*S*)-(1-(4-chlorophenyl)-4-(2,4-dioxopentan-3-yl)-3-methyl-5-oxo-4,5-dihydro-1*H*-pyrazol-4-yl)carbamate (3g).** Product **3g** was obtained according to general procedure using pentane-2,4-dione (11 µL, 0.11 mmol, 1.1 equiv) as β-diketone and catalyst **C4** (1.3 mg, 0.002 mmol, 0.02 equiv). Chromatography on silica gel using hexane/EtOAc = 3:1 as eluent afforded compound **3g** as a colorless solid (34 mg, 0.081 mmol, 81% yield). Mp 170-171 °C (hexane-EtOAc). $[\alpha]_D^{25}$ = +17.9 (c= 0.6, $CHCl_3$). ^1H NMR (500 MHz, $CDCl_3$) δ 7.84 (d, *J*= 8.9 Hz, 2H), 7.34 (d, *J*= 8.9 Hz, 2H), 6.36 (br, 1H), 4.05 (s, 1H), 2.30 (s, 3H), 2.29 (s, 3H), 2.07 (s, 3H), 1.35 (s, 9H). ^{13}C NMR (126 MHz, $CDCl_3$) δ 200.4, 169.9, 158.1, 153.5, 136.3, 130.4, 128.9, 119.9, 81.7, 66.9, 66.6, 32.1, 31.9, 28.1, 14.7. IR (ATR): 3419, 2975, 2905, 1714, 1494, 1461, 1365, 1251, 1152, 836, 810 cm^{-1}. HRMS (ESI-QTOF) m/z $[M+H]^+$ Calcd. For$C_{20}H_{25}ClN_3O_5$ 422.1477; Found 422.1487. Chiral HPLC analysis: Chiralpak AD-H column, hexane/*i*-PrOH 85:15, 0.7 mL/min, λ = 254 nm, major enantiomer (*S*) t_R = 10.0 min, minor enantiomer (*R*) t_R = 31.8 min. (er 88:12). A sample of **3g** (er 88:12) was recrystallized from hexane-ethyl acetate to afford **3g** as white crystals (quasi-racemic mixture, er 58:42) and enantioenriched **3g** from the mother liquors (er 96:4). This last fraction was then used to prepare compound **4g**.

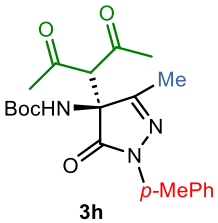

3h

***tert*-Butyl (*S*)-(4-(2,4-dioxopentan-3-yl)-3-methyl-5-oxo-1-(*p*-tolyl)-4,5-dihydro-1*H*-pyrazol-4-yl)carbamate (3h).** Product **3h** was obtained according to general procedure using pentane-2,4-dione (11 µL, 0.11 mmol, 1.1 equiv) as β-diketone and catalyst **C4** (1.3 mg, 0.002 mmol, 0.02 equiv). Chromatography on silica gel using hexane/EtOAc = 3:1 as eluent afforded compound **3h** as a colorless solid (27 mg, 0.068 mmol, 68% yield). Mp 150-151 °C (hexane-EtOAc). $[\alpha]_D^{25}$ = +19.0 (c= 0.5, $CHCl_3$). ^1H NMR (500 MHz, $CDCl_3$) δ 7.73 (d, *J*= 8.4 Hz, 2H), 7.18 (d, *J*= 8.4 Hz, 2H), 6.35 (br, 1H), 4.07 (s, 1H), 2.33 (s, 3H), 2.30 (s, 3H), 2.29 (s, 3H), 2.07 (s, 3H), 1.35 (s, 9H). ^{13}C NMR (126 MHz, $CDCl_3$) δ 200.4, 169.7, 135.3, 135.1, 129.4, 119.0, 77.3, 67.0, 66.7, 32.1, 31.9, 28.1, 21.0, 14.8. IR (ATR): 3423, 2978, 2923, 1714, 1703, 1512, 1472, 1369, 1255, 1156, 1056, 814 cm^{-1}. HRMS (ESI-QTOF) m/z: $[M+H]^+$ Calcd. For $C_{21}H_{28}N_3O_5$ 402.2023; Found 402.2043. Chiral HPLC analysis: Chiralpak AD-H column, hexane/*i*-PrOH 85:15, 0.7 mL/min, λ = 254 nm, major enantiomer (*S*) t_R = 11.5 min, minor enantiomer (*R*) t_R = 44.7 min. (er 89:11).

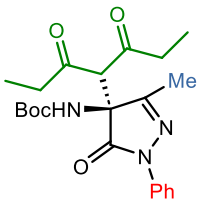

3ab

***tert*-Butyl (*S*)-(4-(3,5-dioxoheptan-4-yl)-3-methyl-5-oxo-1-phenyl-4,5-dihydro-1*H*-pyrazol-4-yl)carbamate (3ab).** Product **3ab** was obtained according to general procedure using heptane-3,5-dione (15 µL, 0.11 mmol, 1.1 equiv) as β-diketone and catalyst **C4** (1.3 mg, 0.002 mmol, 0.02 equiv). Chromatography on silica gel using hexane/EtOAc = 4:1 as eluent afforded compound **3ab** as a colorless solid (27 mg, 0.066 mmol, 66% yield). Mp 119-120 ºC (hexane-EtOAc). $[\alpha]_D^{25}$ = +12.9 (c= 0.6, $CHCl_3$). ^{1}H NMR (500 MHz, $CDCl_3$): δ 7.85 (dd, *J*= 8.7, 1.2 Hz, 2H), 7.37 (dd, *J*= 8.6, 7.4 Hz, 2H), 7.17 (tt, *J*= 7.4, 1,2 Hz, 1H), 6.55 (br, 1H), 4.03 (s, 1H), 2.60 (m, 2H), 2.54 (m, 2H), 2.05 (s, 3H), 1.36 (s, 9H), 1.08 (t, *J*= 7.1 Hz, 3H), 0.99 (t, *J*= 7.1 Hz, 3H). ^{13}C NMR (126 MHz, $CDCl_3$) δ 202.7, 170.1, 137.8, 128.8, 125.3, 118.9, 77.3, 67.0, 65.1, 38.6, 38.4, 28.1, 14.8, 7.4, 7.3. IR (ATR): 3339, 2978, 2942, 1714, 1597, 1497, 1369, 1270, 1152, 1104, 759, 689 cm^{-1}. HRMS (ESI-QTOF) m/z: $[M+H]^+$ Calcd. For $C_{22}H_{30}N_3O_5$ 416.2180; Found 416.2189. Chiral HPLC analysis: Chiralpak AD-H column, hexane/*i*-PrOH 85:15, 0.7 mL/min, λ = 254 nm, major enantiomer (*S*) t_R = 9.2 min, minor enantiomer (*R*) t_R = 23.8 min. (er 85:15).

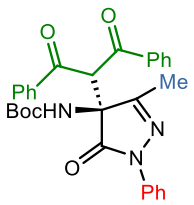

3ac

***tert*-Butyl (*S*)-(4-(1,3-dioxo-1,3-diphenylpropan-2-yl)-3-methyl-5-oxo-1-phenyl-4,5-dihydro-1*H*-pyrazol-4-yl)carbamate (3ac).** Product **3ac** was obtained according to general procedure using 1,3-diphenylpropane-1,3-dione (25 mg, 0.11 mmol, 1.1 equiv) as β-diketone and catalyst **C4** (1.3 mg, 0.002 mmol, 0.02 equiv). Chromatography on silica gel using hexane/EtOAc = 4:1 as eluent afforded compound **3ac** as a colorless solid (38 mg, 0.075 mmol, 75% yield). Mp 201-202 ºC (hexane-EtOAc). $[\alpha]_D^{25}$ = -68.6 (c= 0.7, $CHCl_3$). ^{1}H NMR (500 MHz, $CDCl_3$) δ 7.89 (dd, *J*= 11.9, 8.6 Hz, 4H), 7.51 (m, 4H), 7.39 (m, 4H), 7.22 (dd, *J*= 8.6, 7.2 Hz, 2H), 7.07 (td, *J*= 7.4, 1.3 Hz, 1H), 6.61 (br, 1H), 5.91 (s, 1H), 2.22 (s, 3H), 1.36 (s, 9H). ^{13}C NMR (126 MHz, $CDCl_3$) δ 191.1, 170.1, 137.5, 136.1, 135.2, 134.5, 134.2, 129.1, 129.1, 128.7, 128.5, 128.5, 125.0, 118.6, 77.3, 67.8, 56.6, 28.1, 15.8. IR (ATR): 3276, 3147, 2986, 1729, 1700, 1593, 1490, 1446, 1365, 1270, 1214, 1152, 770, 751, 696, 682 cm^{-1}. HRMS (ESI-QTOF) m/z $[M+H]^+$ Calcd. For $C_{30}H_{30}N_3O_5$ 512.2180; Found 512.2214. Chiral HPLC analysis: Chiralpak AD-H column, hexane/*i*-PrOH 85:15, 0.7 mL/min, λ = 254 nm, major enantiomer (*S*) t_R = 14.2 min, minor enantiomer (*R*) t_R = 35.8 min. (er 88:12).

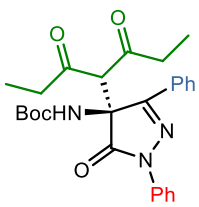

3eb

***tert*-Butyl (*S*)-(4-(3,5-dioxoheptan-4-yl)-5-oxo-1,3-diphenyl-4,5-dihydro-1*H*-pyrazol-4-yl)carbamate (3eb).** Product **3eb** was obtained according to general procedure using heptane-3,5-dione (15 µL, 0.11 mmol, 1.1 equiv) as β-diketone and catalyst **C4** (6.3 mg, 0.01 mmol, 0.1 equiv). Chromatography on silica gel using hexane/EtOAc = 8:1 as eluent afforded compound **3eb** as a colorless oil (29 mg, 0.06 mmol, 60% yield). $[\alpha]_D^{25}$ = +48.4 (c= 0.5, $CHCl_3$). ^{1}H NMR (500 MHz, $CDCl_3$) δ 7.98 (dd, *J*= 8.6, 1.3 Hz, 2H), 7.88 (dd, *J*= 7.3, 2.5 Hz, 2H), 7.43 (m, 5H), 7.23 (m, 1H), 7.12 (br, 1H), 3.94 (s, 1H), 2.59 (dq, *J*= 20.6, 7.1 Hz, 1H), 2.38 (dq, *J*= 19.0, 7.0 Hz, 1H), 2.19 (dq, *J*= 19.2, 7.1 Hz, 1H), 2.03 (dq, *J*= 19.4, 7.0 Hz, 1H), 1.33 (s, 9H), 0.90 (t, *J*= 7.1 Hz, 3H), 0.79 (t, *J*= 7.0 Hz, 3H). ^{13}C NMR (126 MHz, $CDCl_3$) δ 204.0, 202.7, 170.2, 137.9, 130.7, 128.9, 126.8, 125.5, 119.2, 77.3, 66.7, 39.0, 28.1, 7.2, 6.9. IR (ATR): 3369, 2979, 2939, 1731,

1698, 1599, 1489, 1397, 1283, 1158, 1114, 1015, 758, 736, 689 cm^{-1}. HRMS (ESI-QTOF) m/z $[M+H]^+$ Calcd. For $C_{27}H_{32}N_3O_5$ 478.2336; Found 478.2345. Chiral HPLC analysis: Chiralpak AD-H column, hexane/*i*-PrOH 85:15, 0.7 mL/min, λ = 254 nm, major enantiomer (*S*) t_R = 8.9 min, minor enantiomer (*R*) t_R = 22.3 min. (er 93:7).

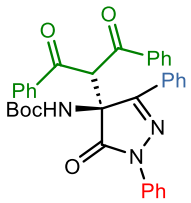

3ec

***tert*-Butyl (*S*)-(4-(1,3-dioxo-1,3-diphenylpropan-2-yl)-5-oxo-1,3-diphenyl-4,5-dihydro-1*H*-pyrazol-4-yl)carbamate (3ec).** Product **3ec** was obtained according to general procedure using 1,3-diphenylpropane-1,3-dione (25 mg, 0.11 mmol, 1.1 equiv) as β-diketone and catalyst **C4** (6.3 mg, 0.01 mmol, 0.1 equiv). Chromatography on a silica gel using hexane/EtOAc = 4:1 as an eluent afforded compound **3ec** as a colorless solid (26 mg, 0.046 mmol, 46% yield). Mp 189-190 °C (hexane-EtOAc). $[\alpha]_D^{25}$ = +41.7 (c= 0.34, $CHCl_3$). ^{1}H NMR (500 MHz, $CDCl_3$) δ 7.88 (ddd, *J*= 8.6, 7.6, 1.3 Hz, 4H), 7.75 (d, *J*= 7.2 Hz, 2H), 7.58 (m, 1H), 7.49 (dd, *J*= 8.5, 1.3 Hz, 2H), 7.40 (m, 5H), 7.21 (m, 6H), 5.80 (s, 1H), 1.39 (s, 9H). ^{13}C NMR (126 MHz, $CDCl_3$) δ 190.4, 170.3, 137.9, 137.0, 136.6, 134.1, 133.8, 130.4, 129.1, 128.9, 128.6, 128.4, 128.2, 128.1, 127.5, 125.4, 118.9, 77.3, 68.6, 51.9, 28.2. IR (ATR): 3420, 3068, 2979, 2928, 1709, 1695, 1595, 1482, 1280, 1258, 1159, 971, 758, 685 cm^{-1}. HRMS (ESI-QTOF) m/z $[M+H]^+$ Calcd. For $C_{35}H_{32}N_3O_5$ 574.2336; Found 574.2342. Chiral HPLC analysis: Chiralpak AD-H column, hexane/*i*-PrOH 80:20, 1 mL/min, λ = 254 nm, major enantiomer (*S*) t_R = 10.9 min, minor enantiomer (*R*) t_R = 23.8 min. (er 93:7).

5.5.2 General procedure for the synthesis of pyrazole derivatives 4 by reaction of adducts 3 with hydrazine hydrate.

To a solution of adduct **3** (0.1 mmol) in 1.0 mL of methanol, hydrated hydrazine (12 µl, 0.2 mmol, 2 equiv) was added at 0 °C and the reaction mixture was then stirred at rt. The progress of the reaction was monitored by TLC analysis. After the completion of the reaction, the solvent was removed under reduced pressure. The crude reaction mixture was purified by flash column chromatography to afford the corresponding product **4**. The enantiomeric excess was determined by chiral-phase HPLC analysis using mixtures of hexane/isopropanol as eluent.

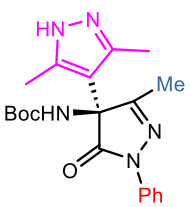

4a

***tert*-Butyl (*S*)-(3,3',5-trimethyl-5'-oxo-1'-phenyl-1',5'-dihydro-1*H*,4'*H*-[4,4'-bipyrazol]-4'-yl)carbamate (4a).** Product **4a** was obtained from **3a** according to general procedure. Chromatography on silica gel using EtOAc as eluent afforded compound **4a** as a colorless solid (31 mg, 0.081 mmol, 81% yield). Mp 220-222 °C (hexane-EtOAc). $[\alpha]_D^{25}$ = +96.5 (c= 0.5, $CHCl_3$). ^{1}H NMR (400 MHz, $CDCl_3$) δ 7.93 (dd, *J*= 8.0, 0.8 Hz, 2H), 7.39 (t, *J*= 7.8 Hz, 2H), 7.18 (tt, *J*= 7.4, 1.2 Hz, 1H), 5.92 (br, 1H), 2.28 (s, 6H), 2.11 (s, 3H), 1.37 (s, 9H). ^{13}C NMR (126 MHz, $CDCl_3$) δ 172.0, 160.5, 154.1, 142.3, 138.0, 128.9, 125.0, 118.6, 107.5, 77.3, 65.6, 28.1, 14.2, 12.9. IR (ATR): 3247, 2978, 2934, 1711, 1692, 1593, 1501, 1365, 1251, 1156, 759, 693 cm^{-1}. HRMS (ESI-QTOF) m/z $[M+Na]^+$ Calcd. For $C_{20}H_{25}N_5NaO_3$ 406.1850; Found 406.1860. Chiral HPLC analysis: Lux Amylose-2 column, hexane/*i*-PrOH 90:10, 1 mL/min, λ = 254 nm, minor enantiomer (*R*) t_R = 19.9 min, major enantiomer (*S*) t_R = 29.1 min. (er 94:6).

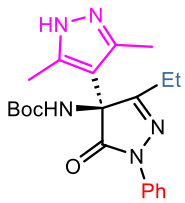

4b

***tert*-Butyl (*S*)-(3'-ethyl-3,5-dimethyl-5'-oxo-1'-phenyl-1',5'-dihydro-1*H*,4'*H*-[4,4'-bipyrazol]-4'-yl)carbamate (4b).** Product **4b** was obtained from **3b** according to general procedure. Chromatography on silica gel using EtOAc as eluent afforded compound **4b** as a colorless oil (27 mg, 0.068 mmol, 68% yield). $[\alpha]_D^{25}$ = +62.8 (c= 0.1, $CHCl_3$). ^{1}H NMR (500 MHz, $CDCl_3$) δ 7.97 (dd, *J*= 8.7, 1.2 Hz, 2H), 7.40 (dd, *J*= 8.7, 7.4 Hz, 2H), 7.18 (tt, *J*= 7.4, 1.2 Hz, 1H), 5.71 (br, 1H), 2.50 (dq, *J*= 17.6, 7.4 Hz, 1H), 2.37 (m, 1H), 2.28 (s, 6H), 1.36 (s, 9H), 1.30 (t, *J*= 7.0 Hz, 3H). ^{13}C NMR (126 MHz, $CDCl_3$) 172.1, 164.0, 154.0, 142.3, 138.2, 128.8, 124.9, 118.5, 108.0, 77.2, 65.6, 28.1, 21.5, 12.9, 9.1. HRMS (ESI-QTOF) m/z $[M+H]^+$ Calcd. For $C_{21}H_{28}N_5O_3$ 398.2187; Found 398.216. Chiral HPLC analysis: Chiralpak AD-H column, hexane/*i*-PrOH 90:10, 1 mL/min, λ = 254 nm, major enantiomer (*S*) t_R = 25.8 min, minor enantiomer (*R*) t_R = 31.8 min. (er 85:15).

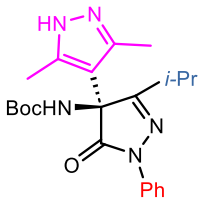

4c

***tert*-Butyl (*S*)-(3'-isopropyl-3,5-dimethyl-5'-oxo-1'-phenyl-1',5'-dihydro-1*H*,4'*H*-[4,4'-bipyrazol]-4'-yl)carbamate (4c).** Product **4c** was obtained from **3c** according to general procedure. Chromatography on silica gel using hexane/EtOAc = 2:1 as an eluent afforded compound **4c** as a colorless oil (32 mg, 0.078 mmol, 78% yield). $[\alpha]_D^{25}$ = +139.8 (c= 0.5, $CHCl_3$). ^{1}H NMR (500 MHz, $CDCl_3$) δ 7.99 (d, *J*= 7.1 Hz, 2H), 7.40 (dd, *J*= 8.5, 7.4 Hz, 2H), 7.18 (t, *J*= 7.4 Hz, 1H), 6.22 (br, 1H), 2.66 (sept, *J*= 6.8 Hz, 1H), 2.23 (s, 6H), 1.36 (s, 9H), 1.32 (d, *J*= 7.0 Hz, 3H), 1.07 (d, *J*= 6.8 Hz, 3H). ^{13}C NMR (126 MHz, $CDCl_3$): 172.3, 167.0, 154.4, 141.9, 138.1, 128.8, 125.0, 118.6, 107.8, 77.2, 66.2, 28.2, 28.1, 21.1, 20.8, 12.8. IR (ATR): 3290, 2975, 2931, 1708, 1597, 1494, 1367, 1159, 759, 737, 693 cm^{-1}. HRMS (ESI-QTOF) m/z $[M+Na]^+$ Calcd. For $C_{22}H_{29}N_5NaO_3$ 434.2163; Found 434.2162. Chiral HPLC analysis: Lux Amylose-2 column, hexane/*i*-PrOH 90:10, 1 mL/min, λ = 254 nm, minor enantiomer (*R*) t_R = 17.5 min, major enantiomer (*S*) t_R = 23.5 min. (er 90:10).

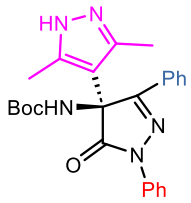

4e

***tert*-Butyl (*S*)-(3,5-dimethyl-5'-oxo-1',3'-diphenyl-1',5'-dihydro-1*H*,4'*H*-[4,4'-bipyrazol]-4'-yl)carbamate (4e).** Product **4e** was obtained from **3e** according to general procedure. Chromatography on silica gel using hexane/EtOAc = 1:1 as eluent afforded compound **4e** as a colorless oil (36 mg, 0.082 mmol, 82% yield). $[\alpha]_D^{25}$ = -190.0 (c= 0.1, $CHCl_3$). ^{1}H NMR (500 MHz, $CDCl_3$) δ 8.13 (br, 1H), 7.99 (dd, *J*= 8.7, 1.2 Hz, 2H), 7.85 (d, *J*= 7.1 Hz, 2H), 7.39 (m, 5H), 7.19 (tt, *J*= 7.4, 1.2 Hz, 1H), 2.30 (s, 6H), 1.19 (s, 9H). ^{13}C NMR (126 MHz, $CDCl_3$) δ 171.5, 167.0, 153.7, 143.1, 138.3, 138.2, 128.9, 128.8, 126.4, 125.1, 118.7, 108.7, 77.2, 64.1, 27.9, 12.8. IR (ATR): 3237, 3123, 3060, 2978, 2931, 1730, 1708, 1594, 1500, 1367, 1159, 759, 737, 689 cm^{-1}. HRMS (ESI-QTOF) m/z $[M+H]^+$ Calcd. For $C_{25}H_{28}N_5O_3$ 446.2187; Found 446.2205. Chiral HPLC analysis: Lux *i*-Amylose-3 column, hexane/*i*-PrOH 90:10, 1 mL/min, λ = 254 nm, major enantiomer (*S*) t_R = 12.8 min, minor enantiomer (*R*) t_R = 32.5 min. (er 94:6).

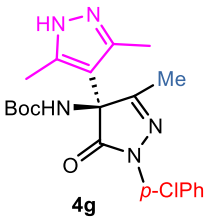

4g

***tert*-Butyl (*S*)-(1'-(4-chlorophenyl)-3,3',5-trimethyl-5'-oxo-1',5'-dihydro-1*H*,4'*H*-[4,4'-bipyrazol]-4'-yl)carbamate (4g).** Product **4g** was obtained from enantioenriched **3g** according to general procedure. Chromatography on silica gel using hexane/EtOAc = 1:3 as eluent afforded compound **4g** as a colorless oil (25 mg, 0.060 mmol, 60% yield). $[\alpha]_D^{25}$ = +51.0 (c= 0.2, $CHCl_3$). ^{1}H NMR (500 MHz, $CDCl_3$) δ 7.91 (d, *J*= 8.9 Hz, 2H), 7.35 (d, *J*= 8.9 Hz, 2H), 5.84 (br, 1H), 2.27 (s, 6H), 2.10 (s, 3H), 1.37 (s, 9H). ^{13}C NMR (126 MHz, $CDCl_3$) δ 171.9, 160.7, 154.0, 142.3, 136.6, 130.1, 128.9, 119.6, 107.4, 77.2, 65.5, 28.1, 14.2, 12.8. IR (ATR): 3268, 2978, 2931, 1708, 1490, 1361, 1254, 1159, 1093, 1011, 910, 828, 727 cm^{-1}. HRMS (ESI-QTOF) m/z $[M+H]^+$ Calcd. For $C_{20}H_{25}ClN_5O_3$ 418.1640; Found 418.1633. HPLC: Lux *i*-Amylose-3 column, hexane/*i*-PrOH 90:10, 1 mL/min, λ = 254 nm, major enantiomer (*S*) t_R = 26.5 min, minor enantiomer (*R*) t_R = 52.5 min. (er 94:6).

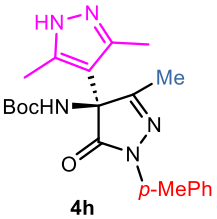

4h

***tert*-Butyl (*S*)-(3,3',5-trimethyl-5'-oxo-1'-(*p*-tolyl)-1',5'-dihydro-1*H*,4'*H*-[4,4'-bipyrazol]-4'-yl)carbamate (4h).** Product **4h** was obtained from **3h** according to general procedure. Chromatography on silica gel using hexane/EtOAc = 1:3 as an eluent afforded compound **4h** as a colorless oil (25 mg, 0.063 mmol, 63% yield). $[\alpha]_D^{25}$ = +61.2 (c= 0.3, $CHCl_3$). ^{1}H NMR (500 MHz, $CDCl_3$) δ 7.80 (d, *J*= 8.6 Hz, 2H), 7.19 (d, *J*= 8.6 Hz, 2H), 6.00 (br, 1H), 2.34 (s, 3H), 2.26 (s, 6H), 2.09 (s, 3H), 1.37 (s, 9H). ^{13}C NMR (126 MHz, $CDCl_3$) δ 171.8, 160.5, 154.1, 142.3, 135.6, 134.7, 129.4, 118.6, 107.6, 77.3, 65.5, 28.1, 20.9, 14.1, 12.8. IR (ATR): 3268, 2982, 2928, 1705, 1509, 1361, 1250, 1159, 815, 730 cm^{-1}. HRMS (ESI-QTOF) m/z $[M+H]^+$ Calcd. For $C_{21}H_{28}N_5O_3$ 398.2187; Found 398.2183. Chiral HPLC analysis: Chiralpak IA, hexane/*i*-PrOH 90:10, 1 mL/min, λ = 254 nm, major enantiomer (*S*) t_R = 23.5 min, minor enantiomer (*S*) t_R = 47.2 min. (er 88:12).

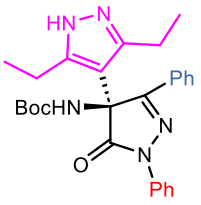

4eb

***tert*-Butyl (S)-(3,5-diethyl-5'-oxo-1',3'-diphenyl-1',5'-dihydro-1*H*,4'*H*-[4,4'-bipyrazol]-4'-yl)carbamate (4eb).** Product **4eb** was obtained from **3eb** according to general procedure. Chromatography on silica gel using hexane/EtOAc = 2:1 as eluent afforded compound **4eb** as a colorless oil (19 mg, 0.040 mmol, 40% yield). $[\alpha]_D^{25}$ = -134.3 (c= 0.2, $CHCl_3$). ^{1}H NMR (500 MHz, $CDCl_3$) δ 7.97 (dd, *J*= 8.6, 1.2 Hz, 2H), 7.82 (d, *J*= 7.6 Hz, 2H), 7.42 (m, 5H), 7.21 (tt, *J*= 7.4, 1.2 Hz, 1H), 2.98 (m, 2H), 2.86 (dq, *J*= 15.5, 7.6 Hz), 1.24 (t, *J*= 7.5, 6H), 1.20 (s, 9H). ^{13}C NMR (126 MHz, $CDCl_3$) δ 166.1, 148.5, 144.0, 133.4, 124.3, 124.2, 121.7, 120.6, 114.1, 104.4, 72.3, 23.2, 15.1, 8.7, 7.3. IR (ATR): 3250, 2975, 2928, 1701, 1594, 1490, 1368, 1159, 756, 693 cm^{-1}. HRMS (ESI-QTOF) m/z $[M+H]^+$ Calcd. For $C_{27}H_{32}N_5O_3$ 474.2500; Found 474.2486. Chiral HPLC analysis: Chiralpak IA, hexane/*i*-PrOH 95:5, 1 mL/min, λ = 254 nm, minor enantiomer (*R*) t_R = 20.1 min, major enantiomer (*S*) t_R = 25.0 min. (er 95:5).

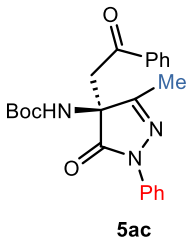

5ac

***tert*-Butyl (*S*)-(3-methyl-5-oxo-4-(2-oxo-2-phenylethyl)-1-phenyl-4,5-dihydro-1*H*-pyrazol-4-yl)carbamate (5ac)**. Product **5ac** was obtained from **3ac** according to general procedure. Chromatography on silica gel using hexane/EtOAc = 3:1 as eluent afforded compound **5ac** as a colorless oil (21 mg, 0.052 mmol, 52% yield). $[\alpha]_D^{25}$ = -17.5 (c= 0.3, CH_2Cl_2). $[[\alpha]_D^{20}$ = -20.2 (c = 1, CH_2Cl_2, er 94:6 for (*S*) enantiomer)].[6] ^{1}H NMR (400 MHz, DMSO-d_6) δ 7.90 (br, 1H), 7.83 (m, 2H), 7.74 (d, *J*= 7.8 Hz, 2H), 7.62 (tt, *J*= 7.4, 1.3 Hz, 1H), 7.49 (t, *J*= 7.8 Hz, 2H), 7.38 (dd, *J*= 8.7, 7.4 Hz, 2H), 7.14 (tt, *J*= 7.4, 1.3 Hz, 1H), 3.74 (d, *J*= 17.2 Hz, 1H), 3.62 (d, *J*= 17.2 Hz, 1H), 1.99 (s, 3H), 1.31 (s, 9H). ^{13}C NMR (100 MHz, DMSO-d_6) δ 195, 172.3, 158.8, 153.8, 138.7, 136.2, 134.2, 129.3, 129.2, 128.4, 124.7, 118.1, 80.0, 63.6, 42.6, 28.4, 13.5. IR (ATR): 2856, 1714, 1594, 1500, 1364, 1251, 1159, 753, 693 cm^{-1}. HRMS (ESI-QTOF) m/z $[M+Na]^+$ Calcd. For $C_{35}H_{25}N_3NaO_4$ 430.1737; Found 430.1759. Chiral HPLC analysis: Chiralpak IA column, hexane/*i*-PrOH 80:20, 1 mL/min, λ = 254 nm, minor enantiomer (*R*) t_R = 6.9 min, major enantiomer (*S*) t_R = 32.4 min. (er 77:23).

5.5.3 General procedure for the synthesis of pyrazole derivatives 6a,e.

A solution of **3a,e** (0.1 mmol), 4-chlorophenylhydrazine hydrochloride (19 mg, 0.11 mmol, 1.1 equiv) and and K_2CO_3 (8 mg, 0.055 mmol, 0.55 equiv) in ethanol (1 mL) was heated to 80 °C for 2-3 h. After that, the solvent of reaction mixture was removed under reduced pressure. The crude product was purified by flash chromatography on silica gel to afford **6a,e**.

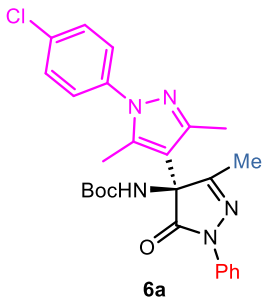

6a

***tert*-Butyl (*S*)-(1-(4-chlorophenyl)-3,3',5-trimethyl-5'-oxo-1'-phenyl-1',5'-dihydro-1*H*,4'*H*-[4,4'-bipyrazol]-4'-yl)carbamate (6a).** Product **6a** was obtained from **3a** according to general procedure. Chromatography on silica gel using hexane/EtOAc = 4:1 as an eluent afforded compound **6a** as a colorless solid (37 mg, 0.075 mmol, 75% yield). Mp 196-197 ^{o}C (hexane-EtOAc). $[\alpha]_D^{25}$ = +59.9 (c= 0.7, $CHCl_3$). ^{1}H NMR (500 MHz, $CDCl_3$) δ 7.94 (dd, *J*= 8.7, 1.2 Hz, 2H), 7.40 (m, 4H), 7.28 (d, *J*= 8.5 Hz, 2H), 7.18 (tt, *J*= 7.4, 1.2 Hz, 1H), 5.41 (br, 1H), 2.40 (s, 3H), 2.33 (s, 3H), 2.19 (s, 3H), 1.39 (s, 9H). ^{13}C NMR (126 MHz, $CDCl_3$) δ 171.5, 159.8, 153.7, 146.6, 138.0, 137.1, 134.4, 129.4, 128.9, 127.1, 125.1, 118.6, 110.0, 79.7, 65.4, 28.1, 14.5, 14.1, 12.3. IR (ATR)**:** 3269, 2982, 2928, 1711, 1598, 1500, 1393, 1364, 1295, 1254, 1163, 1093, 1014, 838, 759, 690, 645 cm^{-1}. HRMS (ESI-QTOF) m/z $[M+H]^+$ Calcd. For $C_{26}H_{29}ClN_5O_3$ 494.1953; Found 494.1931. Chiral HPLC analysis: Chiralpak AD-H column, hexane/*i*-PrOH 90:10, 1 mL/min, λ = 254 nm, major enantiomer (*S*) t_R = 45.0 min, minor enantiomer (*R*) t_R = 74.2 min. (er 84:16).

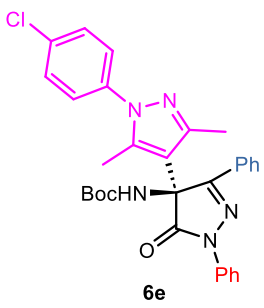

6e

***tert*-Butyl (*S*)-(1-(4-chlorophenyl)-3,5-dimethyl-5'-oxo-1',3'-diphenyl-1',5'-dihydro-1H,4'H-[4,4'-bipyrazol]-4'-yl)carbamate (6e).** Product **6e** was obtained from **3e** according to general procedure. Chromatography on silica gel using hexane/EtOAc = 4:1 as eluent afforded compound **6e** as a colorless oil (22 mg, 0.040 mmol, 40% yield). $[\alpha]_D^{25}$ = -155.0 (c= 0.4, $CHCl_3$). ^{1}H NMR (500 MHz, $CDCl_3$) δ 8.01 (dd, *J*= 8.8, 1.1 Hz, 2H), 7.91 (d, *J*= 6.5 Hz, 2H), 7.44 (m, 5H), 7.42 (d, *J*= 8.7 Hz, 2H), 7.29 (d, *J*= 8.7 Hz, 2H), 7.20 (tt, *J*= 7.4, 1.2 Hz, 1H), 5.54 (br, 1H), 2.41 (s, 3H), 2.31 (s, 3H), 1.22 (s, 9H). ^{13}C NMR (126 MHz, $CDCl_3$) δ 171.7, 153.6, 146.9, 138.4, 137.5, 134.1, 130.7, 130.3, 129.3, 128.9, 126.9, 126.5, 125.1, 118.9, 110.5, 77.2, 64.4, 27.9, 14.2, 12.6. IR (ATR): 3245, 2975, 2854, 1727, 1701, 1596, 1500, 1362, 1260, 1158, 1092, 1016, 829, 756, 735, 691 cm^{-1}. HRMS (ESI-QTOF) m/z: $[M+Na]^+$ Calcd. For $C_{31}H_{30}N_5ClNaO_3$ 578.1929; Found 578.1943. Chiral HPLC analysis: Chiralpak AD-H column, hexane/*i*-PrOH 90:10, 1 mL/min, λ = 254 nm, major enantiomer (*S*) t_R = 10.1 min, minor enantiomer (*R*) t_R = 63.7 min. (er 96:4).

5.5.4 General Procedure for the synthesis of isoxazole derivatives 7a,e.

A solution of **3a,e** (0.1 mmol), hydroxylamine hydrochloride (8 mg, 0.11 mmol, 1.1 equiv) and K_2CO_3 (8 mg, 0.055 mmol, 0.55 equiv) in ethanol (1 mL) was heated to 80 °C for 2-3 h. After that, the solvent of reaction mixture was removed under reduced pressure. The crude product was purified by flash chromatography on silica gel to afford **7a,e**.

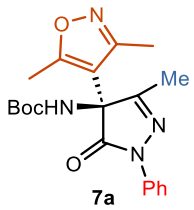

7a

***tert*-Butyl (*S*)-(4-(3,5-dimethylisoxazol-4-yl)-3-methyl-5-oxo-1-phenyl-4,5-dihydro-1*H*-pyrazol-4-yl)carbamate (7a).** Product **7a** was obtained from **3a** according to general procedure. Chromatography on silica gel using hexane/EtOAc = 3:1 as an eluent afforded compound **7a** as a colorless oil (17 mg, 0.044 mmol, 44% yield). $[\alpha]_D^{25}$ = +45.2 (c= 0.5, $CHCl_3$). ^{1}H NMR (500 MHz, $CDCl_3$) δ 7.91 (dd, *J*= 8.8, 1.1 Hz, 2H), 7.41 (dd, *J*= 8.7, 7.4 Hz, 2H), 7.20 (tt, *J*= 7.4, 1.2 Hz, 1H), 5.35 (br, 1H), 2.47 (s, 3H), 2.36 (s, 3H), 2.15 (s, 3H), 1.38 (s, 9H). ^{13}C NMR (126 MHz, $CDCl_3$) δ 170.6, 167.3, 157.8, 153.8, 137.8, 129.0, 125.3, 118.5, 107.2, 77.3, 63.9, 28.1, 14.3, 12.9, 11.8. IR (ATR): 3270, 2982, 2931, 2249, 1705, 1596, 1497, 1362, 1253, 1158, 1063, 1023, 906, 756, 727, 691, 643 cm^{-1}. HRMS (ESI-QTOF) m/z: $[M+Na]^+$ Calcd. For $C_{20}H_{24}N_4NaO_4$ 407.1690; Found 407.1693. Chiral HPLC analysis: Chiralpak AD-H column, hexane/*i*-PrOH 90:10, 1 mL/min, λ = 254 nm, major enantiomer (*S*) t_R = 10.6 min, minor enantiomer (*R*) t_R = 19.5 min. (er 83:17).

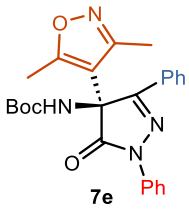

7e

***tert*-Butyl (*S*)-(4-(3,5-dimethylisoxazol-4-yl)-5-oxo-1,3-diphenyl-4,5-dihydro-1*H*-pyrazol-4-yl)carbamate (7e).** Product **7e** was obtained from **3e** according to general procedure. Chromatography on silica gel using hexane/EtOAc = 3:1 as eluent afforded compound **7e** as a colorless oil (36 mg, 0.080 mmol, 80% yield). $[\alpha]_D^{25}$ = -151.4 (c= 0.5, $CHCl_3$). ^{1}H NMR (500 MHz, $CDCl_3$) δ 7.98 (dd, *J*= 8.7, 1.3 Hz, 2H), 7.83 (m, 2H), 7.43 (m, 4H), 7.34

(br, 2H), 7.22 (tt, *J*= 7.4, 1.2 Hz, 1H), 2.38 (s, 6H), 1.20 (s, 9H). ^{13}C NMR (100 MHz, $CDCl_3$) δ 170.7, 167.8, 158.2, 153.8, 138.1, 131.0, 129.0, 128.9, 126.2, 125.4, 118.7, 107.7, 77.2, 62.7, 27.9, 13.0, 11.9. IR (ATR): 3245, 3128, 2978, 2927, 1731, 1705, 1599, 1490, 1380, 1366, 1256, 1150, 1052, 1026, 906, 756, 735, 687 cm^{-1}. HRMS (ESI-QTOF) m/z: $[M+Na]^+$ Calcd. For $C_{25}H_{26}N_4NaO_4$ 469.1846; Found 469.1858. Chiral HPLC analysis: Chiralpak AD-H column, hexane/*i*-PrOH 90:10, 1 mL/min, λ = 254 nm, minor enantiomer (*R*) t_R = 10.1 min, major enantiomer (*S*) t_R = 14.6 min. (er 93:7).

Chapter VI: Cross-nucleophile couplings *via* oxidative chemistry

This chapter is part of the results obtained while working under the supervision of Prof. Karl Anker Jørgensen in the Department of Chemistry of Aarhus University.

As this chapter is Prof. Karl Anker Jørgensen's intellectual property and the results are unpublished, the experimental section is omitted.

6.1 Introduction and background

The reaction between a nucleophile and an electrophile is a typical transformation in organic chemistry as it generates the formation of a covalent bond. In contrast, the reaction between two nucleophiles is a challenging topic for their inherently incompatibility.

The α-position of an aldehyde is expected to be nucleophilic due to the formation of the corresponding enol or enolate. However, this situation can be reversed converting the α-position into an activated electrophile. A pathway to overcome this situation comes by using an aminocatalyst, specifically a primary amine catalyst, in combination with an oxidant,[1] Scheme 6.1.

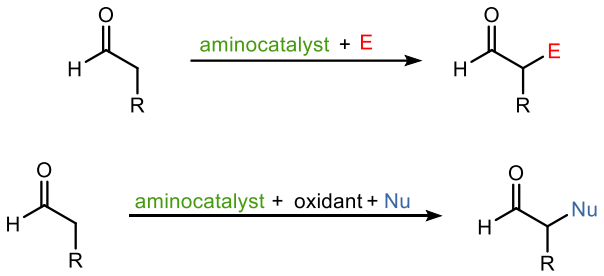

Scheme 6.1: Different aminocatalytic pathways for α-functionalization of aldehydes.

In this context, Jørgensen[2] disclosed the first enantioselective oxidative addition of aliphatic and aromatic carboxylic acids to α-branched aldehydes using a primary aminocatalyst in presence of an oxidant despite the *a priori* nucleophilic activity both reactants have, Scheme 6.2a. The reaction of the starting aldehyde with the aminocatalyst followed by oxidation with silver carbonate allows the formation of the corresponding carbocation and then, the coupling with the carboxylic acid occurs directed by an N—H—O bond between the tertiary amine of the catalyst and the carboxylic acid, Scheme 6.2b.

[1] N. M. Rezayee, J. N. Lamhauge, K. A. Jørgensen *Acc. Chem. Res.* **2022**, *55*, 1703–1717.

[2] L. A. Leth, L. Næsborg, G. J. Reyes-Rodríguez, H. N. Tobiesen, M. V. Iversen, K. A. Jørgensen *J. Am. Chem. Soc.* **2018**, *140*, 12687−12690. *For coupling of α-branched aldehydes with oligopeptides and amino acids see:* H. N. Tobiesen, L. A. Leth, M. V. Iversen, L. Næsborg, S. Bertelsen, K. A. Jørgensen *Angew. Chem. Int. Ed.* **2020**, *59*, 18490–18494.

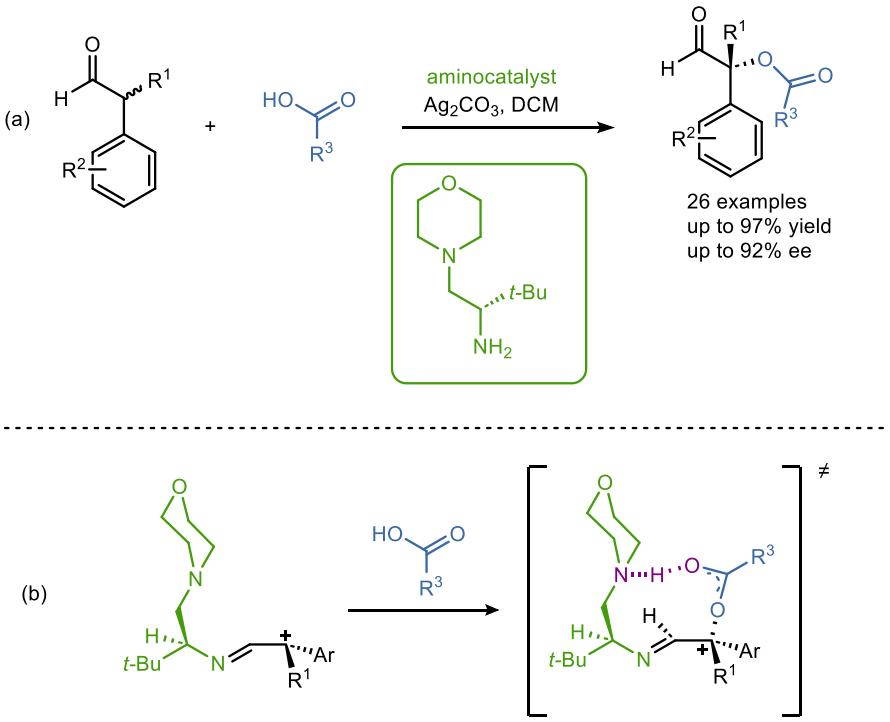

Scheme 6.2: Enantioselective oxidative coupling of carboxylic acids with α-branched aldehydes.

S_N2 substitution is known as the classical mechanism which involves inversion of stereochemistry through a concerted transition state: it is not a stereoselective process as the final stereochemistry depends on the starting material, Scheme 6.3.

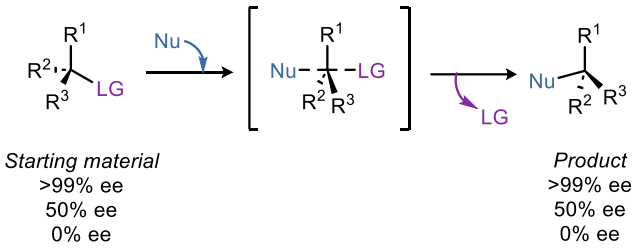

Scheme 6.3: Classical S_N2 mechanism.

Jørgensen and Houk[3] reported the coupling of α-branched aldehydes with indoles, Scheme 6.4, so that an initial racemic sample gave substitution products with up to 91% enantiomeric excesses. It was demonstrated by computational, kinetic, and empirical studies that the mechanism does not occur *via* a cationic intermediate, but through an asymmetric S_N2 dynamic

[3] N. M. Rezayee, V. J. Enemærke, S. T. Linde, J. N. Lamhauge, G. J. Reyes-Rodríguez, K. A. Jørgensen, C. Lu, K. N. Houk *J. Am. Chem. Soc.* **2021**, *143*, 7509−7520.

kinetic resolution. The combination of an α-branched aldehyde with a primary aminocatalyst in presence of DDQ as oxidant allows the existence of a dynamic Walden cycle. Figure 6.1 shows the most favorable transition state for the coupling between (*R*)-**I** and the corresponding indole.

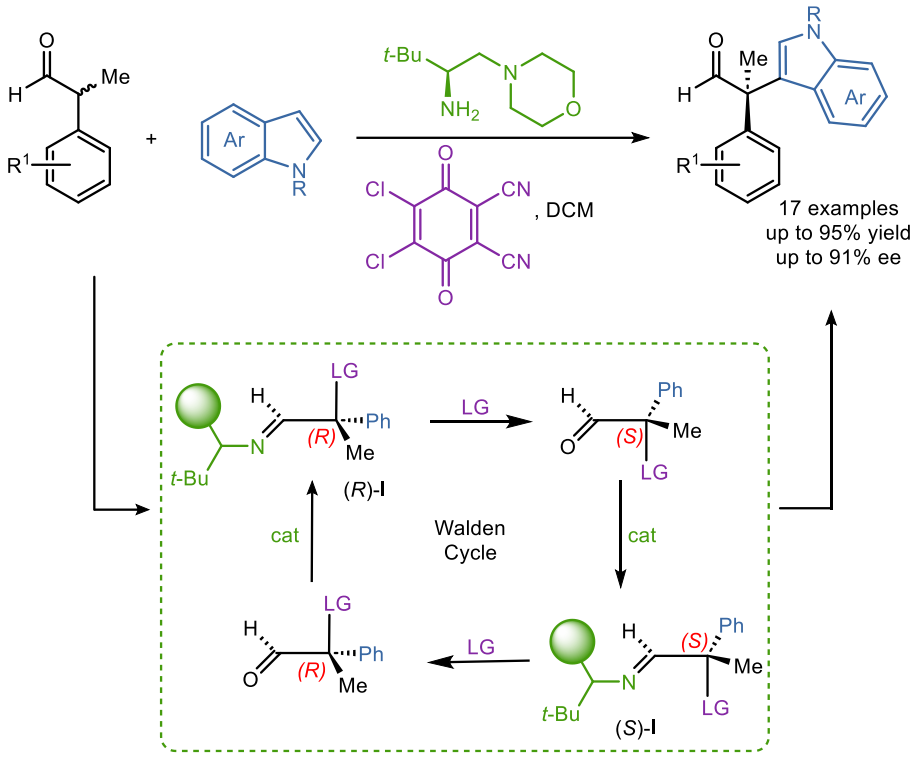

Scheme 6.4*:* Organocatalyzed addition of indoles to α-branched aldehydes *via* oxidative coupling.

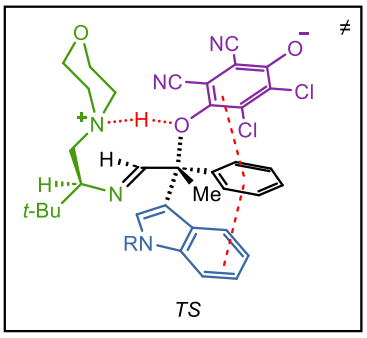

Figure 6.1: Transition state for coupling of (*R*)-**I** with the corresponding indole.

Following the study on *umpolung* reactivity, Jørgensen[4] moved to α-etherification of aldehydes, as ether functionality is an abundantly important scaffold in natural products.[5] A wide variety of hydroxyl-containing nucleophiles were coupled with α-branched aldehydes with up to 95% ee, Scheme 6.5.

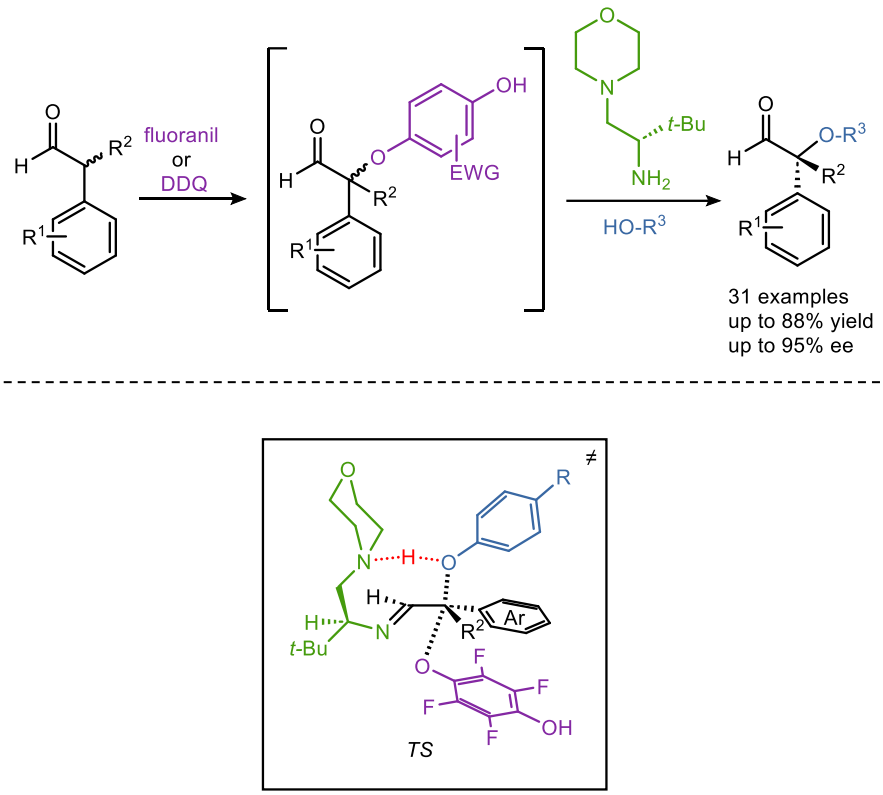

Scheme 6.5: α-Etherification of aldehydes through enantioselective oxidative catalysis.

Two different protocols were developed depending on the nature of the nucleophile. When aromatic hydroxyl-nucleophiles were used, a two-step one-pot protocol was optimized. First, oxidation of starting aldehyde in presence of fluoranil and sacrificial *rac*-aminocatalyst, as the oxidation does not occur without the presence of an aminocatalyst. Then, the nucleophile and the chiral aminocatalyst were added. In contrast, when alcohol nucleophiles were used, the 1,4-benzoquinone DDQ was found to be the optimal oxidant and, changing the solvent after oxidation was necessary to provide the same level of enantioselectivity. More specifically, some of the nucleophiles tolerated were allylic, benzylic and propargylic alcohols, Scheme 6.6.

[4] J. N. Lamhauge, V. Corti, Y. Liu, K. A. Jørgensen *Angew. Chem. Int. Ed.* **2021**, *60*, 18728–18733.
[5] P. Domínguez de María, R. W. van Gemert, A. J. J. Straathof, U. Hanefeld *Nat. Prod. Rep.* **2010**, *27*, 370–392.

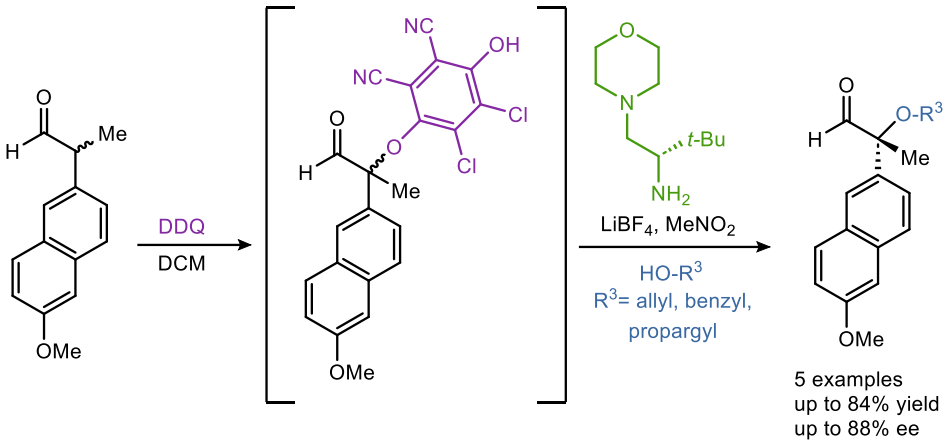

Scheme 6.6: Oxidative α-etherification with alkyl alcohols.

Total synthesis represents a tool which demonstrates the power of organic chemistry. Efforts are employed to develop new pathways and strategies for the synthesis of different natural products. Bruguierols[6] are a class of natural products with biological and antibacterial activity, Figure 6.2a. Only a few examples have been described for the synthesis of this family, so the search for new routes that allow its total synthesis,[7] or that of other derivatives, such as Integrastatin A[8] is a potential topic due to the interesting properties they could have.

[6] B. Panda *Arkivoc* **2019**, *i*, 293–303.
[7] (a) B. Hu, S. Xing, J. Ren, Z. Wang Tetrahedron, **2010**, *66*, 5671–5674, (b) F. J. Fañanás, A. Fernández, D. Cevic, F. Rodríguez *J. Org. Chem.* **2009**, *74*, 932–934, (c) D. Martinez Solorio, M. P. Jennings *J. Org. Chem.* **2007**, *72*, 6621–6623, (d) C. V. Ramana, S. R. Salian, R. G. Gonnade *Eur. J. Org. Chem.* **2007**, 5483–5486.
[8] S. B. Singh, D. L. Zink, D. S. Quamina, F. Pelaez, A. Teran, P. Felock, D. J. Hazuda *Tetrahedron Lett.* **2002**, *43*, 2351 — 2354.

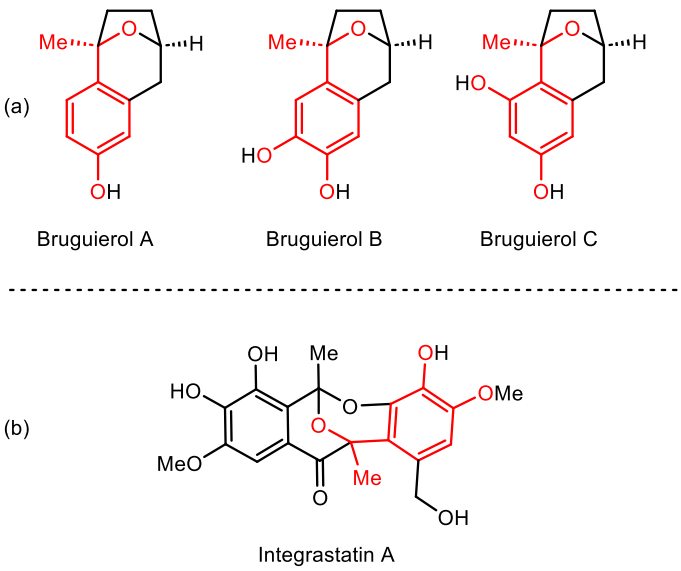

Figure 6.2: Selected natural products.

With this in mind and the results for the oxidative α-etherification in hand, the coupling of alcohol nucleophiles with α-branched aldehydes through oxidative aminocatalysis and its subsequent transformation to synthesize new quaternary isochromanes that constitutes the structural core of Bruguierols, will be presented, Scheme 6.7.

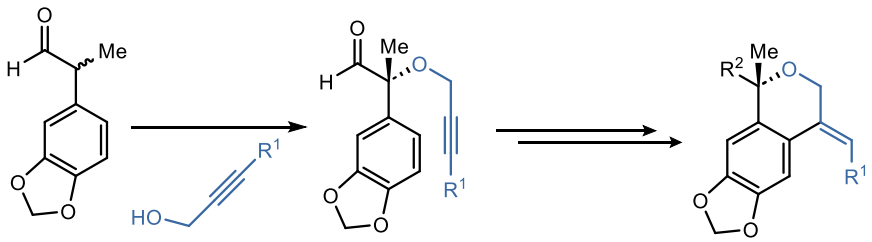

Scheme 6.7: Proposed project.

6.2 Results and discussion

We started by combining α-methyl substituted aldehyde **1** with propargylic alcohol **2a** in the optimized conditions[9] shown in Scheme 6.8. *L-tert*-leucine-derived diamine **A** was found to be the optimal aminocatalyst to develop the reaction as the tertiary amine had demonstrated in previous works to be crucial for the coupling reaction.[3,4] DDQ as oxidant and $LiBF_4$ as additive in nitromethane as solvent at 5 °C complete the reaction conditions. In a one-step protocol, **3a** was

[9] Reaction optimization had been previously carried out by Dr. Philipp Waser.

isolated in 59% yield and 95% ee. A scale-up reaction of the oxidative coupling was carried out (0.6 mmol of **1**) affording **3a** with a slightly improvement in the yield and the same level of enantioselectivity, Scheme 6.8.

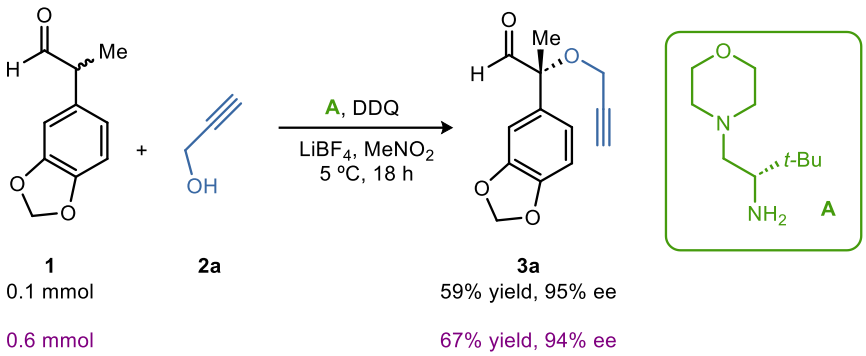

Scheme 6.8: Optimized reaction conditions for the oxidative coupling.

With the optimized conditions in hand, the influence of differently substituted propargylic alcohols was evaluated, Table 1. When phenyl or ester substituted-propargylic alcohols, **2b**-**c**, were used in the reaction, **3b** and **3c** were isolated with moderate yields and high enantiomeric excesses.

Table 1. Substrate scope for propargylic alcohols **2a-c**.[a,b,c]

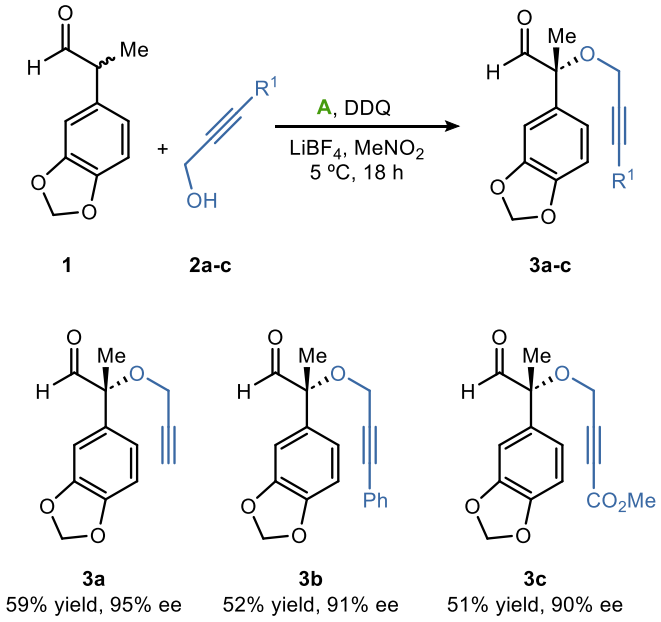

[a]Reaction scale: **1** (0.1 mmol). [b]Yield of **3a-c** after column chromatography. [C] Ee values determined by chiral stationary phase ultra-performance convergence chromatography (UPC^2) analysis.

The reaction mechanism is expected to be the same as the previous one reported when propargylic alcohols were used.[4] First, reaction of the aldehyde with DDQ as oxidant allowing the *umpolung* reactivity and then, nucleophilic attack of the different alcohols giving rise to the corresponding α-substituted aldehydes.

Next, further transformations were studied. Metal-catalyzed 6-exo-dig cyclization with **3a** was not successful as starting aldehyde decomposed in almost all cases. An alternative pathway which included acetalization of **3a** was carried out before cyclization, Scheme 6.9. Treatment of **3a** with trimethyl orthoformate and pyridinium *p*-toluenesulfonate in dichloromethane at room temperature gave rise to acetal-**4** quantitatively.

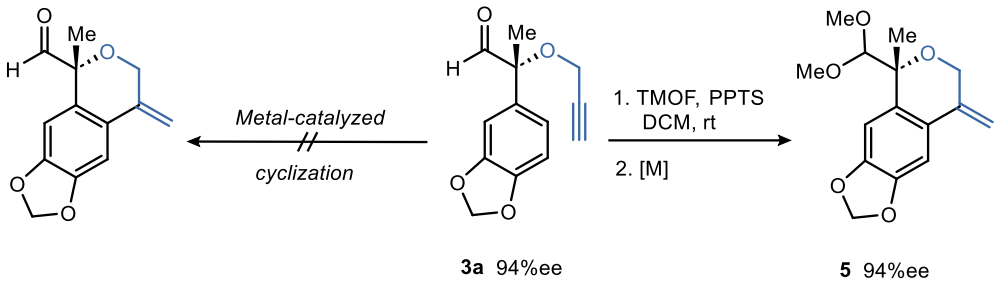

Scheme 6.9: Different pathways for cyclization process.

After acetalization, different conditions for metal-catalyzed cyclization were evaluated in dichloromethane as solvent at room temperature, Table 2. No reaction was observed when IPrAuCl was used (Table 2, entry 1). In contrast, in presence of $AgSbF_6$, **4** rapidly disappeared but no formation of **5** was detected (Table 2, entry 2). The equimolar mixture of IPrAuCl/$AgSbF_6$, entry 3, provided a complex reaction mixture. However, when 1 mol% of previously prepared IPrAuSbF_6 was used, full conversion of **4** was achieved after 5 min, giving rise to cyclized product **5** in 76% yield after column chromatography maintaining the enantiomeric excess (Table 2, entry 4).

Table 2. Control experiments for gold-catalyzed cyclization.

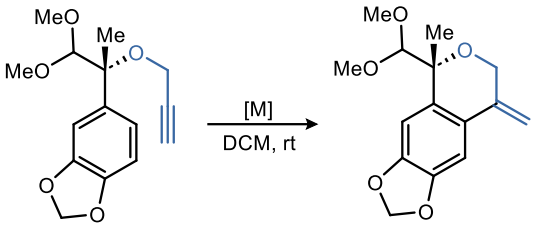

4 94% ee **5** 94% ee

Entry	*Cat (mol%)*	*Time*	*Conversion[a] (%)[b]*
1	IPrAuCl (20)	3 h	0 (0)
2	$AgSbF_6$ (20)	3 h	100 (0)
3	IPrAuCl (20) + $AgSbF_6$ (20)	2 h	100 (0)
4	$IPrAuSbF_6$ (1)	5 min	100 (76)

[a] Conversion measured by ^{1}H-NMR. [b]Yield of isolated **5** after column chromatography.

Cleavage of protecting group with 2,6-lutidine and trimethylsilyl trifluoromethanesulfonate in dichloromethane at low temperature provided the corresponding aldehyde **6** in moderate yield, Scheme 6.10. The subsequent reduction of the aldehyde group with sodium borohydride in methanol gave rise to **7** in 50% yield after two steps, Scheme 6.10. In both steps, no erosion in the enantiomeric excess was detected.

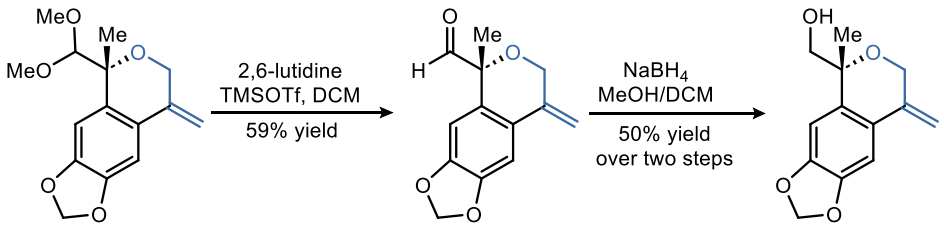

5 94% ee **6** 94% ee **7** 94% ee

Scheme 6.10: Transformations of cyclized product **5**.

6.3 Conclusions

Coupling of propargylic alcohols with α-methyl substituted aldehydes is reported in this chapter. The reaction proceeds under mild conditions in one-step one-pot protocol with moderate yields (51-59%) and high enantioselectivity (90-95% ee). Products undergo further metal-catalyzed cyclization using only 1 mol% of previously prepared $IPrAuSbF_6$ yielding the quaternary

corresponding isochromanes after deprotection and reduction. Yields are good and the enantioselectivity is maintained in all the cases. More experimental work will be necessary to complete the study.

6.4 Experimental section

General information

NMR spectra were acquired on a Bruker AVANCE III HD spectrometer running at 400 MHz for ^{1}H and 100 MHz for ^{13}C. Chemical shifts (δ) are reported in ppm relative to residual solvent signals ($CHCl_3$, 7.26 ppm for ^{1}H NMR; $CDCl_3$, 77.16 ppm for ^{13}C NMR). The following abbreviations are used to indicate the multiplicity in NMR spectra: s, singlet; d, doublet; t, triplet; q, quartet; p, pentet; dd, double doublet; ddd, double double doublet; dt, double triplet; td, triple doublet; tt, triple triplet; m, multiplet; bs, broad signal. ^{13}C NMR spectra were acquired in a broad band decoupled mode. Mass spectra were recorded on a Bruker MicroTOF-Q High-Performance LC-MS system using electrospray (ES+) ionization. Dichloromethane was dried over molecular sieves (4 Å). Analytical thin layer chromatography (TLC) was performed using pre-coated aluminium-backed plates (Merck Kieselgel 60 F254) and visualized by UV radiation, p-anisaldehyde stain, vanillin or $KMnO_4$ stain. For flash chromatography (FC) Sigma-Aldrich silica gel high-purity grade (9385) (SiO_2 60, 230-400 mesh) was used. Optical rotations were measured on a Bellingham + Stanley ADP440+ polarimeter, [α] values are given in $deg \cdot cm^3 \cdot g^{-1} \cdot dm^{-1}$; concentration in $g \cdot (100\ mL)^{-1}$. The enantiomeric excess (ee) of the products was determined by chiral stationary phase Waters ACQUITY UPC^2 (Daicel Chiralpak). Racemic samples for UPC^2 analysis were prepared using DDQ as oxidant and an equimolar mixture of both enantiomers of **A** as catalyst. Propargylic alcohol **2a** was commercially available. Aldehyde **1**,[10] propargylic alcohols **2b-c**[11] and both enantiomers of **A**[3] were prepared according to literature procedures.

6.5 References

1. N. M. Rezayee, J. N. Lamhauge, K. A. Jørgensen *Acc. Chem. Res.* **2022**, *55*, 1703–1717.
2. L. A. Leth, L. Næsborg, G. J. Reyes-Rodríguez, H. N. Tobiesen, M. V. Iversen, K. A. Jørgensen *J. Am. Chem. Soc.* **2018**, *140*, 12687−12690. *For coupling of α-branched aldehydes with oligopeptides and amino acids see:* H. N. Tobiesen, L. A. Leth, M. V. Iversen, L. Næsborg, S. Bertelsen, K. A. Jørgensen *Angew. Chem. Int. Ed.* **2020**, *59*, 18490–18494.

[10] (a) S. Hu, Z. Lu, M. Liu, H. Xu, J. Wu, F. Chen *J. Org. Chem.* **2020**, *85*, 14916–14925, (b) F. A. Cruz, V. M. Dong *J. Am. Chem. Soc.* **2017**, *139*, 1029−1032.

[11] (a) R. Tao, Y. Yin, Y. Duan, Y. Sun, Y. Sun, F. Cheng, J. Pan, C. Lu, Y. Wang *Tetrahedron*, **2017**, *73*, 1762–1768, (b) J. Kratochvíl, Z. Novák, M. Ghavre, L. Nováková, A. Růžička, J. Kuneš, M. Pour *Org. Lett.* **2015**, *17*, 520–523, (c) J. Rehbein, S. Leick, M. Hiersemann *J. Org. Chem.* **2009**, *74*, 1531–1540, (d) M. S. Leonard, P. J. Carroll, M. M. Joullié *J. Org. Chem.* **2004**, *69*, 2526–2531.

3. N. M. Rezayee, V. J. Enemærke, S. T. Linde, J. N. Lamhauge, G. J. Reyes-Rodríguez, K. A. Jørgensen, C. Lu, K. N. Houk *J. Am. Chem. Soc.* **2021**, *143*, 7509−7520.
4. J. N. Lamhauge, V. Corti, Y. Liu, K. A. Jørgensen *Angew. Chem. Int. Ed.* **2021**, *60*, 18728–18733.
5. P. Domínguez de María, R. W. van Gemert, A. J. J. Straathof, U. Hanefeld *Nat. Prod. Rep.* **2010**, *27*, 370–392.
6. B. Panda *Arkivoc* **2019**, *i*, 293–303.
7. (a) B. Hu, S. Xing, J. Ren, Z. Wang Tetrahedron, **2010**, *66*, 5671–5674, (b) F. J. Fañanás, A. Fernández, D. Cevic, F. Rodríguez *J. Org. Chem.* **2009**, *74*, 932–934, (c) D. Martinez Solorio, M. P. Jennings *J. Org. Chem.* **2007**, *72*, 6621–6623, (d) C. V. Ramana, S. R. Salian, R. G. Gonnade *Eur. J. Org. Chem.* **2007**, 5483–5486.
8. S. B. Singh, D. L. Zink, D. S. Quamina, F. Pelaez, A. Teran, P. Felock, D. J. Hazuda *Tetrahedron Lett.*, **2002**, *43*, 2351–2354.
9. Reaction optimization had been previously carried out by Dr. Philipp Waser.
10. (a) S. Hu, Z. Lu, M. Liu, H. Xu, J. Wu, F. Chen *J. Org. Chem.* **2020**, *85*, 14916–14925, (b) F. A. Cruz, V. M. Dong *J. Am. Chem. Soc.* **2017**, *139*, 1029−1032.
11. (a) R. Tao, Y. Yin, Y. Duan, Y. Sun, Y. Sun, F. Cheng, J. Pan, C. Lu, Y. Wang *Tetrahedron*, **2017**, *73*, 1762–1768, (b) J. Kratochvíl, Z. Novák, M. Ghavre, L. Nováková, A. Růžička, J. Kuneš, M. Pour *Org. Lett.* **2015**, *17*, 520–523, (c) J. Rehbein, S. Leick, M. Hiersemann *J. Org. Chem.* **2009**, *74*, 1531–1540, (d) M. S. Leonard, P. J. Carroll, M. M. Joullié *J. Org. Chem.* **2004**, *69*, 2526–2531.

General Conclusions

As demonstrated through this Doctoral Thesis, several pathways have proved to be useful for the synthesis of different pyrazolin-5-one derivatives.

N-Heterocyclic carbenes provided an easy access for the synthesis of spirocyclic pyrazolone γ-butyrolactones and butenolides through a [3+2] annulation reaction between pyrazolin-4,5-diones and enals or 3-bromoenals, respectively. The homoenolate intermediates generated from the unsaturated aldehydes and chiral carbenes derived from (1*S*,2*R*)-*cis*-aminoindanol act as nucleophiles with pyrazol diones to afford the desired spiro compounds.

In another way, a direct route for the synthesis of oxazolidino spiropyrazolinones promoted by a bifunctional squaramide catalyst have been established. The reaction proceeds *via* *N*,*O*-acetalization/aza Michael addition domino reaction between *N*-Boc ketimines derived from pyrazolin-5-ones and γ-hydroxyenones. In a different approach, *N*-Boc ketimines have been used as electrophiles in Mannich reactions with 1,3-dicarbonyl compounds. Mannich adducts undergo further derivatization to finally give rise to 4-pyrazolyl- and 4-isoxazolyl-4-amino-pyrazolones.

Methodology

^{1}H NMR (500 MHz), ^{13}C NMR (126 MHz) and ^{19}F NMR (376 MHz) spectra were recorded in $CDCl_3$ as solvent. Chemical shifts for protons are reported in ppm from TMS with the residual $CHCl_3$ resonance as internal reference. Chemical shifts for carbons are reported in ppm from TMS and are referenced to the carbon resonance of the solvent. Data are reported as follows: chemical shift, multiplicity (s= singlet, d= doublet, t= triplet, q= quartet, m= multiplet, br= broad), coupling constants in Hertz, and integration.

Specific rotations were measured on a Perkin-Elmer 341 digital polarimeter using a 1 mL cell with a 1-dm path length, and a sodium lamp, and concentration is given in g per 100 mL.

Infrared spectra were recorded on a Perkin-Elmer Spectrum One FT-IR spectrometer and are reported in frequency of absorption (only the structurally most important peaks are given).

Flash chromatography was carried out using silica gel (230–240 mesh). TLC analysis was performed on glass-backed plates coated with silica gel 60 and F254 indicator and visualized by either UV irradiation or by staining with phosphomolybdic acid solution.

Chiral HPLC analysis was performed on a JASCO HPLC system (JASCO PU-2089 and UV-2075 UV/Vis detector) with a quaternary pump, and on Hewett-Packard 1090 Series II instrument equipped with a quaternary pump, using Phenomenex Lux-amylose-1, Lux-i-cellulose-5, Lux-Cellulose-1 and Lux-i-Cellulose-5, and Chiralpak OD, IA and AD-H analytical columns (250 × 4.6 mm). Detection was monitored at 210, 220 and 254 nm. ESI mass spectra were obtained on an Agilent 5973 inert GC/MS system.

Commercially available organic and inorganic compounds were used without further purification. Solvents were dried and stored over microwave-activated 4Å molecular sieves.

List of Publications

The results summarized in this Doctoral Thesis have led to four scientific articles.

Chapter II

"NHC-catalysed [3+2]-asymmetric annulation between pyrazolin-4,5-diones and enals: synthesis of novel spirocyclic pyrazolone γ-butyrolactones and computational study of mechanism and stereoselectivity"

Marta Gil-Ordóñez, Alicia Maestro, Pablo Ortega, Pablo G. Jambrina, José M. Andrés *Org. Chem. Front.* **2022**, 9, 420-427. DOI: 10.1039/d1qo01462e

Chapter III

"Access to spiropyrazolone-butenolides through NHC-catalysed [3+2]-asymmetric annulation of 3-bromoenals and 1H-pyrazol-4,5-diones"

Marta Gil-Ordóñez, Alicia Maestro, José M. Andrés *Manuscript submitted and under revision*.

Chapter IV

"Organocatalytic Asymmetric Synthesis of Oxazolidino Spiropyrazolinones via N,O-acetalization/aza Michael addition domino reaction between N-Boc pyrazolinone ketimines and γ-hydroxyenones"

Marta Gil-Ordóñez, Laura Martín, Alicia Maestro, José M. Andrés *Org. Biomol. Chem.* **2023**, *21*, 2361-2369. DOI: 10.1039/d2ob02290g

Chapter V

"*Squaramide-catalyzed asymmetric Mannich reaction between 1,3-dicarbonyl compounds and pyrazolinone ketimines: a pathway to enantioenriched 4-pyrazolyl and 4-isoxazolyl-4-aminopyrazolone derivatives"*

Marta Gil-Ordóñez, Camille Aubry, Cristopher Niño, Alicia Maestro, José M. Andrés *Molecules* **2022**, *27*, 6983. DOI: 10.3390/molecules27206983